



universität
wien

DISSERTATION / DOCTORAL THESIS

Titel der Dissertation / Title of the Doctoral Thesis

High-resolution imaging for photoacoustic tomography
and optical coherence tomography

verfasst von / submitted by

Cong Shi

angestrebter akademischer Grad /
in partial fulfilment of the requirements for the degree of

Doktor der Naturwissenschaften (Dr. rer. nat.)

Wien, June 2017 / Vienna, June 2017

Studienkennzahl lt. Studienblatt /
degree programme code as it appears
on the student record sheet:

A 796 605 405

Dissertationsgebiet lt. Studienblatt/
field of study as it appears on the
student record sheet:

Mathematics

Betreuer / Supervisor:

Univ.-Prof. Dipl.-Ing. Dr. Otmar Scherzer

Mitbetreut / Co-Supervisor:

Univ.-Prof. Dr. Adrian Constantin

Abstract

by Cong Shi

Photoacoustic tomography (PAT) has attracted much interest in the last decades due to the excellent contrast, high spatial resolution and good specificity. However, most of the current research misses one important element, attenuation. Since naturally most of the tissue has viscoelascity, the energy of the acoustic wave would decrease in the course of propagation. Failing to accommodate attenuation could degrade the quality of the final image.

This dissertation consists of three articles on medical imaging.

The first two articles focus on PAT taking into account acoustic attenuation. The first aim is to develop a corresponding mathematical framework. Known research on the attenuated PAT is sparse. Some fundamental problems, such as the degree of ill-posedness for the inverse problem and existence of an explicit reconstruction formula, remain open.

In the first article, after summarizing all the known attenuation models, a unified attenuation model is given. We will analyze the existence and uniqueness for the solution of this attenuation model, as well as the singular values' asymptotic behavior of the forward problem. Furthermore, we also provide a necessary and sufficient condition for finite propagation speed of the wave.

In the second article, we treat the inverse problem, that is, how to reconstruct the initial pressure. There are some known methods to solve this problem, but there exists no explicit reconstruction formula. We will introduce novel reconstruction formulas based on the universal backprojection formula. Numerical results show these formulas work quite well with similar computational complexity as backprojection formulas.

In the third article, we propose a signal separation technique in sub-cellular scale Optical Coherence Tomography (OCT). This is useful since in the OCT images the background signal caused by collagen or other inter-cellular parts is so strong that it covers the useful information inside the cells. The aim in this project is to remove the influence of this strong, slow-varying background signal to isolate the useful information. First we study the modeling of the signals from the background and cell activity, and then we will give an efficient technique utilizing the Singular Value Decomposition (SVD) to achieve our goal.

Acknowledgements

This cumulative dissertation is a collection of scientific articles the author worked on at the Faculty of Mathematics, University of Vienna during the last few years.

Finally it is time for a personal word! The journey started on October 03. 2013 that is the first day for me to go to Vienna, even to Europe. I met so many wonderful people, from inside and outside the work-sphere. It is indeed a pleasure to convey my gratitude to them in my humble acknowledgment.

I want to thank my advisor Otmar Scherzer for introducing me to this field. From the beginning every week he spent half a day for discussing problem with me, which last for several months no matter if he is busy. He has always been there to provide me unflinching encouragement, support and guidance in different ways, providing many chances to go to the conferences to communicate with other researchers. He taught me that mathematician should be rigorous, which make me benefit forever. I am very grateful to Habib Ammari, who gave me a good chance to stay in ETH for 7 months, I am profoundly impressed by his understanding of mathematics, his technical thoroughness, and his brilliant new ideas.

It is a pleasure to pay a great tribute to my amazing collaborator Peter Elbau whose deep fundamental knowledge of mathematics gave me a lot of help and was always positive and optimistic about both good and bad things, which make me benefit a lot. I also feel grateful to Francisco Romero for the fruitful discussion in ETH.

I am particularly thankful to Professor Maïtine Bergounioux (Orléans, France), Professor Liliana Borcea (Michigan, USA) and Professor Faouzi Triki (Grenoble, France), for their valuable and devoted time to review this thesis.

The warm support of my fellow colleagues in CSC is what allowed me to complete this thesis and made me have a wonderful time along the way. The atmosphere at CSC is always warm and cosy, and my colleagues are very passionate whenever I need help. They make me enjoy the research and life in Vienna so much. I would like to offer a special thank you to Min Hadler, our secretary, who provides many help for my life in Vienna. My thanks also go to our IT expert, Axel Kittenberger, is always happy to solve any technique problems.

Thanks to University of Vienna and the Faculty of Mathematics that provided a comfortable and super beautiful working environment throughout the years. Also thanks to ETH and the Faculty of Mathematics for providing working place for me to stay there for several months.

Words fail me to express my gratitude to the best boyfriend in the world, my boyfriend, Chen, for his unconditional support in research and life. He endures all my bad tempers and devotes all of his knowledge and time to me to make me better each day. Without him, I could not be my current self. I want to send my gratitude and apologize to my parents for understanding my study and limit time to accompany them, especially during the last one year of my PhD study. I want to thank all of friends that I will not mention in person here, they have shared so many special moments with me, contributing to a common story now lead me towards a new chapter. Thank you all for the valueless memories.

Cong Shi
University of Vienna

May 24, 2017

Financial supports:

The work presented here was supported by the Austrian Science Fund (FWF) through the National Research Network 'Doctoral Program Dissipation and Dispersion in Nonlinear PDEs '(W1245).

Contents

Abstract	iii
Acknowledgements	v
Contents	vii
List of notation	ix
1 Introduction	1
1.1 Background	1
1.1.1 Photoacoustic tomography with considering attenuation	1
1.1.2 Ill-posedness of inverse problem	2
1.1.3 Eigenvalues of integral operators	4
Integral operator with finite differentiable kernel	4
Integral operator with weak singular kernel	4
1.1.4 Tempered distributions	5
1.1.5 Pseudo-differential operator	6
1.1.6 Stationary phase method	6
1.1.7 Reconstruction in photoacoustic tomography	8
1.1.8 Optical coherence tomography	9
1.2 Contributions	11
1.2.1 Eigenvalue analysis of attenuated photoacoustic operator	11
Strong attenuation medium	14
Weak attenuation medium	14
1.2.2 Reconstruction formulas	15
1.2.3 Dynamic optical coherence tomography	16
1.3 Outline	17
References	18
2 Singular Values of the Attenuated Photoacoustic Imaging Operator	21
2.1 Introduction	21
2.2 The Attenuated Wave Equation	23
2.2.1 Solution of the Attenuated Wave Equation	24
2.2.2 Finite Propagation Speed	30
2.3 Examples of Attenuation Models	32
2.4 The Integrated Photoacoustic Operator	33
2.5 Singular Values of the Integrated Photoacoustic Operator	45
2.5.1 Strongly Attenuating Media	45
2.5.2 Weakly Attenuating Media	46
2.A Eigenvalues of Integral Operators of Hilbert–Schmidt Type	52

2.B	Estimating the Kernel of the Integrated Photoacoustic Operator	60
	References	64
3	Reconstruction formulas for Photoacoustic Imaging in Attenuating Media	67
3.1	Introduction	67
3.2	Attenuation	70
3.3	Reconstruction formulas	77
3.4	Numerical experiments	78
3.A	Appendix	88
	References	91
4	A signal separation technique for sub-cellular imaging using dynamic optical coherence tomography	95
4.1	Introduction	96
4.2	The dynamic forward problem	97
4.2.1	Single particle model	97
4.2.2	Multi-particle dynamical model	99
4.3	Property analysis of the forward problem	100
4.3.1	Direct operator representation	100
4.3.2	Eigenvalue analysis	103
4.4	The inverse problem: Signal separation	104
4.4.1	Analysis of SVD algorithm	105
4.4.2	Analysis of obtaining the intensity of metabolic activity	108
4.5	Numerical experiments	109
4.5.1	Forward problem measurements	110
4.5.2	SVD of the measurements	111
4.5.3	Selection of cut-off singular value	113
4.5.4	Signal reconstruction	114
4.5.5	Discussion and observations	115
4.6	Conclusion	116
4.A	Appendix	116
	References	117
5	Discussion and Outlook	119
A	Deutsche Zusammenfassung	121

List of notation

Chapter 2

$h(\mathbf{x})$	Source term in the wave equation
$p(t, \mathbf{x})$	Pressure wave in non-attenuating media
$p^a(t, \mathbf{x})$	Pressure wave in attenuating media
$\kappa(\omega)$	Complex wave number
κ_{∞}	A non-negative number in $\kappa(\omega)$
$\kappa_*(\omega)$	A complex function in $\kappa(\omega)$
$\tilde{\kappa}(z)$	A holomorphic continuation of $\kappa(\omega)$
c	Propagation speed of wave
Ω	A bounded Lipschitz domain
$\partial\Omega$	The observation surface
Ω_{ϵ}	The object
$E(t, x)$	Electric field
$m(t, \xi)$	Measurements on the observation surface
G_{κ}	The kernel of solution of attenuating wave equation
\mathbb{N}	The positive integer number
\mathbb{Z}	The integer number
\mathbb{R}	The real number
\mathbb{C}	The complex number
\mathbb{H}	The upper half complex plane
$\overline{\mathbb{H}}$	The closure of the upper half complex plane
\mathcal{S}	Schwartz space
\mathcal{S}'	The space of tempered distributions
\mathcal{D}	Space of test functions
\mathcal{D}'	Space of distributions
\mathcal{F}	The Fourier transform
\mathcal{F}^{-1}	The inverse Fourier transform
\mathcal{A}_{κ}	Attenuation operator
$\check{\mathcal{P}}_{\kappa}$	Photoacoustic operator
$\check{\mathcal{P}}_{\kappa}^{(0)}$	Photoacoustic operator with constant attenuation
$\check{\mathcal{P}}_{\kappa}^{(1)}$	Perturbation of the photoacoustic operator
F_{κ}	Kernel of $\check{\mathcal{P}}_{\kappa}^* \check{\mathcal{P}}_{\kappa}$
$F_{\kappa}^{(0)}$	Kernel of $\check{\mathcal{P}}_{\kappa}^* \check{\mathcal{P}}_{\kappa}$ for constant attenuation
$F_{\kappa}^{(1)}$	First perturbation of kernel
$F_{\kappa}^{(2)}$	Second perturbation of kernel
R_{κ}	The integral kernel of operator $\check{\mathcal{P}}_{\kappa}^{(1)*} \check{\mathcal{P}}_{\kappa}^{(1)}$
\mathcal{Q}_{κ}	The operator $\check{\mathcal{P}}_{\kappa}^* \check{\mathcal{P}}_{\kappa} - \check{\mathcal{P}}_{\kappa}^{(0)*} \check{\mathcal{P}}_{\kappa}^{(0)}$
T	A general integral operator

F	Hermitian integral kernel of operator T
U	A bounded open set in \mathbb{R}^m
T_1	A general integral operator
T_2	Finite rank operator
M_j	The supremum of higher order fractional derivatives of kernel F

Chapter 3

$h(\mathbf{x})$	Source term in the wave equation
$p(t, \mathbf{x})$	Pressure wave in non-attenuating media
$q(t, \mathbf{x})$	Integrated pressure wave in non-attenuating media
$p^a(t, \mathbf{x})$	Pressure wave in attenuating media
$q^a(t, \mathbf{x})$	Integrated pressure wave in attenuating media
$\kappa(\omega)$	Complex wave number
k_∞	A non-negative number in $\kappa(\omega)$
$k_*(\omega)$	A complex function in $\kappa(\omega)$
$\tilde{\kappa}(z)$	A holomorphic continuation of $\kappa(\omega)$
c	Propagation speed of wave
Ω	A bounded Lipschitz domain
$\partial\Omega$	The observation surface
Ω_ϵ	The object
$m(t, \xi)$	Measurements on the observation surface
\mathbb{N}	The positive integer number
\mathbb{Z}	The integer number
\mathbb{R}	The real number
\mathbb{C}	the complex number
\mathbb{H}	The upper half complex plane
$\overline{\mathbb{H}}$	The closure of the upper half complex plane
\mathcal{S}	Schwartz space
\mathcal{S}'	The space of tempered distributions
\mathcal{F}	The Fourier transform
\mathcal{F}^{-1}	The inverse Fourier transform
\mathcal{A}_κ	Attenuation operator
\mathcal{B}	Attenuation solution operator
$k(t, \tau)$	The kernel of operator \mathcal{B}
\mathcal{I}	Time integration operator
\mathcal{W}	The wave operator

Chapter 4

Ω	Sample
\mathcal{F}	The Fourier transform
Γ_{ODT}	The ODT signal generated by one particle
$S_0(\omega)$	The spectral density of the light source
$K(x, \omega)$	Reflectivity of the sample
$K_R(x, \omega)$	Reflectivity of the reference mirror
\bar{n}	The index of refraction
c	The speed of the light
τ	The time delay on the reference arm
Δ	The path difference between the reference arm and sample arm
$p(x, z, t)$	Density function at point $x \times z$ at time t
$p_c(x, z, t)$	Density function of collagen particles
$p_m(x, z, t)$	Density function of the density function of metabolic activity particles
K_c	Reflectivity of collagen particles
K_m	Reflectivity of metabolic activity particles
$\Gamma_{ODT}^c(x, t)$	The collagen signal
$\Gamma_{ODT}^m(x, t)$	The metabolic activity signal
v_0	The collagen particle moving speed
$q_c(x, z)$	The density function of all the collagen particles inside area x with initial vertical position z
S	The integral operator with kernel $\Gamma_{ODT}(x, t)$
S_c	The integral operator with kernel $\Gamma_{ODT}^c(x, t)$
S_m	The integral operator with kernel $\Gamma_{ODT}^m(x, t)$
$F(x, y)$	The kernel of integral operator SS^*
$F_{cc}(x, y)$	The kernel of integral operator $S_c S_c^*$
$F_{cm}(x, y)$	The kernel of integral operator $S_c S_m^*$
$F_{mc}(x, y)$	The kernel of integral operator $S_m S_c^*$
$F_{mm}(x, y)$	The kernel of integral operator $S_m S_m^*$

Introduction

1.1 Background

1.1.1 Photoacoustic tomography with considering attenuation

Photoacoustic imaging is a biomedical imaging modality based on the photoacoustic effect. In photoacoustic imaging, non-ionizing laser pulses (such as radio wave or near infrared light) are delivered into tissues. Some of the delivered energy will be absorbed and converted into heat, leading to thermo-elastic expansion and thus leads to the propagation of a pressure wave. The signal is detected by ultrasonic transducers distributed on the boundary of the object, and then analyzed to produce images. As a result, this image is used for imaging optical properties of the object, like optical absorption contrast. Figure 1.1 is a schematic illustration showing the basic principles of photoacoustic imaging. The left figure is the flow chart of PAT process, and the right figure is a typical PAT mechanism (Reproduced from Zhang, E., J. Laufer, and P.C. Beard, Appl. Opt. 47(4): 561-77, 2008.)

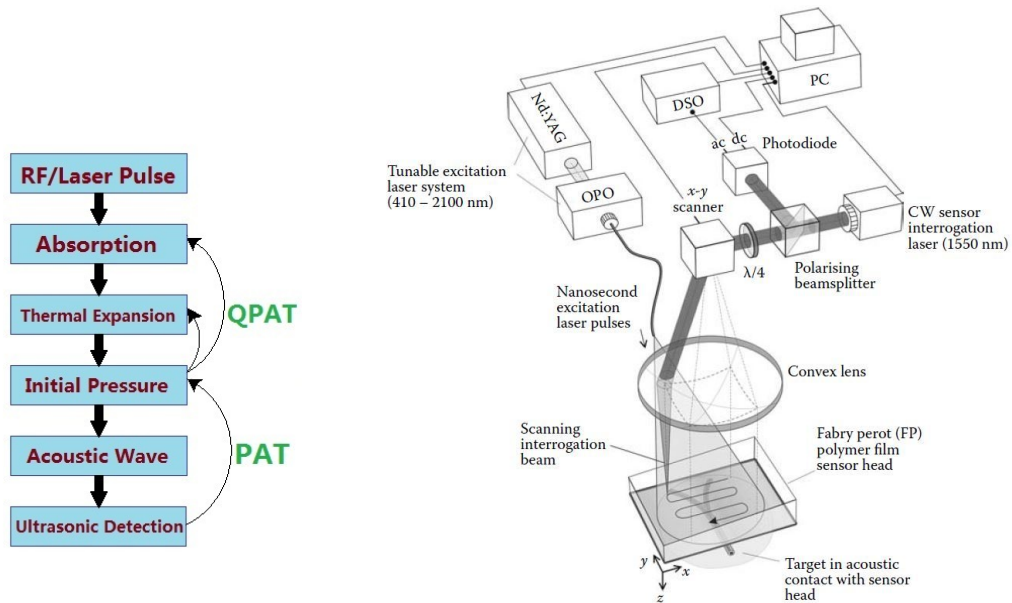


FIGURE 1.1: Illustration of the PAT setup.

In the standard photoacoustic imaging, see e.g. [Wan09], it is assumed that the medium is *non-attenuating*, and the imaging problem consists in visualising the spatially, compactly supported

absorption density function $h : \mathbb{R}^3 \rightarrow \mathbb{R}$, appearing as a source term in the wave equation

$$\begin{aligned} \partial_{tt}p(t, x) - \Delta p(t, x) &= \delta'(t)h(x), & t \in \mathbb{R}, x \in \mathbb{R}^3, \\ p(t, x) &= 0, & t < 0, x \in \mathbb{R}^3, \end{aligned}$$

from measurements $m(t, x)$ of the pressure p for $(t, x) \in (0, \infty) \times \partial\Omega$, where $\partial\Omega$ is the boundary of a compact, convex set Ω containing the support of h .

If the medium is acoustically homogeneous, then the initial pressure wave could be extracted from the measurements of the pressure by inverting a spherical Radon transform. In this regard, we refer to the review papers [KK08; Kuc11]. In non-attenuating media, there are some theoretical and numerical results for the reconstruction. Palamodov [Pal10] has proved the singular values of the spherical mean operator decays polynomially with the order $-\frac{1}{3}$, which could provide a theoretical basis for the explicit reconstruction formula. Also, there are some known reconstruction methods, for example, filtered back-projection formulas and time reversal.

A challenging problem in photoacoustic imaging is to take into account the acoustic attenuation. Until now there is no ill-posedness analysis, and also no explicit reconstruction formula in the attenuating medium. However, using time reversal, one can still reconstruct the initial pressure. In fact, in recent works, Ammari et al. [Amm+13] used a thermo-viscous law model for the attenuation losses and investigated reconstructing sources in attenuating media by modifying the time reversal process as a first order correction of the attenuation effect. Kowar [Kow14] concerned time reversal in photoacoustic tomography of dissipative media that are similar to water. There are also some literatures which use power laws as attenuation compensation and applied time reversal on these kinds of models (see e.g. [CT10; TZC10]).

In this thesis, we developed a mathematical framework for photoacoustic imaging in attenuating media, and provide the ill-posedness analysis for the corresponding inverse problem and explicit reconstruction formulas for the initial pressure. In order to introduce our results, in the next sections we will give the background knowledge of inverse problems, the eigenvalue decay results of integral operators, the classical filtered backprojection formulas, and some tools we use to solve these problems.

1.1.2 Ill-posedness of inverse problem

A comprehensive theory to ill-posed problems in Hilbert spaces has been introduced, e.g. in [EHN96]. Let X and Y be Hilbert spaces and $T : X \rightarrow Y$ be a bounded linear operator. Considering the equation

$$Th = g, \tag{1.1}$$

where $h \in X$ and $g \in Y$. The direct problem or forward problem is to find g from h , while for given data g solving the equation for h is referred to as the inverse problem. In order to analyze the inverse problem, we first introduce Hadamard's definition of well-posedness, which includes three criteria:

- Existence: For all admissible data g , there exists a function h such that $Th = g$, i.e. $g \in \text{ran}(T)$.
- Uniqueness: For all admissible data g , the solution h is unique, i.e. operator T is injective.

- Continuity: The solution h depends continuously on the data g , i.e. the operator T^{-1} is bounded.

Here $\text{ran}(T)$ denotes the range of operator T . For problems with a physical background, the direct problems are usually well-posed in the sense of Hadamard. However, the inverse problem could be ill-posed. The degree of ill-posedness is measured by the decay of the singular values of operator T . Let T be an integral operator of the form

$$T : L^2(\Omega) \rightarrow L^2(\Omega)$$

$$x \rightarrow (Th)(x) := \int_{\Omega} F(x, y)h(y)dy,$$

where $\Omega \in \mathbb{R}^n$ is compact and Jordan-measurable with positive measure, and $F(x, y)$ is the integral kernel corresponding to operator T . Let T^\dagger be the Moore-Penrose (generalized) inverse [EHN96] of T and $(\sigma_n; v_n, u_n)$ be a singular system for the compact linear operator T . Then for $g \in D(T^\dagger)$ which denotes the domain of T^\dagger we have

$$T^\dagger g = \sum_{n=1}^{\infty} \frac{\langle g, u_n \rangle}{\sigma_n} v_n. \quad (1.2)$$

In practice, the data g will contain some noise. (1.2) shows how the noise influences the solution $T^\dagger g$. Namely, the component corresponding to u_n in the noise will be amplified by a factor of σ_n^{-1} , and this factor can grow without bound. For example, let $g_{\delta,n} := g + \delta u_n$ be the measured data with noises, then $\|g_{\delta,n} - g\|_{L^2} = \delta$, but due to (1.2),

$$T^\dagger g - T^\dagger g_{\delta,n} = \frac{\langle \delta u_n, u_n \rangle}{\sigma_n} v_n,$$

and therefore,

$$\|T^\dagger g - T^\dagger g_{\delta,n}\|_{L^2} = \frac{\delta}{\sigma_n}.$$

Hence, the faster the singular values decay, the more severe instability in (1.2) becomes. This makes it possible to quantify the degree of ill-posedness of $Th = g$.

- Mildly(moderately) ill-posed: if $\sigma_n = O(n^{-a})$ holds for some $a \in \mathbb{R}^+$.
- severely ill-posed: if $\sigma_n = O(e^{-bn^a})$ holds for some $a, b \in \mathbb{R}^+$.

Roughly, the rate $\sigma_n = O(n^{-\frac{1}{2}})$ holds in general for computerized tomography in two dimensions, so the corresponding inverse problems are moderately ill-posed. However, "incomplete data problems" in computerized tomography, where X-ray measurements are available only for some directions, are severely ill-posed [EHN96].

The precondition of ill-posedness is that the forward operator T is compact. Here we introduce an important definition: Hilbert-Schmidt operator, which is a bounded operator T on a Hilbert space H with finite Hilbert-Schmidt norm

$$\|T\|_{HS}^2 = \text{tr}(T^*T) := \sum_{n \in I} \|Tu_n\|^2,$$

where $\|\cdot\|$ is the norm of space H and tr is the trace of a nonnegative self-adjoint operator. Hilbert-Schmidt operators are compact. An important class of examples is provided by Hilbert-Schmidt integral operator. Let Ω be a domain in n -dimensional Euclidean space \mathbb{R}^n , a Hilbert-Schmidt kernel is a function $F : \Omega \times \Omega \rightarrow \mathbb{C}$ with

$$\int_{\Omega} \int_{\Omega} |F(x, y)|^2 dx dy < \infty,$$

and associated Hilbert-Schmidt integral operator is the operator $T : L^2(\Omega; \mathbb{C}) \rightarrow L^2(\Omega; \mathbb{C})$ given by

$$(Th)(x) = \int_{\Omega} F(x, y)h(y) dy, \quad x \in \Omega.$$

Then T is a Hilbert-Schmidt operator with Hilbert-Schmidt norm

$$\|T\|_{HS} = \|F\|_{L^2}.$$

1.1.3 Eigenvalues of integral operators

Let T be an integral operator with kernel F . The essential thing is to find the asymptotic behavior of its eigenvalues. In this section we will introduce some results in the literature for the integral operators with finite differentiable kernel and weak singular kernel.

Integral operator with finite differentiable kernel

If $F(x, y)$ is a positive definite Hermitian kernel such that the partial derivative $\frac{\partial^p}{\partial y^p} F(x, y)$ exists and is continuous on the square $[0, 1]^2$ with a positive integer p , then the eigenvalues of integral operator T have the following asymptotic behavior,

$$\lambda_j(T) = o(j^{-(p+1)}) \text{ as } j \rightarrow \infty. \quad (1.3)$$

Integral operator with weak singular kernel

For $0 < \eta < n$ with the space dimension n . If $F(x, y)$ is a weak singular kernel, that is,

$$F(x, y) = \phi(x, y) \cdot |x - y|^{-\eta} \quad (1.4)$$

where $\phi \in L^\infty(\mathbb{R}^n \times \mathbb{R}^n)$. There are several results concerning the eigenvalues of the operator T :

- If $\frac{n}{2} < \eta < n$, then [Kos74] shows that the eigenvalues of the operator T admit the estimate

$$\lambda_j(T) = O(j^{-(1-\frac{\eta}{n})}). \quad (1.5)$$

- If $\eta = n/2$, König proved in [Kön80] that, the eigenvalues λ_j have order

$$\lambda_j(T) = O(j^{-\frac{1}{2}} \log(j+1)). \quad (1.6)$$

- If $0 < \eta < n/2$, it is shown in [CJK91] that the operator T has square-summable eigenvalues.

All of the above results cannot be improved in general.

1.1.4 Tempered distributions

The Schwartz space is the function space

$$\mathcal{S}(\mathbb{R}^n) = \{f \in C^\infty(\mathbb{R}^n) : \|f\|_{\alpha,\beta} < \infty, \forall \alpha, \beta \in \mathbb{Z}_+^n\},$$

where α, β are multi-indices. $C^\infty(\mathbb{R}^n)$ is the set of smooth functions from \mathbb{R}^n to \mathbb{C} , and

$$\|f\|_{\alpha,\beta} = \sup_{x \in \mathbb{R}^n} |x^\alpha D^\beta f(x)|.$$

The space of tempered distributions, usually denoted by \mathcal{S}' is defined as the dual of the Schwartz space. More explicitly, a linear functional $T : \mathcal{S}(\mathbb{R}^n) \rightarrow \mathbb{C}$ is called a tempered distribution if

- $T(\phi_1 + \phi_2) = T(\phi_1) + T(\phi_2)$, for all $\phi_1, \phi_2 \in \mathcal{S}$,
- $T(a\phi) = \bar{a}T(\phi)$, for all $\phi \in \mathcal{S}$, and $a \in \mathbb{C}$,
- For $\phi_j, \phi \in \mathcal{S}$, if $\phi_j \rightarrow \phi$ in \mathcal{S} , then $T\phi_j \rightarrow T\phi$. Convergence in \mathcal{S} means that the supports of ϕ_j are contained in a compact set, and $\nabla^k \phi_j \rightarrow \nabla^k \phi$ for every n -tuple k .

The Dirac delta δ is a widely-used distribution defined by the equation $\langle \delta, \phi \rangle = \phi(0)$ by assuming that ϕ is a Schwartz function. We have the following properties of δ :

- $\langle \delta', \phi \rangle = -\phi'(0)$.
- $\delta(ax) = \frac{\delta(x)}{|a|}$.
- $\int_{-\infty}^{\infty} f(t)\delta(t-T)dt = f(T)$.

Assume the one-dimensional inverse Fourier-transform is given by

$$\check{\varphi}(t) = \frac{1}{\sqrt{2\pi}} \int_{\omega=-\infty}^{\infty} e^{-i\omega t} \varphi(\omega) d\omega.$$

Let $\phi \in \mathcal{S}(\mathbb{R})$ and $\psi \in \mathcal{S}(\mathbb{R}^3)$. The Fourier-transform $\mathcal{F}[\cdot] : \mathcal{S}' \rightarrow \mathcal{S}'$ on the space of tempered distributions is defined by

$$\langle \mathcal{F}[u], \phi \otimes \psi \rangle_{\mathcal{S}', \mathcal{S}} = \langle u, \check{\phi} \otimes \psi \rangle_{\mathcal{S}', \mathcal{S}}.$$

Another important definition is the regular distribution. Let f be locally integrable on \mathbb{R}^n , that is, on every compact set $U \subseteq \mathbb{R}^n$, we have $f \in L^1(U; \mathbb{C})$. Then T_f defined by

$$T_f \phi = \int_{\mathbb{R}^n} f(x) \phi(x) dx$$

is a regular distribution on \mathbb{R}^n , and we can identify T_f with f .

1.1.5 Pseudo-differential operator

In order to analyze the spectrum of the attenuated photoacoustic operator, we will make use of pseudo-differential operators and the corresponding results about their spectrum. The materials here follow Shubin's book [Shu87]. Pseudo-differential operators could be interpreted as a generalization of differential operators. Differential operators are local in the sense that one only needs the value of a function in a neighbourhood of a point to determine the effect of the operator. Pseudo-differential operators are pseudo-local, which means informally that when applied to a distribution they do not create a singularity at points where the distribution is already smooth. Let $D^\alpha = (-i\partial_1)^{\alpha_1} \cdots (-i\partial_n)^{\alpha_n}$, here $\alpha = (\alpha_1, \dots, \alpha_n)$ is a multi-index. Consider $x \in \mathbb{R}^n$. A pseudo-differential operator $P(x, D)$ on \mathbb{R}^n is an operator whose value on the function $u(x)$ is the function of x :

$$P(x, D)u(x) = \frac{1}{(2\pi)^n} \int_{\mathbb{R}^n} e^{ix \cdot \xi} a(x, \xi) \hat{u}(\xi) d\xi,$$

where $\hat{u}(\xi)$ is the Fourier transform of u and the symbol $a(x, \xi)$ in the integrand belongs to a certain symbol class. For instance, if $a(x, \xi)$ is an infinitely differentiable function on $\mathbb{R}^n \times \mathbb{R}^n$ with the property

$$|D_\xi^\alpha D_x^\beta a(x, \xi)| \leq C_{\alpha, \beta} (1 + |\xi|)^{m - |\alpha|}$$

for all $x, \xi \in \mathbb{R}^n$, all multi-indices α, β , some constants $C_{\alpha, \beta}$ and some real number m , then a belongs to the symbol class $S_{1,0}^m$ of Hörmander, and the corresponding operator $P(x, D)$ is called a pseudo-differential operator of order m and belongs to the class $\Psi_{1,0}^m$.

A pseudo-differential operator of order m is called *elliptic* if there exist positive constants R, C_1, C_2 such that its symbol satisfies

$$C_1 |\xi|^m \leq |a(x, \xi)| \leq C_2 |\xi|^m \text{ for all } |\xi| \geq R.$$

Let A be a self-adjoint elliptic differential operator of order $m > 0$ on a closed n -dimensional manifold M and $a_m(x, \xi)$ be the principle symbol of the operator A . Assume that $a_m(x, \xi) > 0$ when $\xi \neq 0$. Then the eigenvalues of A have the following asymptotic relation

$$\lambda_j \sim V(1)^{-m/n} j^{m/n}, \quad j \rightarrow +\infty,$$

for $V(t) = (2\pi)^{-n} \int_{a_m(x, \xi) < t} dx d\xi$.

1.1.6 Stationary phase method

There is a very useful analytical tool which allows us to find asymptotic expansions for integrals that can not, in many cases, be calculated in any other way. This tool is known as stationary phase method. The descriptions here mostly follow Section 7.7 of [Hö3].

The general objective of this method is to find an asymptotic expression as $\tau \rightarrow +\infty$ for integrals of the form

$$\int_{\mathbb{R}^n} e^{i\tau f(\omega)} g(\omega) d\omega.$$

where f, g are infinitely smooth complex-valued functions, and $\Im f \geq 0$. The exact behaviour of the integral depends on the presence of the points $\omega \in \mathbb{R}^n$ where $\nabla f = \Im f = 0$.

When no such points are present in \mathbb{R}^n , the integral decreases faster than $O(\tau^{-k})$ for any $k > 0$, as described in [Hö3, Theorem 7.7.1]. More precisely, let $f, g \in C^\infty(\mathbb{R}^n; \mathbb{C})$ with

- $\text{supp } g$ is compact,
- $\Im f(\omega) \geq 0$.
- $\nabla f(\omega)$ and $\Im f(\omega)$ could not be 0 at same frequency ω .

Then there exists a constant $C_1 > 0$ such that for all $l \in \mathbb{N}$ and all $\tau \geq 0$,

$$\begin{aligned} & \tau^l \left| \int_{\mathbb{R}^n} e^{i\tau f(\omega)} g(\omega) d\omega \right| \\ & \leq C_1 \sum_{\alpha=0}^l \sup_{\omega \in \mathbb{R}^n} |d^\alpha g(\omega)| (|\nabla f(\omega)|^2 + \Im f(\omega))^{\alpha/2-l}. \end{aligned} \quad (1.7)$$

On the other hand, when there are points where $\nabla f = \Im f = 0$, the main contributions to the integral come from these points. In other words, if we consider $f(\omega)$ as a phase function, then these points are exactly where the phase is real and stationary, hence the name "stationary phase method". The method also describes the contribution of such stationary points in the non-degenerate case. Under suitable substitutions, we can assume that the stationary point is $\omega = (0, 0, \dots, 0)$, and that the phase function $f(\omega)$ is equal to $\langle A\omega, \omega \rangle / 2$ where A is the Hessian matrix of f at the stationary point. More explicitly, as mentioned in [[Hö3], Theorem 7.7.3], let A be a symmetric non-degenerate matrix with

- $\Im A \geq 0$,
- $f(\omega) = \langle A\omega, \omega \rangle / 2$, so that $\nabla f(0) = \Im f(0) = 0$.
- $g \in C_0^\infty(\mathbb{R}^n; \mathbb{C})$.

Then for all $l \in \mathbb{N}$, we have

$$\begin{aligned} & \left| \int_{\mathbb{R}^n} e^{i\tau f(\omega)} g(\omega) d\omega - \left(\det \frac{\tau A}{2\pi i} \right)^{-1/2} T_l(\omega) \right| \\ & \leq C(\|A^{-1}\|/\tau)^{n/2+l} \sum_{|\alpha| \leq 2l+n/2+1} \|d^\alpha g\|_{L^2(\mathbb{R}^n)}, \end{aligned} \quad (1.8)$$

where $T_l(\omega)$ is a polynomial of ω^{-1} with degree $l-1$, and its coefficients are determined by derivatives of g at $\omega = (0, 0, \dots, 0)$ of order up to $2l-2$.

1.1.7 Reconstruction in photoacoustic tomography

Here we will address the procedures of actual reconstruction of the source term $h(x)$ from the data m measured by transducers. We assume here that the sound speed is constant and normalized to be equal to 1.

In constant speed case, there are different reconstruction methods, like explicit reconstruction formulas, Fourier expansion methods, filtered backprojection algorithms, series solutions for arbitrary geometries and time reversal methods, which we refer to the review papers [KK08; Kuc11]. It is well known that different analytic inversion formulas in photoacoustic tomography can behave differently in numerical implementation, for example, in terms of their stability. However, numerical implementation seems to show that the analytic (backprojection type) formulas work quite well, although some of them are not equivalent. Here we mainly consider the filtered backprojection type formulas for the inversion of high dimensional Radon transform in \mathbb{R}^n with $n \geq 1$.

To illustrate the method, we use the filtered backprojection formula of classical Radon transform in \mathbb{R}^2 as an example. For a function $h : \mathbb{R}^2 \rightarrow \mathbb{R}$, if the values of the integrals of h along lines are given, then the Radon Transform of h is given by

$$R[h](t, \theta) := \int_{L_{t, \theta}} h ds = \int_{s=-\infty}^{\infty} h \left(t \begin{pmatrix} \cos \theta \\ \sin \theta \end{pmatrix} + s \begin{pmatrix} -\sin \theta \\ \cos \theta \end{pmatrix} \right) ds,$$

where $t \in \mathbb{R}$ and $\theta \in [0, 2\pi)$ and

$$L_{t, \theta} = \left\{ \left(t \begin{pmatrix} \cos \theta \\ \sin \theta \end{pmatrix} + s \begin{pmatrix} -\sin \theta \\ \cos \theta \end{pmatrix} \right) : s \in \mathbb{R} \right\}.$$

Then $h(x_1, x_2)$ could be reconstructed from $R[h]$ by

$$h \begin{pmatrix} x_1 \\ x_2 \end{pmatrix} = \frac{1}{2} R^* (\mathcal{F}_{\omega \rightarrow t}^{-1} [|\omega| \mathcal{F}_{t \rightarrow \omega} [R[h]](\omega, \theta)]) \begin{pmatrix} x_1 \\ x_2 \end{pmatrix}.$$

where R^* is the adjoint operator of the Radon transform R , and \mathcal{F} denotes the one-dimensional Fourier transform. The term $|\omega|$ could be interpreted as a filtering of the data. There are different ways to choose the filter which we denote by E . Then the explicit reconstruction formula of h from its Radon transform data could be written as

$$h = R^* E (R[h]). \quad (1.9)$$

In classical PAT, the forward operator maps the initial pressure to the measurements is given by the *spherical mean operator*, which could be seen as a generalization of Radon transform to the families of spheres in \mathbb{R}^3 . Similar to above, there are also some filtered backprojection formulas in this case.

In non-attenuating media, the most typical type of filtered backprojection formula for reconstructing h is known as the universal (meaning applicable for a series of measurement geometries) backprojection algorithm. Such formulas are usually suitable for at least three imaging geometries: planar, spherical, and cylindrical surfaces. A widely-used formula of this type is due to Xu

& Wang in [XW05], which is given as follows:

$$h(x) = \frac{2}{\Omega_0} \int_{\xi \in \Gamma} \frac{m(|\xi - \mathbf{x}|, \xi) - |\xi - \mathbf{x}| \frac{\partial m}{\partial t}(|\xi - \mathbf{x}|, \xi)}{|\xi - \mathbf{x}|^2} \left(\mathbf{n}_\xi \cdot \frac{\xi - \mathbf{x}}{|\xi - \mathbf{x}|} \right) ds(\Gamma), \quad (1.10)$$

where Ω_0 is 2π for a planar geometry and 4π for cylindrical and spherical geometries, \mathbf{n}_ξ is the outer normal vector for the measurement geometry Γ .

In 2007, Burgholzer and his coworkers in [Bur+07b] gave a universal back projection formula in \mathbb{R}^2 based on Wang's formula in \mathbb{R}^3 :

$$h(x) = -\frac{4}{\Omega_0} \int_C \int_{|\xi - \mathbf{x}|}^{\infty} \left(\frac{(\partial_t(t^{-1}m))(t, \xi)}{\sqrt{t^2 - |\xi - \mathbf{x}|^2}} dt \right) \mathbf{n}_\xi \cdot (\xi - \mathbf{x}) dC, \quad (1.11)$$

where Ω_0 is 2π for a planar detection surface and 4π for a circular cylinder, \mathbf{n}_ξ is the outer normal vector for the surface Γ .

1.1.8 Optical coherence tomography

Optical coherence tomography (OCT) is a medical imaging technique that uses light waves to take micrometer-resolution, three-dimensional images from biological tissue. Optical coherence tomography is based on low-coherence interferometry, typically employing near-infrared light. The use of relatively long wavelength light allows it to penetrate into the scattering medium. It works by measuring the time delay and the intensity of backscattered or back reflected light coming from the biological tissue.

The research on OCT has been growing very fast for the last two decades. We refer the reader, for instance, to [EMS15; Hua+91; Fer96; Fer+03; Pod05; Sch99; TW05].

This imaging method has been continuously improved in terms of speed, resolution and sensitivity. It has also seen a variety of extensions aiming to assess functional aspects of the tissue in addition to morphology. One of these approaches is Doppler OCT (also called ODT), which aims at visualizing movements in the tissues (for example, blood flows). ODT is based on the identical optical design as OCT, but additional signal processing is used to extract information encoded in the carrier frequency of the interferogram. When Doppler OCT is used to observe cell-scale details of a tissue, the highly-scattering collagen usually dominates the signal, obscuring the intra-cellular details. A challenging problem is to remove the influence of the collagen in order to have a better imaging inside the cells. For extracting useful and meaningful information from the ODT Signal, there has been some studies, see [Ape+16; Lee+12; Joo+10; LSD09].

We mention here a few methods currently in use:

- Using the autocorrelation function to calculate the mean-squared displacement (MSD) and time-averaged displacement (TAD) of scattering structures. See, for example, [Joo+10; LSD09].
- Stochastic method. Similar to above, relating the autocorrelation function of the signal with some parameters concerning movement of particles. Here those parameters are estimated using a fitting algorithm, instead of being calculated directly. See [Lee+12].

- Standard deviation. Taking standard deviations of the signal to disregard the stationary part of the signal, and obtain information on the intensity of particle movement. See [\[Ape+16\]](#).

1.2 Contributions

The thesis is organized in a cumulative way, containing manuscripts and publications written in the last few years. The aim of this chapter is to introduce the most important ideas, concepts, and the contributions of the thesis.

1.2.1 Eigenvalue analysis of attenuated photoacoustic operator

In inverse problem, one of the fundamental issues is to analyze the ill-posedness, which could provide theoretical direction for solving the inverse problem. In general, there are two ways to analyze the ill-posedness, one is to do the stability analysis, and the other one is to study the eigenvalue asymptotic behavior of the forward operator. In a non-attenuating medium, the ill-posedness has been given, which is the the eigenvalue decay of the spherical mean operator, see [Pal10]. In attenuating media, we have proved that the eigenvalues decay differently according to the degree of attenuation in the medium.

We propose a general attenuation which contains all the known models, for example, power law[Sza94], Szabo[KS12], Nachman-Smith-Waag [NSW90], Thermo viscous[Kin+00, Chapter 8.2], and Kowar-Scherzer-Bonnefond model[KS11]. In this thesis, the propagation of the waves is described by the attenuated wave equation

$$\begin{aligned} \mathcal{A}_\kappa p(t, x) - \Delta p(t, x) &= \delta'(t)h(x), & t \in \mathbb{R}, x \in \mathbb{R}^3, \\ p(t, x) &= 0, & t < 0, x \in \mathbb{R}^3, \end{aligned} \quad (1.12)$$

where \mathcal{A}_κ is the pseudo-differential operator defined in frequency domain by:

$$\check{\mathcal{A}}_\kappa p(\omega, x) = -\kappa^2(\omega)\check{p}(\omega, x), \quad \omega \in \mathbb{R}, x \in \mathbb{R}^3, \quad (1.13)$$

for some attenuation coefficient $\kappa : \mathbb{R} \rightarrow \mathbb{C}$ which admits a solution of (1.12). Here \check{f} denotes the one-dimensional inverse Fourier transform of f with respect to time t . The *attenuated photoacoustic imaging* problem consists in estimating h from measurements m of p on $\partial\Omega$ over time.

Attenuation can be understood as the physical phenomenon that certain frequency components of acoustic waves are attenuated more rapidly over time. Mathematically this is encoded in the function κ defining the pseudo-differential operator \mathcal{A}_κ . A physically and mathematically meaningful κ has to satisfy the following properties (see [ESS16]):

Definition 1.2.1 We call a non-zero function $\kappa \in C^\infty(\mathbb{R}; \overline{\mathbb{H}})$, where $\mathbb{H} = \{z \in \mathbb{C} : \Im z > 0\}$ denotes the upper half complex plane and $\overline{\mathbb{H}}$ its closure in \mathbb{C} , an *attenuation coefficient* if

1. all the derivatives of κ are polynomially bounded.
2. There exists a holomorphic continuation $\tilde{\kappa} : \overline{\mathbb{H}} \rightarrow \overline{\mathbb{H}}$ of κ on the upper half plane.
3. $\kappa(-\omega) = -\overline{\kappa(\omega)}$ for all $\omega \in \mathbb{R}$.

4. There exists some constant $c > 0$ such that the holomorphic extension $\tilde{\kappa}$ of the attenuation coefficient κ satisfies

$$\Im(\tilde{\kappa}(z) - \frac{z}{c}) \geq 0 \quad \text{for every } z \in \overline{\mathbb{H}}.$$

The formal difference between (1.12) and the standard wave equation is that the second time derivative operator ∂_{tt} is replaced by a pseudo-differential operator \mathcal{A}_κ . The different known models manifest as different $\kappa(\omega)$. Let the sound speed c be 1, then

- Standard photoacoustic model: $\kappa(\omega) = \omega$.
- Power law model: $\kappa(\omega) = \omega + i\alpha(-i\omega)^\gamma$ for $\gamma \in (0, 1)$ and $\alpha > 0$.
- Modified Szabo model: $\kappa(\omega) = \sqrt{\omega^2 + 2\alpha_0 i\omega|\omega|^\gamma}$ for $\gamma \in (0, 1)$ and $\alpha_0 > 0$.
- Thermo viscous model: $\kappa(\omega) = \frac{\omega}{\sqrt{1 - i\tau\omega}}$ for $\tau > 0$.
- Kowar-Scherzer-Bonnefond model: $\kappa(\omega) = \omega \left(1 + \frac{\alpha}{\sqrt{1 + (-i\tau\omega)^\gamma}} \right)$ for $\gamma \in (0, 1)$, $\alpha > 0$ and $\tau > 0$.
- Nachman-Smith-Waag model: $\kappa(\omega) = \omega \sqrt{\frac{1 - i\tilde{\tau}\omega}{1 - i\tau\omega}}$ for $c_0 > 0$, $\tau > 0$ and $\tilde{\tau} \in (0, \tau)$.

According to the different asymptotic behaviors of $\kappa(\omega)$, the known models are grouped into two classes,

- Strong attenuation: The attenuation increases sufficiently fast as the frequency increases. For some constants $\kappa_0 > 0$, $\beta > 0$, $\omega_0 \geq 0$,

$$\Im \kappa(\omega) \geq \kappa_0 |\omega|^\beta \quad \text{for all } \omega \in \mathbb{R} \quad \text{with } |\omega| \geq \omega_0 \quad (1.14)$$

- Weak attenuation: The attenuation decreases sufficiently fast as the frequency increases. Let $\kappa(\omega) = \frac{\omega}{c} + i\kappa_\infty + \kappa_*(\omega)$, $\omega \in \mathbb{R}$, $\kappa_* \in C^\infty(\mathbb{R}) \cap L^2(\mathbb{R})$.

The relation between them could be seen clearly in Figure 1.2.

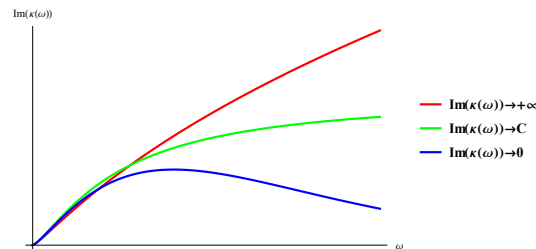


FIGURE 1.2: Classification of attenuation. Red curve corresponds to the strong attenuation, while green and blue curve corresponds to the weak attenuation.

Define the integrated photoacoustic operator $\check{\mathcal{P}}_\kappa : h \mapsto \int_{-\infty}^t p(\tau, \xi) d\tau$, which is given by

$$\check{\mathcal{P}}_\kappa : L^2(\Omega_\varepsilon) \rightarrow L^2(\mathbb{R} \times \partial\Omega), \quad \check{\mathcal{P}}_\kappa h(\omega, \xi) = \frac{1}{4\pi\sqrt{2\pi}} \int_{\Omega_\varepsilon} \frac{e^{i\kappa(\omega)|\xi-y|}}{|\xi-y|} h(y) dy. \quad (1.15)$$

Then, $\check{\mathcal{P}}_\kappa^* \check{\mathcal{P}}_\kappa$ is a self-adjoint operator with the kernel $F_\kappa(x, y)$ given by

$$F_\kappa(x, y) = \frac{1}{32\pi^3} \int_{-\infty}^{\infty} \int_{\partial\Omega} \frac{e^{i\kappa(\omega)|\xi-y| - i\overline{\kappa(\omega)}|\xi-x|}}{|\xi-y||\xi-x|} dS(\xi) d\omega. \quad (1.16)$$

Additionally it is natural to impose that the solution of attenuated wave equation propagates with finite speed. We say that the solution $p \in \mathcal{S}'(\mathbb{R} \times \mathbb{R}^3)$ of the (1.12) *propagates with finite speed* $c > 0$ if

$$\text{supp } p \subset \{(t, x) \in \mathbb{R} \times \mathbb{R}^3 \mid |x| \leq ct + R\}$$

whenever $\text{supp } h \subset B_R(0)$.

The aim is to get the eigenvalue decay of the operator $\check{\mathcal{P}}_\kappa^* \check{\mathcal{P}}_\kappa$. We have proved some basic results for the forward problem.

- The attenuated wave equation

$$\langle \mathcal{A}_\kappa p, \vartheta \rangle_{\mathcal{S}', \mathcal{S}} + \langle \Delta p, \vartheta \rangle_{\mathcal{S}', \mathcal{S}} = - \int_{\mathbb{R}^3} h(x) \partial_t \vartheta(0, x) dx, \quad \vartheta \in \mathcal{S}(\mathbb{R} \times \mathbb{R}^3), \quad (1.17)$$

where the Laplace operator $\Delta : \mathcal{S}'(\mathbb{R} \times \mathbb{R}^3) \rightarrow \mathcal{S}'(\mathbb{R} \times \mathbb{R}^3)$ is defined by

$$\langle \Delta u, \phi \otimes \psi \rangle_{\mathcal{S}', \mathcal{S}} = \langle u, \phi \otimes (\Delta \psi) \rangle_{\mathcal{S}', \mathcal{S}} \quad \text{for all } \phi \in \mathcal{S}(\mathbb{R}), \psi \in \mathcal{S}(\mathbb{R}^3),$$

has a unique solution $p \in \mathcal{S}'(\mathbb{R} \times \mathbb{R}^3)$ with $\text{supp } p \subset [0, \infty) \times \mathbb{R}^3$.

- Considering the causal initial condition, the attenuation wave equation (1.12) propagates with finite speed if and only if $\lim_{\omega \rightarrow \infty} \frac{\tilde{\kappa}(i\omega)}{i\omega} > 0$. The wave propagates with the speed $c = \lim_{\omega \rightarrow \infty} \frac{i\omega}{\tilde{\kappa}(i\omega)}$. The solution p of the attenuated wave equation (1.17) propagates with finite speed $c > 0$ if the holomorphic extension $\tilde{\kappa}$ of the attenuation coefficient κ fulfils

$$\Im(\tilde{\kappa}(z) - \frac{z}{c}) \geq 0 \quad \text{for every } z \in \overline{\mathbb{H}}.$$

Conversely, if there exists a sequence $(z_\ell)_{\ell=1}^\infty \subset \mathbb{H}$ with the properties that

- there exists a parameter $\eta_1 > 0$ such that $\Im(z_\ell) \geq \eta_1$ for all $\ell \in \mathbb{N}$,
- we have $|z_\ell| \rightarrow \infty$ for $\ell \rightarrow \infty$, and
- there exists a parameter $\delta > 0$ such that

$$\Im(\tilde{\kappa}(z_\ell) - \frac{z_\ell}{c}) \leq -\delta |z_\ell| \quad \text{for all } \ell \in \mathbb{N},$$

then p propagates faster than with speed c .

- The kernel $F_\kappa(x, y) \in L^2(\Omega_\varepsilon \times \Omega_\varepsilon)$, which deduces that the operator $\check{\mathcal{P}}_\kappa^* \check{\mathcal{P}}_\kappa : L^2(\Omega_\varepsilon) \rightarrow L^2(\Omega_\varepsilon)$ is a Hilbert-Schmidt operator and thus compact.

Strong attenuation medium

When the object is in a strong attenuation medium, the kernel $F_\kappa(x, y)$ is infinitely smooth. The challenge problem is that the known eigenvalue results are only for the integral operator with finite differentiable kernel. Furthermore, the known results could only get the polynomial eigenvalue decay at the most, as mentioned in [CH99].

One contribution in this thesis is that we give a criterion for a general integral operator with smooth kernel to have exponentially fast decaying eigenvalues through an upper bound on the derivatives of the kernel, see Appendix in Chapter 2.

To get this exponential decay, we give a upper bound for the higher order directional derivatives of the kernel $F_\kappa(x, y)$.

$$\frac{1}{j!} \sup_{x, y \in \Omega_\varepsilon} \sup_{v \in S^2} \left| \frac{\partial^j}{\partial s^j} \right|_{s=0} F_\kappa(x, y + sv) \leq C j^{C(\frac{N}{\beta}-1)j} \quad \text{for all } j \in \mathbb{N}_0, \quad (1.18)$$

for $\beta \in (0, N]$.

Finally, we proved the eigenvalues $(\lambda_n(\check{\mathcal{P}}_\kappa^* \check{\mathcal{P}}_\kappa))_{n \in \mathbb{N}}$ of $\check{\mathcal{P}}_\kappa^* \check{\mathcal{P}}_\kappa$ in decreasing order fulfil

$$\lambda_n(\check{\mathcal{P}}_\kappa^* \check{\mathcal{P}}_\kappa) \leq C n \sqrt[3]{n} \exp\left(-cn^{\frac{\beta}{3N}}\right) \quad \text{for all } n \in \mathbb{N}. \quad (1.19)$$

In inverse problem, this exponential eigenvalue decay of the forward operator indicates that the corresponding inverse problem is severely ill-posed.

Weak attenuation medium

When the object is in a weak attenuation medium, the kernel $F_\kappa(x, y)$ has weak singularity with order 1. However, according to the results mentioned in the background section, when the order of singularity of the kernel is between 0 and $n/2$ where n is the dimension of space, we only know that the corresponding operator has square-summable eigenvalues, but this will not help us to find the asymptotic behavior of eigenvalues. Even when the order of singularity changes, the known results could only provide the upper bound of eigenvalue decay, while we also need a lower bound of eigenvalue decay. In Shubin's book [Shu87], he gave a theorem for both the upper and lower bounds of the eigenvalue decay of a pseudo-differential operator. This is the only tool we could use, but the obstacle is that the upper bounds of every order's derivatives of the kernel is needed for proving that the attenuated photoacoustic operator is a pseudo-differential operator.

To get around this obstacle, we divide the attenuated photoacoustic operator into the sum of two operators, one is the standard photoacoustic operator, another one is a perturbation caused by the attenuation. One contribution in the thesis is that for a standard photoacoustic operator we proved it is an elliptic pseudo-differential operator of order -2 by using the stationary phase method to find the asymptotic expansion of its symbol.

Another contribution is that we proved that the eigenvalue of the perturbation operator decays faster than the standard photoacoustic operator using Mercer's theorem.

Finally, we proved the eigenvalues $(\lambda_n(\check{\mathcal{P}}_\kappa^* \check{\mathcal{P}}_\kappa))_{n \in \mathbb{N}}$ of $\check{\mathcal{P}}_\kappa^* \check{\mathcal{P}}_\kappa$ in decreasing order fulfil

$$C_1 n^{-\frac{2}{3}} \leq \lambda_n(\check{\mathcal{P}}_\kappa^* \check{\mathcal{P}}_\kappa) \leq C_2 n^{-\frac{2}{3}} \quad \text{for all } n \in \mathbb{N}, \quad (1.20)$$

for some constants $C_1, C_2 > 0$.

This polynomial eigenvalue decay of the forward operator indicates that the corresponding inverse problem is mildly ill-posed.

1.2.2 Reconstruction formulas

In the standard photoacoustic imaging, there are some reconstruction formulas, for example, in [And88; XFW02; HSZ09], either in frequency domain or in time domain for planar measurement geometry or closed measurement geometry.

Practically, if people consider attenuation in the medium, in the literatures only time reversal has been used, like [AK07; Kun07]. In Chapter 3 we give explicit reconstruction formulas for initial pressure h in the attenuating media from the measurement p^a on a universal geometry in \mathbb{R}^d with $d = 2, 3$. Let q^a be defined as $q^a(t, \xi) = \int_{-\infty}^t p^a(\tau, \xi) d\tau$, and \mathcal{W} be the operator which maps h to p , where p is the ideal data in non-attenuating media.

- No attenuation:

$$h(\mathbf{x}) = \mathcal{W}^{-1} [p^a],$$

where $\mathcal{W}^{-1} [\cdot]$ is the universal back-projection operator.

- Constant attenuation: $\kappa(\omega) = \omega + \kappa_\infty i$,

$$h(\mathbf{x}) = \mathcal{W}^{-1} \left[\frac{\partial}{\partial t} e^{-\kappa_\infty t} q^a(t, \xi) \right].$$

- General weak attenuation:

$$h(\mathbf{x}) = \mathcal{W}^{-1} \left[\frac{\partial}{\partial t} (I + T)^{-1} e^{-\kappa_\infty t} q^a(t, \xi) \right],$$

where T is an integral operator with the kernel $\mathcal{F} [e^{i\kappa_*(\omega)\tau} - 1] (t - \tau)$.

Properties of operator T :

- T is only related to $\kappa(\omega)$.
- T is not related to the dimension of space.
- T is not related to the shape of measurement geometry.

1.2.3 Dynamic optical coherence tomography

Since the cell membrane and the collagen dominate the signal in the imaging of optical coherence tomography, the aim is to get the information of the metabolic activity inside cells. The first problem is to relate the movements of different particles from collagen and metabolic activity and their signal. Based on a single particle model, we build a new multi-particle model. Another contribution is that we gave a theoretical basis for applying the singular value decomposition algorithm on the total optical coherence tomography signal, then the numerical experiments validated this algorithm.

By dividing the particles into collagen particles and the particles from metabolic activities, then the total OCT signal from one pixel contains the signal from these two parts Γ^c and Γ^m . Each part is sum of the signal from single particles in a domain determined by this pixel and the coherence length. For $j \in \{c, m\}$, the corresponding signal could be written by

$$\Gamma_{ODT}^j(x, t) = \int_{-\infty}^{\infty} \int_{-L}^L S_0(\omega) K_j(x, \omega) p_j(x, z, t) e^{2\pi\omega i(\frac{2\bar{n}}{c}z)} d\omega dz, \quad (1.21)$$

where p_j is the density function, S_0, K_j, \bar{n} are coefficients (see details in [Chapter 4](#)),

We construct four operators $S_c S_c^*, S_m S_c^*, S_c S_m^*, S_m S_m^*$ using the signal $\Gamma_{ODT}^c, \Gamma_{ODT}^m$ as the corresponding kernel. Through the new multi-particle model, the kernel of the operator $\Gamma^c \Gamma^c$ is variable separation form, which deduces that $\Gamma^c \Gamma^c$ only has one singular value. Physically, the collagen signal is much larger than the signal from metabolic activities. This helps to prove that the singular value of collagen operator is much larger than the other singular values. Then the singular values have the following relation.

- $\lambda(S_c S_c^*) \gg \lambda_i(S_m S_m^*)$ for any i .
- $\lambda_1(S_m S_m^*) \geq \lambda_i(S_m S_m^*)$ for $i > 1$.
- $\lambda_i(S_c S_m^*) \leq \sqrt{\lambda(S_c S_c^*) \lambda_1(S_m S_m^*)}$ for any i .

Therefore, if we apply the singular value decomposition on the total signal and remove the bigger singular values, the remaining part corresponds to the signal from the metabolic activities.

1.3 Outline

The thesis consists of 4 chapters, essentially divided into 3 parts.

Part 1 gives the introduction to the field of photoacoustic imaging with considering attenuation, including a short summary of some mathematical methods that are fundamental in this work. Moreover, it aims to give an overview about the main contributions included in this thesis.

Part 2 deals with the photoacoustic tomography with considering attenuation. It consists of Chapters 2 and 3.

Chapter 2 addresses the uniqueness and existence of the solution in the attenuated wave equation, and the eigenvalue results for the attenuated photoacoustic operator. In strong attenuating media, the eigenvalue decays exponentially, while in the weak attenuating media, the eigenvalue decays polynomially.

Chapter 3 is devoted to the explicit reconstruction formulas for the source term in \mathbb{R}^2 and \mathbb{R}^3 , which are based on the universal back-projection formula.

Part 3 deals with the dynamic optical coherence tomography. It consists of Chapter 4.

Chapter 4 aims to present signal from the metabolic activity inside the cells. A dynamic multi-particle model is given for the signals from both metabolic activity and the collagen. Then an algorithm based on singular valued decomposition (SVD) is provided. At the end we present some numerical experiments to verify the algorithm.

Finally in Chapter 5 we sum up the thesis in discussion and outlook, where we also discuss some open questions related to the subject matter.

In the Appendix, a German version of the thesis's abstract can be found, as well as a CV including the author's publications and conference talks (CV is not attached in the formal submission).

All the chapters of the thesis are self-contained and can be read independently. Thesis mainly contains the results presented in the following papers.

- Singular values of the attenuated photoacoustic imaging operators, which is a joint work with Otmar Scherzer and Peter Elbau. It is accepted for publication by the journal of differential equations.
- Reconstruction formulas for Photoacoustic Imaging in Attenuating Media, which is a joint work with Otmar Scherzer. It has been submitted and is currently under review.
- A signal separation technique for sub-cellular imaging using dynamic optical coherence tomography, which is a joint work with Habib Ammari and Francisco Romero, and it is accepted for publication by the journal SIAM Multiscale Modelling Simulation.

All the articles are submitted with alphabetically ordered authors.

References

- [AK07] M. Agranovsky and P. Kuchment. “Uniqueness of reconstruction and an inversion procedure for thermoacoustic and photoacoustic tomography with variable sound speed”. *Inverse Probl.* 23.5 (2007), pp. 2089–2102.
- [Amm+13] Habib Ammari, Elie Bretin, Josselin Garnier, and Abdul Wahab. “Time-reversal algorithms in viscoelastic media”. *European J. Appl. Math.* 24.04 (2013), pp. 565–600.
- [And88] L. E. Andersson. “On the determination of a function from spherical averages”. *SIAM J. Math. Anal.* 19.1 (1988), pp. 214–232.
- [Ape+16] C. Apelian, F. Harms, O. Thouvenin, and A. C. Boccara. “Dynamic full field optical coherence tomography: subcellular metabolic contrast revealed in tissues by temporal analysis of interferometric signals”. *Biomed. Opt. Express* 24.7 (2016), pp. 1511–1524.
- [Bur+07b] P. Burgholzer, J. Bauer-Marschallinger, H. Grün, M. Haltmeier, and G. Paltauf. “Temporal back-projection algorithms for photoacoustic tomography with integrating line detectors”. *Inverse Probl.* 23.6 (2007), S65.
- [CH99] C.-H. Chang and C.-W. Ha. “On eigenvalues of differentiable positive definite kernels”. *Integr. Equ. Oper. Theory* 33.1 (1999), pp. 1–7.
- [CJK91] F. Cobos, S. Janson, and T. Kühn. “On the optimal asymptotic eigenvalue behaviour of weakly singular integral operators”. *Proc. Amer. Math. Soc.* 113.4 (1991), pp. 1017–1022.
- [CT10] B. T. Cox and B. E. Treeby. “Artifact trapping during time reversal photoacoustic imaging for acoustically heterogeneous media”. *IEEE Trans. Med. Imag.* 29.2 (2010), pp. 387–396.
- [EHN96] H. W. Engl, M. Hanke, and A. Neubauer. “Regularization of inverse problems”. *Mathematics and its Applications* 375. Dordrecht: Kluwer Academic Publishers Group, 1996. viii+321.
- [EMS15] P. Elbau, L. Mindrinos, and O. Scherzer. “Mathematical Methods of Optical Coherence Tomography”. In: *Handbook of Mathematical Methods in Imaging*. Ed. by O. Scherzer. Springer New York, 2015, pp. 1169–1204.
- [ESS16] P. Elbau, O. Scherzer, and C. Shi. “Singular Values of the Attenuated Photoacoustic Imaging Operator”. Preprint on ArXiv arXiv:1611.05807. University of Vienna, Austria, 2016.
- [Fer+03] A. F. Fercher, W. Drexler, C. K. Hitzenberger, and T. Lasser. “Optical coherence tomography - principles and applications”. *Rep. Prog. Phys.* 66.2 (2003), pp. 239–303.
- [Fer96] A. F. Fercher. “Optical coherence tomography”. *J. Biomed. Opt.* 1.2 (1996), pp. 157–173.

- [Hö3] L. Hörmander. “The Analysis of Linear Partial Differential Operators I”. 2nd ed. New York: Springer Verlag, 2003.
- [HSZ09] M. Haltmeier, O. Scherzer, and G. Zangerl. “A reconstruction algorithm for photoacoustic imaging based on the nonuniform FFT”. *IEEE Trans. Med. Imag.* 28.11 (2009), pp. 1727–1735.
- [Hua+91] D. Huang, E. A. Swanson, C. P. Lin, J. S. Schuman, G. Stinson, W. Chang, M. R. Hee, T. Flotte, K. Gregory, C. A. Puliafito, and J. G. Fujimoto. “Optical coherence tomography”. *Science* 254.5035 (1991), pp. 1178–1181.
- [Joo+10] C. Joo, C. L. Evans, T. Stepinac, T. Hasan, and J. F. de Boer. “Diffusive and directional intracellular dynamics measured by field-based dynamic light scattering”. *Opt. Express* 18.3 (2010), pp. 2858–2871.
- [Kin+00] L. E. Kinsler, A. R. Frey, A. B. Coppens, and J. V. Sanders. “Fundamentals of Acoustics”. 4th ed. New York: Wiley, 2000.
- [KK08] P. Kuchment and L. Kunyansky. “Mathematics of thermoacoustic tomography”. *European J. Appl. Math.* 19 (2008), pp. 191–224.
- [Kos74] G. P. Kostometov. “Asymptotic behavior of the spectrum of integral operators with a singularity on the diagonal”. *Math. USSR-Sb.* 23.3 (1974), pp. 417–424.
- [Kow14] R. Kowar. “On time reversal in photoacoustic tomography for tissue similar to water”. *SIAM J. Imaging Sciences* 7.1 (2014), pp. 509–527.
- [KS12] R. Kowar and O. Scherzer. “Attenuation Models in Photoacoustics”. In: *Mathematical Modeling in Biomedical Imaging II: Optical, Ultrasound, and Opto-Acoustic Tomographies*. Ed. by H. Ammari. Vol. 2035. Lecture Notes in Mathematics. Berlin Heidelberg: Springer Verlag, 2012, pp. 85–130.
- [KSB11] R. Kowar, O. Scherzer, and X. Bonnefond. “Causality analysis of frequency-dependent wave attenuation”. *Math. Methods Appl. Sci.* 34 (1 2011), pp. 108–124.
- [Kuc11] P. Kuchment. “Mathematics of hybrid imaging. A brief review”. Preprint. Texas A&M University, 2011.
- [Kun07] L. A. Kunyansky. “Explicit inversion formulae for the spherical mean Radon transform”. *Inverse Probl.* 23.1 (2007), pp. 373–383.
- [Kön80] H. König. “Some remarks on weakly singular integral operators”. *Integr. Equ. Oper. Theory* 3.3 (1980), pp. 397–407.
- [Lee+12] J. Lee, W. Wu, J. Y. Jiang, B. Zhu, and D. A. Boas. “Dynamic light scattering optical coherence tomography”. *Opt. Express* 20.20 (2012), pp. 22262–22277.
- [LSD09] Y. Li, J. Schnekenburger, and M. H. Duits. “Intracellular particle tracking as a tool for tumor cell characterization”. *J. Biomed. Opt.* 14.6 (2009), p. 064005.

- [NSW90] A. I. Nachman, J. F. Smith III, and R. C. Waag. “An equation for acoustic propagation in inhomogeneous media with relaxation losses”. *J. Acoust. Soc. Amer.* 88.3 (1990), pp. 1584–1595.
- [Pal10] V. P. Palamodov. “Remarks on the general Funk transform and thermoacoustic tomography”. *Inverse Probl. Imaging* 4.4 (2010), pp. 693–702.
- [Pod05] A. G. Podoleanu. “Optical coherence tomography”. *Brit. J. Radiology* 78 (2005), pp. 976–988.
- [Sch99] J. M. Schmitt. “Optical coherence tomography (OCT): A review”. *IEEE J. Quantum Electron.* 5 (1999), pp. 1205–1215.
- [Shu87] M. A. Shubin. “Pseudodifferential operators and spectral theory”. Trans. by S. I. Andersson. Vol. 200. Springer, 1987.
- [Sza94] T.L. Szabo. “Time domain wave equations for lossy media obeying a frequency power law”. *J. Acoust. Soc. Amer.* 96 (1994), pp. 491–500.
- [TW05] P. H. Tomlins and R. K. Wang. “Theory, developments and applications of optical coherence tomography”. *J. Phys. D: Appl. Phys.* 38 (2005), pp. 2519–2535.
- [TZC10] B. E. Treeby, E. Z. Zhang, and B. T. Cox. “Photoacoustic tomography in absorbing acoustic media using time reversal”. *Inverse Probl.* 26.11 (2010), p. 115003.
- [Wan09] L. V. Wang, ed. “Photoacoustic Imaging and Spectroscopy”. Optical Science and Engineering. Boca Raton: CRC Press, 2009. xii+499.
- [XFW02] Y. Xu, D. Feng, and L. V. Wang. “Exact Frequency-Domain Reconstruction for Thermoacoustic Tomography — I: Planar Geometry”. *IEEE Trans. Med. Imag.* 21.7 (2002), pp. 823–828.
- [XW05] M. Xu and L. V. Wang. “Universal back-projection algorithm for photoacoustic computed tomography”. *Phys. Rev. E* 71.1, 016706 (2005).

Singular Values of the Attenuated Photoacoustic Imaging Operator

Peter Elbau¹
peter.elbau@univie.ac.at

Otmar Scherzer^{1,2}
otmar.scherzer@univie.ac.at

Cong Shi¹
cong.shi@univie.ac.at

¹Computational Science Center
 University of Vienna
 Oskar-Morgenstern-Platz 1
 A-1090 Vienna, Austria

²Johann Radon Institute for Computational
 and Applied Mathematics (RICAM)
 Altenbergerstraße 69
 A-4040 Linz, Austria

Abstract

We analyse the ill-posedness of the photoacoustic imaging problem in the case of an attenuating medium. To this end, we introduce an attenuated photoacoustic operator and determine the asymptotic behaviour of its singular values. Dividing the known attenuation models into strong and weak attenuation classes, we show that for strong attenuation, the singular values of the attenuated photoacoustic operator decay exponentially, and in the weak attenuation case the singular values of the attenuated photoacoustic operator decay with the same rate as the singular values of the non-attenuated photoacoustic operator.

2.1 Introduction

In standard photoacoustic imaging, see e.g. [Wan09], it is assumed that the medium is *non-attenuating*, and the imaging problem consists in visualising the spatially, compactly supported *absorption density function* $h : \mathbb{R}^3 \rightarrow \mathbb{R}$, appearing as a source term in the wave equation

$$\begin{aligned} \partial_{tt}p(t, x) - \Delta p(t, x) &= \delta'(t)h(x), & t \in \mathbb{R}, x \in \mathbb{R}^3, \\ p(t, x) &= 0, & t < 0, x \in \mathbb{R}^3, \end{aligned} \tag{2.1}$$

from measurements $m(t, x)$ of the pressure p for $(t, x) \in (0, \infty) \times \partial\Omega$, where $\partial\Omega$ is the boundary of a compact, convex set Ω containing the support of h .

In this paper, we consider photoacoustic imaging in attenuating media, where the propagation of the waves is described by the attenuated wave equation

$$\begin{aligned} \mathcal{A}_\kappa p(t, x) - \Delta p(t, x) &= \delta'(t)h(x), & t \in \mathbb{R}, x \in \mathbb{R}^3, \\ p(t, x) &= 0, & t < 0, x \in \mathbb{R}^3, \end{aligned} \quad (2.2)$$

where \mathcal{A}_κ is the pseudo-differential operator defined in frequency domain by:

$$\check{\mathcal{A}}_\kappa p(\omega, x) = -\kappa^2(\omega)\check{p}(\omega, x), \quad \omega \in \mathbb{R}, x \in \mathbb{R}^3, \quad (2.3)$$

for some attenuation coefficient $\kappa : \mathbb{R} \rightarrow \mathbb{C}$ which admits a solution of (2.2). Here \check{f} denotes the one-dimensional inverse Fourier transform of f with respect to time t , that is, for $f \in L^1(\mathbb{R})$:

$$\check{f}(\omega) = \frac{1}{\sqrt{2\pi}} \int_{-\infty}^{\infty} f(t) e^{i\omega t} dt.$$

The *attenuated photoacoustic imaging* problem consists in estimating h from measurements m of p on $\partial\Omega$ over time. The formal difference between (2.2) and (2.1) is that the second time derivative operator ∂_{tt} is replaced by a pseudo-differential operator \mathcal{A}_κ . We emphasise that standard photoacoustic imaging corresponds to $\kappa^2(\omega) = \omega^2$.

We review below, see (2.18), that in frequency domain the solution of (2.2) is given by

$$\check{p}(\omega; x) = - \int_{\mathbb{R}^3} \frac{i\omega}{4\pi\sqrt{2\pi}} \frac{e^{i\kappa(\omega)|x-y|}}{|x-y|} h(y) dy.$$

We associate with this solution the *time-integrated* photoacoustic operator in frequency domain:

$$\check{\mathcal{P}}_\kappa h(\omega, x) = \frac{1}{4\pi\sqrt{2\pi}} \int_{\mathbb{R}^3} \frac{e^{i\kappa(\omega)|x-y|}}{|x-y|} h(y) dy.$$

One goal of this paper is to characterise the degree of ill-posedness of the problem of inverting the time-integrated photoacoustic operator by estimating the decay rate of its singular values. We mention however, that although the attenuated photoacoustic operator, giving the solution \check{p} , is related to the integrated photoacoustic operator by just time-differentiation, the singular values and functions of the photoacoustic operator have not been characterized so far.

In this paper, we are identifying two classes of attenuation models (classes of functions κ), which correspond to *weakly* and *strongly* attenuating media. We prove that for weakly attenuating media the singular values $((\lambda_n(\check{\mathcal{P}}_\kappa^* \check{\mathcal{P}}_\kappa))^{\frac{1}{2}})_{n=1}^\infty$ decay equivalently to $n^{-\frac{1}{3}}$, as in the standard photoacoustic imaging case, where this result has been proven in [Pal10]. For the strongly attenuating models, the singular values are decaying exponentially, which is proven by using that in this case the operator $\check{\mathcal{P}}_\kappa^* \check{\mathcal{P}}_\kappa$ is an integral operator with smooth kernel.

2.2 The Attenuated Wave Equation

To model the wave propagation in an attenuated medium, we imitate the wave equation for the electric field $E : \mathbb{R} \times \mathbb{R}^3 \rightarrow \mathbb{R}^3$ in an isotropic linear dielectric medium described by the electric susceptibility $\chi : \mathbb{R} \rightarrow \mathbb{R}$ (extended by $\chi(t) = 0$ for $t < 0$ to negative times):

$$\frac{1}{c^2} \partial_{tt} E(t, x) + \frac{1}{c^2} \int_0^\infty \frac{\chi(\tau)}{\sqrt{2\pi}} \partial_{tt} E(t - \tau, x) d\tau - \Delta E(t, x) = 0,$$

or written in terms of the inverse Fourier transforms \check{E} and $\check{\chi}$ with respect to the time:

$$-\frac{\omega^2}{c^2} (1 + \check{\chi}(\omega)) \check{E}(\omega, x) - \Delta \check{E}(\omega, x) = 0. \quad (2.4)$$

Analogously, we want to incorporate attenuation by replacing the second time derivatives in our equation (2.1) by a pseudo-differential operator \mathcal{A}_κ of the form (2.3) for some function $\kappa : \mathbb{R} \rightarrow \mathbb{C}$ (corresponding to $\frac{\omega}{c} \sqrt{1 + \check{\chi}(\omega)}$ in the electrodynamic model).

We will interpret the equation (2.2) as an equation in the space of tempered distributions $\mathcal{S}'(\mathbb{R} \times \mathbb{R}^3)$ so that the Fourier transform and the δ -distribution are both well-defined. To make sense of \mathcal{A}_κ as an operator on $\mathcal{S}'(\mathbb{R} \times \mathbb{R}^3)$ and to be able to find a solution of (2.2), we impose the following conditions on the function κ .

Definition 2.2.1 We call a non-zero function $\kappa \in C^\infty(\mathbb{R}; \overline{\mathbb{H}})$, where $\mathbb{H} = \{z \in \mathbb{C} \mid \Im z > 0\}$ denotes the upper half complex plane and $\overline{\mathbb{H}}$ its closure in \mathbb{C} , an *attenuation coefficient* if

1. all the derivatives of κ are polynomially bounded. That is, for every $\ell \in \mathbb{N}_0$ there exist constants $\kappa_1 > 0$ and $N \in \mathbb{N}$ such that

$$|\kappa^{(\ell)}(\omega)| \leq \kappa_1 (1 + |\omega|)^N, \quad (2.5)$$

2. there exists a holomorphic continuation $\tilde{\kappa} : \overline{\mathbb{H}} \rightarrow \overline{\mathbb{H}}$ of κ on the upper half plane, that is, $\tilde{\kappa} \in C(\overline{\mathbb{H}}; \overline{\mathbb{H}})$ with $\tilde{\kappa}|_{\mathbb{R}} = \kappa$ and $\tilde{\kappa} : \mathbb{H} \rightarrow \overline{\mathbb{H}}$ is holomorphic; with

$$|\tilde{\kappa}(z)| \leq \tilde{\kappa}_1 (1 + |z|)^{\tilde{N}} \quad \text{for all } z \in \overline{\mathbb{H}}$$

for some constants $\tilde{\kappa}_1 > 0$ and $\tilde{N} \in \mathbb{N}$.

3. we have the symmetry $\kappa(-\omega) = -\overline{\kappa(\omega)}$ for all $\omega \in \mathbb{R}$.

The condition 1 in Definition 2.2.1 ensures that the product $\kappa^2 u$ of κ^2 with an arbitrary tempered distribution $u \in \mathcal{S}'(\mathbb{R})$ is again in $\mathcal{S}'(\mathbb{R})$ and therefore, the operator \mathcal{A}_κ is well-defined.

Definition 2.2.2 Let $\kappa \in C^\infty(\mathbb{R})$ be an attenuation coefficient. Then, we define the *attenuation operator* $\mathcal{A}_\kappa : \mathcal{S}'(\mathbb{R} \times \mathbb{R}^3) \rightarrow \mathcal{S}'(\mathbb{R} \times \mathbb{R}^3)$ by its action on the tensor products $\phi \otimes \psi \in \mathcal{S}(\mathbb{R} \times \mathbb{R}^3)$, given by $(\phi \otimes \psi)(\omega, x) = \phi(\omega)\psi(x)$:

$$\langle \mathcal{A}_\kappa u, \phi \otimes \psi \rangle_{\mathcal{S}', \mathcal{S}} = - \left\langle u, (\mathcal{F}^{-1} \kappa^2 \mathcal{F} \phi) \otimes \psi \right\rangle_{\mathcal{S}', \mathcal{S}}, \quad (2.6)$$

where $\mathcal{F} : \mathcal{S}(\mathbb{R}) \rightarrow \mathcal{S}(\mathbb{R})$, $\mathcal{F}\phi(\omega) = \frac{1}{\sqrt{2\pi}} \int_{-\infty}^\infty \phi(t) e^{-i\omega t} dt$ denotes the Fourier transform. This uniquely defines the operator \mathcal{A}_κ , see for example [Tar07, Lemma 6.2].

Remark: We use \mathcal{F} when we are talking of the Fourier transform as an operator and use in the calculations $\hat{\phi} = \mathcal{F}\phi$ and $\check{\phi} = \mathcal{F}^{-1}\phi$. We will use the notation \mathcal{F} also for the Fourier transform on different spaces (in particular for the three-dimensional Fourier transform on $\mathcal{S}(\mathbb{R}^3)$).

The condition 2 in Definition 2.2.1 is motivated by the fact that the function $\check{\chi}$ in the electrodynamic model (2.4) is the inverse Fourier transform of a function whose support is inside $[0, \infty)$ and can therefore be holomorphically extended to the upper half plane. We will see later, see Proposition 2.2.6, that this condition guarantees that the attenuated wave equation (2.2) has a causal solution in $\mathcal{S}'(\mathbb{R} \times \mathbb{R}^3)$, that is a solution whose support is contained in $[0, \infty) \times \mathbb{R}^3$.

Finally, the condition 3 in Definition 2.2.1 is required so that the attenuation operator \mathcal{A}_κ maps real-valued distributions to real-valued distributions: To see this, let $u \in \mathcal{S}'(\mathbb{R} \times \mathbb{R}^3)$ be a real-valued distribution. Then, for two real-valued functions $\phi \in \mathcal{S}(\mathbb{R})$ and $\psi \in \mathcal{S}(\mathbb{R}^3)$, the relation (2.6) implies

$$\overline{\langle \mathcal{A}_\kappa u, \phi \otimes \psi \rangle_{\mathcal{S}', \mathcal{S}}} = - \left\langle u, \overline{\mathcal{F}^{-1} \kappa^2 \mathcal{F} \phi} \otimes \psi \right\rangle_{\mathcal{S}', \mathcal{S}}.$$

By substituting the variable ω by $-\omega$ in the Fourier integral below, we get that

$$\overline{(\mathcal{F}^{-1} \kappa^2 \mathcal{F} \phi)(t)} = \frac{1}{2\pi} \int_{-\infty}^{\infty} e^{-i\omega t} \overline{\kappa^2(\omega)} \int_{-\infty}^{\infty} e^{i\omega \tau} \phi(\tau) d\tau d\omega = (\mathcal{F}^{-1} \kappa_r^2 \mathcal{F} \phi)(t)$$

with κ_r given by $\kappa_r(\omega) = \overline{\kappa(-\omega)}$. Thus, the condition $\overline{\langle \mathcal{A}_\kappa u, \phi \otimes \psi \rangle_{\mathcal{S}', \mathcal{S}}} = \langle \mathcal{A}_\kappa u, \phi \otimes \psi \rangle_{\mathcal{S}', \mathcal{S}}$ is equivalent to $\kappa^2 = \kappa_r^2$. Besides the case of a constant, real function κ (something we are not interested in), this is equivalent to $\kappa = -\kappa_r$ because of the condition $\Im \tilde{\kappa}(z) \geq 0$ for all $z \in \overline{\mathbb{H}}$.

2.2.1 Solution of the Attenuated Wave Equation

In this section, we want to determine the solution $p \in \mathcal{S}'(\mathbb{R} \times \mathbb{R}^3)$ of (2.2). To this end, we do a Fourier transform of the wave equation and end up with a Helmholtz equation for each value $\omega \in \mathbb{R}$, which in the case $\Im \kappa(\omega) > 0$ has a unique solution in the space of tempered distributions.

Lemma 2.2.3 *Let κ be a complex number with positive imaginary part, that is $\kappa \in \mathbb{H}$, $f \in L^2(\mathbb{R}^3)$ with compact essential support. Then, the Helmholtz equation*

$$\kappa^2 \langle u, \phi \rangle_{\mathcal{S}', \mathcal{S}} + \langle u, \Delta \phi \rangle_{\mathcal{S}', \mathcal{S}} = \int_{\mathbb{R}^3} f(x) \phi(x) dx, \quad \phi \in \mathcal{S}(\mathbb{R}^3),$$

has a unique solution $u \in \mathcal{S}'(\mathbb{R}^3)$, which is explicitly given by

$$\langle u, \phi \rangle_{\mathcal{S}', \mathcal{S}} = -\frac{1}{4\pi} \int_{\mathbb{R}^3} \int_{\mathbb{R}^3} \frac{e^{i\kappa|x-y|}}{|x-y|} f(y) dy \phi(x) dx, \quad \phi \in \mathcal{S}(\mathbb{R}^3). \quad (2.7)$$

Proof: Writing $\phi = \mathcal{F}^{-1} \hat{\phi}$, where $\mathcal{F} : \mathcal{S}(\mathbb{R}^3) \rightarrow \mathcal{S}(\mathbb{R}^3)$ denotes the three-dimensional Fourier transform, we find with the function $\psi \in \mathcal{S}(\mathbb{R}^3)$ defined by $\psi = \kappa^2 \phi + \Delta \phi$, and therefore

$\hat{\psi}(k) = \mathcal{F}\psi(k) = (\kappa^2 - |k|^2)\hat{\phi}(k)$, that

$$\langle u, \psi \rangle_{\mathcal{S}', \mathcal{S}} = \int_{\mathbb{R}^3} f(x) \phi(x) dx = \frac{1}{(2\pi)^{\frac{3}{2}}} \int_{\mathbb{R}^3} f(x) \int_{\mathbb{R}^3} \frac{\hat{\psi}(k)}{\kappa^2 - |k|^2} e^{i\langle k, x \rangle} dk dx. \quad (2.8)$$

The inner integral is the inverse Fourier transform of a product and can thus be written as the convolution of two inverse Fourier transforms:

$$\frac{1}{(2\pi)^{\frac{3}{2}}} \int_{\mathbb{R}^3} \frac{\hat{\psi}(k)}{\kappa^2 - |k|^2} e^{i\langle k, x \rangle} dk = \frac{1}{(2\pi)^3} \int_{\mathbb{R}^3} \psi(x - y) \int_{\mathbb{R}^3} \frac{e^{i\langle k, y \rangle}}{\kappa^2 - |k|^2} dk dy. \quad (2.9)$$

Using spherical coordinates, we obtain by substituting $\rho = |k|$ and $\cos \theta = \frac{\langle k, y \rangle}{|k||y|}$ that

$$\begin{aligned} \int_{\mathbb{R}^3} \frac{e^{i\langle k, y \rangle}}{\kappa^2 - |k|^2} dk &= 2\pi \int_0^\infty \int_0^\pi \frac{e^{i\rho|y|\cos\theta}}{\kappa^2 - \rho^2} \rho^2 \sin\theta d\theta d\rho \\ &= \frac{4\pi}{|y|} \int_0^\infty \frac{\rho \sin(\rho|y|)}{\kappa^2 - \rho^2} d\rho = -\frac{2\pi i}{|y|} \int_{-\infty}^\infty \frac{\rho e^{i\rho|y|}}{\kappa^2 - \rho^2} d\rho. \end{aligned}$$

Extending the integrand on the right hand side to a meromorphic function on the upper half complex plane, we can use the residue theorem to calculate the integral and find by taking into account that $\kappa \in \mathbb{H}$ that

$$\int_{\mathbb{R}^3} \frac{e^{i\langle k, y \rangle}}{\kappa^2 - |k|^2} dk = -2\pi^2 \frac{e^{i\kappa|y|}}{|y|}. \quad (2.10)$$

Inserting (2.10) into (2.9) and further into (2.8), and remarking that ψ is indeed an arbitrary function in $\mathcal{S}(\mathbb{R}^3)$, we end up with (2.7). \square

To translate the initial condition in (2.2) that the solution p vanishes for negative times into Fourier space, we use that the Fourier transform of such a function can be characterised by being polynomially bounded on the upper half complex plane away from the real axis.

We will briefly summarise the theory as we need it. For a detailed exposition, we refer to [Hö3, Chapter 7.4].

Definition 2.2.4 Let $u \in \mathcal{D}'(\mathbb{R})$ be a distribution with $\text{supp } u \subset [0, \infty)$ such that $e_{-\eta}u \in \mathcal{S}'(\mathbb{R})$ for every $\eta > 0$, where we denote by $e_z \in C^\infty(\mathbb{R})$, $z \in \mathbb{C}$, the function $e_z(t) = e^{zt}$.

We define the *adjoint Fourier–Laplace transform* $\check{u} : \mathbb{H} \rightarrow \mathbb{C}$ of u by choosing for every point $z \in \mathbb{H}$ an arbitrary $\eta_z \in (0, \Im m z)$ and by setting

$$\check{u}(z) = \frac{1}{\sqrt{2\pi}} \langle e_{-\eta_z} u, \tilde{e}_{iz+\eta_z} \rangle_{\mathcal{S}', \mathcal{S}}.$$

Here \tilde{e}_z denotes for every $z \in \mathbb{C}$ with $\Re z < 0$ an arbitrary extension of the function $e_z|_{[0, \infty)}$ to the negative axis such that $\tilde{e}_z \in \mathcal{S}(\mathbb{R})$. (The definition does not depend on the choice of the extension, since $\text{supp } u \subset [0, \infty)$, see the proof of [Hö3, Theorem 2.3.3].)

Note that if u is a regular distribution: $\langle u, \phi \rangle_{\mathcal{D}', \mathcal{D}} = \int_{-\infty}^\infty U(t) \phi(t) dt$ for all $\phi \in C_c^\infty(\mathbb{R})$ with an integrable function $U : \mathbb{R} \rightarrow \mathbb{C}$ with $\text{supp } U \subset [0, \infty)$, then this is exactly the holomorphic

extension of the inverse Fourier transform of U to the upper half plane:

$$\check{u}(z) = \frac{1}{\sqrt{2\pi}} \int_0^\infty U(t) e^{izt} dt, \quad z \in \overline{\mathbb{H}}.$$

With this construction, we have that the inverse Fourier transform of the tempered distribution $u_\eta = e_{-\eta}u$ for $\eta > 0$ is the regular distribution corresponding to $\check{u}(\cdot + i\eta)$, that is,

$$\langle \mathcal{F}^{-1}u_\eta, \phi \rangle_{\mathcal{S}', \mathcal{S}} = \int_{-\infty}^\infty \check{u}(\omega + i\eta) \phi(\omega) d\omega. \quad (2.11)$$

Now, the causality of a distribution u , that is, $\text{supp } u \subset [0, \infty)$, can be written in the form of a polynomial bound on its Fourier–Laplace transform \check{u} .

Lemma 2.2.5 *We use again for every $z \in \mathbb{C}$ the notation $e_z \in C^\infty(\mathbb{R})$ for the function $e_z(t) = e^{izt}$.*

1. *Let $u \in \mathcal{D}'(\mathbb{R})$ be a distribution with $\text{supp } u \subset [0, \infty)$ and such that $e_{-\eta}u \in \mathcal{S}'(\mathbb{R})$ for every $\eta > 0$.*

Then, we find for every $\eta_1 > 0$ constants $C > 0$ and $N \in \mathbb{N}$ such that the adjoint Fourier–Laplace transform \check{u} of u fulfils

$$|\check{u}(z)| \leq C(1 + |z|)^N \quad \text{for all } z \in \mathbb{C} \quad \text{with } \Im z \geq \eta_1. \quad (2.12)$$

2. *Conversely, if we have a holomorphic function $\check{u} : \mathbb{H} \rightarrow \mathbb{C}$ such that there exist for every $\eta_1 > 0$ constants $C > 0$ and $N \in \mathbb{N}$ with*

$$|\check{u}(z)| \leq C(1 + |z|)^N \quad \text{for all } z \in \mathbb{C} \quad \text{with } \Im z \geq \eta_1, \quad (2.13)$$

then \check{u} coincides with the adjoint Fourier–Laplace transform of a distribution $u \in \mathcal{D}'(\mathbb{R})$ with $\text{supp } u \subset [0, \infty)$ and the property that $e_{-\eta}u \in \mathcal{S}'(\mathbb{R})$ for all $\eta > 0$.

Proof:

1. Let $\eta_1 > 0$ and $\eta_0 \in (0, \eta_1)$ be arbitrary. We choose a function $\psi \in C^\infty(\mathbb{R})$ with $\psi(t) = 1$ for $t \in (-\infty, 0]$ and $\psi(t) = 0$ for $t \in [1, \infty)$. Then, we write the given distribution u in the form $u = u_1 + u_2$ by setting

$$\langle u_1, \phi \rangle_{\mathcal{D}', \mathcal{D}} = \langle u, \psi \phi \rangle_{\mathcal{D}', \mathcal{D}} \quad \text{and} \quad \langle u_2, \phi \rangle_{\mathcal{D}', \mathcal{D}} = \langle u, (1 - \psi) \phi \rangle_{\mathcal{D}', \mathcal{D}} \quad \text{for all } \phi \in C_c^\infty(\mathbb{R}).$$

Since we have by assumption $e_{-\eta_0}u \in \mathcal{S}'(\mathbb{R})$ and since u_1 has by construction compact support, we get that $e_{-\eta_0}u_2 \in \mathcal{S}'(\mathbb{R})$. Thus, because of $\text{supp}(1 - \psi) \subset [0, \infty)$, there exist constants $A_2 > 0$ and $N_2 \in \mathbb{N}$ such that

$$\left| \langle e_{-\eta_0}u_2, \phi \rangle_{\mathcal{S}', \mathcal{S}} \right| = \left| \langle e_{-\eta_0}u, (1 - \psi) \phi \rangle_{\mathcal{S}', \mathcal{S}} \right| \leq A_2 \sum_{k, \ell=0}^{N_2} \sup_{t \in [0, \infty)} |t^\ell \phi^{(k)}(t)| \quad \text{for all } \phi \in \mathcal{S}(\mathbb{R}). \quad (2.14)$$

Moreover, since $e_{-\eta_0}u_1$ has compact support $\text{supp}(e_{-\eta_0}u_1) \subset [0, 1]$, we find, see for example [HÖ3, Theorem 2.3.10], constants $A_1 > 0$ and $N_1 \in \mathbb{N}$ so that

$$\left| \langle e_{-\eta_0}u_1, \phi \rangle_{\mathcal{E}', \mathcal{E}} \right| \leq A_1 \sum_{k=0}^{N_1} \sup_{t \in [0, 1]} |\phi^{(k)}(t)| \quad \text{for all } \phi \in C^\infty(\mathbb{R}). \quad (2.15)$$

We now define as in Definition 2.2.4 for $z \in \mathbb{C}$ with $\Re z > 0$ an extension $\tilde{e}_z \in \mathcal{S}(\mathbb{R})$ of the function $e_z|_{[0, \infty)}$ and choose for every $z \in \mathbb{H}$ the function $\phi = \tilde{e}_{iz+\eta_0}$ in (2.14) and (2.15). Then, there exists a constant $C > 0$ such that with $N = \max\{N_1, N_2\}$

$$\begin{aligned} |\check{u}(z)| &= \frac{1}{\sqrt{2\pi}} \left| \langle e_{-\eta_0}u, \tilde{e}_{iz+\eta_0} \rangle_{\mathcal{S}', \mathcal{S}} \right| \\ &\leq \frac{1}{\sqrt{2\pi}} \left| \langle e_{-\eta_0}u_1, \tilde{e}_{iz+\eta_0} \rangle_{\mathcal{S}', \mathcal{S}} \right| + \frac{1}{\sqrt{2\pi}} \left| \langle e_{-\eta_0}u_2, \tilde{e}_{iz+\eta_0} \rangle_{\mathcal{S}', \mathcal{S}} \right| \leq C(1 + |z|)^N \end{aligned}$$

holds for every $z \in \mathbb{H}$ with $\Im z \geq \eta_1$.

2. To construct the distribution u , we define from the given function \check{u} for every $\eta > 0$ the distribution $u_\eta \in \mathcal{S}'(\mathbb{R})$ via the relation (2.11), so that the inverse Fourier transform of u_η is given by the regular distribution corresponding to the function $\omega \mapsto \check{u}(\omega + i\eta)$.

Now, we want to show that $e_\eta u_\eta$ is in fact independent of η , so that there exists a distribution u such that $u_\eta = e_{-\eta}u$ for every $\eta > 0$. To do so, we first remark that the derivative $\partial_\eta u_\eta$ of u_η with respect to η fulfils for every $\phi \in \mathcal{S}(\mathbb{R})$

$$\langle \partial_\eta u_\eta, \phi \rangle_{\mathcal{S}', \mathcal{S}} = i \int_{-\infty}^{\infty} \check{u}'(\omega + i\eta) \hat{\phi}(\omega) d\omega = -i \int_{-\infty}^{\infty} \check{u}(\omega + i\eta) \hat{\phi}'(\omega) d\omega = \langle u_\eta, f\phi \rangle_{\mathcal{S}', \mathcal{S}},$$

where $\hat{\phi} = \mathcal{F}\phi$ denotes the Fourier transform of ϕ and $f(t) = -t$, so that $\hat{\phi}' = i\mathcal{F}(f\phi)$. Thus, $\partial_\eta u_\eta = f u_\eta$ and therefore, $\partial_\eta(e_\eta u_\eta) = e_\eta(\partial_\eta u_\eta - f u_\eta) = 0$, proving that $e_\eta u_\eta$ is independent of η .

So, the distribution $u = e_\eta u_\eta \in \mathcal{D}'(\mathbb{R})$ is well-defined and fulfils by construction that $e_{-\eta}u \in \mathcal{S}'(\mathbb{R})$ for every $\eta > 0$.

Next, we want to show that $\text{supp } u \subset [0, \infty)$. Let $\phi \in C_c^\infty(\mathbb{R})$ and write again $\hat{\phi} = \mathcal{F}\phi$. Then, by our construction, we have for every $\eta_1 > 0$ that

$$\langle e_{-\eta_1}u, \phi \rangle_{\mathcal{S}', \mathcal{S}} = \int_{-\infty}^{\infty} \check{u}(\omega + i\eta_1) \hat{\phi}(\omega) d\omega. \quad (2.16)$$

Since $\hat{\phi}$ is the Fourier transform of a function with compact support, we can extend it holomorphically to \mathbb{C} and get for every $N_1 \in \mathbb{N}_0$ a constant $C_1 > 0$ such that the upper bound

$$|\hat{\phi}(z)| = \frac{1}{\sqrt{2\pi}} \left| \int_{-\infty}^{\infty} \phi(t) e^{-izt} dt \right| \leq \frac{C_1}{(1 + |z|)^{N_1}} e^{\sup_{t \in \text{supp } \phi} (t \Im z)}$$

holds.

Therefore, we can shift the line of integration in (2.16) by an arbitrary value $\eta > 0$ upwards in the upper half plane and get with the upper bound (2.13) that

$$\left| \langle e_{-\eta_1} u, \phi \rangle_{S', S} \right| = \left| \int_{-\infty}^{\infty} \check{u}(\omega + i(\eta_1 + \eta)) \hat{\phi}(\omega + i\eta) d\omega \right| \leq A e^{\eta \sup_{t \in \text{supp } \phi} t}$$

for some constant $A > 0$. Choosing now ϕ such that $\text{supp } \phi \subset (-\infty, 0)$ and taking the limit $\eta \rightarrow \infty$, the right hand side tends to zero, showing that $\langle e_{-\eta_1} u, \phi \rangle_{S', S} = 0$ whenever $\text{supp } \phi \subset (-\infty, 0)$. Thus, $e_{-\eta_1} u$, and therefore also u , has only support on $[0, \infty)$.

Finally, we verify that the Fourier–Laplace transform of u is given by \check{u} . Indeed, given any $\omega \in \mathbb{R}$ and $\eta > 0$, we have by construction for every $\eta_1 \in (0, \eta)$ and every extension $\tilde{e}_z \in \mathcal{S}(\mathbb{R})$ of $e_z|_{[0, \infty)}$ for $z \in \mathbb{C}$ with $\Re z > 0$ that

$$\left\langle e_{-\eta_1} u, \tilde{e}_{i(\omega + i\eta) + \eta_1} \right\rangle_{S', S} = \int_{-\infty}^{\infty} \check{u}(\omega_1 + i\eta_1) \mathcal{F} \tilde{e}_{i\omega + (\eta_1 - \eta)}(\omega_1) d\omega_1.$$

Since $\text{supp } u \subset [0, \infty)$, we know that this expression is independent of the concrete choice of the extension \tilde{e}_z . Moreover, both sides are independent of η_1 . Thus, letting on the right hand side \tilde{e}_z converge to e_z and η_1 to η , $\mathcal{F} \tilde{e}_{i\omega + (\eta_1 - \eta)}$ will tend to $\sqrt{2\pi}$ times the δ -distribution at ω , and we therefore get

$$\frac{1}{\sqrt{2\pi}} \left\langle e_{-\eta_1} u, \tilde{e}_{i(\omega + i\eta) + \eta_1} \right\rangle_{S', S} = \check{u}(\omega + i\eta).$$

□

We now return to the solution of the attenuated wave equation (2.2).

Proposition 2.2.6 *Let κ be an attenuation coefficient and $\mathcal{A}_\kappa : \mathcal{S}'(\mathbb{R} \times \mathbb{R}^3) \rightarrow \mathcal{S}'(\mathbb{R} \times \mathbb{R}^3)$ be the corresponding attenuation operator. Let further $h \in L^2(\mathbb{R}^3)$ with compact essential support.*

Then, the attenuated wave equation

$$\langle \mathcal{A}_\kappa p, \vartheta \rangle_{S', S} + \langle \Delta p, \vartheta \rangle_{S', S} = - \int_{\mathbb{R}^3} h(x) \partial_t \vartheta(0, x) dx, \quad \vartheta \in \mathcal{S}(\mathbb{R} \times \mathbb{R}^3), \quad (2.17)$$

where the Laplace operator $\Delta : \mathcal{S}'(\mathbb{R} \times \mathbb{R}^3) \rightarrow \mathcal{S}'(\mathbb{R} \times \mathbb{R}^3)$ is defined by

$$\langle \Delta u, \phi \otimes \psi \rangle_{S', S} = \langle u, \phi \otimes (\Delta \psi) \rangle_{S', S} \quad \text{for all } \phi \in \mathcal{S}(\mathbb{R}), \psi \in \mathcal{S}(\mathbb{R}^3),$$

has a unique solution $p \in \mathcal{S}'(\mathbb{R} \times \mathbb{R}^3)$ with $\text{supp } p \subset [0, \infty) \times \mathbb{R}^3$.

Moreover, p is of the form

$$\langle p, \phi \otimes \psi \rangle_{S', S} = \int_{-\infty}^{\infty} \int_{\mathbb{R}^3} \int_{\mathbb{R}^3} G_\kappa(\omega, x - y) h(y) dy \hat{\phi}(\omega) \psi(x) dx d\omega, \quad (2.18)$$

where $\hat{\phi}$ denotes the Fourier transform of ϕ and G denotes the integral kernel

$$G_\kappa(\omega, x) = -\frac{i\omega}{4\pi\sqrt{2\pi}} \frac{e^{i\kappa(\omega)|x|}}{|x|}, \quad \omega \in \mathbb{R}, x \in \mathbb{R}^3 \setminus \{0\}. \quad (2.19)$$

Proof: Let $p \in \mathcal{S}'(\mathbb{R} \times \mathbb{R}^3)$ be a solution of (2.17) with $\text{supp } p \subset [0, \infty) \times \mathbb{R}^3$. We evaluate the equation (2.17) for $\vartheta = \phi \otimes \psi \in C_c^\infty(\mathbb{R} \times \mathbb{R}^3)$ and write $\mathcal{F}\phi = \hat{\phi}$. It then follows that

$$-\langle p, \mathcal{F}^{-1}(\kappa^2 \hat{\phi}) \otimes \psi \rangle_{\mathcal{S}', \mathcal{S}} + \langle p, \mathcal{F}^{-1} \hat{\phi} \otimes \Delta \psi \rangle_{\mathcal{S}', \mathcal{S}} = \phi'(0) \int_{\mathbb{R}^3} h(x) \psi(x) \, dx. \quad (2.20)$$

For arbitrary $z \in \mathbb{H}$, we define the adjoint Fourier–Laplace transform $\check{p}(z) \in \mathcal{S}'(\mathbb{R}^3)$ of p by

$$\langle \check{p}(z), \psi \rangle_{\mathcal{S}', \mathcal{S}} = \frac{1}{\sqrt{2\pi}} \langle p, \tilde{e}_{iz} \otimes \psi \rangle_{\mathcal{S}', \mathcal{S}},$$

where $\tilde{e}_z \in \mathcal{S}(\mathbb{R})$, $z \in \mathbb{C}$ with $\Re z < 0$, is an arbitrary extension of $\tilde{e}_z(t) = e^{zt}$ for $t \geq 0$, see Definition 2.2.4. Then, $z \mapsto \langle \check{p}(z), \psi \rangle$ is holomorphic in the upper half plane \mathbb{H} and we have

$$\begin{aligned} \langle p, \mathcal{F}^{-1}(\kappa^2 \hat{\phi}) \otimes \psi \rangle_{\mathcal{S}', \mathcal{S}} &= \lim_{\xi \downarrow 0} \langle p, \tilde{e}_{-\xi} \mathcal{F}^{-1}(\kappa^2 \hat{\phi}) \otimes \psi \rangle_{\mathcal{S}', \mathcal{S}} \\ &= \lim_{\xi \downarrow 0} \int_{-\infty}^{\infty} \langle \check{p}(\omega + i\xi), \psi \rangle_{\mathcal{S}', \mathcal{S}} \kappa^2(\omega) \hat{\phi}(\omega) \, d\omega. \end{aligned}$$

We replace κ in the integrand now by its holomorphic extension $\tilde{\kappa} : \overline{\mathbb{H}} \rightarrow \overline{\mathbb{H}}$, see 2 in Definition 2.2.1, and also extend the Fourier transform $\hat{\phi}$ of the compactly supported function ϕ holomorphically to \mathbb{C} . Since $z \mapsto \langle \check{p}(z), \psi \rangle$ is the adjoint Fourier–Laplace transform of a distribution with support on $[0, \infty)$, it is polynomially bounded, see Lemma 2.2.5. Moreover, we have by Definition 2.2.1 of the attenuation coefficient a polynomial bound on $\tilde{\kappa}$ and get therefore with the dominated convergence theorem that

$$\langle p, \mathcal{F}^{-1}(\kappa^2 \hat{\phi}) \otimes \psi \rangle_{\mathcal{S}', \mathcal{S}} = \lim_{\xi \downarrow 0} \lim_{\eta \downarrow 0} \int_{-\infty}^{\infty} \langle \check{p}(\omega + i(\xi + \eta)), \psi \rangle_{\mathcal{S}', \mathcal{S}} \tilde{\kappa}^2(\omega + i\eta) \hat{\phi}(\omega + i\eta) \, d\omega.$$

Since all functions in the integrand are holomorphic in the upper half plane the integral is independent of η and we can therefore remove the limit with respect to η . Using again the dominated convergence theorem, we can evaluate now the limit with respect to ξ and obtain for arbitrary $\eta > 0$ the equality

$$\langle p, \mathcal{F}^{-1}(\kappa^2 \hat{\phi}) \otimes \psi \rangle_{\mathcal{S}', \mathcal{S}} = \int_{-\infty}^{\infty} \langle \check{p}(\omega + i\eta), \psi \rangle_{\mathcal{S}', \mathcal{S}} \tilde{\kappa}^2(\omega + i\eta) \hat{\phi}(\omega + i\eta) \, d\omega.$$

Inserting this into the equation (2.20) and arguing in the same way for the two other terms therein, we see that $\check{p}(z) \in \mathcal{S}'(\mathbb{R}^3)$ solves for every $z \in \mathbb{H}$ the equation

$$\tilde{\kappa}^2(z) \langle \check{p}(z), \psi \rangle_{\mathcal{S}', \mathcal{S}} + \langle \check{p}(z), \Delta \psi \rangle_{\mathcal{S}', \mathcal{S}} = \frac{iz}{\sqrt{2\pi}} \int_{\mathbb{R}^3} h(x) \psi(x) \, dx.$$

Thus, by Lemma 2.2.3, we get for every $z \in \mathbb{H}$ with $\Im \tilde{\kappa}(z) > 0$ that

$$\langle \check{p}(z), \psi \rangle_{\mathcal{S}', \mathcal{S}} = -\frac{iz}{4\pi\sqrt{2\pi}} \int_{\mathbb{R}^3} \int_{\mathbb{R}^3} \frac{e^{i\tilde{\kappa}(z)|x-y|}}{|x-y|} h(y) \, dy \, \psi(x) \, dx \quad (2.21)$$

is the only solution. However, since $\tilde{\kappa}$ is holomorphic, its imaginary part cannot vanish in any

open set unless $\tilde{\kappa}$ were a constant, real function which is excluded by the symmetry condition 3 in Definition 2.2.1. Therefore, we can uniquely extend the formula (2.21) for $\langle \check{p}(z), \psi \rangle_{\mathcal{S}', \mathcal{S}}$ by continuity to all $z \in \overline{\mathbb{H}}$.

It remains to verify that $\text{supp } p \subset [0, \infty) \times \mathbb{R}^3$. To see this, we use that $\Im \tilde{\kappa}(z) \geq 0$ for every $z \in \overline{\mathbb{H}}$ to estimate the integral in (2.21) by

$$\left| \langle \check{p}(z), \psi \rangle_{\mathcal{S}', \mathcal{S}} \right| \leq C|z|$$

with some constant $C > 0$. Therefore, by Lemma 2.2.5, $\langle \check{p}(z), \psi \rangle_{\mathcal{S}', \mathcal{S}}$ is the Fourier–Laplace transform of a distribution with support in $[0, \infty)$. \square

2.2.2 Finite Propagation Speed

Seeing the equation (2.17) as a generalisation of the wave equation, it is natural to additionally impose that the solution propagates with finite speed.

Definition 2.2.7 We say that the solution $p \in \mathcal{S}'(\mathbb{R} \times \mathbb{R}^3)$ of the equation (2.17) *propagates with finite speed* $c > 0$ if

$$\text{supp } p \subset \{(t, x) \in \mathbb{R} \times \mathbb{R}^3 \mid |x| \leq ct + R\}$$

whenever $\text{supp } h \subset B_R(0)$.

We can give an explicit characterisation of the equations whose solutions propagate with finite speed in terms of the holomorphic extension $\tilde{\kappa}$ of the attenuation coefficient κ .

Lemma 2.2.8 *The solution p of the attenuated wave equation (2.17) propagates with finite speed $c > 0$ if the holomorphic extension $\tilde{\kappa}$ of the attenuation coefficient κ fulfils*

$$\Im(\tilde{\kappa}(z) - \frac{z}{c}) \geq 0 \quad \text{for every } z \in \overline{\mathbb{H}}.$$

Conversely, if there exists a sequence $(z_\ell)_{\ell=1}^\infty \subset \mathbb{H}$ with the properties that

- *there exists a parameter $\eta_1 > 0$ such that $\Im(z_\ell) \geq \eta_1$ for all $\ell \in \mathbb{N}$,*
- *we have $|z_\ell| \rightarrow \infty$ for $\ell \rightarrow \infty$, and*
- *there exists a parameter $\delta > 0$ such that*

$$\Im(\tilde{\kappa}(z_\ell) - \frac{z_\ell}{c}) \leq -\delta|z_\ell| \quad \text{for all } \ell \in \mathbb{N},$$

then p propagates faster than with speed c .

Proof: Since the solution $p \in \mathcal{S}'(\mathbb{R} \times \mathbb{R}^3)$ is a regular distribution with respect to the second component, see (2.18), having finite propagation speed is equivalent to the condition that the distribution $p(x) \in \mathcal{S}'(\mathbb{R})$, given by

$$\langle p(x), \phi \rangle_{\mathcal{S}', \mathcal{S}} = \int_{-\infty}^{\infty} \int_{\mathbb{R}^3} G_\kappa(\omega, x - y) h(y) dy \hat{\phi}(\omega) d\omega, \quad x \in \mathbb{R}^3,$$

has $\text{supp } p(x) \subset [\frac{1}{c}(|x| - R), \infty)$. Letting h tend to a three dimensional δ -distribution, we see that the distribution $g(x) \in \mathcal{S}'(\mathbb{R})$, defined by

$$\langle g(x), \phi \rangle_{\mathcal{S}', \mathcal{S}} = \int_{-\infty}^{\infty} G_{\kappa}(\omega, x) \hat{\phi}(\omega) d\omega,$$

has to fulfil $\text{supp } g(x) \subset [\frac{|x|}{c}, \infty)$. If we shift $g(x)$ now by $\frac{|x|}{c}$ via $\tau : \mathcal{S}(\mathbb{R}) \rightarrow \mathcal{S}(\mathbb{R})$, $(\tau\phi)(t) = \phi(t + \frac{|x|}{c})$, this means that the distribution $g_{\tau}(x) \in \mathcal{S}'(\mathbb{R})$, given by

$$\langle g_{\tau}(x), \phi \rangle_{\mathcal{S}', \mathcal{S}} = \langle g(x), \tau^{-1}\phi \rangle_{\mathcal{S}', \mathcal{S}} = \int_{-\infty}^{\infty} G_{\kappa}(\omega, x) e^{-i\frac{\omega|x|}{c}} \hat{\phi}(\omega) d\omega$$

has to have $\text{supp } g_{\tau}(x) \subset [0, \infty)$. Extending the function $\omega \mapsto G_{\kappa}(\omega, x) e^{-i\frac{\omega|x|}{c}}$ to the upper half plane using the explicit formula (2.19) for G_{κ} , we obtain the adjoint Fourier–Laplace transform $z \mapsto \check{g}_{\tau}(z, x)$ of the distribution $g_{\tau}(x)$:

$$\check{g}_{\tau}(z, x) = -\frac{iz}{4\pi\sqrt{2\pi}} \frac{e^{i(\tilde{\kappa}(z) - \frac{z}{c})|x|}}{|x|},$$

see (2.11). According to Lemma 2.2.5, we can therefore equivalently characterise a finite propagation speed in terms of a polynomial bound on the function $\check{g}_{\tau}(\cdot, x)$.

- If $\Im(\kappa(z) - \frac{z}{c}) \geq 0$ for every $z \in \overline{\mathbb{H}}$, then the adjoint Fourier–Laplace transform of $g_{\tau}(x)$ fulfils that for every $x \in \mathbb{R}^3$ there exists a constant $C > 0$ such that

$$|\check{g}_{\tau}(z, x)| \leq C|z|.$$

Thus, the condition (2.13) of Lemma 2.2.5 is satisfied and therefore $\text{supp } g_{\tau}(x) \subset [0, \infty)$, so that p propagates with the finite speed $c > 0$.

- On the other hand, if there exists a sequence $(z_{\ell})_{\ell=1}^{\infty} \subset \mathbb{H}$ with $\Im(z_{\ell}) \geq \eta_1$ for some $\eta_1 > 0$, $|z_{\ell}| \rightarrow \infty$, and $\Im(\tilde{\kappa}(z_{\ell}) - \frac{z_{\ell}}{c}) \leq -\delta|z_{\ell}|$ for some $\delta > 0$, then

$$|\check{g}_{\tau}(z_{\ell}, x)| \geq \frac{|z_{\ell}|}{4\pi|x|\sqrt{2\pi}} e^{\delta|x||z_{\ell}|},$$

so that condition (2.12) of Lemma 2.2.5 is violated and therefore the support of $g_{\tau}(x)$ cannot be contained in $[0, \infty)$. \square

Proposition 2.2.9 *Let κ be an attenuation coefficient with the holomorphic extension $\tilde{\kappa} : \overline{\mathbb{H}} \rightarrow \overline{\mathbb{H}}$. Then, the solution p of the attenuated wave equation (2.17) propagates with finite speed if and only if*

$$\lim_{\omega \rightarrow \infty} \frac{\tilde{\kappa}(i\omega)}{i\omega} > 0.$$

In this case, it propagates with the speed $c = \lim_{\omega \rightarrow \infty} \frac{i\omega}{\tilde{\kappa}(i\omega)}$.

Proof: We make use of the theory of Nevanlinna functions, see for example [Akh65, Chapter 3.1]. Similar to the Riesz–Herglotz formula, which characterises the functions mapping the unit circle to the upper half plane, we have that all holomorphic functions $\tilde{\kappa} : \mathbb{H} \rightarrow \overline{\mathbb{H}}$ have an integral

representation of the form

$$\tilde{\kappa}(z) = Az + B + \int_{-\infty}^{\infty} \frac{1 + z\nu}{\nu - z} d\sigma(\nu), \quad z \in \mathbb{H}, \quad (2.22)$$

where $\sigma : \mathbb{R} \rightarrow \mathbb{R}$ is a monotonically increasing function of bounded variation and $A \geq 0$ and $B \in \mathbb{R}$ are arbitrary parameters, and vice versa, see [Akh65, Formula 3.3].

Then, $\tilde{\kappa}(z) - Az$ is still of the form (2.22) and therefore is a holomorphic function mapping \mathbb{H} to $\overline{\mathbb{H}}$. In particular, it satisfies $\Im(\tilde{\kappa}(z) - Az) \geq 0$ for all $z \in \mathbb{H}$. Thus, if $A > 0$, p propagates with the finite speed $c = \frac{1}{A}$ according to Lemma 2.2.8.

Evaluating $\tilde{\kappa}$ along the imaginary axis, we find that asymptotically as $\omega \rightarrow \infty$

$$\tilde{\kappa}(i\omega) = i\omega \left(A + \frac{B}{i\omega} + \int_{-\infty}^{\infty} \frac{1 + i\omega\nu}{i\omega(\nu - i\omega)} d\sigma(\nu) \right) = i\omega(A + o(1)). \quad (2.23)$$

Thus,

$$A = \lim_{\omega \rightarrow \infty} \frac{\tilde{\kappa}(i\omega)}{i\omega}.$$

Moreover for $A = 0$, we see from (2.23) that for every choice of $c > 0$, we have the behaviour $\tilde{\kappa}(i\omega) - \frac{i\omega}{c} = i\omega(-\frac{1}{c} + o(1))$ and therefore $\Im(\tilde{\kappa}(i\omega) - \frac{i\omega}{c}) \leq -\frac{\omega}{2c}$ for all $\omega \geq \omega_0$ for a sufficiently large ω_0 . Thus, by Lemma 2.2.8, p cannot have finite propagation speed for $A = 0$. \square

2.3 Examples of Attenuation Models

The following examples of attenuation coefficient have been collected in [KS12], where also references to original papers can be found. In this section, we review them and catalog them into two groups which are characterised by different spectral behaviour.

If the attenuation in the medium increases faster than some power of the frequency, we are in the case of strong attenuation.

Definition 2.3.1 We call an attenuation coefficient $\kappa \in C^\infty(\mathbb{R}; \overline{\mathbb{H}})$ a *strong attenuation coefficient* if it fulfils that

$$\Im \kappa(\omega) \geq \kappa_0 |\omega|^\beta \quad \text{for all } \omega \in \mathbb{R} \quad \text{with } |\omega| \geq \omega_0 \quad (2.24)$$

for some constants $\kappa_0 > 0$, $\beta > 0$, and $\omega_0 \geq 0$.

A common example, which has the drawback of an infinite propagation speed, is the thermo-viscous model, see Table 2.1. In [KSB11], the authors modified this model to obtain one with finite propagation speed, see Table 2.2. Other models, trying to match the heuristic power law behaviour of the attenuation are the power law in Table 2.3 and Szabo's model, see Table 2.4, where we chose the modified version introduced in [KS12] as the original one does not lead to a causal model.

In these tables and in the following we always use the principal branch of the complex roots, that is, we define for $\gamma \in \mathbb{C}$

$$(re^{i\varphi})^\gamma = e^{\gamma(\log(r)+i\varphi)} \quad \text{for every } r > 0, \varphi \in (-\pi, \pi).$$

Remark: The attenuation coefficients in Table 2.2, Table 2.3, and Table 2.4 do not fulfil the smoothness assumption $\kappa \in C^\infty(\mathbb{R})$. However, this requirement originates mainly from our choice of solution concept for the attenuated wave equation (2.2) and we may still consider formula (2.25) as definition of the solution p of (2.2) if κ is non-smooth. In particular, the smoothness assumption is not required for the derivation of the decay of the singular values of the integrated photoacoustic operator.

In the case where the attenuation decreases sufficiently fast as the frequency increases, we call the medium weakly attenuating.

Definition 2.3.2 We call an attenuation coefficient $\kappa \in C^\infty(\mathbb{R}; \overline{\mathbb{H}})$ a *weak attenuation coefficient* if it is of the form

$$\kappa(\omega) = \frac{\omega}{c} + i\kappa_\infty + \kappa_*(\omega), \quad \omega \in \mathbb{R},$$

for some constants $c > 0$ and $\kappa_\infty \geq 0$ and a bounded function $\kappa_* \in C^\infty(\mathbb{R}) \cap L^2(\mathbb{R})$.

Clearly, the non-attenuating case where $\kappa(\omega) = \frac{\omega}{c}$ with $c > 0$, so that the attenuated wave equation (2.2) reduces to the linear wave equation, falls under this category and we will later on treat the case of a weak attenuation coefficient as a perturbation of this non-attenuated case.

A non-trivial example of a weak attenuation model is the model by Nachman, Smith, and Waag, see Table 2.5.

2.4 The Integrated Photoacoustic Operator

Let us now return to the attenuated photoacoustic imaging problem. Thus, we consider the operator mapping the source term h in the attenuated wave equation (2.2) (interpreted in the sense of (2.17)) to the measurements, which shall correspond to the solution of the attenuated wave equation on the measurement surface $\partial\Omega$ measured for all time.

According to Proposition 2.2.6, the solution p of the attenuated wave equation is given by (2.18). This means that the temporal inverse Fourier transform of p is the regular distribution corresponding to the function

$$\check{p}(\omega, x) = \int_{\mathbb{R}^3} G_\kappa(\omega, x-y)h(y) \, dy = -\frac{i\omega}{4\pi\sqrt{2\pi}} \int_{\mathbb{R}^3} \frac{e^{i\kappa(\omega)|x-y|}}{|x-y|} h(y) \, dy, \quad \omega \in \mathbb{R}, x \in \mathbb{R}^3, \quad (2.25)$$

where G_κ is defined by (2.19).

We therefore introduce our measurements \check{m} as the function

$$\check{m}(\omega, \xi) = \check{p}(\omega, \xi) \quad \text{for all } \omega \in \mathbb{R}, \xi \in \partial\Omega.$$

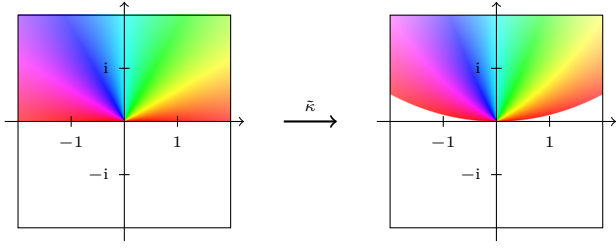
Name:	Thermo-viscous model, see for example [Kin+00, Chapter 8.2]
Attenuation coefficient:	$\kappa : \mathbb{R} \rightarrow \mathbb{C}, \kappa(\omega) = \frac{\omega}{\sqrt{1 - i\tau\omega}}$
Parameters:	$\tau > 0$
Holomorphic extension:	$\tilde{\kappa} : \overline{\mathbb{H}} \rightarrow \mathbb{C}, \tilde{\kappa}(z) = \frac{z}{\sqrt{1 - i\tau z}}$
Upper bound:	$ \tilde{\kappa}(z) \leq z $ for all $z \in \overline{\mathbb{H}}$ This follows from $ 1 - i\tau z \geq \operatorname{Re}(1 - i\tau z) \geq 1$ for $z \in \overline{\mathbb{H}}$.
Propagation speed:	$c = \lim_{\omega \rightarrow \infty} \frac{i\omega}{\tilde{\kappa}(i\omega)} = \lim_{\omega \rightarrow \infty} \sqrt{1 + \tau\omega} = \infty$
Attenuation type:	Strong attenuation coefficient Indeed a Taylor expansion with respect to $\frac{1}{\omega}$ around 0 yields for $\omega \rightarrow \infty$: $\begin{aligned} \Im \kappa(\omega) &= \Im \sqrt{\frac{i\omega}{\tau}} \left(1 + \frac{i}{\tau\omega}\right)^{-\frac{1}{2}} \\ &= \Im \sqrt{\frac{i\omega}{\tau}} (1 + \mathcal{O}(\omega^{-1})) = \sqrt{\frac{\omega}{2\tau}} + \mathcal{O}(\omega^{-1}). \end{aligned}$
Range of $\tilde{\kappa}$:	 <p>To see analytically that $\tilde{\kappa}$ maps the upper half plane $\overline{\mathbb{H}}$ into itself, we first remark that because of the symmetry $\tilde{\kappa}(-\bar{z}) = -\overline{\tilde{\kappa}(z)}$, it is enough to show that the first quadrant $Q_{++} = \{z \in \mathbb{C} \mid \operatorname{Re}(z) \geq 0, \operatorname{Im}(z) \geq 0\}$ is mapped under $\tilde{\kappa}$ into $\overline{\mathbb{H}}$. Since $f : \mathbb{C} \rightarrow \mathbb{C}, f(z) = \frac{1}{1 - i\tau z}$ is a Möbius transform which maps Q_{++} to the half ball $\bar{B}_{\frac{1}{2}}(\frac{1}{2}) \cap Q_{++}$ and $\tilde{\kappa}$ is the composition $\tilde{\kappa}(z) = z\sqrt{f(z)}$, we indeed have $\tilde{\kappa}(Q_{++}) \subset \overline{\mathbb{H}}$.</p>

TABLE 2.1: The thermo-viscous model.

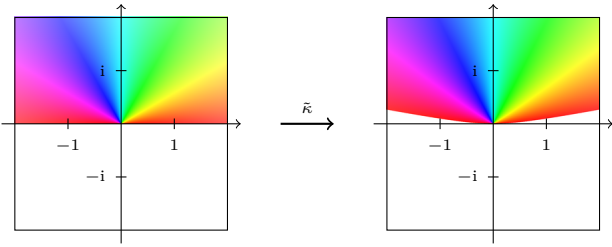
Model:	Kowar–Scherzer–Bonnefond model, see [KSB11]
Attenuation coefficient:	$\kappa : \mathbb{R} \rightarrow \mathbb{C}, \kappa(\omega) = \omega \left(1 + \frac{\alpha}{\sqrt{1 + (-i\tau\omega)^\gamma}} \right)$
Parameters:	$\gamma \in (0, 1), \alpha > 0, \tau > 0$
Holomorphic extension:	$\tilde{\kappa} : \overline{\mathbb{H}} \rightarrow \mathbb{C}, \tilde{\kappa}(z) = z \left(1 + \frac{\alpha}{\sqrt{1 + (-i\tau z)^\gamma}} \right)$
Upper bound:	$ \tilde{\kappa}(z) \leq (1 + \alpha) z $ This follows from $ 1 + (-i\tau z)^\gamma \geq \Re(1 + (-i\tau z)^\gamma) \geq 1$ for $z \in \overline{\mathbb{H}}$.
Propagation speed:	$c = \lim_{\omega \rightarrow \infty} \frac{i\omega}{\tilde{\kappa}(i\omega)} = \lim_{\omega \rightarrow \infty} \frac{1}{1 + \frac{\alpha}{\sqrt{1 + (\tau\omega)^\gamma}}} = 1$
Attenuation type:	Strong attenuation coefficient A Taylor expansion with respect to $\omega^{-\gamma}$ around 0 yields for $\omega \rightarrow \infty$: $\begin{aligned} \Im \kappa(\omega) &= \alpha\omega \Im \left((-i\tau\omega)^{-\frac{\gamma}{2}} (1 + (-i\tau\omega)^{-\gamma})^{-\frac{1}{2}} \right) \\ &= \alpha\omega \Im \left((-i\tau\omega)^{-\frac{\gamma}{2}} + \mathcal{O}(\omega^{-\frac{3}{2}\gamma}) \right) \\ &= \alpha\tau^{-\frac{\gamma}{2}} \sin\left(\frac{\pi\gamma}{4}\right) \omega^{1-\frac{\gamma}{2}} (1 + \mathcal{O}(\omega^{-\gamma})). \end{aligned}$
Range of $\tilde{\kappa}$:	 <p>To see where $\tilde{\kappa}$ maps the upper half plane, we write $\tilde{\kappa}$ in the form</p> $\tilde{\kappa}(z) = z(1 + \alpha\sqrt{f_2(f_1(z))}) \quad \text{with} \quad f_2(z) = \frac{1}{1+z}, \quad f_1(z) = (-i\tau z)^\gamma.$ <p>Now, f_1 maps the first quadrant Q_{++} in a subset of the fourth quadrant $Q_{+-} = \{z \in \mathbb{C} \mid \Re(z) \geq 0, \Im(z) \leq 0\}$. And f_2 is a Möbius transform which maps Q_{+-} to the half ball $\bar{B}_{\frac{1}{2}}(\frac{1}{2}) \cap Q_{++}$.</p> <p>Thus, since the product of two points in the first quadrant Q_{++} is in the upper half plane, $\tilde{\kappa}(Q_{++}) \subset \overline{\mathbb{H}}$ and because of the symmetry $\tilde{\kappa}(-\bar{z}) = -\overline{\tilde{\kappa}(z)}$, we therefore have $\tilde{\kappa}(\overline{\mathbb{H}}) \subset \overline{\mathbb{H}}$.</p>

TABLE 2.2: The Kowar–Scherzer–Bonnefond model.

Instead of considering the operator mapping h to \check{m} , we will divide the data by $-i\omega$, meaning that we consider the map from h to the inverse Fourier transform of the measurements which were integrated over time. Additionally, we want to assume that the measurements are performed

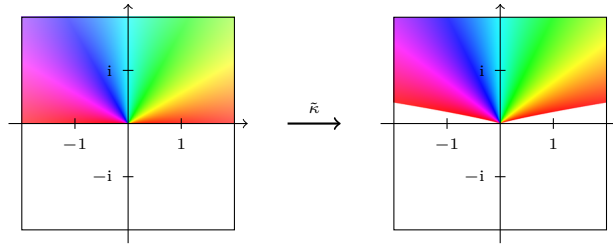
Model:	Power law, see for example [Sza94]
Attenuation coefficient:	$\kappa : \mathbb{R} \rightarrow \mathbb{C}, \kappa(\omega) = \omega + i\alpha(-i\omega)^\gamma$
Parameters:	$\gamma \in (0, 1), \alpha > 0$
Holomorphic extension:	$\tilde{\kappa} : \overline{\mathbb{H}} \rightarrow \mathbb{C}, \tilde{\kappa}(z) = z + i\alpha(-iz)^\gamma$
Upper bound:	$ \tilde{\kappa}(z) \leq z + \alpha z ^\gamma \leq \alpha(1 - \gamma) + (1 + \alpha\gamma) z $ The second inequality uses Young's inequality to estimate $ z ^\gamma \leq \gamma z + 1 - \gamma$.
Propagation speed:	$c = \lim_{\omega \rightarrow \infty} \frac{i\omega}{\tilde{\kappa}(i\omega)} = \lim_{\omega \rightarrow \infty} \frac{1}{1 + \alpha\omega^{\gamma-1}} = 1$
Attenuation type:	Strong attenuation coefficient We have $\Im \kappa(\omega) = \alpha \sin\left((1 - \gamma)\frac{\pi}{2}\right) \omega ^\gamma$.
Range of $\tilde{\kappa}$:	 <p>That the range of $\tilde{\kappa}$ is a subset of $\overline{\mathbb{H}}$ follows immediately from</p> $\Im \tilde{\kappa}(re^{i\varphi}) = r \sin \varphi + \alpha r^\gamma \sin\left(\frac{\pi}{2} + \left(\varphi - \frac{\pi}{2}\right)\gamma\right) \geq 0$ <p>for all $r \geq 0$ and $\varphi \in [0, \pi]$.</p>

TABLE 2.3: The power law model.

outside the support of the source.

Remark: This assumption that the absorption density functions h has compact support in the domain Ω is very common in the theory of photoacoustics, see for instance [AKQ07; KK08].

Definition 2.4.1 Let $\Omega \subset \mathbb{R}^3$ be a bounded Lipschitz domain and κ be either a strong or a weak attenuation coefficient. For $\varepsilon > 0$, we define $\Omega_\varepsilon = \{x \in \Omega \mid \text{dist}(x, \partial\Omega) > \varepsilon\}$.

Then, we call

$$\check{\mathcal{P}}_\kappa : L^2(\Omega_\varepsilon) \rightarrow L^2(\mathbb{R} \times \partial\Omega), \quad \check{\mathcal{P}}_\kappa h(\omega, \xi) = \frac{1}{4\pi\sqrt{2\pi}} \int_{\Omega_\varepsilon} \frac{e^{i\kappa(\omega)|\xi-y|}}{|\xi-y|} h(y) dy \quad (2.26)$$

the *integrated photoacoustic operator* of the attenuation coefficient κ in frequency domain.

Lemma 2.4.2 Let $\Omega \subset \mathbb{R}^3$ be a bounded Lipschitz domain and $\varepsilon > 0$. Then, the integrated photoacoustic operator $\check{\mathcal{P}}_\kappa : L^2(\Omega_\varepsilon) \rightarrow L^2(\mathbb{R} \times \partial\Omega)$ of an attenuation coefficient κ is a bounded

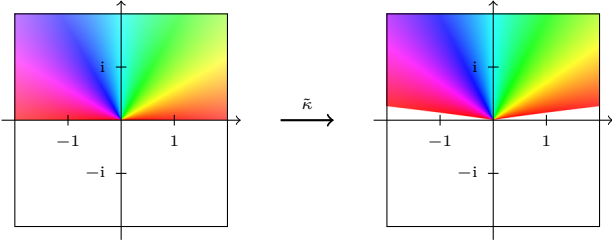
Model:	Modified Szabo model, see [KS12] and, for the original version, [Sza94]
Attenuation coefficient:	$\kappa : \mathbb{R} \rightarrow \mathbb{C}, \kappa(\omega) = \omega\sqrt{1 + \alpha(-i\omega)^{\gamma-1}}$
Parameters:	$\gamma \in (0, 1), \alpha > 0$
Holomorphic extension:	$\tilde{\kappa} : \overline{\mathbb{H}} \rightarrow \mathbb{C}, \tilde{\kappa}(z) = z\sqrt{1 + \alpha(-iz)^{\gamma-1}}$
Upper bound:	$ \tilde{\kappa}(z) \leq z + \sqrt{\alpha} z ^{\frac{\gamma+1}{2}} \leq \frac{1}{2}\alpha(1 - \gamma) + (1 + \frac{\alpha}{2}(1 + \gamma)) z $ The second inequality uses Young's inequality to estimate $ z ^{\frac{1+\gamma}{2}} \leq \frac{1}{2}(1 + \gamma) z + \frac{1}{2}(1 - \gamma)$.
Propagation speed:	$c = \lim_{\omega \rightarrow \infty} \frac{i\omega}{\tilde{\kappa}(i\omega)} = \lim_{\omega \rightarrow \infty} \frac{1}{\sqrt{1 + \alpha\omega^{\gamma-1}}} = 1$
Attenuation type:	Strong attenuation coefficient A Taylor expansion with respect to $\omega^{\gamma-1}$ around 0 yields for $\omega \rightarrow \infty$: $\Im \kappa(\omega) = \Im \left(\omega (1 + 2\alpha(-i\omega)^{\gamma-1})^{\frac{1}{2}} \right) = \omega + \mathcal{O}(\omega^\gamma).$
Range of $\tilde{\kappa}$:	 <p>To determine the range, we write $\tilde{\kappa}$ in the form</p> $\tilde{\kappa}(z) = z\sqrt{1 + f(z)} \quad \text{with} \quad f(z) = \alpha(-iz)^{\gamma-1}.$ <p>Now, since $\gamma - 1 < 0$, f maps the first quadrant Q_{++} to a subset of Q_{++}. Thus, since the product of two points in the first quadrant is in the upper half plane, we have $\tilde{\kappa}(Q_{++}) \subset \overline{\mathbb{H}}$ and because of the symmetry $\tilde{\kappa}(-\bar{z}) = -\overline{\tilde{\kappa}(z)}$ therefore $\tilde{\kappa}(\overline{\mathbb{H}}) \subset \overline{\mathbb{H}}$.</p>

TABLE 2.4: The modified Szabo model.

linear operator and its adjoint is given by

$$\check{\mathcal{P}}_\kappa^* : L^2(\mathbb{R} \times \partial\Omega) \rightarrow L^2(\Omega_\varepsilon), \quad \check{\mathcal{P}}_\kappa^* \check{m}(y) = \frac{1}{4\pi\sqrt{2\pi}} \int_{-\infty}^{\infty} \int_{\partial\Omega} \frac{e^{-i\overline{\kappa(\omega)}|\xi-y|}}{|\xi-y|} \check{m}(\omega, \xi) dS(\xi) d\omega. \quad (2.27)$$

Proof:

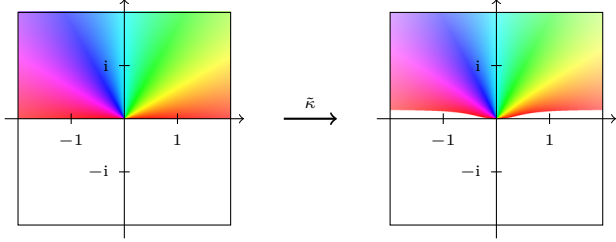
Name:	Nachman–Smith–Waag model, see [NSW90]
Attenuation coefficient:	$\kappa : \mathbb{R} \rightarrow \mathbb{C}, \kappa(\omega) = \frac{\omega}{c_0} \sqrt{\frac{1 - i\tilde{\tau}\omega}{1 - i\tau\omega}}$
Parameters:	$c_0 > 0, \tau > 0, \tilde{\tau} \in (0, \tau)$
Holomorphic extension:	$\tilde{\kappa} : \overline{\mathbb{H}} \rightarrow \mathbb{C}, \frac{z}{c_0} \sqrt{\frac{1 - i\tilde{\tau}z}{1 - i\tau z}}$
Upper bound:	$ \tilde{\kappa}(z) \leq \frac{1}{c_0} z $ for all $z \in \overline{\mathbb{H}}$ This follows from $ 1 - i\tilde{\tau}z \leq 1 - i\tau z $ for $z \in \overline{\mathbb{H}}$.
Propagation speed:	$c = \lim_{\omega \rightarrow \infty} \frac{i\omega}{\tilde{\kappa}(i\omega)} = \lim_{\omega \rightarrow \infty} c_0 \sqrt{\frac{1 + \tau\omega}{1 + \tilde{\tau}\omega}} = c_0 \sqrt{\frac{\tau}{\tilde{\tau}}}$
Attenuation Type:	Weak attenuation coefficient Indeed a Taylor expansion with respect to $\frac{1}{\omega}$ around 0 yields for $\omega \rightarrow \infty$: $\begin{aligned} \kappa(\omega) &= \frac{\omega}{c_0} \sqrt{\frac{\tilde{\tau}}{\tau}} \left(1 + \frac{i}{\tilde{\tau}\omega}\right)^{\frac{1}{2}} \left(1 + \frac{i}{\tau\omega}\right)^{-\frac{1}{2}} \\ &= \frac{\omega}{c_0} \sqrt{\frac{\tilde{\tau}}{\tau}} \left(1 + \frac{i}{2\tilde{\tau}\omega} + \mathcal{O}(\omega^{-2})\right) \left(1 - \frac{i}{2\tau\omega} + \mathcal{O}(\omega^{-2})\right) \\ &= \frac{\omega}{c_0} \sqrt{\frac{\tilde{\tau}}{\tau}} + \frac{i(\tau - \tilde{\tau})}{2c_0\tau\sqrt{\tilde{\tau}\tau}} + \mathcal{O}(\omega^{-1}). \end{aligned}$
Range of $\tilde{\kappa}$:	 <p>The Möbius transform $f : \bar{\mathbb{C}} \rightarrow \bar{\mathbb{C}}, f(z) = \frac{1 - i\tilde{\tau}z}{1 - i\tau z}$ maps the first quadrant Q_{++} to $\bar{B}_r(a) \cap Q_{++}$ where $r = \frac{1}{2}(1 - \frac{\tilde{\tau}}{\tau})$ and $a = \frac{1}{2}(1 + \frac{\tilde{\tau}}{\tau})$. Thus, $\tilde{\kappa}(z) = \frac{z}{c_0} \sqrt{f(z)} \in \overline{\mathbb{H}}$ for $z \in Q_{++}$ and the symmetry $\tilde{\kappa}(-\bar{z}) = -\overline{\tilde{\kappa}(z)}$ then implies that $\tilde{\kappa}(z) \in \overline{\mathbb{H}}$ for every $z \in \overline{\mathbb{H}}$.</p>

TABLE 2.5: The Nachman–Smith–Waag model.

1. We first consider the case of a strong attenuation coefficient. Then, we have for every $\omega \in \mathbb{R}$ and $\xi \in \partial\Omega$ the estimate

$$|\check{\mathcal{P}}_\kappa h(\omega, \xi)|^2 \leq \frac{|\Omega_\varepsilon|}{32\varepsilon^2\pi^3} \|h\|_2^2 e^{-2\varepsilon \Im \kappa(\omega)}.$$

Since, by Definition 2.3.1, $\Im \kappa(\omega) \geq \kappa_0 |\omega|^\beta$ for all $\omega \in \mathbb{R}$ with $|\omega| \geq \omega_0$ for some

sufficiently large $\omega_0 \geq 0$, this shows that $\check{\mathcal{P}}_\kappa : L^2(\Omega_\varepsilon) \rightarrow L^2(\mathbb{R} \times \partial\Omega)$ is a bounded linear operator.

2. In the case of a weak attenuation coefficient, see [Definition 2.3.2](#), we split the operator into $\check{\mathcal{P}}_\kappa = \check{\mathcal{P}}_\kappa^{(0)} + \check{\mathcal{P}}_\kappa^{(1)}$, where we define

$$\check{\mathcal{P}}_\kappa^{(0)} h(\omega, \xi) = \frac{1}{4\pi\sqrt{2\pi}} \int_{\Omega_\varepsilon} \frac{e^{i\frac{\omega}{c}|\xi-y|}}{|\xi-y|} e^{-\kappa_\infty|\xi-y|} h(y) dy \quad (2.28)$$

as the photoacoustic operator with constant attenuation and the perturbation

$$\check{\mathcal{P}}_\kappa^{(1)} h(\omega, \xi) = \frac{1}{4\pi\sqrt{2\pi}} \int_{\Omega_\varepsilon} \frac{e^{i\frac{\omega}{c}|\xi-y|}}{|\xi-y|} e^{-\kappa_\infty|\xi-y|} (e^{i\kappa_*(\omega)|\xi-y|} - 1) h(y) dy. \quad (2.29)$$

Now, $\check{\mathcal{P}}_\kappa^{(0)} h$ is seen to be the inverse Fourier transform of the function $\mathcal{P}_\kappa^{(0)} h$, defined by

$$\mathcal{P}_\kappa^{(0)} h(t, \xi) = \frac{e^{-\kappa_\infty ct}}{4\pi t} \int_{\Omega_\varepsilon \cap \partial B_{ct}(\xi)} h(z) dS(z), \quad t > 0, \quad \xi \in \partial\Omega,$$

and $\mathcal{P}_\kappa^{(0)} h(t, \xi) = 0$ for $t \leq 0$, $\xi \in \partial\Omega$. Now, $\mathcal{P}_\kappa^{(0)} : L^2(\Omega_\varepsilon) \rightarrow L^2(\mathbb{R} \times \partial\Omega)$ can be directly seen to be a bounded linear operator, since we have, recalling that $\kappa_\infty \geq 0$,

$$\begin{aligned} \|\mathcal{P}_\kappa^{(0)} h\|_2^2 &\leq \int_{\partial\Omega} \int_0^\infty \frac{1}{16\pi^2 t^2} \left| \int_{\Omega_\varepsilon \cap \partial B_{ct}(\xi)} h(z) dS(z) \right|^2 dt dS(\xi) \\ &\leq \int_{\partial\Omega} \int_0^\infty \frac{c^2}{4\pi} \int_{\Omega_\varepsilon \cap \partial B_{ct}(\xi)} |h(z)|^2 dS(z) dt dS(\xi). \end{aligned}$$

Thus, combining the two inner integrals to an integral over Ω_ε , we find that

$$\|\mathcal{P}_\kappa^{(0)} h\|_2^2 \leq \frac{c}{4\pi} |\partial\Omega| \|h\|_2^2.$$

This is a special case of the more general result in [\[Pal10, Lemma 4.1\]](#).

Thus, $\mathcal{P}_\kappa^{(0)} : L^2(\Omega_\varepsilon) \rightarrow L^2(\mathbb{R} \times \partial\Omega)$ and therefore, because the Fourier transform on $L^2(\mathbb{R})$ is an isometry, also $\check{\mathcal{P}}_\kappa^{(0)} : L^2(\Omega_\varepsilon) \rightarrow L^2(\mathbb{R} \times \partial\Omega)$ are bounded, linear operators.

For $\check{\mathcal{P}}_\kappa^{(1)} h$, we get the estimate

$$|\check{\mathcal{P}}_\kappa^{(1)} h(\omega, \xi)|^2 \leq \frac{|\Omega_\varepsilon|}{32\varepsilon^2\pi^3} \|h\|_2^2 \sup_{y \in \Omega_\varepsilon} |e^{i\kappa_*(\omega)|\xi-y|} - 1|^2. \quad (2.30)$$

We now remark that we can find for every bounded set $D \subset \mathbb{C}$ a constant $C > 0$ such that

$$|e^z - 1| \leq C|z| \quad \text{for all } z \in D. \quad (2.31)$$

Therefore, since κ_* is according to [Definition 2.3.2](#) bounded and $|\xi - y|$ remains bounded since Ω is bounded, we find a constant $\tilde{C} > 0$ such that

$$\sup_{y \in \Omega_\varepsilon} |e^{i\kappa_*(\omega)|\xi-y|} - 1|^2 \leq \tilde{C} |\kappa_*(\omega)|^2 \quad \text{for all } \omega \in \mathbb{R}, \xi \in \partial\Omega.$$

Since κ_* is additionally square integrable by [Definition 2.3.2](#), we find by inserting this into the estimate (2.30) that $\check{\mathcal{P}}_\kappa^{(1)} : L^2(\Omega_\varepsilon) \rightarrow L^2(\mathbb{R} \times \partial\Omega)$ is a bounded, linear operator, and therefore so is the operator $\check{\mathcal{P}}_\kappa : L^2(\Omega_\varepsilon) \rightarrow L^2(\mathbb{R} \times \partial\Omega)$. \square

To obtain the singular values of the operator $\check{\mathcal{P}}_\kappa$, we consider the operator $\check{\mathcal{P}}_\kappa^* \check{\mathcal{P}}_\kappa$ on $L^2(\Omega_\varepsilon)$. It turns out that this operator is a Hilbert–Schmidt integral operator, in particular therefore compact. So, by the singular theorem for compact operators, its spectrum consists of at most countably many positive eigenvalues and the value zero.

Proposition 2.4.3 *Let $\check{\mathcal{P}}_\kappa : L^2(\Omega_\varepsilon) \rightarrow L^2(\mathbb{R} \times \partial\Omega)$ be the integrated photoacoustic operator of a weak or a strong attenuation coefficient κ for some bounded, convex domain $\Omega \subset \mathbb{R}^3$ with smooth boundary and some $\varepsilon > 0$. Then, $\check{\mathcal{P}}_\kappa^* \check{\mathcal{P}}_\kappa : L^2(\Omega_\varepsilon) \rightarrow L^2(\Omega_\varepsilon)$ is a self-adjoint integral operator with kernel $F \in L^2(\Omega_\varepsilon \times \Omega_\varepsilon)$ given by*

$$F_\kappa(x, y) = \frac{1}{32\pi^3} \int_{-\infty}^{\infty} \int_{\partial\Omega} \frac{e^{i\kappa(\omega)|\xi-y| - i\overline{\kappa(\omega)}|\xi-x|}}{|\xi-y||\xi-x|} dS(\xi) d\omega, \quad (2.32)$$

that is

$$\check{\mathcal{P}}_\kappa^* \check{\mathcal{P}}_\kappa h(x) = \int_{\Omega_\varepsilon} F_\kappa(x, y) h(y) dy. \quad (2.33)$$

In particular, $\check{\mathcal{P}}_\kappa^* \check{\mathcal{P}}_\kappa$ is a Hilbert–Schmidt operator and thus compact.

We remark that the convexity and smoothness assumptions on Ω are only needed for the weak attenuation case. For strong attenuation, a Lipschitz domain Ω is sufficient.

Proof: The representation (2.32) of the integral kernel F_κ of the operator $\check{\mathcal{P}}_\kappa^* \check{\mathcal{P}}_\kappa$ is directly obtained by combining the formulas (2.26) and (2.27) for $\check{\mathcal{P}}_\kappa$ and $\check{\mathcal{P}}_\kappa^*$. To prove that $F \in L^2(\Omega_\varepsilon \times \Omega_\varepsilon)$, we treat the two cases of strong and weak attenuation coefficients separately.

1. For a strong attenuation coefficient, we estimate directly

$$|F_\kappa(x, y)|^2 \leq \frac{|\partial\Omega|}{32\varepsilon^2\pi^3} \int_{-\infty}^{\infty} e^{-2\varepsilon \Im \kappa(\omega)} d\omega \quad \text{for all } x, y \in \Omega_\varepsilon.$$

According to [Definition 2.3.1](#), we have $\Im \kappa(\omega) \geq \kappa_0 |\omega|^\beta$ for all $|\omega| \geq \omega_0$ for some $\omega_0 \geq 0$ and therefore, $|F_\kappa|^2$ is uniformly bounded. Thus, $F_\kappa \in L^2(\Omega_\varepsilon \times \Omega_\varepsilon)$, which implies that $\check{\mathcal{P}}_\kappa^* \check{\mathcal{P}}_\kappa$ is a Hilbert–Schmidt operator and compact, see for example [[Wei80](#), Theorems 6.10 and 6.11].

2. In the case of a weak attenuation coefficient, we write F_κ similar to the proof of [Lemma 2.4.2](#) as the sum of a contribution $F_\kappa^{(0)}$ of a medium with constant attenuation and perturbations

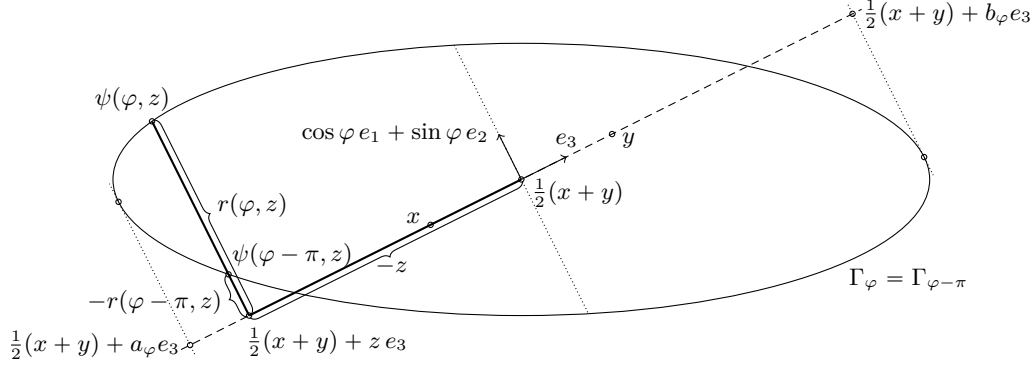


FIGURE 2.1: Parametrisation of the intersection Γ_φ , $\varphi \in (0, \pi)$, of the boundary $\partial\Omega$ and the plane E_φ .

$F_\kappa^{(1)}$ and $F_\kappa^{(2)}$: $F_\kappa = F_\kappa^{(0)} + F_\kappa^{(1)} + F_\kappa^{(2)}$ with

$$F_\kappa^{(j)}(x, y) = \frac{1}{32\pi^3} \int_{-\infty}^{\infty} \int_{\partial\Omega} \frac{e^{i\frac{\omega}{c}(|\xi-y| - |\xi-x|)}}{|\xi-y||\xi-x|} e^{-\kappa_\infty(|\xi-y| + |\xi-x|)} f_\kappa^{(j)}(\omega, \xi, x, y) dS(\xi) d\omega, \quad (2.34)$$

where

$$\begin{aligned} f_\kappa^{(0)}(\omega, \xi, x, y) &= 1, \\ f_\kappa^{(1)}(\omega, \xi, x, y) &= i\kappa_*(\omega)|\xi-y| - \overline{i\kappa_*(\omega)}|\xi-x|, \\ f_\kappa^{(2)}(\omega, \xi, x, y) &= e^{i\kappa_*(\omega)|\xi-y| - \overline{i\kappa_*(\omega)}|\xi-x|} - f_\kappa^{(1)}(\omega, \xi, x, y) - f_\kappa^{(0)}(\omega, \xi, x, y). \end{aligned}$$

- To calculate the double integral in $F_\kappa^{(0)}$, we first parametrise $\partial\Omega$ depending on the values $x, y \in \Omega_\varepsilon$ with $x \neq y$.

We choose a positively oriented, orthonormal basis $(e_j)_{j=1}^3 \subset \mathbb{R}^3$ with $e_3 = \frac{y-x}{|y-x|}$ and consider the curve

$$\Gamma_\varphi = \partial\Omega \cap E_\varphi, \quad E_\varphi = \{\xi \in \mathbb{R}^3 \mid \langle \xi - \frac{1}{2}(x+y), \cos \varphi e_2 - \sin \varphi e_1 \rangle = 0\},$$

given as the intersection of the boundary $\partial\Omega$ and the plane E_φ through $\frac{1}{2}(x+y)$, spanned by the vectors e_3 and $\cos \varphi e_1 + \sin \varphi e_2$.

Setting

$$a_\varphi = \min_{\xi \in \Gamma_\varphi} \langle \xi - \frac{1}{2}(x+y), e_3 \rangle \quad \text{and} \quad b_\varphi = \max_{\xi \in \Gamma_\varphi} \langle \xi - \frac{1}{2}(x+y), e_3 \rangle,$$

we choose the parametrisation $\psi \in C^1(U; \mathbb{R}^3)$ of $\partial\Omega$ (up to a set of measure zero) defined on the open set $U = \{(\varphi, z) \mid z \in (a_\varphi, b_\varphi), \varphi \in (-\pi, 0) \cup (0, \pi)\}$ as

$$\psi(\varphi, z) = \frac{1}{2}(x+y) + r(\varphi, z)(\cos \varphi e_1 + \sin \varphi e_2) + z e_3, \quad (2.35)$$

where we pick for $\varphi \in (0, \pi)$ the function r in such a way that $r(\varphi, z) > -r(\varphi - \pi, z)$ so that the two maps $\psi(\varphi - \pi, \cdot)$ and $\psi(\varphi, \cdot)$ parametrise together Γ_φ , see Figure 2.1.

- If we would formally interchange the order of integration in the definition (2.34) of $F_\kappa^{(0)}$, the integral over ω would lead to a δ -distribution at the zeros of the exponent $\frac{1}{c}(|\xi - x| - |\xi - y|)$. We therefore start by analysing this exponent, which is up to the prefactor $\frac{1}{c}$ given by

$$g(\varphi, z) = |\psi(\varphi, z) - x| - |\psi(\varphi, z) - y|$$

if we use the parametrisation ψ for integrating over $\partial\Omega$.

The zeros of g are exactly those points (φ, z) such that $\psi(\varphi, z)$ is in the bisection plane of x and y . Thus, we have by construction of the parametrisation ψ , see (2.35), that

$$g(\varphi, z) = 0 \quad \text{is equivalent to} \quad z = 0. \quad (2.36)$$

Furthermore, we can prove that

$$\partial_z g(\varphi, z) = \left\langle \frac{\psi(\varphi, z) - x}{|\psi(\varphi, z) - x|} - \frac{\psi(\varphi, z) - y}{|\psi(\varphi, z) - y|}, \partial_z \psi(\varphi, z) \right\rangle \quad (2.37)$$

only vanishes at the two points where $\psi(\varphi, z)$ is the intersection point of the line through x and y with $\partial\Omega$: We assume by contradiction that $\partial_z g(\varphi, z) = 0$ at a point $(\varphi, z) \in U$ with $\psi(\varphi, z)$ not lying on the line through x and y . Then, the first vector $\frac{\psi(\varphi, z) - x}{|\psi(\varphi, z) - x|} - \frac{\psi(\varphi, z) - y}{|\psi(\varphi, z) - y|}$ would be a non-zero vector in E_φ , and the second vector $\partial_z \psi(\varphi, z)$ is by construction a non-zero tangent vector on $\Gamma_\varphi \subset E_\varphi$ at $\psi(\varphi, z)$. Thus, $\partial_z g(\varphi, z) = 0$ would imply that the first vector is a non-trivial multiple of the outer unit normal vector $\nu(\psi(\varphi, z))$ to Γ_φ at $\psi(\varphi, z)$. However, if $w_1, w_2 \in \mathbb{R}^2$ are two unit vectors with $w_1 - w_2 = n$, $n \neq 0$, then $\langle w_1, n \rangle = -\langle w_2, n \rangle$, since for given $w_1 \in S^1$, w_2 is the intersection point of S^1 with the line parallel to n through w_1 . Thus, we would have

$$\left\langle \frac{\psi(\varphi, z) - x}{|\psi(\varphi, z) - x|}, \nu(\psi(\varphi, z)) \right\rangle = - \left\langle \frac{\psi(\varphi, z) - y}{|\psi(\varphi, z) - y|}, \nu(\psi(\varphi, z)) \right\rangle,$$

but, because of the convexity of Ω , the projections $\left\langle \frac{\psi - x}{|\psi - x|}, \nu \circ \psi \right\rangle$ and $\left\langle \frac{\psi - y}{|\psi - y|}, \nu \circ \psi \right\rangle$ have to be both positive, which is a contradiction. Therefore, $\partial_z g(\varphi, z) = 0$ if and only if $\psi(\varphi, z)$ is on the line through x and y .

- After these preparations, we can now reduce the formula (2.34) for $F_\kappa^{(0)}$ to a one-dimensional integral and estimate it explicitly to show that $F_\kappa^{(0)} \in L^2(\Omega_\varepsilon \times \Omega_\varepsilon)$.

We plug in the parametrisation ψ into the definition (2.34) of $F_\kappa^{(0)}$ and find for $x \neq y$

$$F_\kappa^{(0)}(x, y) = \int_{-\pi}^{\pi} \int_{-\infty}^{\infty} \int_{a_\varphi}^{b_\varphi} e^{i\omega g(\varphi, z)} \mu(\varphi, z, x, y) dz d\omega d\varphi, \quad (2.38)$$

where

$$\mu(\varphi, z, x, y) = \frac{1}{32\pi^3} \frac{e^{-\kappa_\infty(|\psi(\varphi, z) - y| + |\psi(\varphi, z) - x|)}}{|\psi(\varphi, z) - y||\psi(\varphi, z) - x|} \sqrt{\det(d\psi^T(\varphi, z) d\psi(\varphi, z))}. \quad (2.39)$$

To evaluate the integrals, we remark that if $\lambda \in C^1(\mathbb{R})$ is a real-valued, strictly monotone function with $\lambda(\mathbb{R}) = I \subset \mathbb{R}$ and $\rho \in L^1(\mathbb{R}^2)$, then

$$\int_{-\infty}^{\infty} \int_{-\infty}^{\infty} e^{i\omega\lambda(z)} \rho(z) dz d\omega = \int_{-\infty}^{\infty} \int_{-\infty}^{\infty} e^{i\omega\zeta} \rho_\lambda(\zeta) d\zeta d\omega, \quad \text{where} \quad \rho_\lambda(\zeta) = \frac{\rho(\lambda^{-1}(\zeta))}{|\lambda'(\lambda^{-1}(\zeta))|} \chi_I(\zeta)$$

with the characteristic function χ_I of the interval I . Now, the inner integral is up to the missing factor $\frac{1}{\sqrt{2\pi}}$ exactly the inverse Fourier transform $\check{\rho}_\lambda$ of ρ_λ so that we get

$$\int_{-\infty}^{\infty} \int_{-\infty}^{\infty} e^{i\omega\lambda(z)} \rho(z) dz d\omega = \sqrt{2\pi} \int_{-\infty}^{\infty} \check{\rho}_\lambda(\omega) d\omega = 2\pi \rho_\lambda(0).$$

Applying this result to the two inner integrals in (2.38), where we use from above that $g(\varphi, \cdot)$ has only two critical points and is therefore piecewise strictly monotone to first split the innermost integral into integrals over intervals where $\partial_z g(\varphi, z) \neq 0$, we find with (2.36) that

$$F_\kappa^{(0)}(x, y) = 2\pi \int_{-\pi}^{\pi} \frac{\mu(\varphi, 0, x, y)}{|\partial_z g(\varphi, 0)|} d\varphi. \quad (2.40)$$

Evaluating (2.37) at $z = 0$, we find with $|\psi(\varphi, 0) - x| = |\psi(\varphi, 0) - y|$, see (2.36), and the explicit formula (2.35) for the parametrisation ψ that

$$\partial_z g(\varphi, 0) = \left\langle \frac{y - x}{|\psi(\varphi, 0) - x|}, \partial_z r(\varphi, 0)(\cos \varphi e_1 + \sin \varphi e_2) + e_3 \right\rangle = \frac{|y - x|}{|\psi(\varphi, 0) - x|}.$$

Plugging this together with formula (2.39) for μ into (2.40), we finally get for $F_\kappa^{(0)}$ the representation

$$F_\kappa^{(0)}(x, y) = \frac{1}{16\pi^2 |y - x|} \int_{-\pi}^{\pi} \frac{e^{-2\kappa_\infty |\psi(\varphi, 0) - x|}}{|\psi(\varphi, 0) - x|} \sqrt{\det(d\psi^T(\varphi, 0) d\psi(\varphi, 0))} d\varphi. \quad (2.41)$$

This is an integral over the intersection $\gamma_{x,y} = \{\xi \in \partial\Omega \mid \langle \xi - \frac{1}{2}(x + y), y - x \rangle = 0\}$ of $\partial\Omega$ and the bisection plane of the points x and y . To express it in a parametrisation invariant form, we write it as a line integral over $\gamma_{x,y}$, which means we want to use the volume element $|\partial_\varphi \psi(\varphi, 0)| d\varphi$. Calculating the outer unit normal vector explicitly from (2.35), we find

$$\nu \circ \psi = \frac{\partial_\varphi \psi \times \partial_z \psi}{\sqrt{\det(d\psi^T d\psi)}} = \frac{r e_1 + \partial_\varphi r e_2 - r \partial_z r e_3}{\sqrt{\det(d\psi^T d\psi)}}.$$

Thus, we get the relation

$$|\partial_\varphi \psi|^2 = r^2 + (\partial_\varphi r)^2 = \det(d\psi^T d\psi) |\nu \circ \psi - \langle \nu \circ \psi, e_3 \rangle e_3|^2.$$

With this, we can write (2.41) as the parametrisation free line integral

$$F_\kappa^{(0)}(x, y) = \frac{1}{16\pi^2|y-x|} \int_{\gamma_{x,y}} \frac{e^{-2\kappa_\infty|\xi-x|}}{|\xi-x|} \left| \nu(\xi) - \left\langle \frac{y-x}{|y-x|}, \nu(\xi) \right\rangle \frac{y-x}{|y-x|} \right|^{-1} dS(\xi). \quad (2.42)$$

In particular, we have

$$|F_\kappa^{(0)}(x, y)| \leq \frac{A}{|x-y|} \quad \text{for all } x, y \in \Omega_\varepsilon \quad \text{with } x \neq y \quad (2.43)$$

for some constant $A > 0$, and therefore $F_\kappa^{(0)} \in L^2(\Omega_\varepsilon \times \Omega_\varepsilon)$.

- To estimate the first perturbation $F_\kappa^{(1)}$, we remark that, according to Definition 2.3.2, κ_* is bounded and square integrable. We can therefore pull in the definition (2.34) of $F_\kappa^{(1)}$ the integration over the variable ω as an inverse Fourier transform inside the surface integral and find that

$$F_\kappa^{(1)}(x, y) = \frac{1}{16\pi^2\sqrt{2\pi}} \int_{\partial\Omega} i e^{-\kappa_\infty(|\xi-y|+|\xi-x|)} \times \left(\frac{\check{\kappa}_*\left(\frac{1}{c}(|\xi-y|-|\xi-x|)\right)}{|\xi-x|} - \frac{\check{\kappa}_*\left(\frac{1}{c}(|\xi-x|-|\xi-y|)\right)}{|\xi-y|} \right) dS(\xi).$$

Choosing now a radius $R > \text{diam } \Omega$, we get by applying Hölder's inequality and increasing the domain of integration that

$$\int_{\Omega_\varepsilon} \int_{\Omega_\varepsilon} |F_\kappa^{(1)}(x, y)|^2 dx dy \leq \frac{|\partial\Omega|}{128\pi^5\varepsilon^2} \int_{\partial\Omega} \int_{B_R(\xi)} \int_{B_R(\xi)} |\check{\kappa}_*\left(\frac{1}{c}(|\xi-y|-|\xi-x|)\right)|^2 dx dy dS(\xi)$$

Thus, switching in the two inner integrals to spherical coordinates around the point ξ , we find

$$\int_{\Omega_\varepsilon} \int_{\Omega_\varepsilon} |F_\kappa^{(1)}(x, y)|^2 dx dy \leq \frac{|\partial\Omega|^2 R^4}{8\pi^3\varepsilon^2} \int_0^R \int_0^R |\check{\kappa}_*\left(\frac{1}{c}(r-\rho)\right)|^2 dr d\rho \leq \frac{|\partial\Omega|^2 R^5 c}{8\pi^3\varepsilon^2} \|\check{\kappa}_*\|_2^2,$$

which shows that $F_\kappa^{(1)} \in L^2(\Omega_\varepsilon \times \Omega_\varepsilon)$.

- The second perturbation $F_\kappa^{(2)}$ can be bounded directly via

$$|F_\kappa^{(2)}(x, y)| \leq \frac{1}{32\pi^3\varepsilon^2} \int_{-\infty}^{\infty} \int_{\partial\Omega} |f_\kappa^{(2)}(\omega, \xi, x, y)| dS(\xi) d\omega \quad (2.44)$$

for all $x, y \in \Omega_\varepsilon$. Using that for every bounded set $D \subset \mathbb{C}$, there exists a constant $C > 0$ such that

$$|e^z - z - 1| \leq C|z|^2 \quad \text{for all } z \in D$$

holds, we find a constant $\tilde{C} > 0$ so that

$$|f_\kappa^{(2)}(\omega, \xi, x, y)| \leq \tilde{C} |\kappa_*(\omega)|^2 \quad \text{for all } \omega \in \mathbb{R}, \xi \in \partial\Omega, x, y \in \Omega_\varepsilon. \quad (2.45)$$

Plugging this into (2.44), we get that

$$|F_\kappa^{(2)}(x, y)| \leq \frac{\tilde{C} |\partial\Omega|}{32\pi^3 \varepsilon^2} \|\kappa_*\|_2^2 \quad \text{for all } x, y \in \Omega_\varepsilon.$$

Thus, in particular, we have $F_\kappa^{(2)} \in L^2(\Omega_\varepsilon \times \Omega_\varepsilon)$.

We conclude therefore that $F_\kappa = F_\kappa^{(0)} + F_\kappa^{(1)} + F_\kappa^{(2)} \in L^2(\Omega_\varepsilon \times \Omega_\varepsilon)$, which shows as in the first part of the proof that $\check{\mathcal{P}}_\kappa^* \check{\mathcal{P}}_\kappa$ is a Hilbert–Schmidt operator and compact. \square

2.5 Singular Values of the Integrated Photoacoustic Operator

We have seen in Proposition 2.4.3 that the operator $\check{\mathcal{P}}_\kappa^* \check{\mathcal{P}}_\kappa$, given by (2.33), is a compact operator. The inversion of the photoacoustic problem is therefore ill-posed. To quantify the ill-posedness, we want to study the decay of the eigenvalues $(\lambda_n(\check{\mathcal{P}}_\kappa^* \check{\mathcal{P}}_\kappa))_{n \in \mathbb{N}}$ of $\check{\mathcal{P}}_\kappa^* \check{\mathcal{P}}_\kappa$, where we enumerate the eigenvalues in decreasing order: $0 \leq \lambda_{n+1}(\check{\mathcal{P}}_\kappa^* \check{\mathcal{P}}_\kappa) \leq \lambda_n(\check{\mathcal{P}}_\kappa^* \check{\mathcal{P}}_\kappa)$ for all $n \in \mathbb{N}$.

We differ again between the two cases of a strong and of a weak attenuation coefficient κ .

2.5.1 Strongly Attenuating Media

To obtain the behaviour of the eigenvalues of $\check{\mathcal{P}}_\kappa^* \check{\mathcal{P}}_\kappa$ in the case of a strong attenuation coefficient κ , see Definition 2.3.1, we will use Corollary 2.A.4 which gives a criterion for a general integral operator with smooth kernel to have exponentially fast decaying eigenvalues in terms of an upper bound on the derivatives of the kernel, see (2.79). We therefore only have to check that the kernel (2.32) of $\check{\mathcal{P}}_\kappa^* \check{\mathcal{P}}_\kappa$ fulfils these estimates. The calculations are straightforward (although a bit tedious) and can be found explicitly in section 2.B.

Proposition 2.5.1 *Let Ω be a bounded Lipschitz domain in \mathbb{R}^3 , $\varepsilon > 0$ and $\check{\mathcal{P}}_\kappa : L^2(\Omega_\varepsilon) \rightarrow L^2(\mathbb{R} \times \partial\Omega)$ be the integrated photoacoustic operator of a strong attenuation coefficient κ .*

Then, the kernel F_κ of $\check{\mathcal{P}}_\kappa^ \check{\mathcal{P}}_\kappa$, explicitly given by (2.32), fulfils the estimate*

$$\frac{1}{j!} \sup_{x, y \in \Omega_\varepsilon} \sup_{v \in S^2} \left| \frac{\partial^j}{\partial s^j} \Big|_{s=0} F_\kappa(x, y + sv) \right| \leq B b^j j^{(\frac{N}{\beta} - 1)j} \quad \text{for all } j \in \mathbb{N}_0, \quad (2.46)$$

for some constants $B, b > 0$, where $N \in \mathbb{N}$ denotes the exponent for $\ell = 0$ in the condition (2.5) and $\beta \in (0, N]$ is the exponent in the condition (2.24) for the strong attenuation coefficient κ .

Proof: Putting the derivatives with respect to s inside the integrals in the definition (2.32) of the kernel F_κ , we get that

$$\frac{\partial^j}{\partial s^j} \Big|_{s=0} F_\kappa(x, y + sv) = \int_{-\infty}^{\infty} \frac{1}{\omega^2} \int_{\partial\Omega} \overline{G_\kappa(\omega, x - \xi)} \frac{\partial^j}{\partial s^j} \Big|_{s=0} G_\kappa(\omega, y - \xi + sv) dS(\xi) d\omega,$$

where G_κ denotes the integral kernel (2.19). We remark that the term $\frac{1}{\omega^2}$ comes from the fact that we consider the integrated photoacoustic operator instead of the operator which maps directly the measurements to the initial data.

Using Proposition 2.B.3 to estimate the derivative of G_κ , we find a constant $C > 0$ so that

$$\begin{aligned} & \left| \frac{1}{j!} \left| \frac{\partial^j}{\partial s^j} \right|_{s=0} F_\kappa(x, y + sv) \right| \\ & \leq C^j \int_{-\infty}^{\infty} \frac{1}{\omega^2} \int_{\partial\Omega} |G_\kappa(\omega, x - \xi)| |G_\kappa(\omega, y - \xi)| \left(\frac{1}{|y - \xi|^j} + \frac{1}{j!} |\kappa(\omega)|^j \right) dS(\xi) d\omega. \end{aligned}$$

From the uniform estimate

$$|G_\kappa(\omega, x - \xi)| \leq \frac{|\omega| e^{-\varepsilon \Im \kappa(\omega)}}{4\pi\varepsilon\sqrt{2\pi}} \quad \text{for all } x \in \Omega_\varepsilon, \xi \in \partial\Omega, \omega \in \mathbb{R},$$

which is directly obtained from the definition (2.19) of G_κ by using that $|x - \xi| \geq \varepsilon$ for all $\xi \in \partial\Omega$ and $x \in \Omega_\varepsilon$, it then follows that

$$\left| \frac{1}{j!} \left| \frac{\partial^j}{\partial s^j} \right|_{s=0} F_\kappa(x, y + sv) \right| \leq \frac{|\partial\Omega| C^j}{32\pi^3 \varepsilon^2} \int_{-\infty}^{\infty} e^{-2\varepsilon \Im \kappa(\omega)} \left(\frac{1}{\varepsilon^j} + \frac{1}{j!} |\kappa(\omega)|^j \right) d\omega.$$

Applying now Lemma 2.B.4 (for the first term in the integrand, we use Lemma 2.B.4 with $j = 0$), we find constants $B, b > 0$ so that

$$\left| \frac{1}{j!} \left| \frac{\partial^j}{\partial s^j} \right|_{s=0} F(x, y + sv) \right| \leq B b^j j^{\left(\frac{N}{\beta} - 1\right)j} \quad \text{for all } x, y \in \Omega_\varepsilon, v \in S^2, j \in \mathbb{N}_0. \quad \square$$

Combining Proposition 2.5.1 with Corollary 2.A.4, we obtain the decay of the singular values of the integrated photoacoustic operator.

Corollary 2.5.2 *Let Ω be a bounded Lipschitz domain in \mathbb{R}^3 , $\varepsilon > 0$, and $\check{\mathcal{P}}_\kappa : L^2(\Omega_\varepsilon) \rightarrow L^2(\mathbb{R} \times \partial\Omega)$ be the integrated photoacoustic operator of a strong attenuation coefficient κ .*

Then, there exist constants $C, c > 0$ so that the eigenvalues $(\lambda_n(\check{\mathcal{P}}_\kappa^ \check{\mathcal{P}}_\kappa))_{n \in \mathbb{N}}$ of $\check{\mathcal{P}}_\kappa^* \check{\mathcal{P}}_\kappa$ in decreasing order fulfil*

$$\lambda_n(\check{\mathcal{P}}_\kappa^* \check{\mathcal{P}}_\kappa) \leq C n^{\frac{N}{\beta}} \exp\left(-cn^{\frac{\beta}{Nm}}\right) \quad \text{for all } n \in \mathbb{N}. \quad (2.47)$$

Proof: According to Proposition 2.5.1, we know that there exist constants $B, b > 0$ so that the integral kernel F_κ of the operator $\check{\mathcal{P}}_\kappa^* \check{\mathcal{P}}_\kappa$ fulfils the estimate (2.46). Applying thus Corollary 2.A.4 with $\mu = \frac{N}{\beta} - 1$ to the operator $\check{\mathcal{P}}_\kappa^* \check{\mathcal{P}}_\kappa$, we obtain the decay rate (2.47). \square

2.5.2 Weakly Attenuating Media

To analyse the operator $\check{\mathcal{P}}_\kappa^* \check{\mathcal{P}}_\kappa$ in the case of a weak attenuation coefficient κ , see Definition 2.3.2, we split $\check{\mathcal{P}}_\kappa$ as in the proof of Lemma 2.4.2 in $\check{\mathcal{P}}_\kappa = \check{\mathcal{P}}_\kappa^{(0)} + \check{\mathcal{P}}_\kappa^{(1)}$, see (2.28) and (2.29). We will show that decomposing the operator as $\check{\mathcal{P}}_\kappa^* \check{\mathcal{P}}_\kappa = \check{\mathcal{P}}_\kappa^{(0)*} \check{\mathcal{P}}_\kappa^{(0)} + \mathcal{Q}_\kappa$, the eigenvalues of the

operator $\mathcal{Q}_\kappa = \check{\mathcal{P}}_\kappa^{(0)*}\check{\mathcal{P}}_\kappa^{(1)} + \check{\mathcal{P}}_\kappa^{(1)*}\check{\mathcal{P}}_\kappa^{(0)} + \check{\mathcal{P}}_\kappa^{(1)*}\check{\mathcal{P}}_\kappa^{(1)}$ decay faster than those of $\check{\mathcal{P}}_\kappa^{(0)*}\check{\mathcal{P}}_\kappa^{(0)}$ so that \mathcal{Q}_κ does not alter the asymptotic decay rate of the eigenvalues of $\check{\mathcal{P}}_\kappa^{(0)*}\check{\mathcal{P}}_\kappa^{(0)}$.

The term $\check{\mathcal{P}}_\kappa^{(0)*}\check{\mathcal{P}}_\kappa^{(0)}$ corresponds to a constant attenuation and its behaviour was already discussed in [Pal10].

Lemma 2.5.3 *Let κ be a weak attenuation coefficient, $\Omega \subset \mathbb{R}^3$ be a bounded, convex domain with smooth boundary, and $\varepsilon > 0$. We define the operator $\check{\mathcal{P}}_\kappa^{(0)} : L^2(\Omega_\varepsilon) \rightarrow L^2(\Omega_\varepsilon)$ by (2.28). Then, there exist constants $C_1, C_2 > 0$ such that we have*

$$C_1 n^{-\frac{2}{3}} \leq \lambda_n(\check{\mathcal{P}}_\kappa^{(0)*}\check{\mathcal{P}}_\kappa^{(0)}) \leq C_2 n^{-\frac{2}{3}} \quad \text{for all } n \in \mathbb{N}. \quad (2.48)$$

Proof: The idea of the proof is to show that the operator $\check{\mathcal{P}}_\kappa^{(0)*}\check{\mathcal{P}}_\kappa^{(0)}$ has the same eigenvalues as an elliptic pseudodifferential operator $\mathcal{T} : L^2(M) \rightarrow L^2(M)$ of order -2 on a closed manifold M . Then, we can apply the result [Shu87, Theorem 15.2] to obtain the asymptotic behaviour of the eigenvalues.

- First, we want to replace the operator $\check{\mathcal{P}}_\kappa^{(0)*}\check{\mathcal{P}}_\kappa^{(0)}$ by a pseudodifferential operator \mathcal{T} on a closed manifold with the same eigenvalues.

We have seen in the proof of Proposition 2.4.3 that the operator $\check{\mathcal{P}}_\kappa^{(0)*}\check{\mathcal{P}}_\kappa^{(0)}$ is an integral operator with integral kernel $F_\kappa^{(0)}$ defined by (2.34). We now generate the closed manifold M by taking two copies of $\overline{\Omega_\varepsilon}$ and identifying their boundary points: $M = (\overline{\Omega_\varepsilon} \times \{1, 2\}) / \sim$ with the equivalence relation $(x, a) \sim (\tilde{x}, \tilde{a})$ if and only if $x = \tilde{x}$ and either $a = \tilde{a}$ or $x \in \partial\Omega_\varepsilon$. This is called the double of the manifold with boundary $\overline{\Omega_\varepsilon}$, see for example [Lee13, Example 9.32]. Then, the operator $\mathcal{T} : L^2(M) \rightarrow L^2(M)$ given by

$$\mathcal{T}h([x, a]) = \frac{1}{2} \sum_{b=1}^2 \int_{\Omega_\varepsilon} F_\kappa^{(0)}(x, y) h([y, b]) \, dy$$

has the same non-zero eigenvalues as $\check{\mathcal{P}}_\kappa^{(0)*}\check{\mathcal{P}}_\kappa^{(0)} : L^2(\Omega_\varepsilon) \rightarrow L^2(\Omega_\varepsilon)$. Indeed, if h is an eigenfunction of \mathcal{T} with eigenvalue $\lambda \neq 0$, then necessarily $h([x, 1]) = h([x, 2])$ for almost every $x \in \Omega_\varepsilon$ and therefore $x \mapsto h([x, 1])$ is an eigenfunction of $\check{\mathcal{P}}_\kappa^{(0)*}\check{\mathcal{P}}_\kappa^{(0)}$ with eigenvalue λ . Conversely, if h is an eigenfunction of $\check{\mathcal{P}}_\kappa^{(0)*}\check{\mathcal{P}}_\kappa^{(0)}$ with eigenvalue λ , then clearly $[x, a] \mapsto h(x)$ is an eigenfunction of \mathcal{T} with eigenvalue λ .

To write \mathcal{T} in the form of a pseudodifferential operator, we extend the kernel $F_\kappa^{(0)}$ to a smooth function $\tilde{F}_\kappa^{(0)} \in C^\infty(\Omega_\varepsilon \times \mathbb{R}^3)$ by choosing an arbitrary cut-off function $\phi \in C_c^\infty(\mathbb{R}^3)$ with $\phi(y) = 1$ for $y \in \Omega_\varepsilon$ and $\text{supp } \phi \subset \Omega$ and setting

$$\tilde{F}_\kappa^{(0)}(x, y) = \frac{\phi(y)}{32\pi^3} \int_{-\infty}^{\infty} \int_{\partial\Omega} \frac{e^{-\kappa_\infty(|\xi-y|+|\xi-x|)}}{|\xi-y||\xi-x|} e^{i\frac{\omega}{c}(|\xi-y|-|\xi-x|)} \, dS(\xi) \, d\omega, \quad x \in \Omega_\varepsilon, \, y \in \mathbb{R}^3. \quad (2.49)$$

Then, defining g up to the normalisation factor $(2\pi)^{\frac{3}{2}}$ as the inverse Fourier transform of $\tilde{F}_\kappa^{(0)}$ with respect to y :

$$g(x, k) = \int_{\mathbb{R}^3} \tilde{F}_\kappa^{(0)}(x, y) e^{-i\langle k, x-y \rangle} \, dy, \quad x \in \Omega_\varepsilon, \, k \in \mathbb{R}^3, \quad (2.50)$$

we can write the kernel $F_\kappa^{(0)}$ with the Fourier inversion theorem in the form

$$F_\kappa^{(0)}(x, y) = \frac{1}{(2\pi)^3} \int_{\mathbb{R}^3} g(x, k) e^{i\langle k, x-y \rangle} dk, \quad x, y \in \Omega_\varepsilon,$$

where g is smooth, since $g(x, \cdot)$ is the Fourier transform of a function with compact support.

- In the expression (2.50) for g , the integral over ω from the definition (2.49) of $\tilde{F}_\kappa^{(0)}$ can be seen as a one-dimensional inverse Fourier transform, which allows us to get rid of two one-dimensional integrals.

To this end, we pull the outer integral over \mathbb{R}^3 inside both other integrals and write it in spherical coordinates around the point ξ : $y = \xi + r\theta$ with $r > 0$ and $\theta \in S^2$. This gives us

$$\begin{aligned} g(x, k) &= \frac{1}{32\pi^3} \int_{\partial\Omega} e^{i\langle k, \xi-x \rangle} \int_{S^2} \int_{-\infty}^{\infty} e^{-i\frac{\omega}{c}|\xi-x|} \\ &\quad \times \int_0^\infty \frac{r e^{-\kappa_\infty(r+|\xi-x|)}}{|\xi-x|} \phi(\xi + r\theta) e^{i(\frac{\omega}{c} + \langle k, \theta \rangle)r} dr d\omega dS(\theta) dS(\xi). \end{aligned}$$

For every $\xi \in \partial\Omega$ and every $\theta \in S^2$, the two inner integrals with respect to r and ω each represent a Fourier transform and we get with $\rho(r) = \frac{r e^{-\kappa_\infty(r+|\xi-x|)}}{|\xi-x|} \phi(\xi + r\theta) \chi_{[0, \infty)}(r)$ that

$$\begin{aligned} \int_{-\infty}^{\infty} e^{-i\frac{\omega}{c}|\xi-x|} \int_0^\infty \rho(r) e^{i(\frac{\omega}{c} + \langle k, \theta \rangle)r} dr d\omega &= \sqrt{2\pi} \int_{-\infty}^{\infty} \check{\rho}\left(\frac{\omega}{c} + \langle k, \theta \rangle\right) e^{-i\frac{\omega}{c}|\xi-x|} d\omega \\ &= 2\pi c e^{i|\xi-x|\langle k, \theta \rangle} \rho(|\xi-x|). \end{aligned}$$

Thus, we find

$$g(x, k) = \frac{c}{16\pi^2} \int_{\partial\Omega} \int_{S^2} e^{-2\kappa_\infty|\xi-x|} \phi(\xi + |\xi-x|\theta) e^{i(|\xi-x|\langle k, \theta \rangle + \langle k, \xi-x \rangle)} dS(\theta) dS(\xi). \quad (2.51)$$

- We are now interested in the leading order asymptotics of $g(x, k)$ as $|k| \rightarrow \infty$. To obtain this, we will apply the stationary phase method, see for example [HÖ3, Theorem 7.7.5].

So, let $\psi \in C^\infty(U; \mathbb{R}^3)$ be a parametrisation of $\partial\Omega$ and $\Theta \in C^\infty(V; \mathbb{R}^3)$ be a parametrisation of S^2 with some open sets $U, V \subset \mathbb{R}^2$. Then, according to the stationary phase method, the asymptotics is determined by the region around the critical points of the phase function

$$\Phi_{x,k}(\eta, \vartheta) = |\psi(\eta) - x| \langle k, \Theta(\vartheta) \rangle + \langle k, \psi(\eta) - x \rangle$$

in the integrand in (2.51). The optimality conditions

$$0 = \partial_{\vartheta_i} \Phi_{x,k}(\eta, \vartheta) = |\psi(\eta) - x| \langle k, \partial_{\vartheta_i} \Theta(\vartheta) \rangle, \quad i = 1, 2,$$

with respect to ϑ imply that k is normal to the tangent space of S^2 in the point $\Theta(\vartheta)$ at a critical point (η, ϑ) of $\Phi_{x,k}$, that is $\Theta(\vartheta) = \pm \frac{k}{|k|}$. The optimality conditions

$$0 = \partial_{\eta_i} \Phi_{x,k}(\eta, \vartheta) = \left\langle \partial_{\eta_i} \psi(\eta), \pm |k| \frac{\psi(\eta) - x}{|\psi(\eta) - x|} + k \right\rangle, \quad i = 1, 2,$$

with respect to η then imply for a critical point (η, ϑ) of $\Phi_{x,k}$ that the projections of the two vectors $-\frac{\psi(\eta) - x}{|\psi(\eta) - x|}$ and $\Theta(\vartheta) = \pm \frac{k}{|k|}$ on the tangent space of $\partial\Omega$ at $\psi(\eta)$ coincide. Since both vectors have unit length, this means that up to the sign of the normal component they have to be equal. Additionally, we use that, because of the cut-off term $\phi(\psi(\eta) + |\psi(\eta) - x|\Theta(\vartheta))$ in the integrand, the critical points at which the vector $\Theta(\vartheta)$ points outwards the domain Ω at $\psi(\eta)$ do not contribute to the integral. Therefore, a relevant critical point (η, ϑ) is such that $\Theta(\vartheta)$ is pointing inwards at $\psi(\eta)$ and since $-\frac{\psi(\eta) - x}{|\psi(\eta) - x|}$ is also pointing inwards, we are left with the two critical points $(\eta^{(\ell)}, \vartheta^{(\ell)})$ given by

$$\Theta(\vartheta^{(\ell)}) = (-1)^\ell \frac{k}{|k|} = -\frac{\psi(\eta^{(\ell)}) - x}{|\psi(\eta^{(\ell)}) - x|}, \quad \ell = 1, 2.$$

In particular, we have $\Phi_{x,k}(\eta^{(\ell)}, \vartheta^{(\ell)}) = 0$.

For the second derivatives of $\Phi_{x,k}$ at the critical points, we find

$$\begin{aligned} \partial_{\eta_i \eta_j} \Phi_{x,k}(\eta^{(\ell)}, \vartheta^{(\ell)}) &= \frac{(-1)^\ell |k|}{|\psi(\eta) - x|} \left(\left\langle \partial_{\eta_i} \psi(\eta^{(\ell)}), \partial_{\eta_j} \psi(\eta^{(\ell)}) \right\rangle - \left\langle \partial_{\eta_i} \psi(\eta^{(\ell)}), \frac{k}{|k|} \right\rangle \left\langle \partial_{\eta_j} \psi(\eta^{(\ell)}), \frac{k}{|k|} \right\rangle \right), \\ \partial_{\vartheta_i \vartheta_j} \Phi_{x,k}(\eta^{(\ell)}, \vartheta^{(\ell)}) &= |\psi(\eta^{(\ell)}) - x| \left\langle k, \partial_{\vartheta_i \vartheta_j} \Theta(\vartheta^{(\ell)}) \right\rangle, \\ \partial_{\eta_i \vartheta_j} \Phi_{x,k}(\eta^{(\ell)}, \vartheta^{(\ell)}) &= 0. \end{aligned}$$

For the determinants of the derivatives with respect to η and ϑ , we obtain (this can be readily checked for parametrisations ψ and Θ corresponding to normal coordinates at the points $(\psi(\eta^{(\ell)}), \Theta(\vartheta^{(\ell)}))$)

$$\begin{aligned} \det(\partial_{\eta_i \eta_j} \Phi_{x,k}(\eta^{(\ell)}, \vartheta^{(\ell)}))_{i,j=1}^2 &= \frac{\left\langle k, \nu(\psi(\eta^{(\ell)})) \right\rangle^2}{|\psi(\eta^{(\ell)}) - x|^2} \det(d\psi^T(\eta^{(\ell)}) d\psi(\eta^{(\ell)})), \\ \det(\partial_{\vartheta_i \vartheta_j} \Phi_{x,k}(\eta^{(\ell)}, \vartheta^{(\ell)}))_{i,j=1}^2 &= |k|^2 \det(d\Theta^T(\vartheta^{(\ell)}) d\Theta(\vartheta^{(\ell)})), \end{aligned}$$

where $\nu : \partial\Omega \rightarrow S^2$ denotes the outer unit normal vector field on $\partial\Omega$.

Therefore, the stationary phase method, see for example [Hö3, Theorem 7.7.5], implies for $x \in \Omega_\varepsilon$, $k \in \mathbb{R}^3$, and $\mu > 0$ that we have asymptotically for $\mu \rightarrow \infty$

$$\begin{aligned} g(x, \mu k) &= \frac{c}{16\pi^2} \int_{U \times V} e^{-2\kappa_\infty |\psi(\eta) - x|} \phi(\psi(\eta) + |\psi(\eta) - x|\Theta(\vartheta)) e^{i\mu \Phi_{x,k}(\eta, \vartheta)} \\ &\quad \times \sqrt{\det(d\psi^T(\eta) d\psi(\eta)) \det(d\Theta^T(\vartheta) d\Theta(\vartheta))} d(\eta, \vartheta) \\ &= \frac{c}{4|k|\mu^2} \sum_{\ell=1}^2 \frac{|\psi(\eta^{(\ell)}) - x|}{|\langle k, \nu(\psi(\eta^{(\ell)})) \rangle|} e^{-2\kappa_\infty |\psi(\eta^{(\ell)}) - x|} + \mathcal{O}\left(\frac{1}{\mu^3}\right). \end{aligned}$$

Thus, g is of the form

$$g(x, k) = g_{-2}(x, k) + \mathcal{O}(|k|^{-3})$$

with $g_{-2}(x, \cdot)$ being a positive function which is homogeneous of order -2 .

Therefore, a parameterix of the pseudodifferential operator \mathcal{T} on $L^2(M)$ is an elliptic pseudodifferential operator of order 2 and thus has, according to [Shu87, Theorem 15.2], eigenvalues which grow as $n^{\frac{2}{3}}$. Consequently, the eigenvalues of \mathcal{T} and thus also those of $\check{\mathcal{P}}_\kappa^* \check{\mathcal{P}}_\kappa$ decay as $n^{-\frac{2}{3}}$. \square

To estimate the eigenvalues of the term $\check{\mathcal{P}}_\kappa^{(1)*} \check{\mathcal{P}}_\kappa^{(1)}$ in $\check{\mathcal{P}}_\kappa^* \check{\mathcal{P}}_\kappa$, we show with Mercer's theorem that the operator is trace class.

Lemma 2.5.4 *Let κ be a weak attenuation coefficient, $\Omega \subset \mathbb{R}^3$ be a bounded, convex domain with smooth boundary, and $\varepsilon > 0$. We define the operator $\check{\mathcal{P}}_\kappa^{(1)} : L^2(\Omega_\varepsilon) \rightarrow L^2(\Omega_\varepsilon)$ by (2.29). Then, we have that*

$$\lim_{n \rightarrow \infty} n \lambda_n(\check{\mathcal{P}}_\kappa^{(1)*} \check{\mathcal{P}}_\kappa^{(1)}) = 0. \quad (2.52)$$

Proof: Using the definition (2.29) of $\check{\mathcal{P}}_\kappa^{(1)}$, we find that

$$\check{\mathcal{P}}_\kappa^{(1)*} \check{\mathcal{P}}_\kappa^{(1)} h(x) = \int_{\Omega_\varepsilon} R_\kappa(x, y) h(y) \, dy$$

with the integral kernel

$$R_\kappa(x, y) = \frac{1}{32\pi^3} \int_{-\infty}^{\infty} \int_{\partial\Omega} r_\kappa(\xi, \omega, x, y) \, dS(\xi) \, d\omega,$$

$$r_\kappa(\xi, \omega, x, y) = \frac{e^{i\frac{\omega}{c}(|\xi-y| - |\xi-x|)}}{|\xi-y||\xi-x|} e^{-\kappa_\infty(|\xi-y| + |\xi-x|)} (e^{i\kappa_*(\omega)|\xi-y|} - 1)(e^{-i\overline{\kappa_*(\omega)}|\xi-x|} - 1).$$

Since for every bounded set $D \subset \mathbb{C}$, there exists a constant C such that

$$|e^z - 1| \leq C|z| \quad \text{for all } z \in D,$$

we find a constant $\tilde{C} > 0$ such that the integrand r_κ is uniformly estimated by an integrable function:

$$|r_\kappa(\xi, \omega, x, y)| \leq \tilde{C} |\kappa_*(\omega)|^2 \quad \text{for all } x, y \in \overline{\Omega_\varepsilon}, \xi \in \partial\Omega, \omega \in \mathbb{R}.$$

Taking now an arbitrary sequence $(x_k, y_k)_{k \in \mathbb{N}} \subset \Omega_\varepsilon$ converging to an element $(x, y) \in \overline{\Omega_\varepsilon}$, we get with the dominated convergence theorem and the continuity of r_κ that

$$\lim_{k \rightarrow \infty} R_\kappa(x_k, y_k) = \frac{1}{32\pi^3} \int_{-\infty}^{\infty} \int_{\partial\Omega} \lim_{k \rightarrow \infty} r_\kappa(\xi, \omega, x_k, y_k) \, dS(\xi) \, d\omega = R_\kappa(x, y).$$

Thus, R_κ is continuous and therefore Mercer's theorem, see for example [CH53, Chapter III, Section 5 and 9], implies that

$$\sum_{n=1}^{\infty} \lambda_n(\check{\mathcal{P}}_\kappa^{(1)*} \check{\mathcal{P}}_\kappa^{(1)}) < \infty.$$

Since $(\lambda_n(\check{\mathcal{P}}_\kappa^{(1)*} \check{\mathcal{P}}_\kappa^{(1)}))_{n=1}^{\infty}$ is by definition a decreasing sequence, Abel's theorem, see for example [Har21, §173], gives us (2.52). \square

From the decay rates of the singular values of $\check{\mathcal{P}}_\kappa^{(0)}$ and $\check{\mathcal{P}}_\kappa^{(1)}$, we can directly deduce the decay rate of the perturbation $\check{\mathcal{P}}_\kappa^* \check{\mathcal{P}}_\kappa - \check{\mathcal{P}}_\kappa^{(0)*} \check{\mathcal{P}}_\kappa^{(0)}$.

Lemma 2.5.5 *Let κ be a weak attenuation coefficient, $\Omega \subset \mathbb{R}^3$ be a bounded, convex domain with smooth boundary, and $\varepsilon > 0$.*

Then, the operator

$$\mathcal{Q}_\kappa : L^2(\Omega_\varepsilon) \rightarrow L^2(\Omega_\varepsilon), \quad \mathcal{Q}_\kappa = \check{\mathcal{P}}_\kappa^* \check{\mathcal{P}}_\kappa - \check{\mathcal{P}}_\kappa^{(0)*} \check{\mathcal{P}}_\kappa^{(0)} \quad (2.53)$$

with $\check{\mathcal{P}}_\kappa^{(0)} : L^2(\Omega_\varepsilon) \rightarrow L^2(\Omega_\varepsilon)$ being defined by (2.28) fulfils

$$\lim_{n \rightarrow \infty} n^{\frac{5}{6}} |\lambda_n(\mathcal{Q}_\kappa)| = 0. \quad (2.54)$$

Here $(\lambda_n(\mathcal{Q}_\kappa))_{n \in \mathbb{N}}$ denotes the eigenvalues of \mathcal{Q}_κ , sorted in decreasing order: $|\lambda_{n+1}(\mathcal{Q}_\kappa)| \leq |\lambda_n(\mathcal{Q}_\kappa)|$ for all $n \in \mathbb{N}$.

Proof: We start with the positive semi-definite operator $\check{\mathcal{P}}_\kappa^* \check{\mathcal{P}}_\kappa$. We split $\check{\mathcal{P}}_\kappa$ as in the proof of Lemma 2.4.2 in $\check{\mathcal{P}}_\kappa = \check{\mathcal{P}}_\kappa^{(0)} + \check{\mathcal{P}}_\kappa^{(1)}$ with $\check{\mathcal{P}}_\kappa^{(1)}$ given by (2.29). Then, we can write \mathcal{Q}_κ in the form

$$\mathcal{Q}_\kappa = \check{\mathcal{P}}_\kappa^* \check{\mathcal{P}}_\kappa - \check{\mathcal{P}}_\kappa^{(0)*} \check{\mathcal{P}}_\kappa^{(0)} = \check{\mathcal{P}}_\kappa^{(1)*} \check{\mathcal{P}}_\kappa^{(0)} + \check{\mathcal{P}}_\kappa^{(0)*} \check{\mathcal{P}}_\kappa^{(1)} + \check{\mathcal{P}}_\kappa^{(1)*} \check{\mathcal{P}}_\kappa^{(1)}.$$

To estimate the eigenvalues of the operator $\check{\mathcal{P}}_\kappa^{(1)*} \check{\mathcal{P}}_\kappa^{(0)} + \check{\mathcal{P}}_\kappa^{(0)*} \check{\mathcal{P}}_\kappa^{(1)}$, we use that for all $m, n \in \mathbb{N}$ the inequalities

$$\begin{aligned} |\lambda_{m+n-1}(\check{\mathcal{P}}_\kappa^{(1)*} \check{\mathcal{P}}_\kappa^{(0)} + \check{\mathcal{P}}_\kappa^{(0)*} \check{\mathcal{P}}_\kappa^{(1)})| &\leq s_m(\check{\mathcal{P}}_\kappa^{(0)*} \check{\mathcal{P}}_\kappa^{(1)}) + s_n(\check{\mathcal{P}}_\kappa^{(0)*} \check{\mathcal{P}}_\kappa^{(1)}) \quad \text{and} \\ s_{m+n-1}(\check{\mathcal{P}}_\kappa^{(0)*} \check{\mathcal{P}}_\kappa^{(1)}) &\leq s_m(\check{\mathcal{P}}_\kappa^{(0)}) s_n(\check{\mathcal{P}}_\kappa^{(1)}) \end{aligned}$$

hold, see for example [GK69, Chapter II.2.3, Corollary 2.2], where $s_n(T) = \sqrt{\lambda_n(T^*T)}$ denotes the singular values of a compact operator T sorted in decreasing order: $s_{n+1}(T) \leq s_n(T)$ for all $n \in \mathbb{N}$. Here, we used that $s_n(T) = s_n(T^*)$, see for example [GK69, Chapter II.2.2]. Inserting the decay rates (2.48) and (2.52) for $(s_n(\check{\mathcal{P}}_\kappa^{(0)}))_{n=1}^\infty$ and $(s_n(\check{\mathcal{P}}_\kappa^{(1)}))_{n=1}^\infty$ into these inequalities, we find that

$$\lim_{n \rightarrow \infty} n^{\frac{5}{6}} |\lambda_n(\check{\mathcal{P}}_\kappa^{(1)*} \check{\mathcal{P}}_\kappa^{(0)} + \check{\mathcal{P}}_\kappa^{(0)*} \check{\mathcal{P}}_\kappa^{(1)})| = 0.$$

Estimating, again with [GK69, Chapter II.2.3, Corollary 2.2], the eigenvalues of the sum \mathcal{Q}_κ of the two operators $\check{\mathcal{P}}_\kappa^{(1)*} \check{\mathcal{P}}_\kappa^{(0)} + \check{\mathcal{P}}_\kappa^{(0)*} \check{\mathcal{P}}_\kappa^{(1)}$ and $\check{\mathcal{P}}_\kappa^{(1)*} \check{\mathcal{P}}_\kappa^{(1)}$, we find that

$$|\lambda_{m+n-1}(\mathcal{Q}_\kappa)| \leq |\lambda_m(\check{\mathcal{P}}_\kappa^{(1)*} \check{\mathcal{P}}_\kappa^{(0)} + \check{\mathcal{P}}_\kappa^{(0)*} \check{\mathcal{P}}_\kappa^{(1)})| + \lambda_n(\check{\mathcal{P}}_\kappa^{(1)*} \check{\mathcal{P}}_\kappa^{(1)})$$

for all $m, n \in \mathbb{N}$, which yields with the behaviour (2.52) of the eigenvalues of $\check{\mathcal{P}}_\kappa^{(1)*} \check{\mathcal{P}}_\kappa^{(1)}$ the result (2.54). \square

Combining Lemma 2.5.3 and Lemma 2.5.5, we obtain that the singular values of the photoacoustic operator $\check{\mathcal{P}}_\kappa$ decay as in the unperturbed case.

Theorem 2.5.6 *Let $\check{\mathcal{P}}_\kappa : L^2(\Omega_\varepsilon) \rightarrow L^2(\mathbb{R} \times \partial\Omega)$ be the integrated photoacoustic operator of a weak attenuation coefficient κ for some bounded, convex domain $\Omega \subset \mathbb{R}^3$ with smooth boundary*

and some $\varepsilon > 0$. Then, there exist constants $C_1, C_2 > 0$ such that we have

$$C_1 n^{-\frac{2}{3}} \leq \lambda_n(\check{\mathcal{P}}_\kappa^* \check{\mathcal{P}}_\kappa) \leq C_2 n^{-\frac{2}{3}} \quad \text{for all } n \in \mathbb{N}. \quad (2.55)$$

Proof: Defining again the operators $\check{\mathcal{P}}_\kappa^{(0)}$, see (2.28), and \mathcal{Q}_κ , see (2.53), we know from [GK69, Chapter II.2.3, Corollary 2.2] for all $m, n \in \mathbb{N}$ that

$$\lambda_{m+n-1}(\check{\mathcal{P}}_\kappa^* \check{\mathcal{P}}_\kappa) \leq \lambda_m(\check{\mathcal{P}}_\kappa^{(0)*} \check{\mathcal{P}}_\kappa^{(0)}) + |\lambda_n(\mathcal{Q}_\kappa)|$$

and

$$\lambda_{m+n-1}(\check{\mathcal{P}}_\kappa^{(0)*} \check{\mathcal{P}}_\kappa^{(0)}) - |\lambda_n(\mathcal{Q}_\kappa)| \leq \lambda_m(\check{\mathcal{P}}_\kappa^* \check{\mathcal{P}}_\kappa).$$

Therefore, Lemma 2.5.3 and Lemma 2.5.5 imply bounds of the form (2.55). \square

2.A Eigenvalues of Integral Operators of Hilbert–Schmidt Type

In this section, we derive estimates for the eigenvalues of operators T of the form

$$T : L^2(U) \rightarrow L^2(U), \quad (Th)(x) = \int_U F(x, y)h(y) \, dy \quad (2.56)$$

on a bounded, open set $U \subset \mathbb{R}^m$ with an Hermitian integral kernel $F \in C(\bar{U} \times \bar{U})$ (that is, $F(x, y) = \overline{F(y, x)}$). In particular, such an operator T is a self-adjoint Hilbert–Schmidt operator, and we want to additionally assume that T is positive semi-definite. So, the eigenvalues $(\lambda_n(T))_{n \in \mathbb{N}}$ of T are non-negative and we enumerate them in decreasing order:

$$0 \leq \lambda_{n+1}(T) \leq \lambda_n(T) \quad \text{for all } n \in \mathbb{N}.$$

To obtain the asymptotic decay rate of the eigenvalues of such an operator T , we proceed as in [CH99] where a characterisation for a decay rate of the form $\lambda_n(T) = \mathcal{O}(n^{-k})$ was presented in terms of an upper estimate on the derivatives of the kernel F . The extension to an exponential decay rate is rather straightforward.

First, we show that when approximating an operator T_1 by a finite rank operator T_2 , we can estimate the eigenvalues above the rank of the finite rank operator T_2 in terms of the supremum norm of the difference of their kernels, see for example [Wey12, Satz II].

Lemma 2.A.1 *Let $U \subset \mathbb{R}^m$ be a bounded, open set, $T_i : L^2(U) \rightarrow L^2(U)$, $i = 1, 2$, be two integral operators with Hermitian integral kernels $F_i \in C(\bar{U} \times \bar{U})$. Moreover, let T_1 be positive semi-definite and T_2 have finite rank $r \in \mathbb{N}_0$.*

Then, the eigenvalues $(\lambda_n(T_1))_{n \in \mathbb{N}}$ of T_1 (sorted in decreasing order) satisfy

$$\sum_{n=r+1}^{\infty} \lambda_n(T_1) \leq (2r+1)|U|\|F_1 - F_2\|_{\infty}.$$

Proof: The min-max theorem (see for example [GK69, Chapter II.2.3]) states that for every self-adjoint, compact operator T and every fixed $m \in \mathbb{N}$

$$|\lambda_m(T)| = \min_{\text{rank}(A) \leq m-1} \|T - A\|, \quad (2.57)$$

where the minimum is taken over all operators $A : L^2(U) \rightarrow L^2(U)$ with rank less than or equal to $m - 1$.

Let us fix $n \in \mathbb{N}$ now. Applying (2.57) with $T = T_1 - T_2$ shows that there exists an operator A with $\text{rank}(A) \leq n - 1$ such that

$$|\lambda_n(T_1 - T_2)| = \|T_1 - T_2 - A\|. \quad (2.58)$$

Because $\text{rank}(T_2) \leq r$ and $\text{rank}(A) \leq n - 1$, $\text{rank}(T_2 + A) \leq n + r - 1$, and we therefore have

$$\|T_1 - T_2 - A\| \geq \min_{\text{rank}(\tilde{A}) \leq n+r-1} \|T_1 - \tilde{A}\|. \quad (2.59)$$

Using (2.57) with $T = T_1$ and $m = n + r$ we find that

$$\min_{\text{rank}(\tilde{A}) \leq n+r-1} \|T_1 - \tilde{A}\| = |\lambda_{n+r}(T_1)| = \lambda_{n+r}(T_1), \quad (2.60)$$

since T_1 is positive semi-definite. Combining the three relations (2.58), (2.59), and (2.60), we get

$$\lambda_{n+r}(T_1) \leq |\lambda_n(T_1 - T_2)| \quad \text{for all } r, n \in \mathbb{N}.$$

Taking the sum over all $n \in \mathbb{N}$, we get

$$\sum_{n=r+1}^{\infty} \lambda_n(T_1) \leq \sum_{n=1}^{\infty} |\lambda_n(T_1 - T_2)|. \quad (2.61)$$

The eigenvalues of $T_1 - T_2$ do not need to be all non-negative, however, since T_2 has rank at most r , the operator $T_1 - T_2$ cannot have more than r negative eigenvalues. Moreover, their norm is bounded by

$$|\lambda_n(T_1 - T_2)| \leq \|T_1 - T_2\| \leq \|F_1 - F_2\|_{L^2(U \times U)} \leq |U| \|F_1 - F_2\|_{\infty}. \quad (2.62)$$

Thus, we can estimate the sum in (2.61) by

$$\begin{aligned} \sum_{n=1}^{\infty} |\lambda_n(T_1 - T_2)| &= \sum_{n=1}^{\infty} \lambda_n(T_1 - T_2) + 2 \sum_{\lambda_n(T_1 - T_2) < 0} |\lambda_n(T_1 - T_2)| \\ &\leq \sum_{n=1}^{\infty} \lambda_n(T_1 - T_2) + 2r|U| \|F_1 - F_2\|_{\infty}. \end{aligned} \quad (2.63)$$

Moreover, choosing an orthonormal eigenbasis $(\psi_n)_{n=1}^{\infty} \subset L^2(U)$ of the compact, self-adjoint operator $T_1 - T_2$, we get with Mercer's theorem, see for example [CH53, Chapter III, §5 and

§9], that

$$F_1(x, y) - F_2(x, y) = \sum_{n=1}^{\infty} \lambda_n(T_1 - T_2) \psi_n(x) \overline{\psi_n(y)},$$

and therefore

$$\sum_{n=1}^{\infty} \lambda_n(T_1 - T_2) = \int_U (F_1(x, x) - F_2(x, x)) dx \leq |U| \|F_1 - F_2\|_{\infty}. \quad (2.64)$$

Combining (2.61), (2.63), and (2.64) gives

$$\sum_{n=r+1}^{\infty} \lambda_n(T_1) \leq (2r+1) |U| \|F_1 - F_2\|_{\infty}. \quad \square$$

Thus, approximating the kernel in our integral operator by one of its Taylor polynomials, we get a convergence rate for the eigenvalues depending on the approximation error of the Taylor polynomial. To improve this estimate, we first subdivide the domain U in smaller domains, so that the approximation error of the Taylor polynomial is smaller.

Regarding an upper bound for the eigenvalues, it is indeed enough to keep the subdomains along the diagonal of $U \times U$, see [CH99, Lemma 1].

Lemma 2.A.2 *Let $U \subset \mathbb{R}^m$ be a bounded, open set and $T_1 : L^2(U) \rightarrow L^2(U)$ be a positive semi-definite integral operator with Hermitian kernel $F_1 \in C(\bar{U} \times \bar{U})$. Let further $Q_\ell \subset U$, $\ell = 1, \dots, N$, be open, pairwise disjoint sets such that $U \subset \bigcup_{\ell=1}^N \bar{Q}_\ell$ and define the kernel $F_2 : \bar{U} \times \bar{U} \rightarrow \mathbb{C}$ by*

$$F_2 = F_1 \sum_{\ell=1}^N \chi_{Q_\ell \times Q_\ell}.$$

Then, the integral operator $T_2 : L^2(U) \rightarrow L^2(U)$ with the integral kernel F_2 is also positive semi-definite and fulfils

$$\sum_{n=r+1}^{\infty} \lambda_n(T_1) \leq \sum_{n=r+1}^{\infty} \lambda_n(T_2) \quad \text{for every } r \in \mathbb{N}_0. \quad (2.65)$$

Proof: For each $\ell \in \{1, \dots, N\}$, let $P_\ell : L^2(U) \rightarrow L^2(U)$, $P_\ell h = h \chi_{Q_\ell}$ be the orthogonal projection onto the subspace $L^2(Q_\ell)$. In particular, because the sets Q_ℓ are pairwise disjoint, we have

$$P_k P_\ell = \delta_{k,\ell} P_\ell. \quad (2.66)$$

With this notation, we can write

$$T_2 = \sum_{\ell=1}^N P_\ell T_1 P_\ell. \quad (2.67)$$

Now, we first show that T_2 is indeed positive semi-definite. Let us assume by contradiction that this is not the case. Then, there exists a function $h \in L^2(U)$ so that $\langle h, T_2 h \rangle < 0$. Thus, because

of the representation (2.67) of T_2 , we find an index $\ell \in \{1, \dots, N\}$ such that

$$\langle P_\ell h, T_1 P_\ell h \rangle = \langle h, P_\ell T_1 P_\ell h \rangle < 0.$$

However, this contradicts the fact that T_1 should be positive semi-definite.

To get a relation between the eigenvalues of T_1 and T_2 , we construct a sequence $(T^{(k)})_{k=0}^N$ of positive semi-definite operators interpolating between $T^{(0)} = T_1$ and $T^{(N)} = T_2$. We define recursively for every $k \in \{1, \dots, N\}$

$$T^{(k)} = \frac{1}{2}[T^{(k-1)} + (1 - 2P_k)T^{(k-1)}(1 - 2P_k)] \quad \text{with} \quad T^{(0)} = T_1. \quad (2.68)$$

Before continuing, we want to verify that this definition indeed yields $T^{(N)} = T_2$. We first remark that, because of the orthogonality relation (2.66), the equation (2.68) can be written as

$$\begin{aligned} T^{(k)} P_k &= P_k T^{(k-1)} P_k & \text{and} \\ T^{(k)} P_\ell &= (1 - P_k) T^{(k-1)} P_\ell & \text{for } \ell \neq k. \end{aligned}$$

Thus, we get recursively for every ℓ that

$$\begin{aligned} T^{(N)} P_\ell &= (1 - P_N) T^{(N-1)} P_\ell \\ &= (1 - P_N) \cdots (1 - P_{\ell+1}) T^{(\ell)} P_\ell \\ &= (1 - P_N) \cdots (1 - P_{\ell+1}) P_\ell T^{(\ell-1)} P_\ell \\ &= (1 - P_N) \cdots (1 - P_{\ell+1}) P_\ell (1 - P_{\ell-1}) \cdots (1 - P_1) T_1 P_\ell \\ &= P_\ell T_1 P_\ell. \end{aligned}$$

So, again using the representation (2.67) of T_2 , we see that

$$T^{(N)} = T^{(N)} \sum_{\ell=1}^N P_\ell = \sum_{\ell=1}^N P_\ell T_1 P_\ell = T_2.$$

Now, by Ky Fan's maximum principle, see for example [GK69, Chapter II.4], we can write the sum of the $r \in \mathbb{N}$ largest eigenvalues of $T^{(k)}$, $k \in \{1, \dots, N\}$, in the form

$$\sum_{n=1}^r \lambda_n(T^{(k)}) = \sup \left\{ \sum_{n=1}^r \langle h_n, T_2^{(k)} h_n \rangle \mid (h_n)_{n=1}^r \subset L^2(U), \langle h_n, h_{n'} \rangle = \delta_{n,n'} \right\},$$

Inserting the recursive definition (2.68) for $T^{(k)}$, we get from the subadditivity of the supremum the estimate

$$\sum_{n=1}^r \lambda_n(T^{(k)}) \leq \frac{1}{2} \sum_{n=1}^r \left[\lambda_n(T^{(k-1)}) + \lambda_n((1 - 2P_k)T^{(k-1)}(1 - 2P_k)) \right].$$

Since $(1 - 2P_k)^2 = 1$ and eigenvalues are invariant under conjugation (that is, we have $\lambda_n(AT^{(k-1)}A^{-1}) = \lambda_n(T^{(k-1)})$ for every invertible operator A), this simplifies to

$$\sum_{n=1}^r \lambda_n(T^{(k)}) \leq \sum_{n=1}^r \lambda_n(T^{(k-1)}).$$

We therefore get recursively the inequality

$$\sum_{n=1}^r \lambda_n(T_2) \leq \sum_{n=1}^r \lambda_n(T_1). \quad (2.69)$$

Additionally, since h is an eigenfunction of T_2 if and only if the functions $P_\ell h$ are for every $\ell \in \{1, \dots, N\}$ either zero or an eigenfunction of $P_\ell T_1 P_\ell$ with the same eigenvalue, we have that

$$\sum_{n=1}^{\infty} \lambda_n(T_2) = \sum_{\ell=1}^N \sum_{n'=1}^{\infty} \lambda_{n'}(P_\ell T_1 P_\ell).$$

According to Mercer's theorem, see for example [CH53, Chapter III, §5 and §9], we therefore get as in (2.64) that

$$\sum_{n=1}^{\infty} \lambda_n(T_2) = \sum_{\ell=1}^N \int_{Q_\ell} F_1(x, x) \, dx = \int_U F_1(x, x) \, dx = \sum_{n=1}^{\infty} \lambda_n(T_1). \quad (2.70)$$

Finally, combining (2.69) and (2.70), we obtain the estimate (2.65). \square

Now, putting together Lemma 2.A.1 and Lemma 2.A.2, we obtain a decay rate for the eigenvalues of the integral operator depending on the convergence rate of the Taylor series of its kernel.

Proposition 2.A.3 *Let $U \subset \mathbb{R}^m$ be a bounded, open set, $T : L^2(U) \rightarrow L^2(U)$ be a positive semi-definite integral operator with an Hermitian kernel $F \in C^k(\bar{U} \times \bar{U})$, $k \in \mathbb{N}$, and define*

$$M_j = \frac{1}{j!} \sup_{x, y \in U} \sup_{v \in S^{m-1}} \left| \frac{\partial^j}{\partial s^j} F(x, y + sv) \right|_{s=0}, \quad j \in \mathbb{N}, \quad j \leq k.$$

Then, there exist constants $A > 0$ and $a > 0$ such that for every $n \in \mathbb{N}$

$$\lambda_n(T) \leq A \min_{j \in J_{k,n}} \left[M_j \left(a \sqrt[n]{\frac{2}{n}} \right)^j (j + m)^{j+m} \right], \quad (2.71)$$

where we take the minimum over all values j in the set

$$J_{k,n} = \left\{ j \in \mathbb{N} \mid a(j + m) \leq \sqrt[n]{\frac{n}{2}}, \quad j \leq k \right\}.$$

Proof: For some $\delta \in (0, 1)$, we partition the domain U in pairwise disjoint open sets Q_ℓ , $\ell = 1, \dots, N$, with diameter not greater than δ such that $\bigcup_{\ell=1}^N \bar{Q}_\ell \supset U$. We remark that there exists a constant $a > 0$ so that we can find for every $\delta \in (0, 1)$ such a partition with N sets where

$$N < \left(\frac{a}{\delta}\right)^m \quad (2.72)$$

(for example by picking a cube with side length $D = \text{diam}(U)$ containing $U \subset \mathbb{R}^m$ and choosing a partition in $\lceil \frac{D}{L} \rceil^m$ cubes of side length $L = \frac{\delta}{\sqrt{m}}$, which gives an estimate of the form (2.72) with $a = D\sqrt{m} + 1$).

According to Lemma 2.A.2, we can now get an upper bound for the behaviour of the lower eigenvalues of T by considering the eigenvalues of the integral operator $\tilde{T} : L^2(U) \rightarrow L^2(U)$ with kernel $F \sum_{\ell=1}^N \chi_{Q_\ell \times Q_\ell}$ or, equivalently, the eigenvalues of the integral operators $T_\ell : L^2(Q_\ell) \rightarrow L^2(Q_\ell)$ with the integral kernels $F \chi_{Q_\ell \times Q_\ell}$.

To obtain an estimate for the eigenvalues of the operators T_ℓ , we consider instead of T_ℓ the finite rank operator which we get by approximating the kernel F on $Q_\ell \times Q_\ell$ by a polynomial and then apply Lemma 2.A.1, see [Wey12, §2].

So, we pick in every set Q_ℓ an arbitrary point z_ℓ and expand F on $Q_\ell \times Q_\ell$ in a Taylor polynomial of degree $j - 1$ for some $j \leq k$ with respect to the second variable around the points z_ℓ . Then, we get

$$F(x, y) = F_{j,\ell}(x, y) + C_{j,\ell}(x, y), \quad x, y \in Q_\ell,$$

with the Taylor polynomial $F_{j,\ell}$ explicitly given by

$$F_{j,\ell}(x, y) = \sum_{\{\alpha \in \mathbb{N}_0^m \mid |\alpha| \leq j-1\}} \frac{1}{\alpha!} \partial_y^\alpha F(x, z_\ell) (y - z_\ell)^\alpha,$$

and with the remainder term $C_{j,\ell}$, which can be uniformly estimated by

$$|C_{j,\ell}(x, y)| \leq M_j \delta^j \quad \text{for all } x, y \in Q_\ell. \quad (2.73)$$

Since $F_{j,\ell}$ is not necessarily Hermitian, we symmetrise it by defining the kernel $\tilde{F}_{j,\ell}$ on $Q_\ell \times Q_\ell$ as

$$\tilde{F}_{j,\ell}(x, y) = \frac{1}{2} (F_{j,\ell}(x, y) + \overline{F_{j,\ell}(y, x)}).$$

Then, $\tilde{F}_{j,\ell}$ is of the form $\tilde{F}_{j,\ell}(x, y) = \sum_{i=1}^{r_j} a_{i,\ell}(x) b_{i,\ell}(y)$ for some functions $a_{i,\ell}, b_{i,\ell} \in C(\bar{Q}_\ell)$ with r_j given by two times the number of elements in the set $\{\alpha \in \mathbb{N}_0^m \mid |\alpha| \leq j-1\}$, which is $r_j = 2 \binom{j+m-1}{m}$. Thus, the integral operator $\tilde{T}_{j,\ell} : L^2(Q_\ell) \rightarrow L^2(Q_\ell)$ with kernel $\tilde{F}_{j,\ell}$ has a finite rank which is not greater than r_j . Moreover, we get from (2.73) the uniform estimate

$$\sup_{x, y \in Q_\ell} |F(x, y) - \tilde{F}_{j,\ell}(x, y)| \leq M_j \delta^j.$$

Therefore, Lemma 2.A.1 gives us directly that

$$\sum_{n=r_j+1}^{\infty} \lambda_n(T_\ell) \leq (2r_j + 1) M_j |Q_\ell| \delta^j. \quad (2.74)$$

Now, since every eigenvalue of the integral operator \tilde{T} corresponds exactly to one eigenvalue of one of the operators T_ℓ , we have that

$$\sum_{n=1}^{\infty} \lambda_n(\tilde{T}) = \sum_{\ell=1}^N \sum_{n=1}^{\infty} \lambda_n(T_\ell), \quad (2.75)$$

and since the eigenvalues of every operator are enumerated in decreasing order, we have that

$$\sum_{n=1}^{Nr_j} \lambda_n(\tilde{T}) \geq \sum_{\ell=1}^N \sum_{n=1}^{r_j} \lambda_n(T_\ell). \quad (2.76)$$

Thus, we get from [Lemma 2.A.2](#) for the eigenvalues of the operator T by combining (2.75), (2.76), and using the estimate (2.74) that

$$\sum_{n=Nr_j+1}^{\infty} \lambda_n(T) \leq \sum_{n=Nr_j+1}^{\infty} \lambda_n(\tilde{T}) \leq \sum_{\ell=1}^N \sum_{n=r_j+1}^{\infty} \lambda_n(T_\ell) \leq (2r_j + 1)M_j|U|\delta^j. \quad (2.77)$$

For fixed $n \in \mathbb{N}$ and $j \in \mathbb{N}$, we now want to choose the parameter $N \in \mathbb{N}$ in such a way that $Nr_j < n$ and that we can make the parameter δ as small as possible. We pick

$$\delta = a \sqrt[m]{\frac{r_j}{n}},$$

where we assume that j is chosen such that $r_j < \frac{n}{a^m}$, so that $\delta < 1$ is fulfilled (an upper bound on δ is needed for an estimate of the form (2.72)). Because of $r_j = 2^{\binom{j+m-1}{m}} \leq 2(j+m-1)^m$, this condition on r_j can be ensured by imposing

$$j + m \leq \frac{1}{a} \sqrt[m]{\frac{n}{2}}. \quad (2.78)$$

Then, according to (2.72), there exists a partition $(Q_\ell)_{\ell=1}^N$ with

$$N < \left(\frac{a}{\delta}\right)^m = \frac{n}{r_j}.$$

Evaluating (2.77) at these parameters, we find that

$$\lambda_n(T) \leq \sum_{\tilde{n}=Nr_j+1}^{\infty} \lambda_{\tilde{n}}(T) \leq (2r_j + 1)M_j|U|\delta^j \leq (2r_j + 1)M_j|U|a^j \left(\frac{r_j}{n}\right)^{\frac{j}{m}}.$$

Simplifying the expression by estimating $r_j \leq 2(j+m-1)^m \leq 2(j+m)^m$ and $2r_j + 1 \leq 4(j+m)^m$, we finally get that

$$\lambda_n(T) \leq 4|U|M_j \left(a \sqrt[m]{\frac{2}{n}}\right)^j (j+m)^{j+m},$$

where we can choose $j \in \{1, \dots, k\}$ arbitrary as long as the condition (2.78) is fulfilled. \square

In particular, Proposition 2.A.3 includes the trivial case where the kernel F is a polynomial of degree K , in which case $M_{K+1} = 0$ and we obtain $\lambda_n(T) = 0$ for all $n \geq 2(a(K + m + 1))^m$, since then $K + 1 \in J_{K+1,n}$. Moreover, we find that for a general $F \in C^k(\bar{U} \times \bar{U})$, we may always pick $j = k$ for $n \geq 2(a(k + m))^m$ to obtain that the eigenvalues decay at least as

$$\lambda_n(T) \leq Cn^{-\frac{k}{m}}$$

for some constant $C > 0$.

For smooth kernels F , the optimal choice of j depends on the behaviour of the supremum M_j of the directional derivative as a function of j .

Corollary 2.A.4 *Let $U \subset \mathbb{R}^m$ be a bounded, open set and $T : L^2(U) \rightarrow L^2(U)$ be the positive semi-definite integral operator with the smooth, Hermitian kernel $F \in C^\infty(\bar{U} \times \bar{U})$.*

If we have for some constants $B, b, \mu > 0$ the inequality

$$\frac{1}{j!} \sup_{x, y \in U} \sup_{v \in S^{m-1}} \left| \frac{\partial^j}{\partial s^j} \Big|_{s=0} F(x, y + sv) \right| \leq Bb^j j^{\mu j}, \quad (2.79)$$

then there exist constants $C, c > 0$ so that the eigenvalues decay at least as

$$\lambda_n(T) \leq Cn^{\frac{1}{\sqrt[n]{n}}} \exp\left(-cn^{\frac{1}{m(1+\mu)}}\right), \quad n \in \mathbb{N}. \quad (2.80)$$

Proof: Using Proposition 2.A.3 with the upper bound (2.79) for the constants M_j , we find that there exist constants $A, a > 0$ so that

$$\lambda_n(T) \leq AB \min_{j+m \leq \frac{1}{a} \sqrt[n]{\frac{n}{2}}} \left[\left(ab \sqrt[n]{\frac{2}{n}} \right)^j j^{\mu j} (j+m)^{j+m} \right] \quad \text{for all } n \in \mathbb{N}.$$

To simplify this, we estimate $j^{\mu j} \leq (j+m)^{\mu(j+m)}$ and obtain with $\tilde{j} = j+m$

$$\lambda_n(T) \leq \tilde{A}n \min_{\tilde{j} \leq \frac{1}{a} \sqrt[n]{\frac{n}{2}}} \left[\left(ab \sqrt[n]{\frac{2}{n}} \right)^{\tilde{j}} \tilde{j}^{(1+\mu)\tilde{j}} \right] \quad \text{for all } n \in \mathbb{N} \quad (2.81)$$

for some constant $\tilde{A} > 0$.

To evaluate the minimum in (2.81), we consider for

$$\alpha_n = ab \sqrt[n]{\frac{2}{n}} \quad (2.82)$$

the function

$$f_n : (0, \infty) \rightarrow (0, \infty), \quad f_n(\zeta) = (\alpha_n \zeta^{1+\mu})^\zeta.$$

Then, by solving the optimality condition

$$0 = f'_n(\zeta) = ((1+\mu) \log \zeta + 1 + \mu + \log \alpha_n) f_n(\zeta),$$

we find that f_n attains its minimum at

$$\zeta_n = e^{-1} \alpha_n^{-\frac{1}{1+\mu}}, \quad (2.83)$$

see Figure 2.2.

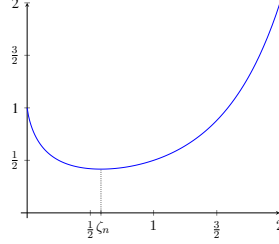


FIGURE 2.2: Graph of the function $f_n(\zeta) = (\alpha_n \zeta^{1+\mu})^\zeta$ for $\alpha_n = \frac{1}{2}$ and $\mu = \frac{1}{2}$.

Since we only need the asymptotic behaviour for $n \rightarrow \infty$, let us pick a value $n_0 \in \mathbb{N}$ such that

$$\begin{aligned} \zeta_n &> 1, & \text{that is } \alpha_n < e^{-(1+\mu)} < 1, & \text{ and} \\ \zeta_n &< \frac{1}{a} \sqrt[m]{\frac{n}{2}} = \frac{b}{\alpha_n}, & \text{that is } \alpha_n^{\frac{\mu}{1+\mu}} < be, \end{aligned}$$

for all $n \geq n_0$. This can be always achieved since $\alpha_n \rightarrow 0$ as $n \rightarrow \infty$.

Now, the minimum in (2.81) is restricted to the set of natural numbers $\tilde{j} \leq \frac{1}{a} \sqrt[m]{\frac{n}{2}}$ so that we cannot simply insert for \tilde{j} the minimum point ζ_n of the function f_n . Instead, we estimate the minimum from above by the value of f_n at the largest integer $\lfloor \zeta_n \rfloor$ below ζ_n :

$$\lambda_n(T) \leq \tilde{A}n \min_{\tilde{j} \leq \frac{1}{a} \sqrt[m]{\frac{n}{2}}} f_n(\tilde{j}) \leq \tilde{A}n f_n(\lfloor \zeta_n \rfloor).$$

Since $\alpha_n < 1$ and $\zeta_n > 1$ for all $n \geq n_0$, we get from the explicit formula (2.83) for ζ_n that

$$f(\lfloor \zeta_n \rfloor) \leq \alpha_n^{\zeta_n - 1} \zeta_n^{(1+\mu)\zeta_n} = \frac{1}{\alpha_n} (\alpha_n \zeta_n^{1+\mu})^{\zeta_n} = \frac{1}{\alpha_n e^{(1+\mu)\zeta_n}}.$$

Thus, using the expressions (2.82) and (2.83) for α_n and ζ_n , we find constants $C, c > 0$ such that

$$\lambda_n(T) \leq Cn \sqrt[m]{n} \exp\left(-cn \frac{1}{m(1+\mu)}\right) \quad \text{for all } n \in \mathbb{N}. \quad \square$$

2.B Estimating the Kernel of the Integrated Photoacoustic Operator

To be able to use Corollary 2.A.4 to estimate the eigenvalues of the operator $\check{\mathcal{P}}_\kappa^* \check{\mathcal{P}}_\kappa$, we need to find an upper bound for the derivatives of the integral kernel F_κ of the operator $\check{\mathcal{P}}_\kappa^* \check{\mathcal{P}}_\kappa$, which is

given by (2.32). Since

$$F_\kappa(x, y) = \int_{-\infty}^{\infty} \int_{\partial\Omega} \frac{1}{\omega^2} \overline{G_\kappa(\omega, \xi - x)} G_\kappa(\omega, \xi - y) dS(\xi) d\omega,$$

where G_κ denotes the fundamental solution of the Helmholtz equation, given by (2.19), we start with the directional derivatives of the function $G_\kappa(\omega, \cdot)$. Since $G_\kappa(\omega, \cdot)$ is radially symmetric, this means we can write it for arbitrary $\omega \in \mathbb{R}$ and $x \in \mathbb{R}^3 \setminus \{0\}$ in the form

$$G_\kappa(\omega, x) = g_{\kappa, \omega}(\tfrac{1}{2}|x|^2) \quad \text{with} \quad g_{\kappa, \omega}(\rho) = -\frac{i\omega}{4\pi\sqrt{2\pi}} \frac{e^{i\kappa(\omega)\sqrt{2\rho}}}{\sqrt{2\rho}} \quad \text{for } \rho > 0, \quad (2.84)$$

this problem reduces to the calculation of one dimensional derivatives of the function $g_{\kappa, \omega}$.

Lemma 2.B.1 *Let $\phi \in C^\infty(\mathbb{R})$ be defined by*

$$\phi(s) = \frac{1}{2}|x + sv|^2$$

for some arbitrary $x \in \mathbb{R}^m$ and $v \in S^{m-1}$. Then, we have for every function $\gamma \in C^\infty(\mathbb{R})$ that

$$(\gamma \circ \phi)^{(j)}(0) = \sum_{k=0}^{\lfloor \frac{j}{2} \rfloor} \frac{j!}{2^k k! (j-2k)!} \langle v, x \rangle^{j-2k} \gamma^{(j-k)}(\tfrac{1}{2}|x|^2). \quad (2.85)$$

Proof: Since $\phi'(0) = \langle v, x \rangle$, $\phi''(0) = 1$, and all higher derivatives of ϕ are zero, the formula of Faà di Bruno, see for example [Com74, Chapter 3.4, Theorem A], simplifies to

$$(\gamma \circ \phi)^{(j)}(0) = \sum_{\alpha \in A_{2,j}} \frac{j!}{\alpha_1! \alpha_2!} \left(\frac{\langle v, x \rangle}{1!} \right)^{\alpha_1} \left(\frac{1}{2!} \right)^{\alpha_2} \gamma^{(\alpha_1 + \alpha_2)}(\tfrac{1}{2}|x|^2),$$

where $A_{2,j} = \{\alpha \in \mathbb{N}_0^2 \mid \alpha_1 + 2\alpha_2 = j\}$. Setting $k = \alpha_2$ and thus $\alpha_1 = j - 2k$, we obtain the formula in the form (2.85). \square

Thus, the directional derivatives of $G_\kappa(\omega, \cdot)$ can be calculated from the derivatives of $g_{\kappa, \omega}$, which we may estimate directly.

Lemma 2.B.2 *Let $\gamma_a \in C^\infty((0, \infty))$ denote the function*

$$\gamma_a(\rho) = \frac{e^{a\sqrt{2\rho}}}{\sqrt{2\rho}}, \quad \rho > 0, \quad a \in \mathbb{C}. \quad (2.86)$$

Then, we have for every $j \in \mathbb{N}_0$ and all $\rho > 0$ the inequality

$$|\gamma_a^{(j)}(\rho)| \leq 2^j(j+1)! \left(e^{j+1} + \frac{1}{j!} \left(\frac{\rho}{2} \right)^{\frac{j}{2}} |a|^j \right) \frac{|\gamma_a(\rho)|}{\rho^j}. \quad (2.87)$$

Proof: Let us first assume that $a \neq 0$ and write $\gamma_a(\rho) = \frac{1}{a} \frac{d}{d\rho} e^{a\sqrt{2\rho}}$. Thus, we have for every $j \in \mathbb{N}_0$ that

$$\gamma_a^{(j)}(\rho) = \frac{1}{a} \frac{d^{j+1}}{d\rho^{j+1}} e^{a\sqrt{2\rho}}.$$

Applying to this the formula of Faà di Bruno, see for example [Com74, Chapter 3.4, Theorem A], we find with $A_{j+1} = \{\alpha \in \mathbb{N}_0^{j+1} \mid \sum_{k=1}^{j+1} k\alpha_k = j+1\}$ that

$$\begin{aligned} \gamma_a^{(j)}(\rho) &= \sum_{\alpha \in A_{j+1}} \frac{(j+1)!}{\alpha!} (2\rho)^{-\frac{\alpha}{2}} \prod_{k=2}^{j+1} \left((-1)^{k+1} \frac{(2k-3)!!}{k!} (2\rho)^{\frac{1}{2}-k} \right)^{\alpha_k} a^{|\alpha|-1} e^{a\sqrt{2\rho}} \\ &= \sum_{\alpha \in A_{j+1}} \frac{(j+1)!}{\alpha!} \prod_{k=2}^{j+1} \left((-1)^{k+1} \frac{(2k-3)!!}{k!} \right)^{\alpha_k} (2\rho)^{\frac{1}{2}|\alpha|-j-1} a^{|\alpha|-1} e^{a\sqrt{2\rho}}. \end{aligned}$$

This formula also extends continuously to the case $a = 0$.

Estimating it from above by using that $\frac{(2k-3)!!}{k!} \leq \frac{2^{k-1}(k-1)!}{k!} \leq 2^{k-1}$, we obtain that

$$|\gamma_a^{(j)}(\rho)| \leq \sum_{\alpha \in A_{j+1}} \frac{(j+1)!}{\alpha!} \left(\frac{\rho}{2} \right)^{\frac{1}{2}|\alpha|} |a|^{|\alpha|-1} \frac{e^{\Re a \sqrt{2\rho}}}{\rho^{j+1}}.$$

Now, using the combinatorial identity

$$\sum_{\alpha \in A_{j+1} \cap P_{j+1, \ell+1}} \frac{(j+1)!}{\alpha!} = \binom{j}{\ell} \frac{(j+1)!}{(\ell+1)!}$$

for $P_{j+1, \ell+1} = \{\alpha \in \mathbb{N}_0^{j+1} \mid |\alpha| = \ell+1\}$, see for example [Com74, Chapter 3.3, Theorem B], we find that

$$|\gamma_a^{(j)}(\rho)| \leq \sum_{\ell=0}^j \binom{j}{\ell} \frac{(j+1)!}{(\ell+1)!} \left(\frac{\rho}{2} \right)^{\frac{\ell+1}{2}} |a|^\ell \frac{e^{\Re a \sqrt{2\rho}}}{\rho^{j+1}}.$$

We may further estimate this by using $\binom{j}{\ell} \leq \sum_{k=0}^j \binom{j}{k} = 2^j$ and

$$\sum_{\ell=0}^j \frac{s^\ell}{(\ell+1)!} \leq e^{j+1} + \frac{s^j}{j!} \quad \text{for every } s > 0 \quad (2.88)$$

(since $\sum_{\ell=0}^j \frac{s^\ell}{(\ell+1)!} \leq \sum_{\ell=0}^j \frac{s^\ell}{(j+1)!} = \frac{s^j}{j!}$ if $s \geq j+1$ and $\sum_{\ell=0}^j \frac{s^\ell}{(\ell+1)!} \leq \sum_{\ell=0}^j \frac{(j+1)^\ell}{\ell!} \leq e^{j+1}$ otherwise) to obtain (2.87). \square

Putting together Lemma 2.B.1 and Lemma 2.B.2, we find an estimate for the directional derivatives of the function G_κ .

Proposition 2.B.3 *Let G_κ be given by (2.19) for some arbitrary function $\kappa : \mathbb{R} \rightarrow \mathbb{C}$. Then, there exists a constant $C > 0$ so that we have for every $j \in \mathbb{N}_0$, $x \in \mathbb{R}^3 \setminus \{0\}$, and $v \in S^2$ the inequality*

$$\frac{1}{j!} \left| \frac{\partial^j}{\partial s^j} \right|_{s=0} G_\kappa(\omega, x + sv) \Big| \leq |G_\kappa(\omega, x)| C^j \left(\frac{1}{|x|^j} + \frac{1}{j!} |\kappa(\omega)|^j \right). \quad (2.89)$$

Proof: Writing G_κ in the form (2.84), Lemma 2.B.1 implies (with $\gamma = g_{\kappa,\omega}$) that

$$\left| \frac{\partial^j}{\partial s^j} \Big|_{s=0} G_\kappa(\omega, x + sv) \right| \leq \sum_{k=0}^{\lfloor \frac{j}{2} \rfloor} \frac{j!}{2^k k! (j-2k)!} |x|^{j-2k} |g_{\kappa,\omega}^{(j-k)}(\frac{1}{2}|x|^2)|.$$

Inserting the estimate for $g_{\kappa,\omega}^{(j-k)}$ obtained from Lemma 2.B.2 (using that $g_{\kappa,\omega} = -\frac{i\omega}{4\pi\sqrt{2\pi}}\gamma_{i\kappa(\omega)}$ with $\gamma_{i\kappa(\omega)}$ being defined by (2.86) and evaluating at $\rho = \frac{1}{2}|x|^2$), we find that

$$\left| \frac{\partial^j}{\partial s^j} \Big|_{s=0} G_\kappa(\omega, x + sv) \right| \leq j! \frac{|G_\kappa(\omega, x)|}{|x|^j} \sum_{k=0}^{\lfloor \frac{j}{2} \rfloor} \frac{(j-k+1)!}{k!(j-2k)!} 2^{2j-3k} \left(e^{j-k+1} + \frac{1}{(j-k)!} \left(\frac{|x| |\kappa(\omega)|}{2} \right)^{j-k} \right).$$

Using further that $\frac{(j-k+1)!}{k!(j-2k)!} = (j-k+1) \binom{j-k}{k} \leq (j-k+1) 2^{j-k}$, we find that there exists a constant $\tilde{C} > 0$ so that

$$\frac{1}{j!} \left| \frac{\partial^j}{\partial s^j} \Big|_{s=0} G_\kappa(\omega, x + sv) \right| \leq \frac{|G_\kappa(\omega, x)|}{|x|^j} \tilde{C}^j \left(1 + \sum_{k=\lfloor \frac{j}{2} \rfloor}^j \frac{1}{k!} \left(\frac{|x| |\kappa(\omega)|}{2} \right)^k \right).$$

Estimating the sum herein by using relation (2.88), we obtain the inequality (2.89). \square

Proposition 2.B.3 allows us to estimate the derivatives of the function G_κ , however, to apply Corollary 2.A.4 to $\check{P}_\kappa^* \check{P}_\kappa$ for the integrated photoacoustic operator \check{P}_κ , we need to estimate the derivatives of the kernel F_κ of $\check{P}_\kappa^* \check{P}_\kappa$, given by (2.32). For the integral over the frequency which appears in this estimate, we use the following result in the proof of Proposition 2.5.1.

Lemma 2.B.4 *Let $\varepsilon > 0$ and $\kappa : \mathbb{R} \rightarrow \bar{\mathbb{H}}$ be a measurable function fulfilling the inequality (2.5) for $\ell = 0$ with some constants $\kappa_1 > 0$ and $N \in \mathbb{N}$ and the inequality (2.24) with some constants $\omega_0 > 0$, $\kappa_0 > 0$, and $\beta > 0$.*

Then, there exist constants $B, b > 0$ so that we have for every $j \in \mathbb{N}_0$ the estimate

$$\frac{1}{j!} \int_{-\infty}^{\infty} |\kappa(\omega)|^j e^{-2\varepsilon \Im \kappa(\omega)} d\omega \leq B b^j j^{\left(\frac{N}{\beta}-1\right)j}.$$

Proof: By our assumptions on κ , we have that there is a constant $C \geq 0$ such that $\Im \kappa(\omega) \geq \kappa_0 |\omega|^\beta - C$ for all $\omega \in \mathbb{R}$. Thus,

$$\frac{1}{j!} \int_{-\infty}^{\infty} |\kappa(\omega)|^j e^{-2\varepsilon \Im \kappa(\omega)} d\omega \leq \frac{2e^{2C\varepsilon} \kappa_1^j}{j!} \int_0^{\infty} (1+\omega)^{Nj} e^{-2\varepsilon \kappa_0 \omega^\beta} d\omega.$$

By Jensen's inequality, applied to the convex function $f(r) = r^{Nj}$, we can estimate

$$(1+\omega)^{Nj} = 2^{Nj} \left(\frac{1}{2} + \frac{1}{2}\omega \right)^{Nj} \leq 2^{Nj-1} (1+\omega^{Nj}).$$

Then, we find with the substitution $\nu = \omega^\beta$ that

$$\begin{aligned} \frac{1}{j!} \int_{-\infty}^{\infty} |\kappa(\omega)|^j e^{-2\varepsilon \Im \kappa(\omega)} d\omega &\leq \frac{(2^N \kappa_1)^j e^{2C\varepsilon}}{\beta j!} \int_0^{\infty} \nu^{\frac{1}{\beta}-1} (1 + \nu^{\frac{N}{\beta}}) e^{-2\varepsilon \kappa_0 \nu} d\nu \\ &= \frac{(2^N \kappa_1)^j e^{2C\varepsilon}}{\beta \Gamma(j+1)} \left((2\varepsilon \kappa_0)^{-\frac{1}{\beta}} \Gamma\left(\frac{1}{\beta}\right) + (2\varepsilon \kappa_0)^{-\frac{Nj+1}{\beta}} \Gamma\left(\frac{Nj+1}{\beta}\right) \right), \end{aligned}$$

where

$$\Gamma(\rho) = \int_0^{\infty} \nu^{\rho-1} e^{-\nu} d\nu, \quad \rho > 0,$$

denotes the gamma function.

Recalling Stirling's formula, see for example [AS72, Section 6.1.42], we know that the gamma function can be bounded from below and above by

$$\sqrt{\frac{2\pi}{\rho}} \left(\frac{\rho}{e}\right)^\rho \leq \Gamma(\rho) \leq \sqrt{\frac{2\pi}{\rho}} \left(\frac{\rho}{e}\right)^\rho e^{\frac{1}{12\rho}} \quad \text{for every } \rho > 0.$$

Thus, we find constants $B, b > 0$ so that

$$\frac{1}{j!} \int_{-\infty}^{\infty} |\kappa(\omega)|^j e^{-2\varepsilon \Im \kappa(\omega)} d\omega \leq B b^j j^{(\frac{N}{\beta}-1)j}$$

for all $j \in \mathbb{N}_0$. □

Acknowledgement

The work is support by the “Doctoral Program Dissipation and Dispersion in Nonlinear PDEs” (W1245). OS is also supported by the FWF-project “Interdisciplinary Coupled Physics Imaging” (FWF P26687).

The authors thank Adrian Nachman (from the University of Toronto) for stimulating discussions on pseudodifferential operators.

References

- [Akh65] N. I. Akhiezer. “The Classical Moment Problem and some Related Questions in Analysis”. Trans. by N. Kemmer. University Mathematical Monographs. Edinburgh and London: Oliver & Boyd, 1965.
- [AKQ07] M. L. Agranovsky, K. Kuchment, and E. T. Quinto. “Range descriptions for the spherical mean Radon transform”. *J. Funct. Anal.* 248.2 (2007), pp. 344–386.
- [AS72] M. Abramowitz and I.A. Stegun. “Handbook of Mathematical Functions”. New York: Dover, 1972.

- [CH53] R. Courant and D. Hilbert. “Methods of mathematical physics. Vol. I”. Interscience Publishers, Inc., New York, N.Y., 1953. xv+561.
- [CH99] C.-H. Chang and C.-W. Ha. “On eigenvalues of differentiable positive definite kernels”. *Integr. Equ. Oper. Theory* 33.1 (1999), pp. 1–7.
- [Com74] L. Comtet. “Advanced Combinatorics. The Art of Finite and Infinite Expansions”. Dordrecht, Netherlands: D. Reidel, 1974. xi+343.
- [GK69] I. C. Gohberg and M. G. Krein. “Introduction to the Theory of Linear Nonselfadjoint Operators in Hilbert Space”. Vol. 18. Translations of Mathematical Monographs. American Mathematical Society, 1969. 378 pp.
- [Hö3] L. Hörmander. “The Analysis of Linear Partial Differential Operators I”. 2nd ed. New York: Springer Verlag, 2003.
- [Har21] G. H. Hardy. “A Course of Pure Mathematics”. 3rd ed. London: Cambridge at the University Press, 1921.
- [Kin+00] L. E. Kinsler, A. R. Frey, A. B. Coppens, and J. V. Sanders. “Fundamentals of Acoustics”. 4th ed. New York: Wiley, 2000.
- [KK08] P. Kuchment and L. Kunyansky. “Mathematics of thermoacoustic tomography”. *European J. Appl. Math.* 19 (2008), pp. 191–224.
- [KS12] R. Kowar and O. Scherzer. “Attenuation Models in Photoacoustics”. In: *Mathematical Modeling in Biomedical Imaging II: Optical, Ultrasound, and Opto-Acoustic Tomographies*. Ed. by H. Ammari. Vol. 2035. Lecture Notes in Mathematics. Berlin Heidelberg: Springer Verlag, 2012, pp. 85–130.
- [KSB11] R. Kowar, O. Scherzer, and X. Bonnefond. “Causality analysis of frequency-dependent wave attenuation”. *Math. Methods Appl. Sci.* 34 (1 2011), pp. 108–124.
- [Lee13] J. M. Lee. “Introduction to Smooth Manifolds”. 2nd ed. Vol. 218. Graduate Texts in Mathematics. Springer, New York, 2013. xvi+708.
- [NSW90] A. I. Nachman, J. F. Smith III, and R. C. Waag. “An equation for acoustic propagation in inhomogeneous media with relaxation losses”. *J. Acoust. Soc. Amer.* 88.3 (1990), pp. 1584–1595.
- [Pal10] V. P. Palamodov. “Remarks on the general Funk transform and thermoacoustic tomography”. *Inverse Probl. Imaging* 4.4 (2010), pp. 693–702.
- [Shu87] M. A. Shubin. “Pseudodifferential operators and spectral theory”. Trans. by S. I. Andersson. Vol. 200. Springer, 1987.
- [Sza94] T.L. Szabo. “Time domain wave equations for lossy media obeying a frequency power law”. *J. Acoust. Soc. Amer.* 96 (1994), pp. 491–500.
- [Tar07] L. Tartar. “An Introduction to Sobolev Spaces and Interpolation Spaces”. Lecture Notes of the Unione Matematica Italiana 3. Berlin, Heidelberg: Springer, 2007.

- [Wan09] L. V. Wang, ed. “Photoacoustic Imaging and Spectroscopy”. Optical Science and Engineering. Boca Raton: CRC Press, 2009. xii+499.
- [Wei80] J. Weidmann. “Linear Operators in Hilbert Spaces”. Vol. 68. Graduate Texts in Mathematics. New York: Springer, 1980.
- [Wey12] H. Weyl. “Das asymptotische Verteilungsgesetz der Eigenwerte linearer partieller Differentialgleichungen (mit einer Anwendung auf die Theorie der Hohlraumstrahlung)”. German. *Math. Ann.* 71.4 (1912), pp. 441–479.

3

Reconstruction formulas for Photoacoustic Imaging in Attenuating Media

Otmar Scherzer^{1,2}
otmar.scherzer@univie.ac.at

Cong Shi¹
cong.shi@univie.ac.at

¹Computational Science Center
University of Vienna
Oskar-Morgenstern-Platz 1
A-1090 Vienna, Austria

²Johann Radon Institute for Computational
and Applied Mathematics (RICAM)
Altenbergerstraße 69
A-4040 Linz, Austria

Abstract

In this paper we study the problem of photoacoustic inversion in a *weakly* attenuating medium. We present explicit reconstruction formulas in such media and show that the inversion based on such formulas is moderately ill-posed. Moreover, we present a numerical algorithm for imaging and demonstrate in numerical experiments the feasibility of this approach.

3.1 Introduction

When a probe is excited by a short electromagnetic (EM) pulse, it absorbs part of the EM-energy, and expands as a reaction, which in turn produces a pressure wave. In *photoacoustic experiments*, using measurements of the pressure wave, the ability of the medium to transfer absorbed EM-energy into pressure waves is visualized and used for diagnostic purposes. Common visualizations, see [Wan09], are based on the assumptions that the specimen can be *uniformly illuminated*, is acoustically *non-attenuating*, and that the *sound-speed* and *compressibility* are constant.

In mathematical terms, the photoacoustic imaging problem consists in calculating the compactly supported *absorption density function* $h : \mathbb{R}^3 \rightarrow \mathbb{R}$, appearing as a source term in the wave

equation

$$\begin{aligned}\partial_{tt}p(t, \mathbf{x}) - \Delta p(t, \mathbf{x}) &= \delta'(t)h(\mathbf{x}), & t \in \mathbb{R}, \mathbf{x} \in \mathbb{R}^3, \\ p(t, \mathbf{x}) &= 0, & t < 0, \mathbf{x} \in \mathbb{R}^3,\end{aligned}\tag{3.1}$$

from some measurements over time of the pressure p on a two-dimensional manifold Γ outside of the specimen, that is outside of the support of the absorption density function. This problem has been studied extensively in the literature (see e.g. [KK08; WA11; Kuc14], to mention just a few survey articles).

Biological tissue has a non-vanishing viscosity, thus there is thermal consumption of energy. These effects can be described mathematically by *attenuation*. Common models of such are the *thermo-viscous* model [Kin+00], its modification [KSB11], Szabo's power law [Sza94; Sza95] and a causal modification [KS12], Hanyga & Sereďyńska [HS03], Sushilov & Cobbold [SC05], and the Nachman–Smith–Waag model [NSW90]. Photoacoustic imaging in attenuating medium then consists in computing the absorption density function h from measurements of the attenuated pressure p^a on a surface containing the object of interest. The attenuated pressure equation reads as follows

$$\begin{aligned}\mathcal{A}_\kappa[p^a](t, \mathbf{x}) - \Delta p^a(t, \mathbf{x}) &= \delta'(t)h(\mathbf{x}), & t \in \mathbb{R}, \mathbf{x} \in \mathbb{R}^3, \\ p^a(t, \mathbf{x}) &= 0, & t < 0, \mathbf{x} \in \mathbb{R}^3,\end{aligned}\tag{3.2}$$

where \mathcal{A}_κ is the pseudo-differential operator defined in frequency domain (see (3.4)). The formal difference between (3.1) and (3.2) is that the second time derivative operator ∂_{tt} is replaced by a pseudo-differential operator \mathcal{A}_κ .

The literature on Photoacoustics in attenuating media concentrates on time-reversal and attenuation compensation based on power laws: We mention the k -wave toolbox implementation and the according papers [CT10; TZC10], [Bur+07a; Hua+12]. In [ESS16] several attenuation laws from the literature have been cataloged into two classes, namely *weak* and *strong* attenuation laws. Power laws lead, in general, to severely ill-posed photoacoustic imaging problem, while mathematically sophisticatedly derived models, like the Nachman-Smith-Waag model [NSW90], lead to moderately ill-posed problems.

The paper is based on the premise that Photoacoustics is moderately ill-posed, and we therefore concentrate on photoacoustic inversion in weakly attenuating media, which have not been part of extensive analytical and numerical studies in the literature. Another goal of this work is to derive *explicit* reconstruction formulas for the absorption density function h in attenuating media. Previously there have been derived asymptotical expansions in the case of small absorbers [Amm+12; KS13].

Notation

We use the following notations:

- For $s = 0, 1, 2, \dots$ we denote by $\mathcal{S}(\mathbb{R} \times \mathbb{R}^s)$ the Schwartz-space of complex valued functions and its dual space, the space of *tempered distribution*, is denoted by $\mathcal{S}'(\mathbb{R} \times \mathbb{R}^s)$.

We abbreviate $\mathcal{S} = \mathcal{S}(\mathbb{R} \times \mathbb{R}^3)$ and $\mathcal{S}' = \mathcal{S}'(\mathbb{R} \times \mathbb{R}^3)$.

- For $\phi \in \mathcal{S}(\mathbb{R})$ we define the Fourier-transform by

$$\hat{\phi}(\omega) = \frac{1}{\sqrt{2\pi}} \int_{t=-\infty}^{\infty} e^{i\omega t} \phi(t) dt,$$

and the one-dimensional inverse Fourier-transform is given by

$$\check{\phi}(t) = \frac{1}{\sqrt{2\pi}} \int_{\omega=-\infty}^{\infty} e^{-i\omega t} \phi(\omega) d\omega.$$

- Let $\varphi \in \mathcal{S}(\mathbb{R})$ and $\psi \in \mathcal{S}(\mathbb{R}^3)$. The Fourier-transform $\mathcal{F}[\cdot] : \mathcal{S}' \rightarrow \mathcal{S}'$ on the space of tempered distributions is defined by

$$\langle \mathcal{F}[u], \varphi \otimes \psi \rangle_{\mathcal{S}', \mathcal{S}} = \langle u, \check{\varphi} \otimes \psi \rangle_{\mathcal{S}', \mathcal{S}}. \quad (3.3)$$

Note that for functions $u \in \mathcal{S}$ we have

$$\langle \mathcal{F}[u], \varphi \otimes \psi \rangle_{\mathcal{S}', \mathcal{S}} = \int_{\mathbb{R} \times \mathbb{R}^3} u(t, \mathbf{x}) \overline{\check{\varphi}(t) \psi(\mathbf{x})} dt d\mathbf{x}.$$

We are identifying distributions and functions and we are writing in the following for all $u \in \mathcal{S}'$

$$\begin{aligned} \mathcal{F}[u](\omega, \mathbf{x}) &= \frac{1}{\sqrt{2\pi}} \int_{t=-\infty}^{\infty} e^{i\omega t} u(t, \mathbf{x}) dt \text{ and} \\ \mathcal{F}^{-1}[y](t, \mathbf{x}) &= \frac{1}{\sqrt{2\pi}} \int_{\omega=-\infty}^{\infty} e^{-i\omega t} y(\omega, \mathbf{x}) d\omega. \end{aligned}$$

- We define the attenuation operator $\mathcal{A}_\kappa[\cdot] : \mathcal{S}' \rightarrow \mathcal{S}'$ by

$$\langle \mathcal{A}_\kappa[u], \phi \otimes \psi \rangle_{\mathcal{S}', \mathcal{S}} = - \left\langle u, \widetilde{\kappa^2 \hat{\phi}} \otimes \psi \right\rangle_{\mathcal{S}', \mathcal{S}}. \quad (3.4)$$

This means that if $u \in \mathcal{S}(\mathbb{R} \times \mathbb{R}^3)$ then

$$\mathcal{A}_\kappa[u](t, \mathbf{x}) = -\mathcal{F}^{-1}[\kappa^2 \mathcal{F}[u]](t, \mathbf{x}), \quad \omega \in \mathbb{R}, \mathbf{x} \in \mathbb{R}^3. \quad (3.5)$$

- $\mathcal{I}[\cdot]$ denotes the *time integration operator on the space of tempered distributions* and is given by

$$\langle \mathcal{I}[u], \phi \otimes \psi \rangle_{\mathcal{S}', \mathcal{S}} = - \langle u, \phi' \otimes \psi \rangle_{\mathcal{S}', \mathcal{S}}, \quad (3.6)$$

and we write formally for $u \in \mathcal{S}'$

$$u \rightarrow \mathcal{I}[u](t, \mathbf{x}) = \int_{-\infty}^t u(\tau, \mathbf{x}) d\tau. \quad (3.7)$$

- (3.2) and (3.1) (here $\kappa(\omega) = \omega^2$) are understood in a distributional sense, which means that for all $\phi \in \mathcal{S}(\mathbb{R})$ and $\psi \in \mathcal{S}(\mathbb{R}^3)$

$$\begin{aligned} & \left\langle p^a, \widetilde{\kappa^2 \hat{\phi}} \otimes \psi \right\rangle_{\mathcal{S}', \mathcal{S}} + \langle p^a, \phi \otimes \Delta_{\mathbf{x}} \psi \rangle_{\mathcal{S}', \mathcal{S}} \\ &= \phi'(0) \langle h, \psi \rangle_{\mathcal{S}'(\mathbb{R}^3), \mathcal{S}(\mathbb{R}^3)} . \end{aligned} \quad (3.8)$$

3.2 Attenuation

Attenuation describes the physical phenomenon that certain frequency components of acoustic waves are attenuated more rapidly over time. Mathematically this is encoded in the function κ defining the pseudo-differential operator \mathcal{A}_κ . A physically and mathematically meaningful κ has to satisfy the following properties (see [ESS16]):

Definition 3.2.1 We call a non-zero function $\kappa \in C^\infty(\mathbb{R}; \overline{\mathbb{H}})$, where $\mathbb{H} = \{z \in \mathbb{C} : \Im z > 0\}$ denotes the upper half complex plane and $\overline{\mathbb{H}}$ its closure in \mathbb{C} , an *attenuation coefficient* if

1. all the derivatives of κ are polynomially bounded. That is, for every $\ell \in \mathbb{N}_0$ there exist constants $\kappa_1 > 0$ and $N \in \mathbb{N}$ such that

$$|\kappa^{(\ell)}(\omega)| \leq \kappa_1 (1 + |\omega|)^N, \quad (3.9)$$

2. There exists a holomorphic continuation $\tilde{\kappa} : \overline{\mathbb{H}} \rightarrow \overline{\mathbb{H}}$ of κ on the upper half plane, that is, $\tilde{\kappa} \in C(\overline{\mathbb{H}}; \overline{\mathbb{H}})$ with $\tilde{\kappa}|_{\mathbb{R}} = \kappa$ and $\tilde{\kappa} : \mathbb{H} \rightarrow \overline{\mathbb{H}}$ is holomorphic, and there exists constants $\tilde{\kappa}_1 > 0$ and $\tilde{N} \in \mathbb{N}$ such that

$$|\tilde{\kappa}(z)| \leq \tilde{\kappa}_1 (1 + |z|)^{\tilde{N}} \quad \text{for all } z \in \overline{\mathbb{H}}.$$

3. κ is symmetric: That is, $\kappa(-\omega) = -\overline{\kappa(\omega)}$ for all $\omega \in \mathbb{R}$.
4. There exists some constant $c > 0$ such that the holomorphic extension $\tilde{\kappa}$ of the attenuation coefficient κ satisfies

$$\Im(\tilde{\kappa}(z) - \frac{z}{c}) \geq 0 \quad \text{for every } z \in \overline{\mathbb{H}}.$$

Remark: The four conditions in Definition 3.2.1 on κ encode the following physical properties of the attenuated wave equation (see [ESS16]):

The condition (3.9) in Definition 3.2.1 ensures that the product $\kappa^2 u$ of κ^2 with an arbitrary tempered distribution $u \in \mathcal{S}'$ is again in \mathcal{S}' and therefore, the operator $\mathcal{A}_\kappa : \mathcal{S}' \rightarrow \mathcal{S}'$ is well-defined on the space of tempered distributions.

The second condition guarantees that the solution of the attenuated wave equation is causal.

Condition three ensures that real valued distributions (such as the pressure) are mapped to real valued distributions. That is p^a is real valued if the absorption density h is real.

The forth condition guarantees that the solution $p^a \in \mathcal{S}'(\mathbb{R} \times \mathbb{R}^3)$ of the equation (3.2) propagates with finite speed $c > 0$. That is

$$\text{supp } p^a \subset \{(t, x) \in \mathbb{R} \times \mathbb{R}^3 : |x| \leq ct + R\}$$

whenever $\text{supp } h \subset B_R(0)$.

In the literature there have been documented two classes of attenuation models:

Definition 3.2.2 We call an attenuation coefficient $\kappa \in C^\infty(\mathbb{R}; \overline{\mathbb{H}})$ (see Definition 3.2.1)

- a *weak attenuation* coefficient if there exists a constant $0 \leq k_\infty \in \mathbb{R}$ and a bounded function $k_* \in C^\infty(\mathbb{R}; \mathbb{C}) \cap L^2(\mathbb{R}; \mathbb{C})$ such that

$$\kappa(\omega) = \omega + ik_\infty + k_*(\omega) \text{ for all } \omega \in \mathbb{R}. \quad (3.10)$$

In particular, κ is *constantly attenuating*, if κ is a weak attenuation coefficient with $k_* \equiv 0$. That is, there exists a constant $k_\infty \geq 0$ such that

$$\kappa(\omega) = \omega + ik_\infty \text{ for all } \omega \in \mathbb{R}. \quad (3.11)$$

- κ is called *strong attenuation coefficient* if there exist constants $\kappa_0 > 0$, $\beta > 0$, and $\omega_0 > 0$

$$\Im \kappa(\omega) \geq \kappa_0 |\omega|^\beta \text{ for all } \omega \in \mathbb{R} \text{ with } |\omega| \geq \omega_0. \quad (3.12)$$

For such attenuation coefficients we proved in [ESS16] well-posedness of the attenuated wave equation:

Lemma 3.2.3 Let κ be an attenuation coefficient. Then the solution p^a of the equation (3.2) exists and is a real-valued tempered distribution in $\mathbb{R} \times \mathbb{R}^3$.

Moreover, $q^a := \mathcal{I}[p^a]$ is a tempered distribution and satisfies the equation

$$\begin{aligned} \mathcal{A}_\kappa[q^a](t, \mathbf{x}) - \Delta q^a(t, \mathbf{x}) &= \delta(t)h(\mathbf{x}), & t \in \mathbb{R}, \mathbf{x} \in \mathbb{R}^3, \\ q^a(t, \mathbf{x}) &= 0, & t < 0, \mathbf{x} \in \mathbb{R}^3, \end{aligned} \quad (3.13)$$

and in Fourier domain

$$\kappa^2(\omega)\mathcal{F}[q^a](\omega, \mathbf{x}) + \Delta_{\mathbf{x}}\mathcal{F}[q^a](\omega, \mathbf{x}) = -\frac{1}{\sqrt{2\pi}}h(\mathbf{x}). \quad (3.14)$$

Proof: The first item has been proven in [ESS16]. The second item is an immediate consequence of the definition of a tempered distribution. \square

Remark: (3.13) has to be understood in a distributional sense: That is $q^a \in \mathcal{S}'$ and satisfies for every $\phi \in \mathcal{S}(\mathbb{R})$ and $\psi \in \mathcal{S}(\mathbb{R}^3)$ the equation

$$\langle \mathcal{A}_\kappa[q^a], \phi \otimes \psi \rangle_{\mathcal{S}', \mathcal{S}} - \langle q^a, \phi \otimes \Delta_{\mathbf{x}}\psi \rangle_{\mathcal{S}', \mathcal{S}} = \phi(0) \langle h, \psi \rangle_{\mathcal{S}'(\mathbb{R}^3), \mathcal{S}(\mathbb{R}^3)}. \quad (3.15)$$

If $\kappa(\omega) = \omega$ (that is the case of the standard wave equation) $q = q^a$ solves the following equation in a distributional sense

$$\begin{aligned} \partial_{tt}q(t, \mathbf{x}) - \Delta_{\mathbf{x}}q(t, \mathbf{x}) &= \delta(t)h(\mathbf{x}), & t \in \mathbb{R}, \mathbf{x} \in \mathbb{R}^3, \\ q(t, \mathbf{x}) &= 0, & t < 0, \mathbf{x} \in \mathbb{R}^3, \end{aligned} \quad (3.16)$$

and its Fourier-transform $\mathcal{F}[q]$ satisfies the Helmholtz equation

$$\omega^2 \mathcal{F}[q](\omega, \mathbf{x}) + \Delta_{\mathbf{x}} \mathcal{F}[q](\omega, \mathbf{x}) = -\frac{1}{\sqrt{2\pi}} h(\mathbf{x}), \quad \omega \in \mathbb{R}, \mathbf{x} \in \mathbb{R}^3. \quad (3.17)$$

Again $q \in \mathcal{S}'(\mathbb{R} \times \mathbb{R}^3)$ and satisfies (3.16) in a distributional sense:

$$\langle q, \partial_{tt}\phi \otimes \psi \rangle_{\mathcal{S}', \mathcal{S}} - \langle q, \phi \otimes \Delta_{\mathbf{x}}\psi \rangle_{\mathcal{S}', \mathcal{S}} = \phi(0) \langle h, \psi \rangle_{\mathcal{S}'(\mathbb{R}^3), \mathcal{S}(\mathbb{R}^3)}. \quad (3.18)$$

The solution of (3.16) can also be written as the solution of the initial value problem:

$$\begin{aligned} \partial_{tt}q(t, \mathbf{x}) - \Delta_{\mathbf{x}}q(t, \mathbf{x}) &= 0, & t > 0, \mathbf{x} \in \mathbb{R}^3, \\ q(0, \mathbf{x}) &= 0, & \mathbf{x} \in \mathbb{R}^3, \\ \partial_t q(0, \mathbf{x}) &= h(\mathbf{x}), & \mathbf{x} \in \mathbb{R}^3. \end{aligned} \quad (3.19)$$

In the following we derive a functional relation between q and q^a , which is the basis of analytical back-projection formulas in attenuating media.

Theorem 3.2.4 *Let $\phi \in \mathcal{S}(\mathbb{R})$ and define*

$$\nu_+[\phi](\tau) := \frac{1}{\sqrt{2\pi}} \int_{\omega=-\infty}^{\infty} e^{-i\overline{\kappa(\omega)}\tau} \hat{\phi}(\omega) d\omega \text{ for all } \tau \geq 0.$$

Then there exists a sequence $(a_m)_{m \geq 1}$ of real numbers satisfying $\sum_{m \geq 1} a_m 2^{mj} = (-1)^j$ and a function $\vartheta \in C_0^\infty(\mathbb{R}; \mathbb{R})$ such that $\vartheta(\tau) = 1$ when $|\tau| < 1$ and $\vartheta(\tau) = 0$ when $|\tau| \geq 2$ such that the function $\nu : \mathbb{R} \rightarrow \mathbb{C}$, defined by

$$\nu(\tau) := \nu[\phi](\tau) := \begin{cases} \nu_+[\phi](\tau) & \text{for all } \tau \geq 0, \\ \sum_{m=0}^{\infty} a_m \nu_+[\phi](-2^m \tau) \vartheta(-2^m \tau) & \text{for all } \tau < 0, \end{cases} \quad (3.20)$$

is an element of the Schwartz space $\mathcal{S}(\mathbb{R})$.

Proof: 1. Using that for all $k \in \mathbb{N}_0$

$$\psi_k(\tau, \omega) := \partial_\tau^k e^{-i\overline{\kappa(\omega)}\tau} = (-i)^k \overline{\kappa(\omega)}^k e^{-i\overline{\kappa(\omega)}\tau} \text{ for all } \omega, \tau \in \mathbb{R},$$

it follows from Definition 3.2.2 that, uniformly in τ , for all $\omega \in \mathbb{R}$

$$\left| \psi_k(\tau, \omega) \hat{\phi}(\omega) \right| \leq |\kappa(\omega)|^k e^{-\Im \kappa(\omega)\tau} \left| \hat{\phi}(\omega) \right| \leq |\kappa(\omega)|^k \left| \hat{\phi}(\omega) \right|.$$

From (3.9) and $\hat{\phi} \in \mathcal{S}(\mathbb{R})$ (in particular $\kappa \in L^\infty(\mathbb{R}; \mathbb{C})$ and $\hat{\phi} \in C(\mathbb{R}; \mathbb{C})$), $\omega \rightarrow$

$|\kappa(\omega)|^k |\hat{\phi}(\omega)| \in L^1(\mathbb{R}; \mathbb{R})$. Thus by interchanging integration and differentiation it follows that for $R \rightarrow \infty$

$$d^k \nu_+[\phi](\tau) = \frac{1}{\sqrt{2\pi}} \int_{\omega=-\infty}^{\infty} \psi_k(\tau, \omega) \hat{\phi}(\omega) d\omega \text{ for all } \tau \geq 0 \quad (3.21)$$

and that these functions are continuous. Thus $\nu_+[\phi] \in C^\infty([0, \infty); \mathbb{C})$.

2. From [See64] it follows that $\nu[\phi]$ defined in (3.20) is in $C^\infty(\mathbb{R}; \mathbb{C})$ and extends the function $\nu_+[\phi]$ defined on $[0, \infty)$.
3. We are proving that $\nu_+[\phi]$ and all its derivative are faster decaying than polynomials in τ for $\tau \rightarrow +\infty$.

For this purpose we use the *stationary phase method* summarized in Theorem 3.A.1:

Let $\theta \in C_0^\infty(\mathbb{R}; \mathbb{R})$ be a mollifier satisfying $\theta(\omega) = 1$ when $|\omega| < 1$ and $\theta(\omega) = 0$ when $|\omega| \geq 2$. For $k \in \mathbb{N}$ and $R > 0$ fixed, we apply the stationary phase method with

$$\omega \rightarrow f(\omega) = -\overline{\kappa(\omega)} \text{ and } \omega \rightarrow g_R(\omega) := \psi_k(\tau, \omega) \theta(\omega/R).$$

Below we are verifying the assumptions of the stationary phase method:

- $f \in C^\infty(\mathbb{R}; \mathbb{C})$ by Definition 3.2.1 and $g_R \in C_0^\infty(\mathbb{R}; \mathbb{C})$, because it is the product of a $C^\infty(\mathbb{R}; \mathbb{C})$ function and the compactly supported function $\omega \rightarrow \theta(\omega/R)$.
- The second property

$$\Im f = \Im \kappa \geq 0. \quad (3.22)$$

is an immediate consequence of the assumption $\kappa \in C^\infty(\mathbb{R}; \overline{\mathbb{H}})$ in Definition 3.2.1.

Thus (3.49) can be applied with the functions $f = -\overline{\kappa}$ and g_R , and using Lemma 3.A.2 (3.50) it follows that

$$\begin{aligned} & \tau^l \left| \int_{\omega=-\infty}^{\infty} e^{i\tau f(\omega)} g_R(\omega) d\omega \right| \\ & \leq C_1 \sum_{\alpha=0}^l \sup_{\omega \in \mathbb{R}} |d^\alpha g_R(\omega)| (|f'(\omega)|^2 + \Im f(\omega))^{\alpha/2-l} \\ & \leq C_1 \sum_{\alpha=0}^l \sup_{\omega \in \mathbb{R}} |d^\alpha g_R(\omega)| C_2^{\alpha/2-l}. \end{aligned} \quad (3.23)$$

Next, we consider the limit $R \rightarrow \infty$. Because $\theta \in C_0^\infty(\mathbb{R}; \mathbb{R})$ and $g \in \mathcal{S}(\mathbb{R})$ and

$$d^\alpha g_R(\omega) = \sum_{\beta=0}^{\alpha} d^{\alpha-\beta} g(\omega) \binom{\alpha}{\beta} \frac{1}{R^\beta} d^\beta \theta(\omega),$$

it follows that

$$|d^\alpha g_R(\omega) - d^\alpha g(\omega)| \leq \left| \sum_{\beta=1}^{\alpha} d^{\alpha-\beta} g(\omega) \binom{\alpha}{\beta} \frac{1}{R^\beta} d^\beta \theta(\omega) \right| = \mathcal{O}(R^{-1}).$$

and from (3.22) and the assumption $\tau \geq 0$ it follows

$$\begin{aligned} & \left| \int_{\omega=-\infty}^{\infty} e^{i\tau f(\omega)} g_R(\omega) d\omega - \int_{\omega=-\infty}^{\infty} e^{i\tau f(\omega)} g(\omega) d\omega \right| \\ & \leq \int_{\omega=-\infty}^{\infty} e^{-\tau \Im f(\omega)} |g_R(\omega) - g(\omega)| d\omega \leq \int_{\omega=-\infty}^{\infty} |g_R(\omega) - g(\omega)| d\omega. \end{aligned}$$

Using the definition of g_R it follows that

$$\begin{aligned} \int_{\omega=-\infty}^{\infty} |g_R(\omega) - g(\omega)| d\omega & \leq \int_{\omega=-\infty}^{\infty} |g(\omega)| |1 - \theta(\omega/R)| d\omega \\ & \leq \int_{|\omega| \geq R} |g(\omega)| d\omega. \end{aligned}$$

□

Since $g \in \mathcal{S}(\mathbb{R})$ the last integral tends to 0 for $R \rightarrow \infty$ and thus (3.49) holds even for the functions $\omega \rightarrow f(\omega) = -\kappa(\omega)$ and $\omega \rightarrow g(\omega) = \psi_k(\tau, \omega)$, although they are not satisfying the assumptions of Theorem 3.A.1.

Because (according to Theorem 3.2.4), for every $\phi \in \mathcal{S}(\mathbb{R})$, $\nu[\phi] \in \mathcal{S}(\mathbb{R})$, the operator from the following definition is well-defined.

Definition 3.2.5 The *attenuation solution operator* $\mathcal{B}[\cdot] : \mathcal{S}' \rightarrow \mathcal{S}'$ is defined by

$$\begin{aligned} \langle \mathcal{B}[\rho], \phi \otimes \psi \rangle_{\mathcal{S}', \mathcal{S}} & = \langle \rho, \nu[\phi] \otimes \psi \rangle_{\mathcal{S}', \mathcal{S}} \\ & \text{for all } \rho \in \mathcal{S}' \text{ and } \phi \in \mathcal{S}(\mathbb{R}), \psi \in \mathcal{S}(\mathbb{R}^3). \end{aligned} \quad (3.24)$$

Remark: In a weakly attenuating medium $\kappa(\omega) = \omega + ik_\infty + k_*(\omega)$, and therefore, for every $t, \tau \in \mathbb{R}$

$$\begin{aligned} k(t, \tau) & := \mathcal{F}^{-1} \left[e^{i(\cdot + i\kappa_\infty + k_*(\cdot))\tau} \right] (t) \\ & = e^{-k_\infty \tau} \mathcal{F}^{-1} \left[e^{ik_*(\cdot)\tau} \right] (t - \tau) \\ & = e^{-k_\infty \tau} \mathcal{F}^{-1} \left[1 + (e^{ik_*(\cdot)\tau} - 1) \right] (t - \tau) \\ & = \sqrt{2\pi} e^{-k_\infty \tau} \delta(t - \tau) + e^{-k_\infty \tau} \mathcal{F}^{-1} \left[e^{ik_*(\cdot)\tau} - 1 \right] (t - \tau). \end{aligned} \quad (3.25)$$

Because there exists a constant $C > 0$ such that

$$\left| e^{ik_*(\omega)\tau} - 1 \right| \leq C |k_*(\omega)\tau| \text{ for all } \omega, \tau \in \mathbb{R},$$

it follows from [Definition 3.2.2](#) (stating that $k_* \in L^2(\mathbb{R}; \mathbb{C})$) and Plancharel's identity that

$$\begin{aligned} \omega &\rightarrow e^{ik_*(\omega)\tau} - 1 \in L^2(\mathbb{R}; \mathbb{C}) \text{ and} \\ t &\rightarrow e^{-k_\infty \tau} \mathcal{F}^{-1} \left[e^{ik_*(\cdot)\tau} - 1 \right] (t - \tau) \in L^2(\mathbb{R}; \mathbb{C}) \text{ for all } \tau \in \mathbb{R} . \end{aligned}$$

Now, assume that $\rho \in C^0(\mathbb{R} \times \mathbb{R}^3; \mathbb{C}) \cap \mathcal{S}'$ with support in $[0, \infty) \times \mathbb{R}^3$, $\phi \in \mathcal{S}(\mathbb{R})$ and $\psi \in \mathcal{S}(\mathbb{R}^3)$

$$\begin{aligned} &\langle \rho, \nu[\phi] \otimes \psi \rangle_{\mathcal{S}', \mathcal{S}} \\ &= \int_{\mathbb{R}^3} \int_{\tau=-\infty}^{\infty} \rho(\tau, \mathbf{x}) \overline{\nu[\phi](\tau)} \overline{\psi(\mathbf{x})} \, d\tau \, d\mathbf{x} \\ &= \frac{1}{\sqrt{2\pi}} \int_{\mathbb{R}^3} \overline{\psi(\mathbf{x})} \int_{\tau=-\infty}^{\infty} \rho(\tau, \mathbf{x}) \int_{\omega=-\infty}^{\infty} e^{i\kappa(\omega)\tau} \hat{\phi}(\omega) \, d\omega \, d\tau \, d\mathbf{x} . \end{aligned}$$

Using Parseval's identity we get

$$\begin{aligned} &\langle \rho, \nu[\phi] \otimes \psi \rangle_{\mathcal{S}', \mathcal{S}} \\ &= \frac{1}{\sqrt{2\pi}} \int_{\mathbb{R}^3} \int_{\tau=-\infty}^{\infty} \rho(\tau, \mathbf{x}) \overline{\psi(\mathbf{x})} \int_{t=-\infty}^{\infty} k(t, \tau) \overline{\phi(t)} \, dt \, d\tau \, d\mathbf{x} \\ &= \int_{\mathbb{R}^3} \int_{t=-\infty}^{\infty} \overline{\psi(\mathbf{x})} \phi(t) \underbrace{\left(\frac{1}{\sqrt{2\pi}} \int_{\tau=-\infty}^{\infty} k(t, \tau) \rho(\tau, \mathbf{x}) \, d\tau \right)}_{=\mathcal{B}[\rho](t, \mathbf{x})} \, dt \, d\mathbf{x} . \end{aligned} \tag{3.26}$$

Then for $\rho \in C^0(\mathbb{R} \times \mathbb{R}^3; \mathbb{C}) \cap \mathcal{S}'$ it follows from [\(3.26\)](#) and [\(3.25\)](#) that

$$\boxed{e^{k_\infty t} \mathcal{B}[\rho](t, \mathbf{x}) = (\mathcal{I}d + \mathcal{T})[\rho](t, \mathbf{x}) ,} \tag{3.27}$$

where

$$\mathcal{T}[\rho](t, \mathbf{x}) = \frac{1}{\sqrt{2\pi}} \int_{\tau=-\infty}^{\infty} e^{k_\infty(t-\tau)} \mathcal{F}^{-1} \left[e^{ik_*(\omega)\tau} - 1 \right] (t - \tau) \rho(\tau, \mathbf{x}) \, d\tau . \tag{3.28}$$

Theorem 3.2.6 *Let $q = \mathcal{I}[p]$ and $q^a = \mathcal{I}[p^a]$, where p and p^a are the solutions of the equations [\(3.1\)](#) and [\(3.2\)](#), respectively. Then*

$$q^a = \mathcal{B}[q] . \tag{3.29}$$

Proof: Let $\phi \in \mathcal{S}(\mathbb{R})$ and $\psi \in \mathcal{S}(\mathbb{R}^3)$. Then, from [\(3.29\)](#), the definition of the Fourier-transform [\(3.3\)](#), the definition of $\mathcal{B}[\cdot]$ in [\(3.24\)](#), because $\nu[\phi] \in \mathcal{S}(\mathbb{R})$ (see [\(3.20\)](#)) and because q solves

(3.16) it follows that

$$\begin{aligned}
& \langle \mathcal{A}_\kappa[\mathcal{B}[q]], \phi \otimes \psi \rangle_{S', S} - \langle \mathcal{B}[q], \phi \otimes \Delta_{\mathbf{x}} \psi \rangle_{S', S} \\
&= - \left\langle \mathcal{B}[q], \widetilde{\kappa^2 \hat{\phi}} \otimes \psi \right\rangle_{S', S} - \langle \mathcal{B}[q], \phi \otimes \Delta_{\mathbf{x}} \psi \rangle_{S', S} \\
&= - \left\langle q, \nu \left[\widetilde{\kappa^2 \hat{\phi}} \right] \otimes \psi \right\rangle_{S', S} - \langle q, \nu[\phi] \otimes \Delta_{\mathbf{x}} \psi \rangle_{S', S} \\
&= - \left\langle q, \nu \left[\widetilde{\kappa^2 \hat{\phi}} \right] \otimes \psi \right\rangle_{S', S} - \langle q, \partial_{\tau\tau} \nu[\phi] \otimes \psi \rangle_{S', S} \\
&\quad + \nu[\phi](0) \langle h, \psi \rangle_{S'(\mathbb{R}^3), S(\mathbb{R}^3)}
\end{aligned} \tag{3.30}$$

We are representing every term on the right hand side:

1. From [Theorem 3.2.4](#) it follows that

$$\nu[\phi](0) = \frac{1}{\sqrt{2\pi}} \int_{\omega=-\infty}^{\infty} \hat{\phi}(\omega) d\omega = \check{\phi}(0) = \phi(0)$$

and thus

$$\nu[\phi](0) \langle h, \psi \rangle_{S'(\mathbb{R}^3), S(\mathbb{R}^3)} = \phi(0) \langle h, \psi \rangle_{S'(\mathbb{R}^3), S(\mathbb{R}^3)}.$$

2. The first term on the right hand side of (3.30) can be represented as follows:

$$\left\langle q, \nu \left[\widetilde{\kappa^2 \hat{\phi}} \right] \otimes \psi \right\rangle_{S', S} = \left\langle q, \frac{1}{\sqrt{2\pi}} \int_{\omega=-\infty}^{\infty} \overline{\kappa^2(\omega)} e^{-i\overline{\kappa(\omega)} \cdot} \hat{\phi}(\omega) d\omega \otimes \psi \right\rangle_{S', S}.$$

3. For the second term we find that

$$\begin{aligned}
\langle q, \partial_{\tau\tau} \nu[\phi] \otimes \psi \rangle_{S', S} &= \left\langle q, \frac{1}{\sqrt{2\pi}} \int_{\omega=-\infty}^{\infty} \partial_{\tau\tau} e^{-i\overline{\kappa(\omega)} \cdot} \hat{\phi}(\omega) d\omega \otimes \psi \right\rangle_{S', S} \\
&= - \left\langle q, \frac{1}{\sqrt{2\pi}} \int_{\omega=-\infty}^{\infty} \overline{\kappa^2(\omega)} e^{-i\overline{\kappa(\omega)} \cdot} \hat{\phi}(\omega) d\omega \otimes \psi \right\rangle_{S', S}.
\end{aligned}$$

The sum of the first and second term vanishes and thus from (3.30) it follows that

$$\begin{aligned}
& \langle \mathcal{A}_\kappa[\mathcal{B}[q]], \phi \otimes \psi \rangle_{S', S} - \langle \mathcal{B}[q], \phi \otimes \Delta_{\mathbf{x}} \psi \rangle_{S', S} \\
&= \phi(0) \langle h, \psi \rangle_{S'(\mathbb{R}^3), S(\mathbb{R}^3)},
\end{aligned}$$

which shows that $\mathcal{B}[q]$ solves (3.15). Since the solution of this equation is unique it follows that $q^a = \mathcal{B}[q]$. \square

3.3 Reconstruction formulas

In this section we provide explicit reconstruction formulas for the absorption density h (the right hand side of (3.2)) in **attenuating** media. The basis of these formulas are exact reconstruction formulas in **non-attenuating** media.

In the case of non-attenuating media the problem of photoacoustic tomography consists in determining the absorption density h from measurement data of

$$m(t, \xi) := p(t, \xi) \text{ for all } t > 0, \xi \in \Gamma,$$

where Γ denotes the measurement surface and p is the solution of (3.1).

Let \mathcal{W} be the operator which maps h to p . The most universal (meaning applicable for a series of measurement geometries Γ) formula for $\mathcal{W}^{-1}[\cdot]$ is due to Xu & Wang [XW05]. Several different formulas of such kind were presented and analyzed in [KK08; Nat12; Kuc12]. The formula of Xu & Wang [XW05] in \mathbb{R}^3 reads as follows:

$$h(x) = \frac{2}{\Omega_0} \int_{\xi \in \Gamma} \frac{p(|\xi - x|, \xi) - |\xi - x| \frac{\partial p}{\partial t}(|\xi - x|, \xi)}{|\xi - x|^2} \left(\mathbf{n}_\xi \cdot \frac{\xi - x}{|\xi - x|} \right) ds(\Gamma) \quad (3.31)$$

where Ω_0 is 2π for a planar geometry and 4π for cylindrical and spherical geometries and \mathbf{n}_ξ is the outer normal vector for the measurement surface Γ .

From Theorem 3.2.6 we get an explicit reconstruction formula in the case of attenuating media:
Theorem 3.3.1 *Under the assumption that the universal back-projection can be applied in the non-attenuating case, we have*

$$h = \mathcal{W}^{-1} [\partial_t \mathcal{B}^{-1} [(t, \xi) \rightarrow q^a(t, \xi)]] . \quad (3.32)$$

In the following we study the attenuation operator $\mathcal{B}[\cdot]$ and its inverse in weakly attenuating media.

From (3.27) it follows

$$h = \mathcal{W}^{-1} \left[\partial_t (\mathcal{I}d + \mathcal{T})^{-1} [(t, \xi) \rightarrow e^{k_\infty t} q^a(t, \xi)] \right] . \quad (3.33)$$

In particular, in the case of a constantly attenuating medium the kernel of the integral operator $\mathcal{B}[\cdot]$ simplifies to ($k_*(\omega) = 0$)

$$\frac{1}{\sqrt{2\pi}} \mathcal{F}^{-1} \left[e^{i\kappa(\cdot)\tau} \right] (t) = \frac{1}{\sqrt{2\pi}} e^{-k_\infty \tau} \mathcal{F}^{-1} \left[e^{i\cdot\tau} \right] (t) = e^{-k_\infty \tau} \delta(t - \tau).$$

Thus from (3.26) it follows that

$$\boxed{\mathcal{B}[q](t, \mathbf{x}) = \frac{1}{\sqrt{2\pi}} e^{-k_\infty t} q(t, \mathbf{x}) .} \quad (3.34)$$

Thus the operator $\mathcal{B}[\cdot]$ is a multiplication operator and the reconstruction formula (3.33) rewrites to

$$h = \mathcal{W}^{-1} \left[(t, \xi) \rightarrow \partial_t \left(e^{k_\infty t} q^a(t, \xi) \right) \right]. \quad (3.35)$$

Using that $q = e^{k_\infty t} q^a$, we get explicit formulas for the time derivatives of q :

$$\begin{aligned} \partial_t q(t, \xi) &= e^{k_\infty t} (k_\infty q^a(t, \xi) + \partial_t q^a(t, \xi)), \\ \partial_{tt} q(t, \xi) &= e^{k_\infty t} (k_\infty^2 q^a(t, \xi) + 2k_\infty \partial_t q^a(t, \xi) + \partial_{tt} q^a(t, \xi)). \end{aligned}$$

Therefore, inserting the representation of the derivatives in (3.31) we get

$$\boxed{\begin{aligned} \tilde{q}^a(t, \xi) &= \partial_t q^a(t, \xi) - t \partial_{tt} q^a(t, \xi), \\ h(\mathbf{x}) &= \frac{2}{\Omega_0} \int_{\xi \in \Gamma} \frac{\tilde{q}^a(|\xi - \mathbf{x}|, \xi)}{|\xi - \mathbf{x}|^2} \left(\mathbf{n}_\xi \cdot \frac{\xi - \mathbf{x}}{|\xi - \mathbf{x}|} \right) ds(\Gamma). \end{aligned}} \quad (3.36)$$

3.4 Numerical experiments

In this section we describe an algorithm for photoacoustic inversion in a weakly attenuating medium, in which case the attenuation coefficient is $\omega \rightarrow \kappa(\omega) = \omega + ik_\infty + k_*(\omega)$, with $k_* \in L^2(\mathbb{R}; \mathbb{C}) \cap C^\infty(\mathbb{R}; \mathbb{C})$.

The numerical inversions and examples will be performed in \mathbb{R}^2 for the two-dimensional attenuated wave equation. This is consistent with a distributional solution of (3.2) in \mathbb{R}^3 where $(x, y, z) \rightarrow h(x, y)$ is considered a distribution in \mathbb{R}^3 , which is independent of the third variable. In this case p^a can be considered a two-dimensional distribution (3.2), which solves the two-dimensional attenuated wave equation:

$$\begin{aligned} \mathcal{A}_\kappa[p^a](t, x_1, x_2) - \Delta p^a(t, x_1, x_2) &= \delta'(t) h(x_1, x_2), & t \in \mathbb{R}, (x_1, x_2) \in \mathbb{R}^2, \\ p^a(t, x_1, x_2) &= 0, & t < 0, (x_1, x_2) \in \mathbb{R}^2. \end{aligned} \quad (3.37)$$

The two-dimensional universal back-projection formula from [Bur+07a], which is used below, is given by

$$h(x) = -\frac{4}{\Omega_0} \int_{\xi \in \Gamma} \int_{t=|\xi-\mathbf{x}|}^{\infty} \left(\frac{(\partial_t(t^{-1}p))(t, \xi)}{\sqrt{t^2 - |\xi - \mathbf{x}|^2}} dt \right) \mathbf{n}_\xi \cdot (\xi - \mathbf{x}) ds(\Gamma), \quad (3.38)$$

where Ω_0 is 2π for a line measurement geometry and 4π for a circular measurement geometry, \mathbf{n}_ξ is the outer normal vector for the curve Γ .

We assume that the attenuated photoacoustic pressure p^a is measured on a set of N points on a measurement curve Γ at N_T uniformly distributed time points

$$t_i = i\Delta_T, \quad i = 1, \dots, N_T \quad \text{where} \quad \Delta_T = \frac{T}{N_T}.$$

In our experiments Γ will either be a circle of radius R , where the N measurement points are radially uniformly distributed,

$$\xi_j = R(\cos(j\Delta_\xi), \sin(j\Delta_\xi)), \quad j = 0, 1, \dots, N-1 \text{ where } \Delta_\xi = \frac{2\pi}{N}$$

or on a segment of length $2l$ of the x -axis, in which case

$$\xi_j = (2j\Delta_x - 1, 0), \text{ where } \Delta_x = l/N.$$

In this case we consider h to be supported in the upper half-space.

The evaluation of the integral operator $\mathcal{I}[\cdot]$ is numerically realized as follows: For every measurement point $\{\xi_j : j = 0, 1, \dots, N-1\}$

$$q^a(t_i, \xi_j) = \Delta_T \sum_{n=1}^i p^a(t_n, \xi_j). \quad (3.39)$$

The relation $q^a = \mathcal{B}[q]$ from (3.29) is realized numerically as follows: Because we assume a weakly attenuation medium $\mathcal{B}[\cdot]$ (defined in (3.24)) is an integral operator with kernel k defined in (3.25). We use the Taylor-series expansion of the exponential function $\tau \rightarrow e^{ik_*(\omega)\tau}$ and get

$$\mathcal{F}^{-1} \left[e^{ik_*(\omega)\tau} - 1 \right] (t) = \sum_{k=1}^{\infty} \frac{\tau^k}{k!} \mathcal{F}^{-1} \left[(ik_*(\omega))^k \right] (t). \quad (3.40)$$

Inserting (3.40) into (3.28) and taking into account (3.27) and (3.29) we get for all $i = 1, \dots, N_T$ that

$$\begin{aligned} & q^a(t_i, \xi_j) \\ &= e^{-k_\infty t_i} q(t_i, \xi_j) + \frac{1}{\sqrt{2\pi}} \int_{\tau=-\infty}^{\infty} e^{-k_\infty \tau} \sum_{k=1}^{\infty} \frac{\tau^k}{k!} r_k(t_i - \tau) q(\tau, \xi_j) d\tau, \end{aligned} \quad (3.41)$$

where

$$s \rightarrow r_k(s) := \mathcal{F}^{-1} \left[i^k k_*^k(\omega) \right] (s).$$

The integral on the right hand side of (3.41) is approximated for numerical purposes as follows:

$$\frac{\Delta_T}{\sqrt{2\pi}} \sum_{m=1}^{N_T} e^{-k_\infty t_m} \sum_{k=1}^{\infty} \frac{t_m^k}{k!} r_k(t_i - t_m) q(t_m, \xi_j). \quad (3.42)$$

This expression is represented as a matrix-vector multiplication with vector $\vec{q}_j = (q(t_m, \xi_j))_{m=1, \dots, N_T}$ and matrix with entries

$$b_{im} = \frac{\Delta_T}{\sqrt{2\pi}} e^{-k_\infty t_m} \sum_{k=1}^{\infty} \frac{t_m^k}{k!} r_k(t_i - t_m) \text{ with } 1 \leq i \leq N_T, \text{ and } 1 \leq m \leq N_T. \quad (3.43)$$

Then it follows from (3.41) that

$$\vec{q}_j^a = (e^{-k_\infty t_i} I + B) \vec{q}_j, \quad (3.44)$$

which is the discretized version of (3.27). To get numerical values for the entries of B , the terms $r_k(t_i - t_m)$ have to be numerically calculated. For $k = 1$,

$$r_1(t) = \frac{1}{\sqrt{2\pi}} \int_{\omega=-\infty}^{\infty} ik_*(\omega) e^{-i\omega t} d\omega, \quad (3.45)$$

which can be evaluated by numerical integration for all t_i . When $k > 1$, r_k is a convolution of r_{k-1} and r_1 and thus

$$r_k(t) = \frac{1}{\sqrt{2\pi}} (r_1 * r_{k-1})(t) = \frac{1}{\sqrt{2\pi}} \int_0^t r_1(\tau) r_{k-1}(t - \tau) d\tau. \quad (3.46)$$

Numerically, we approximate the convolution by

$$r_k(t_i) \approx \frac{\Delta_T}{\sqrt{2\pi}} \sum_{m=1}^i r_1(t_m) r_{k-1}(t_i - t_m).$$

We summarize the inversion process in a pseudo-code, where we truncate the Taylor-series (3.40) at the tenth coefficient (the number ten has been found from numerical simulations):

Data: The measurements are denoted by $P_{i,j}^a = p^a(t_i, \xi_j)$ for all $i = 1, \dots, N_T$ and $j = 0, \dots, N - 1$

Result: Numerical calculation of the absorption density $h_l = h(x_l)$

```

for  $1 \leq i \leq N_T$  do
    |  $r_{i,1} \leftarrow \frac{1}{\sqrt{2\pi}} \int_{\omega=-\infty}^{\infty} e^{-i\omega t_i} (ik_*(\omega)) d\omega;$ 
end
for  $1 \leq k \leq 10$  do
    | for  $1 \leq m \leq n \leq N_T$  do
    | |  $(F_k)_{i,m} \leftarrow \frac{1}{\sqrt{2\pi}} r_{i-m,k} t_m^k e^{-k_\infty t_m};$ 
    | end
    | for  $1 \leq i \leq N_T$  do
    | |  $r_{i,k+1} = \frac{\Delta_T}{\sqrt{2\pi}} \cdot (\sum_{m=1}^i r_{m,k} r_{i-m,k});$ 
    | end
end
 $B \leftarrow \text{diag}(e^{-k_\infty t_1}, e^{-k_\infty t_2}, \dots) + \Delta_T \sum_{k=1}^{10} \frac{F_k}{k!};$ 
for  $1 \leq i \leq N_T$  do
    |  $Q_{i,j}^a \leftarrow Q_{i-1,j}^a + \Delta_T P_{i,j}^a;$ 
end
 $Q \leftarrow Q^a B^{-1};$ 
for  $1 \leq i \leq N_T$  do
    |  $P_{i,j} \leftarrow \frac{Q_{i,j} - Q_{i-1,j}}{\Delta_T};$ 
end

```

Calculate h_l by applying the back-projection operator $\mathcal{W}^{-1}[\cdot]$ on $P_{i,j}$;

Algorithm 1: Pseudocode for reconstructing the absorption density h .

Numerical experiments

We assume that h is a function with compact support in \mathbb{R}^2 . We calculated p , the solution of (3.1) using the k-wave toolbox [TC10]. By integrating p at the points $\xi_j, j = 0, \dots, N - 1$ over time with (3.39) we get $q(t_i, \xi_j)$ for $i = 1, \dots, N_T$ and $j = 0, \dots, N - 1$. Then we find $q^a(t_i, \xi_j)$ by matrix-vector multiplication (3.44).

In order to avoid *inverse crimes* we used different discretization points in space and time for the simulation of the forward data and the inversion. The forward problem is simulated with $N_T = 500$ and $N = 896$, while the inverse problem is solved with $N_T = 443$ and $N = 849$. The absorption density function $h : \mathbb{R}^2 \rightarrow \mathbb{R}$ with support in $(-0.8, 0.8)^2$ is the Shepp-Logan phantom [SV74]. In all numerical experiments the material parameter $k_\infty = 0.45$.

Circular measurement geometry

In these examples the measurement geometry is a circle with radius $R = 1.7$ on which there are recorded data on $N = 849$ uniformly distributed measurement points. Moreover, the time length is 6 and thus $\Delta_T = 6/N_T = 6/443$.

We consider a constantly attenuating medium, with attenuation coefficient $\kappa(\omega) = \omega + ik_\infty$. Figure 3.2 shows the ground truth (top left) and the simulated pressure data p^a on Γ over time. Two reconstructions are presented: The first one is obtained by applying the universal back-projection formula (3.38) (middle left), while the middle right image shows the reconstruction obtained with algorithm 1. The quantitative values of ground truth and the two reconstructions are plotted on the bottom.

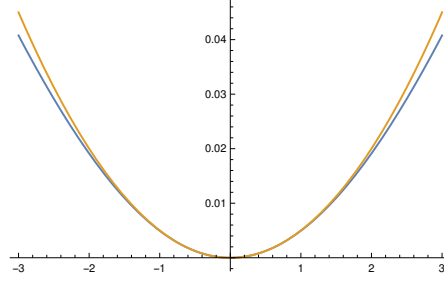


FIGURE 3.1: Blue curve corresponds to $\Im \kappa(\omega)$ of NSW model. Red curve corresponds to power law $0.005\omega^2$.

Next we consider the Nachman, Smith and Waag (NSW) [NSW90] attenuation model:

$$\kappa(\omega) = \omega \sqrt{\frac{1 - i\omega\tilde{\tau}}{1 - i\omega\tau}} = \omega + \frac{\tau - \tilde{\tau}}{2\tau\tilde{\tau}}i + k_*(\omega) \quad (3.47)$$

where $k_*(\omega) = \mathcal{O}(|\omega|^{-1})$. Therefore, κ is a weak attenuation coefficient with $k_\infty = \frac{\tau - \tilde{\tau}}{2\tau\tilde{\tau}}$. In Figure 3.3 we present ground truth, simulated measurements p^a , and compare three imaging techniques:

- Applying the universal back-projection formula $\mathcal{W}^{-1}[p^a]$ (3.38) (thus neglecting the attenuation).
- The compensated back-projection formula

$$\mathcal{W}^{-1} \left[(t, \xi) \mapsto \partial_t \left(e^{k_\infty t} q^a(t, \xi) \right) \right], \quad (3.48)$$

which neglects $k_*(\omega)$ but takes into account k_∞ .

- Reconstruction using (3.32) with the numerical code described in algorithm 1.

The parameters of attenuation coefficient in the NSW model are $\tilde{\tau} = 0.1$ and $\tau = 0.11$. For small frequencies the NSW coefficients behaves like a power law of order 2. However, asymptotically, for large frequencies, it behaves like $\omega + \frac{\tau - \tilde{\tau}}{2\tau\tilde{\tau}}i$. The NSW-coefficient has been plotted in Figure 3.1. In order to demonstrate the stability of the algorithm, we also performed reconstructions from noisy data, where a uniformly distributed noise is added with a variance of 20% of the maximal intensity. The reconstruction results are depicted in the last image of Figure 3.2 and Figure 3.3, respectively.

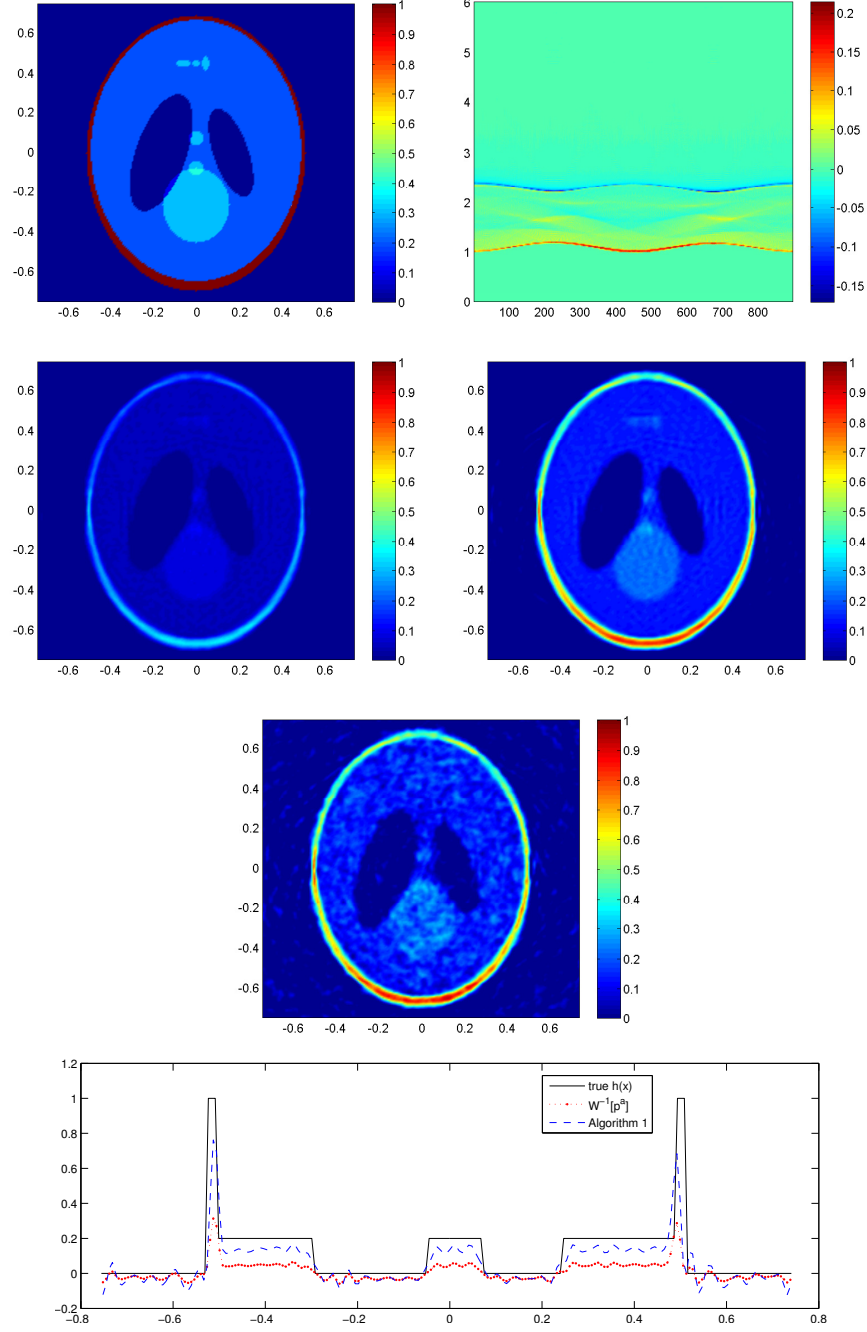


FIGURE 3.2: Measurements along a circle and constantly attenuating model. Top left: Ground truth. Top Right: the simulated pressure data p^a . Middle: Reconstruction by universal back-projection (not taking into account attenuation), and by [algorithm 1](#) with noise-free and 20% noise. Bottom: Cross section through ground truth and reconstructions.

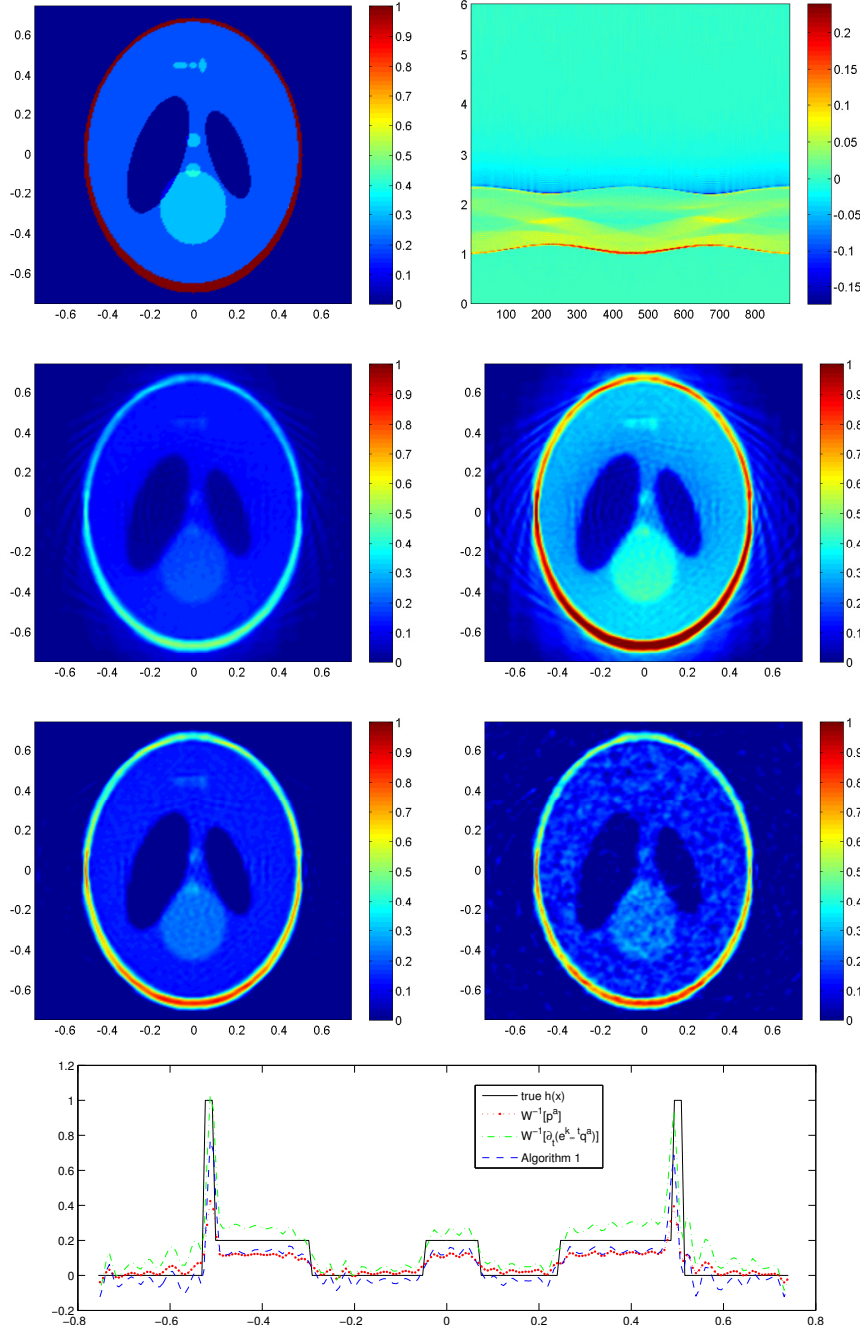


FIGURE 3.3: Measurements along a circle and NSW model. Top left: Ground truth. Top Right: the simulated pressure data p^a . Middle: Reconstruction by universal back-projection (not taking into account attenuation), by compensated attenuation (3.48) and by algorithm 1 with noise-free and 20% noise. Bottom: Cross section through ground truth and reconstructions.

Measurements on a line

The measurement points are $N = 849$ uniformly distributed on a line segment with length $l = 10.2$. The distance of the line to the center of the phantom is 1.7. The time length is 8 and thus $\Delta_T = 8/443$.

We consider a constantly attenuating medium, with attenuation coefficient $\kappa(\omega) = \omega + ik_\infty$. [Figure 3.4](#) shows the ground truth (top left) and the simulated pressure data p^a on Γ over time. Two reconstructions are presented: The first one is obtained by applying the universal back-projection formula (3.38) (middle left) and the middle right image shows the reconstruction obtained with [algorithm 1](#). The quantitative values of ground truth and the two reconstructions are plotted on the bottom.

In [Figure 3.5](#) we present ground truth, simulated measurements p^a using NSW model, and compare three imaging techniques, the universal back-projection formula neglecting attenuation, the compensated back-projection formula (3.48), which neglects $k_*(\omega)$ but takes into account k_∞ , and reconstruction with [algorithm 1](#). The parameters of the NSW attenuation coefficient are again $\tilde{\tau} = 0.1$ and $\tau = 0.11$. The reconstruction results from noisy data are depicted in the last image of [Figure 3.4](#) and [Figure 3.5](#), where uniformly distributed noise is added with a variance of 20% of the maximal intensity value. Numerical results show that the algorithm is quite stable even with 20% noise.

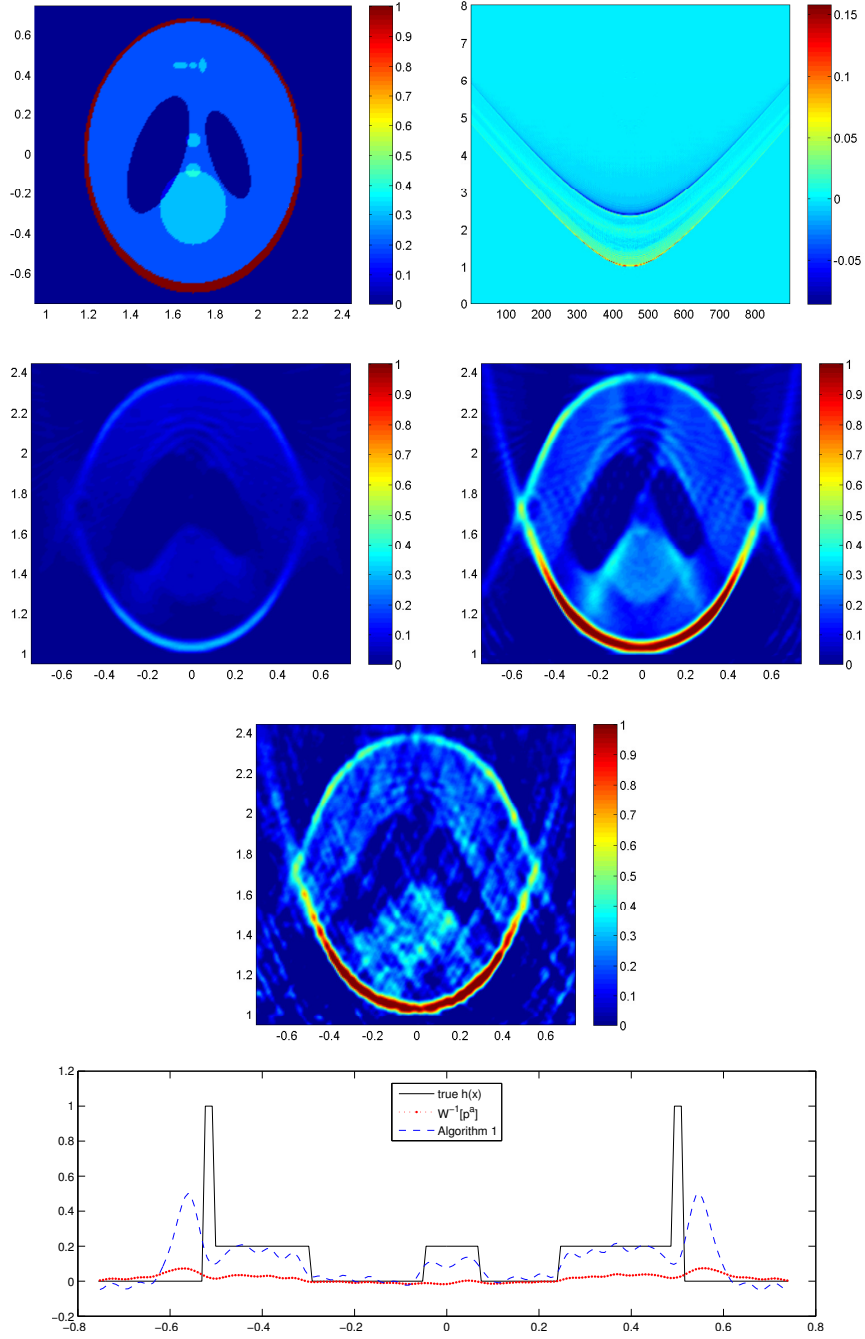


FIGURE 3.4: Measurements along a line and constantly attenuating model. Top left: Ground truth. Top Right: the simulated pressure data p^a . Middle: Reconstruction by universal back-projection (not taking into account attenuation), and by [algorithm 1](#) with noise-free and 20% noise. Bottom: Cross section through ground truth and reconstructions.

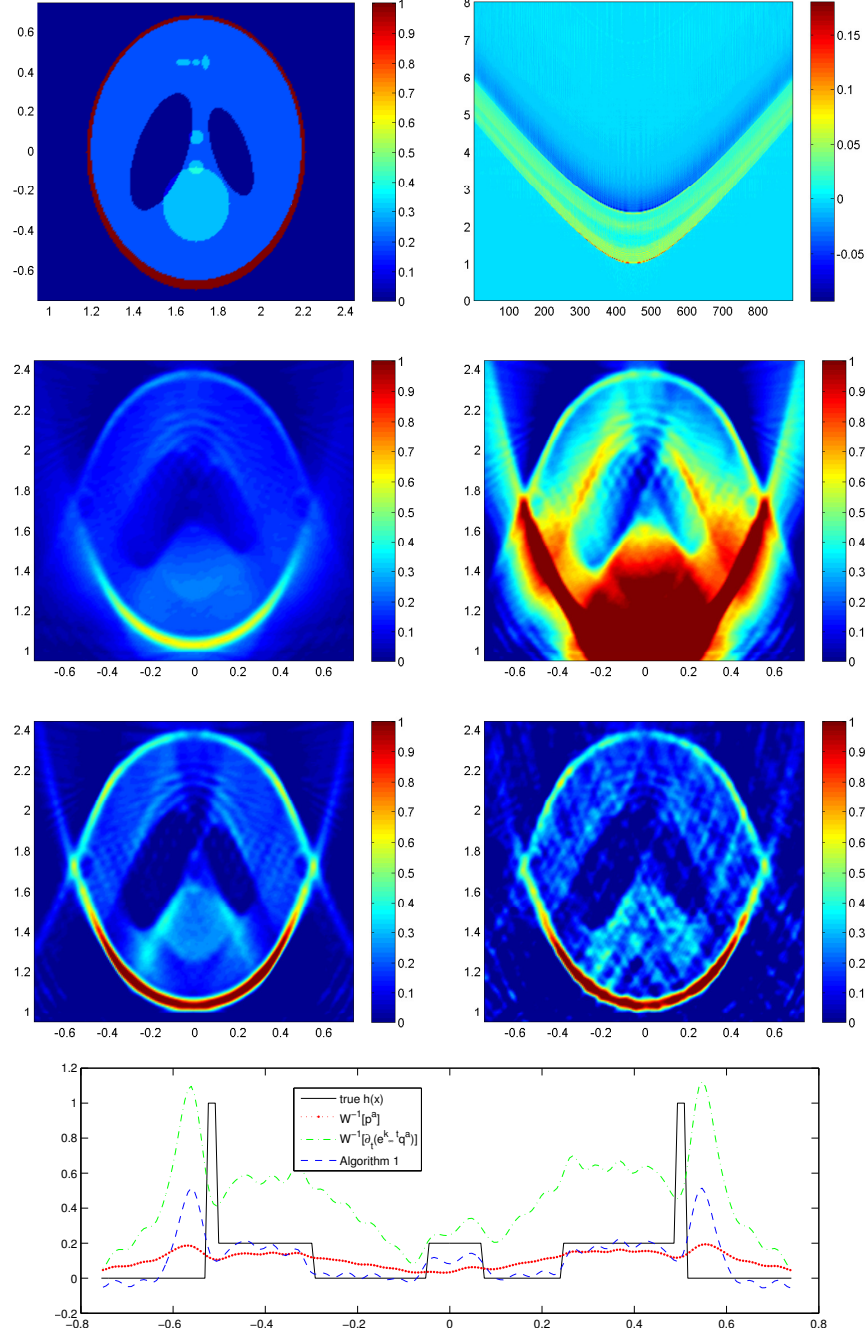


FIGURE 3.5: Measurements along a line and NSW model. Top left: Ground truth. Top Right: the simulated pressure data p^a . Middle: Reconstruction by universal back-projection (not taking into account attenuation), by compensated attenuation (3.48) and by algorithm 1 with noise-free and 20% noise. Bottom: Cross section through ground truth and reconstructions.

Conclusion

We have presented explicit reconstruction formulas for photoacoustic imaging in acoustically attenuating media, which are based on the universal back-projection formula. We have presented a numerical algorithm and showed numerical reconstructions, which were compared with attenuation compensation techniques. The numerical simulations show that the new technique can produce better visualization in 2D with a similar numerical complexity.

Acknowledgment

The work is support by the “Doctoral Program Dissipation and Dispersion in Nonlinear PDEs” (W1245). OS is also supported by the FWF-project “Interdisciplinary Coupled Physics Imaging” (FWF P26687).

3.A Appendix

Theorem 3.A.1 [*HÖ3*, Section 7.7] Let $f, g \in C^\infty(\mathbb{R}; \mathbb{C})$ satisfying

- $\text{supp } g$ is compact and
- $\Im f(\omega) \geq 0$.

Then there exists a constant $C_1 > 0$ such that for all $l \in \mathbb{N}$ and all $\tau \geq 0$,

$$\begin{aligned} & \tau^l \left| \int_{\omega=-\infty}^{\infty} e^{i\tau f(\omega)} g(\omega) d\omega \right| \\ & \leq C_1 \sum_{\alpha=0}^l \sup_{\omega \in \mathbb{R}} |d^\alpha g(\omega)| (|f'(\omega)|^2 + \Im f(\omega))^{\alpha/2-l}. \end{aligned} \quad (3.49)$$

Lemma 3.A.2 Let κ be an attenuation coefficient (cf. [Definition 3.2.1](#)), then there exists a constant $C_2 > 0$ such that

$$|\kappa'(\omega)|^2 + \Im \kappa(\omega) \geq C_2. \quad (3.50)$$

Proof: The fourth assumption of [Definition 3.2.1](#) ensures that the maximal speed of propagation c is finite. Then from [[ESS16](#), Proposition 2.9], it follows that the holomorphic extension $\tilde{\kappa}$ (cf. [Definition 3.2.1](#)) of κ to the upper half plane can be represented as

$$\tilde{\kappa}(z) = Az + B + \int_{\nu=-\infty}^{\infty} \frac{1 + z\nu}{\nu - z} d\sigma(\nu), \quad z \in \mathbb{H}, \quad (3.51)$$

where $A = \frac{1}{c} > 0$, $B \in \mathbb{R}$ are constants, and $\sigma : \mathbb{R} \rightarrow \mathbb{R}$ is a monotonically increasing function of bounded variation.

From [Nus72, Formula (C9)] we know that if $\tilde{\kappa}$ satisfies (3.51), then

$$\nu \rightarrow \Im \kappa(\nu) = \pi(1 + \nu^2)\sigma'(\nu) \text{ for all } \nu \in \mathbb{R}. \quad (3.52)$$

Because, by assumption $\kappa \in C^\infty(\mathbb{R}; \mathbb{C})$, and because $\sigma : \mathbb{R} \rightarrow \mathbb{R}$ is a monotonically increasing function of bounded variation, we conclude from (3.52) that $\sigma' \in C^\infty(\mathbb{R}; \mathbb{R}) \cap L^1(\mathbb{R}; \mathbb{R})$. Moreover, for all fixed $z \in \mathbb{H}$, because $\nu - z \neq 0$ for all $\nu \in \mathbb{R}$, we have $\nu \rightarrow \frac{1+\nu^2}{(\nu-z)^2}$ is uniformly bounded and thus the function

$$\nu \rightarrow \frac{1 + \nu^2}{(\nu - z)^2} \sigma'(\nu) \in L^1(\mathbb{R}; \mathbb{C}).$$

Differentiation of (3.51) with respect to z and taking into account that $\sigma' \in C^\infty(\mathbb{R}; \mathbb{R}) \cap L^1(\mathbb{R}; \mathbb{R})$ yields

$$\tilde{\kappa}'(z) = A + \int_{\nu=-\infty}^{\infty} \frac{(1 + \nu^2)}{(\nu - z)^2} \sigma'(\nu) d\nu, \quad z \in \mathbb{H}.$$

Let now $z = \omega + i\eta$ and take real parts in the above formula to get

$$\Re \tilde{\kappa}'(\omega + i\eta) = A + \int_{\nu=-\infty}^{\infty} (1 + \nu^2) \frac{(\nu - \omega)^2 - \eta^2}{((\nu - \omega)^2 + \eta^2)^2} \sigma'(\nu) d\nu. \quad (3.53)$$

We are proving now that there exists a constant $C_r > 0$ such that

$$\Re \kappa'(\omega) = \lim_{\eta \rightarrow 0^+} \Re \tilde{\kappa}'(\omega + i\eta) \geq A - 2(1 + C_r) \sqrt{(1 + \omega^2)\sigma'(\omega)}. \quad (3.54)$$

Let

$$\begin{aligned} \mathcal{A}_+ &:= \{\nu \in \mathbb{R} : |\nu - \omega|^2 \geq (1 + \omega^2)\sigma'(\omega)\}, \\ \mathcal{A}_- &:= \{\nu \in \mathbb{R} : |\nu - \omega|^2 < (1 + \omega^2)\sigma'(\omega)\}, \\ \mathcal{A}_0 &:= \{\hat{\nu} \in \mathbb{R} : |\hat{\nu}|^2 < (1 + \omega^2)\sigma'(\omega)\}. \end{aligned}$$

For $\omega \in \mathbb{R}$ and $\eta > 0$ let

$$\nu \rightarrow \rho_{\omega, \eta}(\nu) := (1 + \nu^2) \frac{(\nu - \omega)^2 - \eta^2}{((\nu - \omega)^2 + \eta^2)^2} \sigma'(\nu) \text{ for all } \omega \neq \nu \in \mathbb{R}.$$

The function $\rho_{\omega, \eta}$ can be estimated as follows:

$$\rho_{\omega, \eta}(\nu) = \frac{1 + \nu^2}{(\nu - \omega)^2 + \eta^2} \underbrace{\frac{(\nu - \omega)^2 - \eta^2}{(\nu - \omega)^2 + \eta^2}}_{\leq 1} \sigma'(\nu)$$

Moreover, since $\nu \in \mathcal{A}_+$, we find that

$$\frac{1 + \nu^2}{(\nu - \omega)^2 + \eta^2} \leq \frac{1 + \nu^2}{(\nu - \omega)^2} = \underbrace{\frac{1 + \nu^2}{1 + (\nu - \omega)^2}}_{\leq 2(1 + \omega^2)} \underbrace{\frac{1 + (\nu - \omega)^2}{(\nu - \omega)^2}}_{\leq 1 + ((1 + \omega^2)\sigma'(\omega))^{-1}},$$

where the inequality $\frac{1+\nu^2}{1+(\nu-\omega)^2} \leq 2(1+\omega^2)$ is a consequence of the algebraic identity $2(1+\omega^2)(1+(\nu-\omega)^2) - (1+\nu^2) = 2\omega^2(\nu-\omega)^2 + (\nu-2\omega)^2 + 1 > 0$. Therefore with $C_\omega = 2(1+\omega^2)(1+((1+\omega^2)\sigma'(\omega))^{-1})$ it follows that

$$|\rho_{\omega,\eta}(\nu)| \leq C_\omega \sigma'(\nu),$$

and because $\sigma' \in L^1(\mathbb{R}; \mathbb{R})$ the latter means that the functions $\{\rho_{\omega,\eta} : \eta > 0\}$ are uniformly dominated by an $L^1(\mathbb{R}; \mathbb{R})$ function. Therefore we can apply the dominated convergence theorem and get

$$\lim_{\eta \rightarrow 0^+} \int_{\mathcal{A}_+} \rho_{\omega,\eta}(\nu) d\nu = \int_{\mathcal{A}_+} \rho_{\omega,0}(\nu) d\nu \geq 0. \quad (3.55)$$

To estimate $\int_{\mathcal{A}_-} \rho_{\omega,\eta}(\nu) d\nu$, we use the Taylor's expansion of $\omega \rightarrow (1+(\hat{\nu}+\omega)^2)\sigma'(\hat{\nu}+\omega)$ and get

$$(1+(\hat{\nu}+\omega)^2)\sigma'(\hat{\nu}+\omega) = (1+\omega^2)\sigma'(\omega) + \hat{\nu}((1+\omega^2)\sigma''(\omega) + 2\omega\sigma'(\omega)) + r(\hat{\nu}), \quad (3.56)$$

with

$$|r(\hat{\nu})| \leq C_r \hat{\nu}^2 \text{ for all } \hat{\nu} \in \mathcal{A}_-.$$

Using the substitution $\nu \rightarrow \hat{\nu} := \nu - \omega$ and (3.56) we get

$$\begin{aligned} & \lim_{\eta \rightarrow 0^+} \int_{\mathcal{A}_-} \rho_{\omega,\eta}(\nu) d\nu \\ &= \lim_{\eta \rightarrow 0^+} \int_{\mathcal{A}_0} (1+(\hat{\nu}+\omega)^2)\sigma'(\hat{\nu}+\omega) \frac{\hat{\nu}^2 - \eta^2}{(\hat{\nu}^2 + \eta^2)^2} d\hat{\nu} \\ &= (1+\omega^2)\sigma'(\omega) \lim_{\eta \rightarrow 0^+} \int_{\mathcal{A}_0} \frac{\hat{\nu}^2 - \eta^2}{(\hat{\nu}^2 + \eta^2)^2} d\hat{\nu} \\ &\quad + ((1+\omega^2)\sigma''(\omega) + 2\omega\sigma'(\omega)) \lim_{\eta \rightarrow 0^+} \int_{\mathcal{A}_0} \hat{\nu} \frac{\hat{\nu}^2 - \eta^2}{(\hat{\nu}^2 + \eta^2)^2} d\hat{\nu} \\ &\quad + \lim_{\eta \rightarrow 0^+} \int_{\mathcal{A}_0} r(\hat{\nu}) \frac{\hat{\nu}^2 - \eta^2}{(\hat{\nu}^2 + \eta^2)^2} d\hat{\nu} \end{aligned} \quad (3.57)$$

Plugging in the integral formulas

$$\int_{-a}^a \frac{\nu^2 - \eta^2}{(\nu^2 + \eta^2)^2} d\nu = \frac{-2a}{a^2 + \eta^2} \text{ and } \int_{-a}^a \nu \frac{\nu^2 - \eta^2}{(\nu^2 + \eta^2)^2} d\nu = 0$$

into (3.57) we get for the first term with $a = \sqrt{(1 + \omega^2)\sigma'(\omega)}$

$$\begin{aligned} & (1 + \omega^2)\sigma'(\omega) \lim_{\eta \rightarrow 0^+} \int_{\mathcal{A}_0} \frac{\hat{\nu}^2 - \eta^2}{(\hat{\nu}^2 + \eta^2)^2} d\hat{\nu} \\ &= (1 + \omega^2)\sigma'(\omega) \lim_{\eta \rightarrow 0^+} \frac{-2\sqrt{(1 + \omega^2)\sigma'(\omega)}}{(1 + \omega^2)\sigma'(\omega) + \eta^2} = -2\sqrt{(1 + \omega^2)\sigma'(\omega)}, \end{aligned} \quad (3.58)$$

and the second integral term in (3.57) is vanishing, and for the third term we get

$$\left| \int_{\mathcal{A}_0} r(\hat{\nu}) \frac{\hat{\nu}^2 - \eta^2}{(\hat{\nu}^2 + \eta^2)^2} d\hat{\nu} \right| \leq C_r \int_{\mathcal{A}_0} 1 d\hat{\nu} \leq 2C_r \sqrt{(1 + \omega^2)\sigma'(\omega)}. \quad (3.59)$$

Using the estimates (3.58) and (3.59) in (3.57) we get

$$\lim_{\eta \rightarrow 0^+} \int_{\mathcal{A}_-} \rho_{\omega, \eta}(\nu) d\nu \geq -2(1 + C_r) \sqrt{(1 + \omega^2)\sigma'(\omega)}. \quad (3.60)$$

Considering the integral (3.53) as the sum of the two integrals over \mathcal{A}_{\pm} and using the estimates (3.55) and (3.60) we get

$$\lim_{\eta \rightarrow 0^+} \Re \tilde{\kappa}'(\omega + i\eta) \geq A - 2(1 + C_r) \sqrt{(1 + \omega^2)\sigma'(\omega)}.$$

Therefore, $|\Re \kappa'(\omega)| \geq \max(0, A - 2(1 + C_r) \sqrt{(1 + \omega^2)\sigma'(\omega)})$ and together with (3.52) it follows that

$$\begin{aligned} & |\kappa'(\omega)|^2 + \Im \kappa(\omega) \\ & \geq \pi(1 + \omega^2)\sigma'(\omega) + |\Re \kappa'(\omega)|^2 \\ & \geq \pi(1 + \omega^2)\sigma'(\omega) + \left(\max \left\{ 0, A - 2(1 + C_r) \sqrt{(1 + \omega^2)\sigma'(\omega)} \right\} \right)^2 \\ & \geq \underbrace{\frac{\pi A^2}{4(1 + C_r)^2 + \pi}}_{:=C_2}, \end{aligned}$$

where in the last inequality we estimated the minimum of the quadratic function $\rho \rightarrow A^2 - 4A(1 + C_r)\rho + (4(1 + C_r)^2 + \pi)\rho^2$. \square

References

- [Amm+12] H. Ammari, E. Bretin, J. Garnier, and A. Wahab. “Noise source localization in an attenuating medium”. *SIAM J. Appl. Math.* 72.1 (2012), pp. 317–336.
- [Bur+07a] P. Burgholzer, H. Grün, M. Haltmeier, R. Nuster, and G. Paltauf. “Compensation of acoustic attenuation for high-resolution photoacoustic imaging with line detectors”. In: *Photons Plus Ultrasound: Imaging and Sensing 2007: The Eighth Conference*

- on Biomedical Thermoacoustics, Optoacoustics, and Acousto-optics*. Ed. by A. A. Oraevsky and L. V. Wang. Vol. 6437. Proceedings of SPIE. San Jose, CA, USA: SPIE, 2007, p. 643724.
- [CT10] B. T. Cox and B. E. Treeby. “Artifact trapping during time reversal photoacoustic imaging for acoustically heterogeneous media”. *IEEE Trans. Med. Imag.* 29.2 (2010), pp. 387–396.
- [ESS16] P. Elbau, O. Scherzer, and C. Shi. “Singular Values of the Attenuated Photoacoustic Imaging Operator”. Preprint on ArXiv arXiv:1611.05807. University of Vienna, Austria, 2016.
- [Hö03] L. Hörmander. “The Analysis of Linear Partial Differential Operators I”. 2nd ed. New York: Springer Verlag, 2003.
- [HS03] A. Hanyga and M. Sereďyńska. “Power-law attenuation in acoustic and isotropic anelastic media”. *Geophys. J. Int.* 155 (2003), pp. 830–838.
- [Hua+12] C. Huang, L. Nie, R. W. Schoonover, L. V. Wang, and M. A. Anastasio. “Photoacoustic computed tomography correcting for heterogeneity and attenuation”. *J. Biomed. Opt.* 17 (2012), p. 061211.
- [Kin+00] L. E. Kinsler, A. R. Frey, A. B. Coppers, and J. V. Sanders. “Fundamentals of Acoustics”. 4th ed. New York: Wiley, 2000.
- [KK08] P. Kuchment and L. Kunyansky. “Mathematics of thermoacoustic tomography”. *European J. Appl. Math.* 19 (2008), pp. 191–224.
- [KS12] R. Kowar and O. Scherzer. “Attenuation Models in Photoacoustics”. In: *Mathematical Modeling in Biomedical Imaging II: Optical, Ultrasound, and Opto-Acoustic Tomographies*. Ed. by H. Ammari. Vol. 2035. Lecture Notes in Mathematics. Berlin Heidelberg: Springer Verlag, 2012, pp. 85–130.
- [KS13] K. Kalimeris and O. Scherzer. “Photoacoustic imaging in attenuating acoustic media based on strongly causal models”. *Math. Methods Appl. Sci.* 36.16 (Feb. 2013), pp. 2254–2264.
- [KSB11] R. Kowar, O. Scherzer, and X. Bonnetfond. “Causality analysis of frequency-dependent wave attenuation”. *Math. Methods Appl. Sci.* 34 (1 2011), pp. 108–124.
- [Kuc12] P. Kuchment. “Mathematics of hybrid imaging: a brief review”. In: *The Mathematical Legacy of Leon Ehrenpreis*. Ed. by I. Sabadini and D. C. Struppa. Berlin: Springer, 2012, pp. 183–208.
- [Kuc14] P. Kuchment. “The Radon Transform and Medical Imaging”. Philadelphia: Society for Industrial and Applied Mathematics, 2014.
- [Nat12] F. Natterer. “Photo-acoustic inversion in convex domains”. *Inverse Probl. Imaging* 6.2 (2012), pp. 1–6.

- [NSW90] A. I. Nachman, J. F. Smith III, and R. C. Waag. “An equation for acoustic propagation in inhomogeneous media with relaxation losses”. *J. Acoust. Soc. Amer.* 88.3 (1990), pp. 1584–1595.
- [Nus72] H. M. Nussenzveig. “Causality and dispersion relations”. Academic Press, New York-London, 1972, pp. xii+435.
- [SC05] N. V. Sushilov and R. S. C. Cobbold. “Frequency-domain wave equation and its time-domain solution in attenuating media”. *J. Acoust. Soc. Amer.* 115 (2005), pp. 1431–1436.
- [See64] R. T. Seeley. “Extension of C^∞ functions defined in a half space”. *Proc. Amer. Math. Soc.* 15 (1964), pp. 625–626.
- [SV74] L. A. Shepp and Y. Vardi. “A statistical model for positron emission tomography”. *IEEE Trans. Nucl. Sci.* NS-21 (1974), pp. 21–43.
- [Sza94] T.L. Szabo. “Time domain wave equations for lossy media obeying a frequency power law”. *J. Acoust. Soc. Amer.* 96 (1994), pp. 491–500.
- [Sza95] T.L. Szabo. “Causal theories and data for acoustic attenuation obeying a frequency power law”. *J. Acoust. Soc. Amer.* 97 (1995), pp. 14–24.
- [TC10] B. E. Treeby and B. T. Cox. “K-Wave: MATLAB toolbox for the simulation and reconstruction of photoacoustic wave fields”. *J. Biomed. Opt.* 15 (2 2010), p. 021314.
- [TZC10] B. E. Treeby, E. Z. Zhang, and B. T. Cox. “Photoacoustic tomography in absorbing acoustic media using time reversal”. *Inverse Probl.* 26.11 (2010), p. 115003.
- [WA11] K. Wang and M. A. Anastasio. “Photoacoustic and thermoacoustic tomography: image formation principles”. In: *Handbook of Mathematical Methods in Imaging*. Ed. by O. Scherzer. New York: Springer, 2011, pp. 781–817.
- [Wan09] L. V. Wang, ed. “Photoacoustic Imaging and Spectroscopy”. Optical Science and Engineering. Boca Raton: CRC Press, 2009. xii+499.
- [XW05] M. Xu and L. V. Wang. “Universal back-projection algorithm for photoacoustic computed tomography”. *Phys. Rev. E* 71.1, 016706 (2005).

4

A signal separation technique for sub-cellular imaging using dynamic optical coherence tomography

Habib Ammari²
habib.ammari@math.ethz.ch

Francisco Romero²
francisco.romero@sam.math.ethz.ch

Cong Shi¹
cong.shi@univie.ac.at

¹Computational Science Center
University of Vienna
Oskar-Morgenstern-Platz 1
A-1090 Vienna, Austria

²Department of Mathematics
ETH Zürich
Rämistrasse 101,
CH-8092 Zürich, Switzerland

Abstract

This paper aims at imaging the dynamics of metabolic activity of cells. Using dynamic optical coherence tomography, we introduce a new multi-particle dynamical model to simulate the movements of the collagen and the cell metabolic activity and develop an efficient signal separation technique for sub-cellular imaging. We perform a singular-value decomposition of the dynamic optical images to isolate the intensity of the metabolic activity. We prove that the largest eigenvalue of the associated Casorati matrix corresponds to the collagen. We present several numerical simulations to illustrate and validate our approach.

Mathematics Subject Classification (MSC2000): 92C55, 78A46, 65Z05

Keywords: Doppler optical coherence tomography, signal separation, spectral analysis, singular value decomposition, dynamic cell imaging.

4.1 Introduction

Since dynamic properties are essential for a disease prognosis and a selection of treatment options, a number of methods to explore these dynamics has been developed. When optical imaging methods are used to observe cell-scale details of a tissue, the highly-scattering collagen usually dominates the signal, obscuring the intra-cellular details. A challenging problem is to remove the influence of the collagen in order to have a better imaging inside the cells.

There have been many studies on optical imaging to extract useful information. In [Lee+12] the authors use stochastic method, which follows from a probabilistic model for particle movements, and then they express the autocorrelation function of the signal in terms of some parameters including different components of the velocity and the fraction of moving particles. Those parameters are then estimated using a fitting algorithm. In [Joo+10; LSD09], the autocorrelation function of the signal can be written as a complex-valued exponential function of the particle displacements. Through the relation between the real and imaginary parts of this autocorrelation function, the authors analyze the temporal autocorrelation on the complex-valued signals to obtain the mean-squared displacement (MSD) and also time-averaged displacement (TAD) (which is the velocity) of scattering structures. Very recently, in [Ape+16], Apelian et. al. use difference imaging method, which consists in directly removing the stationary parts from the images by taking differences or standard deviations. The motivation of this paper comes from [Ape+16].

Some researchers use Doppler optical coherence tomography to obtain high resolution tomographic images of static and moving constituents simultaneously in highly scattering biological tissues, for example, [Che+99] and in [DF08, Chapter 21].

In this paper, using dynamic optical coherence tomography we introduce a signal separation technique for sub-cellular imaging and give a detailed mathematical analysis of extracting useful information. This includes giving a new multi-particle dynamical model to simulate the movement of the collagen and metabolic activity, and also providing some results relating the eigenvalues and the feasibility of using singular value decomposition (SVD) in optical imaging, which as far as we know is original.

The paper has three main contributions. First, we give a new model as an extension of the single particle optical Doppler tomography, which allows us to justify the SVD approach for the separation between the collagen signal and metabolic activity signal. Then we perform eigenvalue analysis for the operator with the intensity as an integral kernel, and prove that the largest eigenvalue corresponds to the collagen. This means that using a SVD of the images and removing the part corresponding to the largest eigenvalue is a viable method for removing the influence of collagen signals. Finally, based on SVD, we give a new method for isolating the intensity of the metabolic activity.

The paper is structured as follows. In Section 2 we introduce our multi-particle dynamical model based on a classical model in [DF08]. In Section 3, we discuss the forward operator with total signal as its integral kernel, and give its eigenvalue analysis, showing that the part corresponding to the collagen signal have rank one, which provides the theoretical foundation for using SVD. In Section 4, we discuss the mathematical rationality for using a SVD method and the method of isolating the metabolic signal. In Section 5 we give some numerical experiments. Some concluding remarks are presented in the final section.

4.2 The dynamic forward problem

Optical Coherence Tomography (OCT) is a medical imaging technique that uses light to capture high resolution images of biological tissues by measuring the time delay and the intensity of backscattered or back reflected light coming from the sample. The research on OCT has been growing very fast for the last two decades. We refer the reader, for instance, to [EMS15; Hua+91; Fer96; Fer+03; Pod05; Sch99; TW05]. This imaging method has been continuously improved in terms of speed, resolution and sensitivity. It has also seen a variety of extensions aiming to assess functional aspects of the tissue in addition to morphology. One of these approaches is Doppler OCT (called ODT), which aims at visualizing movements in the tissues (for example, blood flows). ODT is based on the identical optical design as OCT, but additional signal processing is used to extract information encoded in the carrier frequency of the interferogram.

The purpose of this paper is to analyze the mathematics of ODT in the context of its application for imaging sub-cellular dynamics. We prove that a signal separation technique performs well and allows imaging of sub-cellular dynamics. We refer the reader to [AA17; Alb+17; Alb+16] for recently developed signal separation approaches in different biomedical imaging frameworks. These include ultrasound imaging, photoacoustic imaging, and electrical impedance tomography.

4.2.1 Single particle model

We first consider a single moving particle. In [DF08, Chapter 21], the optical Doppler tomography is modeled as follows. Assume that there is one moving particle at a point x in the sample Ω and denote by ν the z -component of its velocity. Then the ODT signal generated by this particle is given by

$$\Gamma_{ODT}(x, t) = 2 \int_0^\infty S_0(\omega) K(x, \omega) K_R(x, \omega) \cos(2\pi\omega(\tau + \frac{\Delta}{c}) + 2\pi\omega\frac{2\bar{n}vt}{c}) d\omega, \quad (4.1)$$

where ω is the frequency, $S_0(\omega)$ is the spectral density of the light source, $K(x, \omega)$ and $K_R(x, \omega)$ are the reflectivities of the sample and the reference mirror respectively, \bar{n} is the index of refraction, c is the speed of the light, τ is the time delay on the reference arm, and Δ is the path difference between the reference arm and sample arm.

Since \cos is an even function, the above integral can be rewritten as

$$\Gamma_{ODT}(x, t) = \int_{-\infty}^\infty S_0(\omega) K(x, \omega) K_R(x, \omega) e^{2\pi\omega i(\tau + \frac{\Delta}{c}) + 2\pi\omega i\frac{2\bar{n}vt}{c}} d\omega. \quad (4.2)$$

To give an explanation for the exponential term of the above formula, we choose a suitable coordinate system such that the beam propagates along the z -direction, and suppose that the particle moves in this direction from point A to point B with velocity v , which also means covering a distance of vt (see Figure 4.1). Physically, the received signal Γ_{ODT} is determined by the effective path-length difference between the sample and reference arms. In addition, for this moving particle the effective path-length difference is represented by the quantity $c\tau + \Delta + 2\bar{n}vt$, which could also be seen as the z -coordinate of the particle (see Figure 4.1).

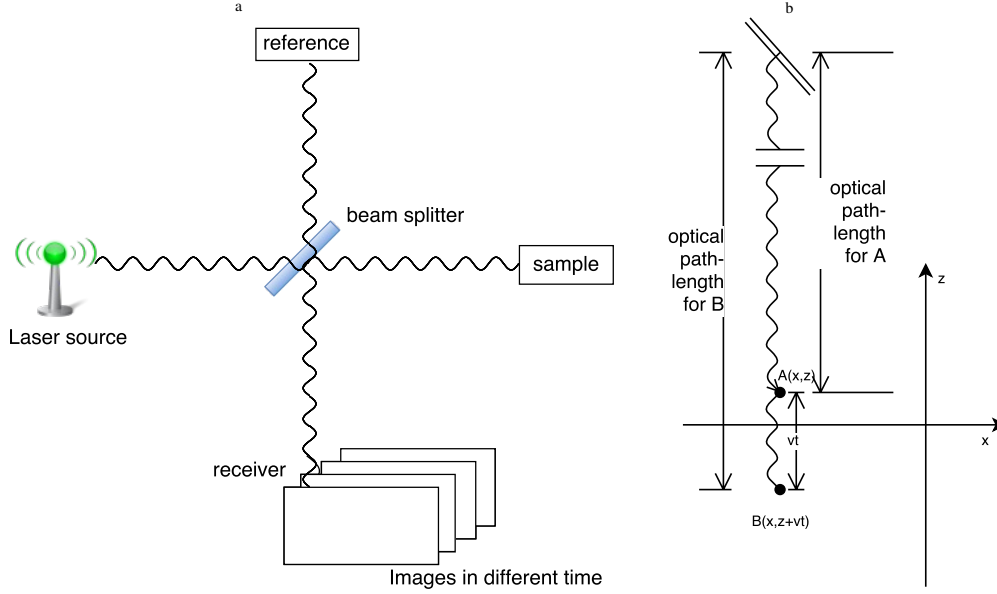


FIGURE 4.1: a) Illustration of the imaging setup. b) A particle moves from A to B covering a distance of vt . When the particle is at B , the light travels an additional distance of $2vt$ inside a medium with refractive index \bar{n} , so the effective path-length of the sample arm increases by $2\bar{n}vt$.

Note that (4.2) is only applicable to a single particle at x moving with a constant velocity v . For a particle with a more general movement, the path-length difference is no longer a linear function with respect to t . Nevertheless, we define $\varphi(t)$ as the z -coordinate of the particle at time t , which is a generalization of $c\tau + \Delta + 2\bar{n}vt$. Also, in our case the reference arm is a mirror, so without loss of generality, we make the assumption that $K_R(x, \omega) = 1$. Then the following expression for signal $\Gamma_{ODT}(x, t)$ holds

$$\Gamma_{ODT}(x, t) = \int_{-\infty}^{\infty} S_0(\omega) K(x, \omega) e^{2\pi i \omega \left(\frac{2\bar{n}}{c} \varphi(t) \right)} d\omega.$$

This is not just a simplification of the model (4.1), but also a small modification, since the particles with regular and random movements produce difference signals. Here we look into more details of particle movements. For the sake of simplicity, we assume that the collagen particles move with a constant speed v , so $\varphi(t) = \varphi(0) + vt$. On the other hand, for the particles belonging to the metabolic activity part, $\varphi(t)$ behaves as a random function, since we do not have much information with regard to them.

Remark. Figure 4.2.1 is derived in [DF08] by considering what is essentially our $\varphi(t)$ (written as Δ_d there, see formula (21.11) and (21.15) of [DF08].) This justifies our treatment for general particles above. We emphasize that we generalized the model in [DF08] to accommodate particles with variable velocities.

4.2.2 Multi-particle dynamical model

We have seen the effect of the image $\Gamma_{ODT}(x, t)$ for one moving particle. We now consider the more realistic case of a medium (could be cell or tissue) with a large number of particles in motion. In actual imaging, for each pixel which we denote also by x , there would be many particles, all with different movement patterns.

We choose an appropriate coordinate system, such that for any particle on the plane $z = 0$, its effective path-length difference is zero. Let L be the coherence length. Physically, only the particles with path-length difference smaller than L , or equivalently $z \in [-L, L]$, will be present in the image. In fact, if the differences between the two arms are larger than the coherence length, then the lights from two arms do not interfere anymore, and thus do not contribute to the received signal. This means that the imaging region is a "thin slice" within the sample with thickness $2L$ (see Figure 4.2). Then we divide the slice into small regions, such that each region corresponds to a pixel of the final image. See Figure 4.2 for the imaged small region, which is given by $x \times [-L, L]$, and for the correspondence between them and pixels of the final image.

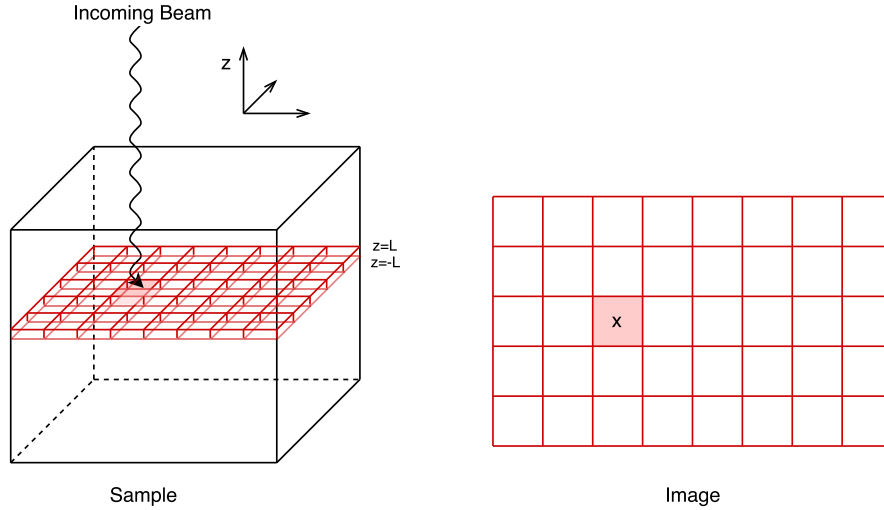


FIGURE 4.2: One "slice" in the sample, and its division into small regions corresponding to the pixels of the image.

Since there are many particles in this region, we describe their distribution using a density function p . Moreover, for any function $f(z)$, we have that the integral $\int_{z_1}^{z_2} f(z)p(x, z, t)dz$ is equal to the sum of $f(z)$ over all particles in $x \times [z_1, z_2]$. We know that the received light intensity in the small region $x \times [-L, L]$ could be seen as the sum of light intensity over all particles in this region. Therefore for uniform medium, we can write it as an integral in terms of the density function $p(x, z, t)$,

$$\Gamma_{ODT}(x, t) = \int_{-\infty}^{\infty} \int_{-L}^L S_0(\omega) K(x, \omega) e^{2\pi\omega i(\frac{2n}{c}z)} p(x, z, t) d\omega dz,$$

noting that the reflectivity coefficient K must be the same for all involved particles. According to the definition of $p(x, z, t)$, we consider it as the sum of the density function of collagen particles

and the density function of metabolic activity particles, namely,

$$p(x, z, t) = p_c(x, z, t) + p_m(x, z, t). \quad (4.3)$$

Consequently, their respective reflectivities will be denoted K_c and K_m , giving us the ODT measurements formula

$$\Gamma_{ODT}(x, t) = \Gamma_{ODT}^c(x, t) + \Gamma_{ODT}^m(x, t), \quad (4.4)$$

where $\Gamma_{ODT}^c(x, t)$ corresponds to the collagen signal and $\Gamma_{ODT}^m(x, t)$ corresponds to the metabolic activity signal, with formulas

$$\Gamma_{ODT}^j(x, t) = \int_{-\infty}^{\infty} \int_{-L}^L S_0(\omega) K_j(x, \omega) p_j(x, z, t) e^{2\pi\omega i(\frac{2n}{c}z)} d\omega dz, \quad \text{for } j \in \{c, m\}. \quad (4.5)$$

Physically, since the collagen moves as a whole, we could assume that the collagen particles move with one uniform (and very small) velocity v_0 , which means any such particles will be at position $z + v_0 t$ at time t . Let $q_c(x, z)$ denote the density function of all the collagen particles inside area x with initial vertical position z . Then we have

$$p_c(x, z + v_0 t, t) = q_c(x, z). \quad (4.6)$$

Furthermore, from this expression we could see when $t = 0$, $q_c(x, z) = p_c(x, z, 0)$.

In the case of metabolic activity we do not assume any conditions on the density function $p_m(x, v, z)$, because there is no physical law of motions for us to use. In the numerical experiments, because of the large number of particles, a random medium generator is used to simulate the particle distribution while keeping the computational cost low.

Since x is a small area inside the sample, when we choose x , it could include both collagen particles and metabolic activity particles. The aim is to separate the two classes of particles. In practice, the contributions of collagen particles to the intensity is much larger than the contributions of the metabolic activity. This allows us to understand that the reflectivity of collagen particles K_c is much larger (realistic quantities are about 10^2 to 10^4 times) than the reflectivity of metabolic activity particles K_m , and

$$|\Gamma_{ODT}^c(x, t)| \gg |\Gamma_{ODT}^m(x, t)|. \quad (4.7)$$

In this section, we have given a multi-particle dynamical model, to separate the collagen signal and the metabolic activity signal. The next step is to analyze the properties of this model.

4.3 Property analysis of the forward problem

4.3.1 Direct operator representation

Based on the multi-particle dynamical model, in order to analyze the properties of collagen and metabolic activity, we first represent their corresponding operators.

Let S be the integral operator with the kernel $\Gamma_{ODT}(x, t)$, which is a real-valued function given by (4.5). Similarly, Let S_c and S_m be integral operators with kernels $\Gamma_{ODT}^c(x, t)$ and $\Gamma_{ODT}^m(x, t)$, respectively. The collagen signal has high correlation between different points, while the metabolic signals have relatively lower correlation, so it would be useful to look at the correlation of the whole signal. The correlation between two points x and y can be represented as $\int \Gamma_{ODT}(x, t) \overline{\Gamma_{ODT}(y, t)} dt$, which is exactly the integral kernel of the operator SS^* , where S^* is the adjoint operator of S . We denote the kernel of SS^* by

$$F(x, y) = \int_0^T \Gamma_{ODT}(x, t) \overline{\Gamma_{ODT}(y, t)} dt, \quad (4.8)$$

for some fixed $T > 0$. Substituting the representation of $\Gamma_{ODT}(x, t)$ in (4.4) into (4.8), we arrive to

$$F(x, y) = F_{cc}(x, y) + F_{cm}(x, y) + F_{mc}(x, y) + F_{mm}(x, y),$$

where for $j, k \in \{c, m\}$, $F_{jk}(x, y)$ is given by

$$\begin{aligned} F_{jk}(x, y) = & \int_{\mathbb{R}^2 \times [-L, L]^2 \times [0, T]} S_0(\omega_1) S_0(\omega_2) K_j(x, \omega_1) K_k(y, \omega_2) p_j(x, z_1, t) \\ & \times p_k(y, z_2, t) e^{\frac{4\pi i \bar{n}}{c}(\omega_1 z_1 - \omega_2 z_2)} d\omega_1 d\omega_2 dz_1 dz_2 dt, \end{aligned} \quad (4.9)$$

with $z_1, z_2 \in [-L, L]$ and $\omega_1, \omega_2 \in \mathbb{R}, t \in [0, T]$. Likewise, the integral operators with kernel $F_{jk}(x, y)$ are exactly the operators $S_j S_k^*$ for $j, k \in \{c, m\}$. In the case of the collagen signal, note that the operator $S_c S_c^*$ contains the solely collagen information.

First we consider its kernel F_{cc} . Applying the uniform movements of collagen particles (4.6) along the z -direction yields

$$\begin{aligned} F_{cc}(x, y) = & \int_{\mathbb{R}^2 \times [-L, L]^2 \times [0, T]} S_0(\omega_1) S_0(\omega_2) K_c(x, \omega_1) K_c(y, \omega_2) q_c(x, z_1 - v_0 t) \\ & \times q_c(y, z_2 - v_0 t) e^{\frac{4\pi i \bar{n}}{c}(\omega_1 z_1 - \omega_2 z_2)} d\omega_1 d\omega_2 dz_1 dz_2 dt. \end{aligned} \quad (4.10)$$

In order to simplify this expression even further, let us introduce a couple of assumptions.

Physically, since the scale of collagen and inter-cellular structures (such as collagen) are much larger than the coherence length L , the particle distribution inside a small slice $|z| < L$ should be more or less uniform. Therefore, it is reasonable to assume that $q_c(x, z)$ does not actually depend on z inside such a small slice, namely, $q_c(x, z) = q_c(x)$.

Furthermore, in practice the tissue being imaged is nearly homogeneous, and therefore the reflectivity spectrum, (or more intuitively, the "color" of the tissue) should stay the same everywhere. The only difference in reflectivity between two points should be a difference of total reflectivity (using our "color" analogy, the two points would look like, e.g. "different shades of red", and not "red and yellow"). Therefore, for any two pixels x_1 and x_2 , by looking at the reflectivities $K_c(x_1, \omega)$ and $K_c(x_2, \omega)$ as functions of frequency ω , they are directly proportional. Thus it is reasonable to assume that $K_c(x, \omega)$ could be written in the variable separation form $K_{c_1}(x) K_{c_2}(\omega)$.

Under these two assumptions, the expression of $F_{cc}(x, y)$ can be simplified considerably:

$$\begin{aligned}
 F_{cc}(x, y) &= TK_{c_1}(x)K_{c_1}(y)q_c(x)q_c(y) \\
 &\times \int_{\mathbb{R}^2 \times [-L, L]^2} S_0(\omega_1)S_0(\omega_2)K_{c_2}(\omega_1)K_{c_2}(\omega_2)e^{\frac{4\pi i \bar{n}}{c}(\omega_1 z_1 - \omega_2 z_2)} d\omega_1 d\omega_2 dz_1 dz_2 \\
 &= TK_{c_1}(x)K_{c_1}(y)q_c(x)q_c(y) \\
 &\times \int_{[-L, L]^2} \mathcal{F}(S_0 K_{c_2})\left(-\frac{4\pi \bar{n} z_1}{c}\right) \mathcal{F}(S_0 K_{c_2})\left(\frac{4\pi \bar{n} z_2}{c}\right) dz_1 dz_2
 \end{aligned} \tag{4.11}$$

where the Fourier transform of a function $f(\omega)$ is defined as $\mathcal{F}f(\tau) = \int_{\mathbb{R}} f(\omega) e^{-i\omega\tau} d\omega$.

This is the fundamental formula for analyzing collagen signal, since from this formula, we could see that $F_{cc}(x, y)$ is variable separable with respect to x and y . This property gives us a hint to compute the eigenvalues of the collagen signal.

For the correlation terms $F_{cm}(x, y)$ and $F_{mc}(x, y)$, which contains both the collagen and metabolic activity signals, we use again the uniform movement assumption for p_c while keeping the metabolic part p_m . Inserting (4.6) into (4.9), we have

$$\begin{aligned}
 F_{mc}(x, y) &= K_{c_1}(y)q_c(y) \int_{[-L, L]^2 \times [0, T]} \mathcal{F}(S_0 K_{c_2})\left(\frac{4\pi \bar{n} z_2}{c}\right) \\
 &\times \mathcal{F}(S_0 K_m)\left(x, -\frac{4\pi \bar{n} z_1}{c}\right) p_m(x, z_1, t) dz_1 dz_2 dt,
 \end{aligned} \tag{4.12}$$

and

$$\begin{aligned}
 F_{cm}(x, y) &= K_{c_1}(x)q_c(x) \int_{[-L, L]^2 \times [0, T]} \mathcal{F}(S_0 K_{c_2})\left(-\frac{4\pi \bar{n} z_1}{c}\right) \\
 &\times \mathcal{F}(S_0 K_m)\left(y, \frac{4\pi \bar{n} z_2}{c}\right) p_m(y, z_2, t) dz_1 dz_2 dt.
 \end{aligned} \tag{4.13}$$

From representations (4.12) and (4.13), we could see that $F_{mc}(x, y)$ and $F_{cm}(x, y)$ have also variable separated forms with respect to x and y .

In the case of the metabolic activity kernel $F_{mm}(x, y)$, by keeping the representation p_m , it is clear that

$$\begin{aligned}
 F_{mm}(x, y) &= \int_{[-L, L]^2 \times [0, T]} \mathcal{F}(S_0 K_m)\left(x, -\frac{4\pi \bar{n} z_1}{c}\right) \mathcal{F}(S_0 K_m)\left(y, \frac{4\pi \bar{n} z_2}{c}\right) \\
 &\times p_m(x, z_1, t) p_m(y, z_2, t) dz_1 dz_2 dt.
 \end{aligned} \tag{4.14}$$

To sum up, the main feature of our multi-particle dynamical model is that, except the sole metabolic activity signal, all the other parts have kernels of variable separable form. Therefore, it is important to relate this property to the separation of the signals. This will be the aim of the next subsection.

4.3.2 Eigenvalue analysis

Since the light source has a limited frequency range, the function $S_0(\omega)$ has compact support. Therefore, using (4.5), the functions $\Gamma_{ODT}^c(x, t)$ and $\Gamma_{ODT}^m(x, t)$ are given by integrals of a bounded integrand over a bounded region, so they are bounded functions on $\Omega \times [0, T]$.

Then the operators S_c and S_m are integral operators with L^2 kernels. Therefore, they are *Hilbert-Schmidt integral operators* by definition. Since the composition of two Hilbert-Schmidt operators is trace-class (see [GG77]), the operators $S_c S_c^*$, $S_c S_m^*$, $S_m S_c^*$, and $S_m S_m^*$ are trace-class operators, and their trace is given by

$$\begin{aligned} \text{tr}(S_c S_c^*) &= \|S_c\|_{HS}^2, & \text{tr}(S_c S_m^*) &= \langle S_c, S_m \rangle_{HS}; \\ \text{tr}(S_m S_m^*) &= \|S_m\|_{HS}^2, & \text{tr}(S_m S_c^*) &= \langle S_m, S_c \rangle_{HS}, \end{aligned}$$

where the Hilbert-Schmidt inner product is written by

$$\langle S_j, S_k \rangle_{HS} = \int_{\Omega \times [0, T]} \Gamma_{ODT}^j(x, t) \overline{\Gamma_{ODT}^k(x, t)} dx dt,$$

and the Hilbert-Schmidt norm is written by

$$\|S_c\|_{HS}^2 = \int_{\Omega \times [0, T]} |\Gamma_{ODT}^j(x, t)|^2 dx dt,$$

for any $j, k \in \{m, c\}$.

In order to argue for the feasibility of using a SVD, we will calculate the corresponding eigenvalues, showing that the collagen signal has one very large eigenvalue relative to the metabolic activity. We assume that the eigenvalues are ordered decreasingly, so λ_1 is the largest one.

We first recall that for an operator A with rank one, the unique non-zero eigenvalue λ is equal to the trace of A . From the expression of $F_{cc}(x, y)$, we could see that $F_{cc}(x, y)$ has rank one because of the separable form with respect to x and y , so the operator $S_c S_c^*$ has only one nonzero eigenvalue, which we denote by $\lambda(S_c S_c^*)$. Now we compare $\lambda(S_c S_c^*)$ and the eigenvalues of the operator $S_m S_m^*$.

Lemma 4.3.1 *Let $S_c S_c^*$ and $S_m S_m^*$ be the integral operators with kernels F_{cc} and F_{mm} defined in (4.11) and (4.14), respectively. If the intensities of collagen and metabolic activity satisfy (4.7), then we have*

$$\lambda(S_c S_c^*) \gg \lambda_i(S_m S_m^*), \quad \forall i \geq 1.$$

Proof: On one hand, $F_{cc}(x, y)$ has rank one, so it is clear that

$$\lambda(S_c S_c^*) = \text{tr}(S_c S_c^*). \quad (4.15)$$

On the other hand, since the eigenvalues of operator $S_m S_m^*$ are all positive, any eigenvalue $\lambda_i(S_m S_m^*)$ satisfies

$$\lambda_i(S_m S_m^*) < \sum_{i=1}^{\infty} \lambda_i(S_m S_m^*) = \text{tr}(S_m S_m^*). \quad (4.16)$$

Then it suffices to prove that $\text{tr}(S_c S_c^*) \gg \text{tr}(S_m S_m^*)$. From the definition of trace of an operator, we readily get $\text{tr}(S_c S_c^*) = \int_{x \in \Omega} F_{cc}(x, x) dx$. Substituting the expression (4.8) into the above formula yields

$$\begin{aligned} \text{tr}(S_c S_c^*) &= \int_{x \in \Omega} \frac{1}{2} \int_{-\infty}^{\infty} \Gamma_{ODT}^c(x, t) \overline{\Gamma_{ODT}^c(x, t)} dt dx \\ &= \frac{1}{2} \int_{x \in \Omega} \int_{-\infty}^{\infty} |\Gamma_{ODT}^c(x, t)|^2 dt dx. \end{aligned}$$

The same analysis can be carried out by looking at $\text{tr}(S_m S_m^*)$,

$$\text{tr}(S_m S_m^*) = \frac{1}{2} \int_{x \in \Omega} \int_{-\infty}^{\infty} |\Gamma_{ODT}^m(x, t)|^2 dt dx. \quad \square$$

Recall that the intensity of collagen signal is much larger than metabolic activity signal, which is the assumption in (4.7). Hence, we obtain the trace comparison $\text{tr}(S_c S_c^*) \gg \text{tr}(S_m S_m^*)$.

Now we compare the eigenvalue $\lambda(S_c S_m^*)$ with $\lambda(S_c S_c^*)$ and $\lambda_1(S_m S_m^*)$.

Lemma 4.3.2 *Let $S_c S_c^*$, $S_c S_m^*$ and $S_m S_m^*$ be the integral operators with kernels defined in (4.11), (4.12) and (4.14). Then their eigenvalues satisfy*

$$\lambda_i(S_c S_m^*) \leq \sqrt{\lambda(S_c S_c^*) \lambda_1(S_m S_m^*)}$$

for all i .

Proof: Recall the definition of the operator norm of an operator A , namely, $\|A\|_{OP} = \sup\{\frac{\|Av\|}{\|v\|}, v \in V \text{ with } v \neq 0\}$, which yields $\lambda(S_c S_m^*) \leq \|S_c S_m^*\|_{OP}$. Since the operator norm is equal to the largest singular value, direct calculation shows that

$$\begin{aligned} \|S_c S_m^*\|_{OP} &\leq \|S_c\|_{OP} \|S_m^*\|_{OP} \\ &= \sigma_1(S_c) \sigma_1(S_m^*) \\ &= \sqrt{\lambda(S_c S_c^*)} \sqrt{\lambda_1(S_m S_m^*)}, \end{aligned}$$

where σ_1 denotes the largest singular value. \square

In this section, we discussed eigenvalue analysis for the forward operator of multi-particle dynamical model. More explicitly, we showed that the largest eigenvalue corresponds to the collagen signal, the middle eigenvalues mix the collagen signal and metabolic activity signal, and the remaining eigenvalue corresponds to the metabolic activity signal. Also in our model the solely collagen signal has rank one, which provides a good reason to use SVD in solving the inverse problem.

4.4 The inverse problem: Signal separation

Our main purpose in this paper is to image the dynamics of metabolic activity of cells. Highly backscattering structures like collagen dominate the dynamic OCT signal, masking low-backscattering structures such as metabolic activity. As shown in the modeling part, we divide the scattering

particles in the tissue into the high-backscattering collagen part, and the low-backscattering metabolic activity part. Based on this division, the resulting image $\Gamma_{ODT}(x, t)$ could also be written as the sum of the collagen $\Gamma_{ODT}^c(x, t)$ and the metabolic activity part $\Gamma_{ODT}^m(x, t)$. The inverse problem is to recover the intensity of metabolic activity of cells from the image $\Gamma_{ODT}(x, t)$. In this paper, we use singular value decomposition (SVD) method to approximate the metabolic activity part, then using a particular formula (see (4.23)) to get its corresponding intensity.

4.4.1 Analysis of SVD algorithm

Since we have proved the high backscattering signal corresponds to a rank one kernel and this part is far larger than the rest, It is natural to associate it to the first singular value of the SVD expansion. We claim that in order to remove the high backscattering signal, it is reasonable to remove the first term in the SVD expansion of the image. Given the orthogonal nature of the SVD decomposition, it is not possible to ensure a clean signal separation. Nonetheless at the end of this section we provide a result that illustrates how the error committed with this decomposition is actually small.

Let $x_1, x_2, \dots, x_j, \dots$ denote the pixels of the image. Define the matrices $A, A_c \in \mathbb{C}^{n_x \times n_t}$ by

$$\begin{aligned} A_{j,k} &= \Gamma_{ODT}(x_j, t_k) \\ (A_c)_{j,k} &= \Gamma_{ODT}^c(x_j, t_k), \end{aligned}$$

where $j \in \{1, \dots, n_x\}$, $k \in \{1, \dots, n_t\}$.

Recall that a non-negative real number σ is a singular value for a matrix A , if and only if there exists unit vectors $u \in \mathbb{R}^{n_x}$ and $v \in \mathbb{R}^{n_t}$ such that

$$Av = \sigma u \text{ and } A^*u = \sigma v,$$

where the vectors u and v are called left-singular and right-singular vectors of A for the singular value σ .

Assuming that the singular values of A are ordered decreasingly, that is, $\sigma_1 \geq \sigma_2 \geq \dots$, and let u_i and v_i be the singular vectors for σ_i . We emphasize that the vectors u_i and v_i are orthonormal sets in \mathbb{C}^{n_x} and \mathbb{C}^{n_t} respectively. Thus, the SVD of the matrix A is given by

$$A = \sum_{i=1}^{n_t} \sigma_i u_i \bar{v}_i^T. \quad (4.17)$$

Since the matrix A is composed of a large rank one part A_c and a small part coming from metabolic signal Γ_{ODT}^m , we can say that $A - A_c$ is "relatively small" with respect to A . It is well known that the first term in the SVD expansion of A is the rank one matrix A_1 such that $\|A - A_1\|_{op}$ is minimal. Therefore, it is natural to think that A_c is "close" to A_1 in some way. But $A_1 = \sigma_1 u_1 \bar{v}_1^T$ is generally not the same as A_c , because as we will see in section 4.A, the eigenvectors of the kernels F_{cc} , F_{cm} and F_{mc} are generally not orthogonal. Since SVD always gives an orthogonal set of eigenvectors, we conclude that the SVD approach itself does not give the eigenvectors exactly. Nevertheless, we can show that the SVD result is still a good approximation to the true eigenvectors.

	Total signal Γ_{ODT}	First term in the SVD of Γ_{ODT}	collagen signal Γ_{ODT}^c
Matrix	A	A_1	A_c
First singular value	σ_1	σ_1	σ_c
First singular vector	u_1, v_1	u_1, v_1	u_c, v_c
Other singular values	$\sigma_2 > \sigma_3 > \dots > \sigma_i$	0	0

TABLE 4.1: Singular values and singular vectors.

To bridge the gap between the collagen signal Γ_{ODT}^c and the first term of SVD expansion of Γ_{ODT} , we investigate the relationship between their singular values and singular vectors. Γ_{ODT}^c has only one nonzero singular value σ_c , with the corresponding singular vectors u_c and v_c .

We claim in the following theorem that the singular value σ_1 and the corresponding singular vector u_1 are good approximations of the singular value σ_c and singular vector u_c . See Table 4.1 for the notations of their singular values and singular vectors.

Theorem 4.4.1 *Let $\sigma_i, u_i, v_i, A_c, u_c$ and v_c be described in Table 4.1. Assume that the collagen signal dominates, that is,*

$$\frac{\|A - A_c\|_{op}}{\|A_c\|_{op}} = 1/N \quad (4.18)$$

for a large N . Then there exist constants $C > 0$ and $\epsilon \in \{-1, 1\}$ such that

$$\frac{|\sigma_c - \sigma_1|}{\sigma_c} \leq C/N,$$

and

$$\|u_c - \epsilon u_1\|_{l^2} \leq C/N.$$

Proof: We define a matrix-valued function

$$F : s \mapsto (A_c + sN(A - A_c))^*(A_c + sN(A - A_c)). \quad (4.19)$$

Through this construct of F , we obtain

$$F(0) = A_c^* A_c \text{ and } F\left(\frac{1}{N}\right) = A^* A.$$

Applying Rellich's perturbation theorem on hermitian matrices F (see, for example, [Rel69]) to get the following two properties. There exists a set of n analytic functions $\lambda_1(s), \lambda_2(s), \dots$,

such that they are all the eigenvalues of $F(s)$. Also, there exists a set of vector-valued analytic functions $u_1(s), u_2(s), \dots$, such that $F(s)u_i(s) = \lambda_i(s)u_i(s)$, and $\langle u_i(s), u_j(s) \rangle = \delta_{ij}$.

In view of the definition of $u_i(s)$ and $\lambda_i(s)$, we show four useful properties, for some $\epsilon \in \{-1, 1\}$,

$$\begin{aligned} u_1(0) &= u_c, & u_1(1/N) &= \epsilon u_1, \\ \lambda_1(0) &= \sigma_c^2 = \|A_c\|_{op}^2, & \lambda_1(1/N) &= \sigma_1^2, \end{aligned} \quad (4.20)$$

where the last property comes from the fact $\lambda_1(1/N)$ is the largest eigenvalue of $F(1/N) = A^*A$ when $N \gg 1$.

The objective is to get upper bounds for $\|u_c - \epsilon u_1\|_{l^2}$ and $|\sigma_c - \sigma_1|$. Using (4.20), we have $u_c - \epsilon u_1 = u_1(0) - u_1(1/N)$ and $\sigma_c - \sigma_1 = \sqrt{\lambda_1(0)} - \sqrt{\lambda_1(1/N)}$. Since $u_1(s)$ and $\lambda_1(s)$ are analytic, a Taylor expansion at 0 yields

$$\begin{aligned} \|u_c - \epsilon u_1\|_{l^2} &= \left\| \frac{u_1'(0)}{N} \right\|_{l^2} + O(1/N^{3/2}), \\ |\sigma_c - \sigma_1| &= \frac{\lambda_1'(0)}{2\sqrt{\lambda_1(0)}N} + O(1/N^2). \end{aligned} \quad (4.21)$$

The next step is to seek for proper upper bounds for $\lambda_1'(0)$ and $u_1'(0)$.

For the upper bound of $\lambda_1'(0)$, we differentiate $F(s)u_i(s) = \lambda_i(s)u_i(s)$ with respect to s and then take $s = 0$ to obtain

$$F'(0)u_i(0) + F(0)u_i'(0) = \lambda_i(0)u_i'(0) + \lambda_i'(0)u_i(0). \quad (4.22)$$

Since we always have $\|u_i(s)\|_{\ell^2} = 1$, a direct calculation shows that

$$\langle u_i(s), u_i'(s) \rangle = \frac{1}{2} \frac{d}{ds} \|u_i(s)\|^2 = 0.$$

By taking an inner product of both sides of (4.22) with $u_i(0)$, we get

$$\begin{aligned} \lambda_i'(0) &= \lambda_i'(0) \|u_i(0)\|_{l^2}^2 \\ &= \langle u_i(0), F'(0)u_i(0) \rangle + \langle u_i(0), F(0)u_i'(0) \rangle \\ &= \langle u_i(0), F'(0)u_i(0) \rangle + \langle F(0)u_i(0), u_i'(0) \rangle \\ &= \langle u_i(0), F'(0)u_i(0) \rangle + \lambda_i(0) \langle u_i(0), u_i'(0) \rangle \\ &= \langle u_i(0), F'(0)u_i(0) \rangle. \end{aligned}$$

Hence, $\lambda_i'(0)$ satisfies $|\lambda_i'(0)| \leq \|F'(0)\|_{op}$. By the definition of $F(s)$, we have $\|F'(0)\|_{op} = N\|A_c^*(A - A_c) + (A - A_c)^*A_c\| \leq 2N\|A_c\|_{op}\|A - A_c\|_{op}$. Replacing N with (4.18) yields $|\lambda_i'(0)| \leq 2\|A_c\|_{op}^2$. Therefore, by inserting the expression $\lambda_1(0)$ in (4.20) into (4.21), we get $|\sigma_c - \sigma_1| \leq \frac{\sigma_c}{N} + O(1/N^2)$.

For the upper bound of $u_1'(0)$, we look again at (4.22). By taking an inner product with $u_1'(0)$, we immediately obtain

$$\langle u_1'(0), F'(0)u_1(0) \rangle + \langle u_1'(0), F(0)u_1'(0) \rangle = \lambda_1(0) \|u_1'(0)\|_{l^2}^2.$$

Recall that the matrix A_c is of rank one. So, there exists a positive constant c , such that $A_c^* A_c = cu_1(0)u_1^T(0)$, which reads

$$F(0)u_1'(0) = cu_1(0)(u_1^T(0)u_1'(0)) = cu_1(0)\langle u_1(0), u_1'(0) \rangle = 0.$$

Therefore, direct calculation shows that $\|u_1'(0)\|_{l^2} \leq \frac{\|F'(0)u_1(0)\|_{l^2}}{\lambda_1(0)} \leq \frac{\|F'(0)\|_{op}}{\|A_c\|_{op}^2} \leq 2$.

The rest of the proof follows by substituting the above bound into (4.21), then we have $\|u_c - \epsilon u_1\|_{l^2} \leq \frac{2}{N} + O(1/N^{3/2})$. \square

Remark 1. Theorem 4.4.1 shows that the eigenvector difference of two classes is the order of $\frac{1}{N}$, where N could be seen as the ratio between collagen signal and metabolic signal, so when N is large enough, the difference could be ignored, therefore, it is reasonable to use the eigenvectors of the SVD to approximate the true eigenvectors.

Remark 2. In the proof of Theorem 4.4.1, we did not use any representation of A and A_c , so in a more general case, for any matrix $A = A_c + o(A_c)$ where rank of A_c is 1, the first singular value and first singular vector of A could be used to approximate the singular value and the singular vector of A_c .

4.4.2 Analysis of obtaining the intensity of metabolic activity

Recall that our objective is to get the intensity of the metabolic activity after removing the influence of the collagen signal. We have proved that the largest singular value corresponds to the collagen signal, and the following few singular values correspond to the correlation part between collagen signal and metabolic activity, the rest of the singular values contains information related to the metabolic activity.

Let T be the set of these "rest" singular values. In practice, we only know the total signal $\Gamma_{ODT}(x, t)$ (or the matrix A). By performing a SVD for $\Gamma_{ODT}(x, t)$, we take the terms only corresponding to the singular values in T in the SVD expansion. The next problem is to reconstruct the intensity of the particle movements of metabolic activity. In the numerical experiments, by observation the sum $\sum_{i \in T} \sigma_i^2 |u_i(x_j)|^2$ gives a very good approximation to the intensity of metabolic activity at the pixel x_j . A theorem is given to explain why it works.

Physically, we expect the metabolic activity signal to be centered around 0, so in each pixel x_j , the norm $\|A_m(x_j, t)\|_{\ell^2}^2$ could be seen as the standard deviation of the metabolic signal, which could represent the intensity of metabolic activities in pixel x_j . However, the eigenvectors of the operators with the kernels F_{cc} , F_{cm} and F_{mc} are not orthogonal (this statement may be justified by arguing as in section 4.A). Thus when using a SVD, we do not get the exact "pure" metabolic activity signal A_m , but only an approximation, which we denote by A_{m_1} . We first give an interpretation that $\sum_{i \in T} \sigma_i^2 |u_i(x_j)|^2$ could be written as a ℓ^2 norm of the matrix A_{m_1} .

Theorem 4.4.2 Let A be the matrix after the discretization of $\Gamma_{ODT}(x, t)$ with respect to x and t , such that the j -th row of A corresponds to the pixel x_j , and the k -th column of A corresponds to the time t_k . Let T be a subset of singular values of A , and A_{m_1} be the result of taking only the

singular values in T from A . Then for any pixel x_j , we have

$$\sum_{i \in T} \sigma_i^2 |u_i(x_j)|^2 = \sum_k |A_{m_1}(x_j, t_k)|^2. \quad (4.23)$$

Proof: We apply the SVD algorithm to the matrix A to get $A = USV^*$, where $U = (u_1, u_2, \dots)$, $V = (v_1, v_2, \dots)$ are unitary matrices, and S is a diagonal matrix containing the singular values of A .

We construct a new diagonal matrix S_T , which is obtained from S by keeping all the singular values in T , but changing everything else to zero. By the definition of A_{m_1} , we readily derive $A_{m_1} = US_T V^*$.

Note that $\sigma_i u_i(x_j)$ is the element at row j , column i of the matrix US . By the construction of S_T , we know $\sigma_i u_i(x_j)$ is the element at row j , column i of the matrix US_T for every $i \in T$. Therefore, the sum $\sum_{i \in T} \sigma_i^2 |u_i(x_j)|^2$ is equal to the square-sum of the j -th row of the matrix US_T , which gives

$$\|US_T(x_j, \cdot)\|_{\ell^2}^2 = \sum_{i \in T} \sigma_i^2 |u_i(x_j)|^2. \quad (4.24)$$

On the other hand, the relation $A_{m_1} = (US_T)V^*$ means that for each x_j , $A_{m_1}(x_j, \cdot) = (US_T)(x_j, \cdot)V^*$.

A direct calculation from the definition of ℓ^2 norm of vectors shows that

$$\sum_k |A_{m_1}(x_j, t_k)|^2 = \|A_{m_1}(x_j, \cdot)\|_{\ell^2}^2 = A_{m_1}(x_j, \cdot)A_{m_1}(x_j, \cdot)^*.$$

Using $V^*V = I$ and substituting $(US_T)(x_j, \cdot)V^*$ for $A_{m_1}(x_j, \cdot)$ yields

$$\sum_k |A_{m_1}(x_j, t_k)|^2 = US_T(x_j, \cdot)(US_T(x_j, \cdot))^* = \|US_T(x_j, \cdot)\|_{\ell^2}^2. \quad (4.25)$$

Combining (4.24) and (4.25) completes the proof. \square

Then let us look at the ℓ^2 norm of the difference between the two matrices A_m and A_{m_1} . Proceeding as in the proof of [Theorem 4.4.1](#), we can estimate $\|A_m - A_{m_1}\|$. When N in (4.18) is large enough, it is reasonable to approximate A_m by A_{m_1} . This fact enables us to say that $\|A_{m_1}(x_j, t)\|_{\ell^2}^2 \approx \|A_m(x_j, t)\|_{\ell^2}^2$ for each pixel x_j .

Therefore, we conclude that $\sum_{i \in T} \sigma_i^2 |(u_i)_j|^2$ over the set T of "rest" singular values is indeed a good approximation for the metabolic activity intensity.

4.5 Numerical experiments

In this section we model the forward measurements of our problem. Using the SVD decomposition we filter out the signal, finally obtaining images of the hidden weak sources.

4.5.1 Forward problem measurements

To simulate the signal measurements using ((4.5)), we only need to simulate the density function $p(x, z, t)$ of the media to be illuminated. For each pixel x , there are two types of superimposed media. One is the collagen media characterized for having a strong signal and slow movement. The second medium is the metabolic activity, that has a fast movement relative to the time samples. According to [Ape+16], the collagen signal intensity is around 100 times stronger than the metabolic one.

Given these properties, both media are modeled differently. The collagen particles are simulated as an extended random medium on z that displaces slowly on time; see [Kli02]. For each pixel x , an independent one-dimensional random medium $r_x(\cdot)$ is generated, and then $p(x, z, t) = r_x(z + tv)$ with v being the constant movement velocity. The metabolic activity is simulated as an uniform white noise, whose intensity represents its magnitude. Background or instrumental noise is added everywhere in a similar fashion, but with smaller intensity.

After the medium is simulated, ((4.5)) is applied to reproduce the measured signal, where for integration purposes, the broadband light is approximated by Dirac deltas in certain frequencies. All the model parameters are set such that we obtain similar measurements to the ones obtained in [Ape+16]. In Figure 4.3 we can see, for a single pixel, the simulated signal as a function of time.

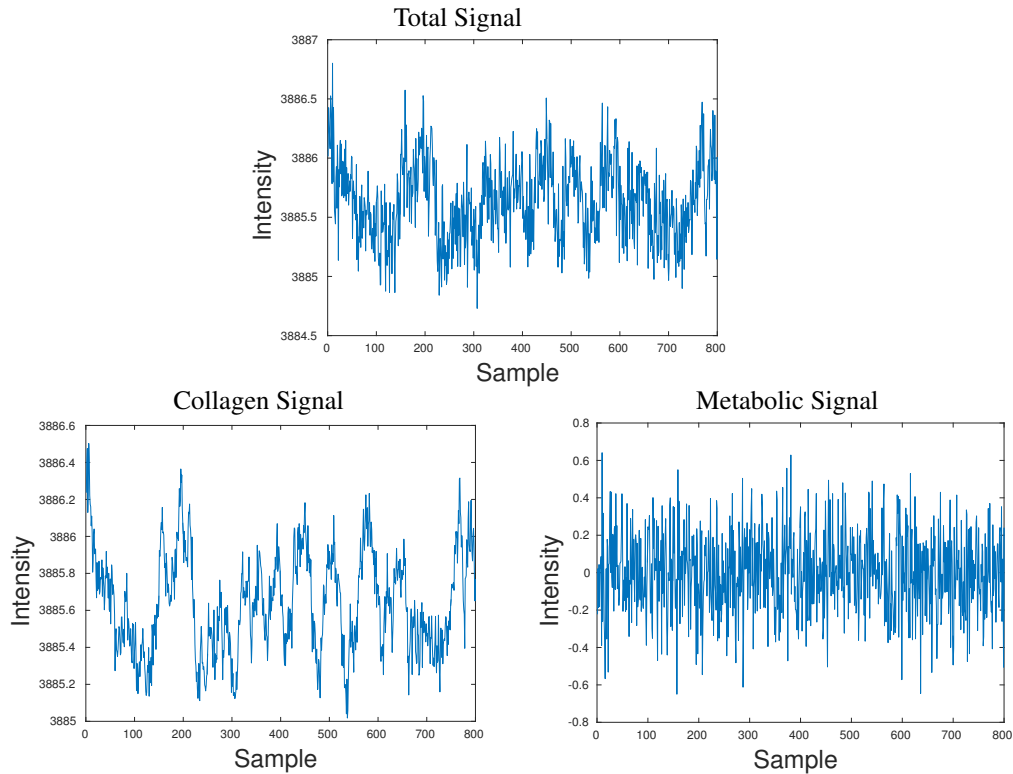


FIGURE 4.3: On top we can see the total signal measured at a fixed pixel. If decomposed into the one corresponding to the collagen structures and metabolic signal, we obtain the bottom images, left and right hand side respectively.

In the following, we consider a two-dimensional 21x21 grid of pixels. The collagen signal, albeit being generated by an independent random media, has the same parameters everywhere, thus sharing a similar behavior. In Figure 4.4, we present the considered metabolic activity intensity map and two snapshots at different times of the total signal.

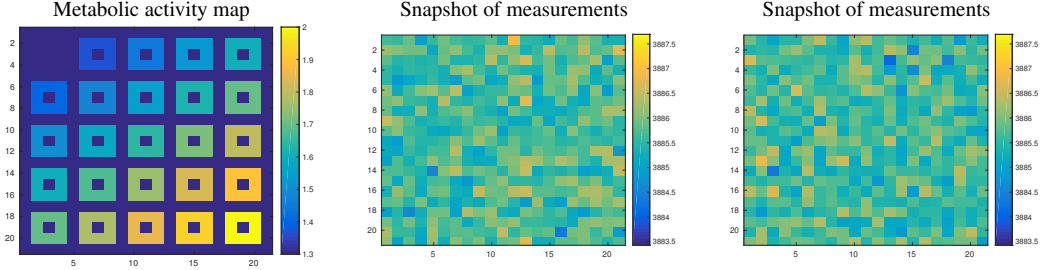


FIGURE 4.4: On the left we can see the considered metabolic map, it describes the intensity of the metabolic signal presented in Figure 4.3. The other two images correspond to raw sampling of the media at different times.

4.5.2 SVD of the measurements

To use the singular value decomposition on the signal, we reshape the raw data $\Gamma_{ODT}(x, t)$ under a Casorati matrix form, where the two-dimensional pixels on the x variable are rearranged as a one-dimensional variable, and hence the total signal is written as a matrix A where each dimension corresponds respectively to the space and time variables. The total signal consists on the addition of the metabolic and collagen signals, namely $A = A_m + A_c$. Our objective is to recover the spatial information of the metabolic signal A_m .

We apply the SVD decomposition (4.17) over the total signal A , where the dimension of each space corresponds to the amount of pixels of the image and the time samples respectively. Each space vector $\{u_i\}$ point out which pixels are participating in the i th singular value. To obtain an image of the pixels participating in a particular subset of singular values $T \subset \mathbb{N}$, we use the following formula (see Section 4.2 for why it works):

$$I(j) = \sqrt{\sum_{i \in T} \sigma_i^2 u_i(j)^2}, \quad (4.26)$$

where the indices j are for indexing the image's pixels. When the signal has mean 0, (4.26) corresponds to the standard deviation that was already considered as an imaging formula in [Ape+16].

In Figure 4.5, we can see an image of each space vector $\{u_i\}$ ordered by their associated singular value, these vectors correspond to the decomposition of the total signal A . The other two pictures on the right of it, correspond to the singular space vectors but for each unmixed signal A_c and A_m , separately. As it can be seen, the spatial vectors of both signals get mixed in the total signal, but the metabolic activity ones get embedded in a clustered fashion, although there is a distortion of these vectors, this is unavoidable given the nature of the SVD.

The location of the spatial vectors is related to their respective singular values, that are presented in Figure 4.6. It is observed, that the moment in which the spatial vectors of the total signal start

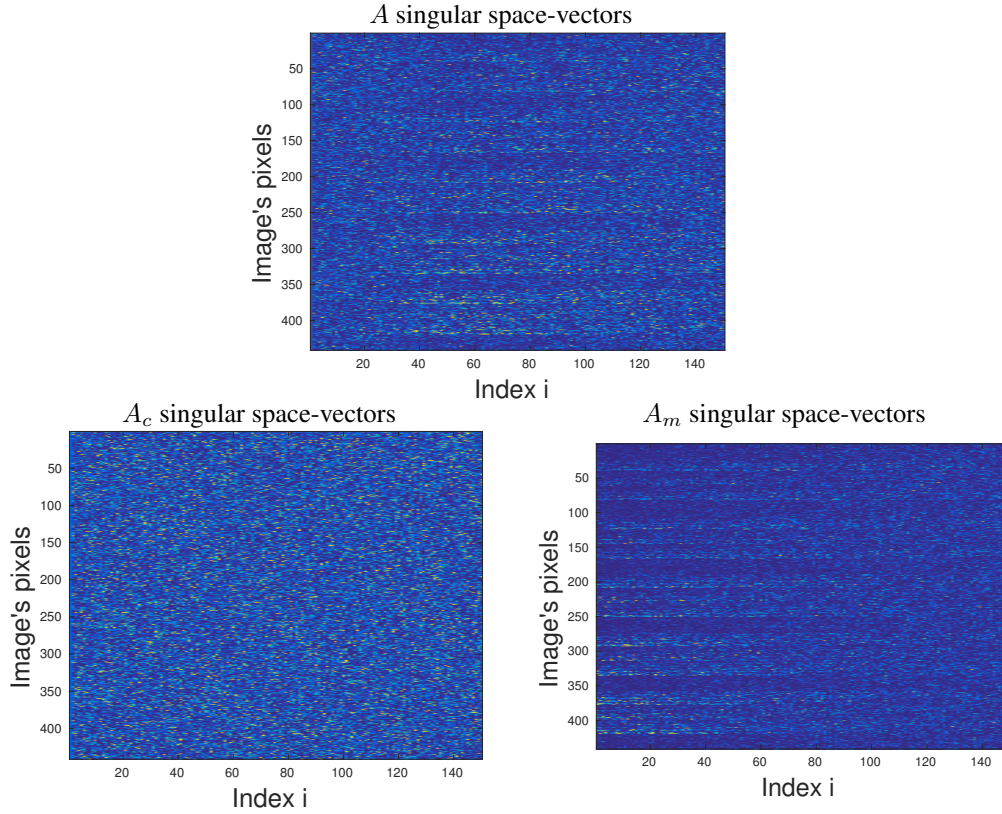


FIGURE 4.5: These images are the space matrices obtained with the SVD, where each column of these matrices corresponds to a singular space-vector, naturally ordered from left to right by their respective singular value index. Notice that each row of these matrices represents each pixel of the image presented in Figure 4.4 and the color intensity indicates how much weight does each singular vector placed in that particular pixel. From the bottom-right image we can see that the first singular space-vectors from the metabolic signal are clearly clustered on some pixels (that correspond to the zones in where there is metabolic activity), whereas from the bottom-left image we notice that the singular space-vectors do not concentrate in any specific location, as the collagen is present everywhere. Observing the image on the top, that is the total signal, we notice that after dropping the firsts singular space-vectors, we also observe a clustered behavior.

This information is the one we seek to recover from the total signal.

to look like the ones from the metabolic activity, is close to the moment in which the singular values from the metabolic activity get close to those in the total signal. In a mathematical way, we say that the index $j \in \mathbb{N}$ in which the spatial vectors u_i start to resemble those of the metabolic activity, corresponds to

$$j = \operatorname{argmin}\{\sigma_j(A) < \sigma_1(A_m)\} - k, \quad \text{with } k \text{ small.} \quad (4.27)$$

In practice, for the tested examples (up to 24x24 grid of pixels, and 500 to 1000 time samples) $k \approx 10$ achieve the best results.

The clustered behavior of the singular vectors arise from the model itself, as it generates fast

decaying singular values for the collagen signal, whereas the metabolic singular values decay in a more slow fashion. Hence, it is possible to assign an interval of the total signal space vectors as an approximation to the metabolic activity A_m .

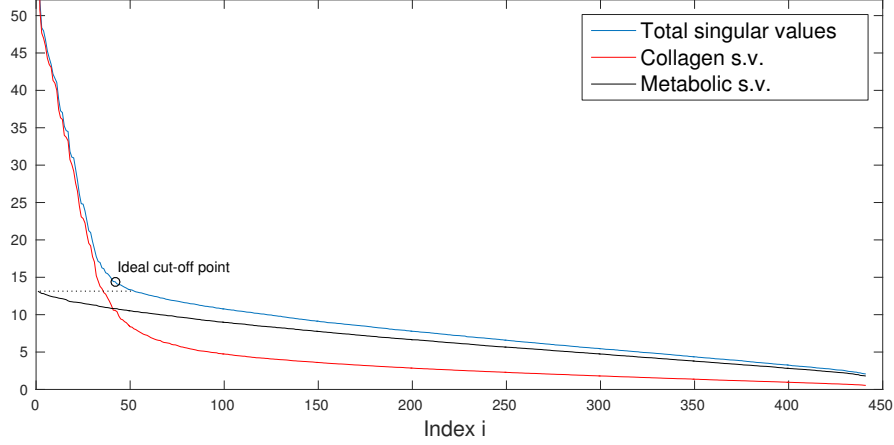


FIGURE 4.6: Singular values for the signals. The circle represents the optimal starting index j at which we should consider the singular space-vectors of the total signal to contain mostly information on the singular space-vectors of the metabolic activity. The first singular value of the total signal and the collagen signal is outside the plot, with an approximate value of 2.3×10^6 .

4.5.3 Selection of cut-off singular value

The before mentioned criteria to choose an adequate interval of singular-space vectors to apply the imaging (4.26) is not possible in practice, as we have no a priori information on where the metabolic singular values $\sigma_i(A_m)$ lie. Since the idea is to consider an interval of singular space vectors, the first and last elements must be defined. The length of the interval corresponds to the range of the matrix A_m , with some added terms coming from the matrix A_c . This can be left as a free parameter to be decided by the controller. As a general guideline, it corresponds to the quantity of pixels in which it is expected to find the metabolic activity.

For the considered first singular space vector, also called cut-off one, there is a criteria that arises from the model. Given the differences between the metabolic and collagen signal, the latter in the time variable has some regularity and self correlation. This characteristic is transferred to the first singular time-vectors. In Figure 4.7 we can see plots of these time-vectors for each signal.

Our proposed technique consists in measuring the regularity of the time vectors using the total variation semi-norm, the smaller the value the more regular. With this information we seek to estimate the $\operatorname{argmin}\{\sigma_j(A) < \sigma_1(A_m)\}$ and thus, using ((4.27)), select the cut-off point. In the case of a discrete signal, the total variation can be stated as

$$\|v\|_{\text{TV}} = \sum_{i=1}^{N-1} |v(i+1) - v(i)|.$$

Applying the total variation norm to the total signal singular time-vectors v_i , we can see that the regularity drops until arriving to, in mean, a slowly increasing plateau. To find it, in an operator

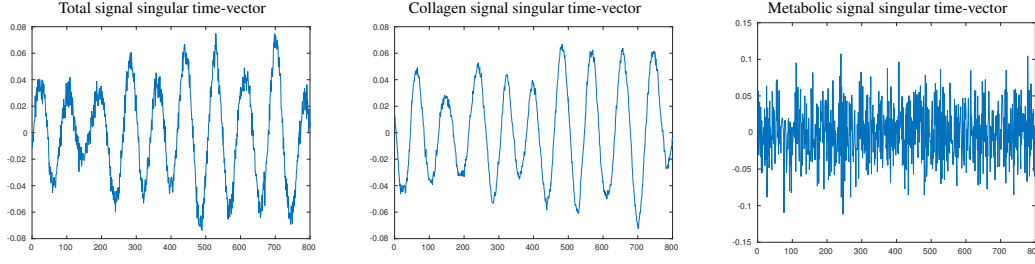


FIGURE 4.7: Plots of the singular time-vectors for each signal, at the second singular value. The collagen time vectors are more regular and correlated compared to the metabolic signal, albeit this property is gradually loosed as we augment the index of the time vectors. Since the SVD of the total signal is dominated by the collagen signal, its time vectors inherit the same property.

free way, it is possible to fit a 2 piece continuous quadratic spline in the total variation plot, and estimate the first metabolic singular value index as the index l in which the spline changes. In our simulations this l is a good approximation for the first singular value of the metabolic activity, meaning that $\sigma_l \approx \sigma_1(A_m)$; see Figure 4.8, thus by subtracting the value k in (4.27), we obtain a cut-off point. Keep in mind that this considered method does not make use of a priori information.

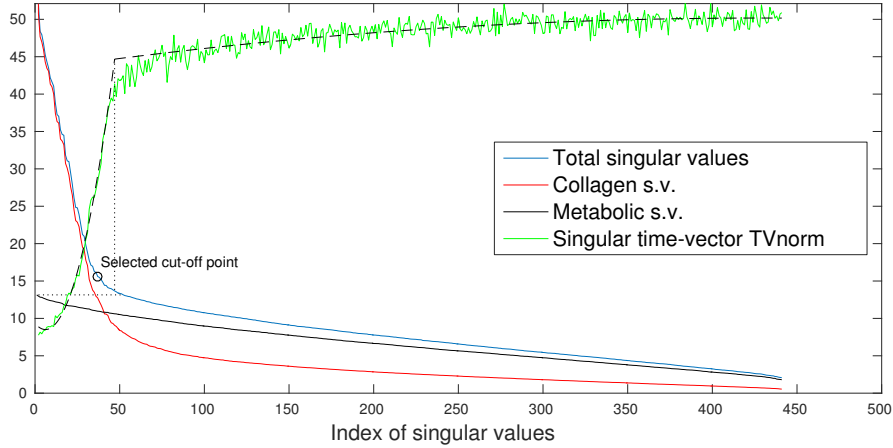


FIGURE 4.8: Same plot as in Figure 4.6, but including the total variation of the singular time-vectors of the total signal. The total variation is scaled to fit the plot with the singular values.

4.5.4 Signal reconstruction

Employing the cut-off criteria in subsection 4.5.3 and (4.26) to our simulation, we can reconstruct the metabolic activity. In Figure 4.9 we have on the left-hand side the best possible reconstruction using the SVD technique, that is the one we could do if we could isolate completely the signal A_m from the total signal A . On the right-hand side, we have the actual reconstruction. It is worth mentioning that we are not able to reconstruct the exact metabolic

map, as (4.26) is used on the simulated media, and thus the image obtained out of the isolated signal A_m is the one we are aiming to reconstruct.

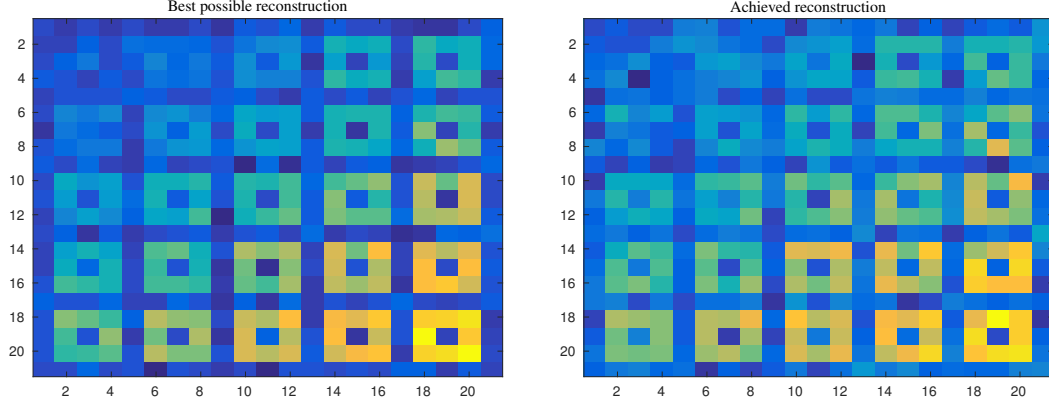


FIGURE 4.9: Reconstruction of the metabolic map presented in Figure 4.4. The left image correspond to using directly (4.26) on the isolated A_m signal. The right-hand side image correspond to using our reconstruction method on the total signal. Once the images are normalized, the committed error with respect to the original metabolic map is 0.011 and 0.017, respectively

4.5.5 Discussion and observations

Since the SVD uses information of all pixels simultaneously to filter out the collagen signal, this technique works better the larger the considered image size is, as the main point is to use the joint information of all the pixels in the image, in contrast to frequency filtering that considers only point-wise information. Numerically, this effect is notorious, as the larger the image size, the more clustered are the singular space-vectors associated to the metabolic activity and thus it is easier to filter out the collagen signal.

With respect to the time samples, keep in mind that all simulations considered a fixed sample rate, and it is observed that the filtering process degrades if too many time samples are considered (i.e. lengthier measurement experiences). When this happens (for our 21x21 grid size, this is above 1000 time samples), the singular values of the collagen signal start decaying in a slower rate, accomplishing a less clustered behavior of the metabolic singular space-vectors, and thus achieving a worse signal separation. Therefore, if there are too many available time samples, one possible recommendation is to do several reconstructions using subsets of these time samples and then averaging the results.

The reasons of this behavior when too many time samples are accessible, are specific to the singular value decomposition and not the sample rate or the noise level. It is possible that the sample rate gets small enough to the point that we could track specific metabolic movements inside the cell, if this is the case, the model becomes invalid and new assumptions must be placed.

4.6 Conclusion

In this paper, we performed a mathematical analysis of extracting useful information for sub-cellular imaging based on dynamic optical coherence tomography. By using a novel multi-particle dynamical model, we analyzed the spectrum of the operator with the intensity as an integral kernel, and shown that the dominant collagen signal is rank-one. Therefore, a SVD approach can theoretically separate the metabolic activity signal from the collagen signal. We proved that the SVD eigenvectors are good approximation to the collagen signal, proving that the SVD approach is feasible and reliable as a method to remove the influence of collagen signals. And we also discovered a new formula that gives the intensity of metabolic activity from the SVD analysis. This is further confirmed by our numerical results on simulated data sets.

4.A Appendix

In this appendix we will illustrate the fact that the eigenvectors of the kernels $F_{cc}(x, y)$, $F_{cm}(x, y)$ and $F_{mc}(x, y)$ are in general not orthogonal. Since all of them have variable separable forms with respect to x and y , which is the basis of our analysis, so here we only prove the nonorthogonality between eigenvectors of the kernels $F_{cc}(x, y)$ in (4.11) and $F_{cm}(x, y)$ in (4.12).

Let A be the matrix obtained from discretizing the signal Γ_{ODT} . The singular values of A are the square roots of the eigenvalues of the matrix A^*A , and the singular vectors of A are the corresponding eigenvectors of A^*A . We notice that A^*A is a discretization of the integral kernel $F(x, y)$. We first demonstrate the relation between kernels with variable separable forms and eigenvectors.

Lemma 4.A.1 *For any function $f(x, y) \in L^2(\Omega \times \Omega)$, if there exist functions $f_1(x)$ and $f_2(y)$, such that $f(x, y) = f_1(x)f_2(y)$, then the operator $T : L^2(\Omega) \rightarrow L^2(\Omega)$ with kernel $f(x, y)$ can have only one nonzero eigenvalue. Furthermore, the eigenvector of T corresponding to the unique nonzero eigenvalue is given by $f_1(x)$ or $f_2(y)$.*

Proof: Using the variable separation form $f(x, y) = f_1(x)f_2(y)$ yields

$$\begin{aligned} (Th)(x) &= \int_{\Omega} f(x, y)h(y)dy \\ &= \int_{\Omega} f_1(x)f_2(y)h(y)dy \\ &= f_1(x) \int_{\Omega} f_2(y)h(y)dy. \end{aligned} \tag{4.28}$$

Suppose that λ is a nonzero eigenvalue of T , and $g(x)$ is the corresponding eigenvector, so that $Tg(x) = \lambda g(x)$. Comparing this with (4.28) implies

$$\lambda g(x) = f_1(x) \int_{\Omega} f_2(y)g(y)dy. \quad \square$$

Therefore, the eigenvector $g(x)$ is a multiple of $f_1(x)$, and the corresponding eigenvalue $\lambda = \int_{\Omega} f_2(y)f_1(y)dy$.

Denote the functions $\varphi^c(x)$ and $\varphi^m(x)$ by

$$\begin{aligned}\varphi^c(x) &= K_{c_1}(x)q_c(x), \\ \varphi^m(x) &= \int_{[-L,L]^2 \times [0,T]} \mathcal{F}(S_0 K_{c_2})\left(\frac{4\pi\bar{n}z_2}{c}\right) \\ &\quad \times \mathcal{F}(S_0 K_m)\left(x, -\frac{4\pi\bar{n}z_1}{c}\right) p_m(x, z_1, t) dz_1 dz_2 dt\end{aligned}$$

Then the kernels F_{cc} and F_{cm} can be written as

$$\begin{aligned}F_{cc}(x, y) &= C_1 \varphi^c(x) \varphi^c(y), \\ F_{cm}(x, y) &= C_2 \varphi^c(x) \varphi^m(y),\end{aligned}$$

where C_1 and C_2 are constants.

Applying [Lemma 4.A.1](#) to the kernels F_{cc} and F_{cm} , we know that the corresponding eigenvectors are φ^c and φ^m respectively.

Since this integral $\int_{\Omega} \varphi^c(x) \varphi^m(x) dx$ depends much on the random term $p_m(x, z, t)$, it will not be zero almost all of the time. Hence, in our construction, the vectors φ^c and φ^m are in general not orthogonal.

References

- [AA17] G. S. Alberti and H. Ammari. “Disjoint sparsity for signal separation and applications to hybrid inverse problems in medical imaging”. *Appl. Comput. Harmon. Anal.* 42.2 (2017), pp. 319–349.
- [Alb+16] G. S. Alberti, H. Ammari, B. Jin, J. K. Seo, and W. Zhang. “The linearized inverse problem in multifrequency electrical impedance tomography”. *SIAM J. Imaging Sciences* 9.4 (2016), pp. 1525–1551.
- [Alb+17] G. S. Alberti, H. Ammari, F. Romero, and T. Wintz. “Mathematical analysis of ultrafast ultrasound imaging”. *SIAM J. Appl. Math.* 77.1 (2017), pp. 1–25.
- [Ape+16] C. Apelian, F. Harms, O. Thouvenin, and A. C. Boccara. “Dynamic full field optical coherence tomography: subcellular metabolic contrast revealed in tissues by temporal analysis of interferometric signals”. *Biomed. Opt. Express* 24.7 (2016), pp. 1511–1524.
- [Che+99] Z. P. Chen, Y. H. Zhao, S. M. Srinivas, S. J. Nelson, N. Prakash, and R. D. Frostig. “Optical doppler tomography”. *IEEE J. Sel. Topics Quantum Electron.* 5.4 (1999), pp. 1134–1142.
- [DF08] W. Drexler and J. G. Fujimoto. “Optical Coherence Tomography”. Berlin, Heidelberg: Springer, 2008.

- [EMS15] P. Elbau, L. Mindrinos, and O. Scherzer. “Mathematical Methods of Optical Coherence Tomography”. In: *Handbook of Mathematical Methods in Imaging*. Ed. by O. Scherzer. Springer New York, 2015, pp. 1169–1204.
- [Fer+03] A. F. Fercher, W. Drexler, C. K. Hitzenberger, and T. Lasser. “Optical coherence tomography - principles and applications”. *Rep. Prog. Phys.* 66.2 (2003), pp. 239–303.
- [Fer96] A. F. Fercher. “Optical coherence tomography”. *J. Biomed. Opt.* 1.2 (1996), pp. 157–173.
- [GG77] I. C. Gohberg and S. Goldberg. “Basic operator theory”. Birkhäuser, 1977.
- [Hua+91] D. Huang, E. A. Swanson, C. P. Lin, J. S. Schuman, G. Stinson, W. Chang, M. R. Hee, T. Flotte, K. Gregory, C. A. Puliafito, and J. G. Fujimoto. “Optical coherence tomography”. *Science* 254.5035 (1991), pp. 1178–1181.
- [Joo+10] C. Joo, C. L. Evans, T. Stepinac, T. Hasan, and J. F. de Boer. “Diffusive and directional intracellular dynamics measured by field-based dynamic light scattering”. *Opt. Express* 18.3 (2010), pp. 2858–2871.
- [Kli02] L. Klimeš. “Correlation functions of random media”. 159.7-8 (2002), pp. 1811–1831.
- [Lee+12] J. Lee, W. Wu, J. Y. Jiang, B. Zhu, and D. A. Boas. “Dynamic light scattering optical coherence tomography”. *Opt. Express* 20.20 (2012), pp. 22262–22277.
- [LSD09] Y. Li, J. Schnekenburger, and M. H. Duits. “Intracellular particle tracking as a tool for tumor cell characterization”. *J. Biomed. Opt.* 14.6 (2009), p. 064005.
- [Pod05] A. G. Podoleanu. “Optical coherence tomography”. *Brit. J. Radiology* 78 (2005), pp. 976–988.
- [Rel69] F. Rellich. “Perturbation theory of eigenvalue problems”. CRC Press, 1969.
- [Sch99] J. M. Schmitt. “Optical coherence tomography (OCT): A review”. *IEEE J. Quantum Electron.* 5 (1999), pp. 1205–1215.
- [TW05] P. H. Tomlins and R. K. Wang. “Theory, developments and applications of optical coherence tomography”. *J. Phys. D: Appl. Phys.* 38 (2005), pp. 2519–2535.

5

Discussion and Outlook

Photoacoustic tomography has been of significant interest in recent years due to the high contrast and high resolution images. In this work, we concentrate on the inverse problems related to acoustic wave equation in attenuating media from wavefield measurements. We successfully handle attenuation effect in acoustic media, analyze the ill-posedness of the inverse problems in different attenuating media. Furthermore, explicit reconstruction formulas are given and numerical results show the viability of these formulas.

In order to address the ill-posedness of inverse problems, we first prove the existence and uniqueness of solution of attenuated wave equation in the distributional sense. Then, we propose a necessary and sufficient condition for the finite propagation speed of wave. By giving the definitions of weak attenuation and strong attenuation, we divide the known photoacoustic models to two classes. We consider a self-adjoint integral operator which is generated by the integrated photoacoustic operator. Through proving the L^2 property of its kernel, we get that the self-adjoint operator is a Hilbert-Schmidt operator and thus compact. Based on this property, we analyzed the decay rate of its eigenvalues. In strong attenuating media, the kernel of this integral operator is infinitely smooth, and we give the bound of its directional derivatives of every order. Using this information, we prove that the singular values of the attenuated photoacoustic operator decay exponentially. On the other hand, in the weak attenuation case the kernel of the integral operator is weak singular. By dividing the integral operator into the sum of constant attenuating operator and a perturbation, we prove the singular values of the attenuated photoacoustic operator decay with the same rate as the singular values of the non-attenuated photoacoustic operator, which is polynomial with the order $-\frac{1}{3}$.

The research about spectral analysis provides fundamental theoretical basis and important tools for analysing the degree of ill-posedness of inverse problems. More generally, our method to analyze the eigenvalue asymptotic behavior of integral operator is applicable to any integral operators with infinity smooth kernels or weak singular kernels. Thus, we could apply these methods on other similar problems which may lie outside of the scope of imaging problems. Also, these methods could be extended to analyze the eigenvalue asymptotic behaviors of the related nonlinear problems.

After giving the ill-posedness of the attenuated PAT problem, we introduce some reconstruction formulas for the initial pressure in the attenuated wave equation, that is, explicit reconstruction formulas in the time domain based on the universal back-projection formula. Numerical experiments show the formula works quite well. The reconstruction methods give more accurate approximations for the initial pressure, which can be used in the subsequent quantitative PAT.

There are still some open problems. Since until now it is hard to make a standard rule to distinguish good attenuation models. An interesting problem is to recover both the initial pressure $h(x)$ and complex wave number $\kappa(\omega)$ by providing more information.

Also, in the thesis, we consider a homogenous medium. That is, we assumed the acoustic properties of the medium, as defined by the complex wave number $\kappa(\omega)$, does not change throughout the tissue we're imaging. In practice, according to the different properties of the tissue, the acoustic properties could be spatially varying, so the problem is how to recover the initial pressure $h(x)$ in the attenuating media with a varying complex wave number $\kappa(\omega, x)$. The non-attenuating counterpart of this problem deals with a variable sound-speed $c(x)$, and there are some known works for this case. In this regard we refer to [AK07; Kun07].

Moreover, the reconstruction formulas we gave in the thesis are for plane, cylinder or sphere. More generally, if the observation surface is only assumed to be smooth and convex, what will the reconstruction formulas look like? In non-attenuating media, we refer to [Nat12].

Another topic in the thesis is about optical coherence tomography. Our work on OCT present a general technique to remove the influence of a strong and slow-varying background signal, to unveil useful information on the cellular scale.

Using dynamic optical coherence tomography, based on a single particle model we give a new multi-particle dynamical model to simulate the movements of the collagen and the cell metabolic activity. We prove that the largest singular value of the associated Casorati matrix corresponds to the collagen. Then, we present an efficient signal separation technique for sub-cellular imaging. To isolate the signal from the metabolic activity, we perform a singular-value decomposition on the dynamic optical images. Several numerical results are given to illustrate and validate our approach.

This signal separation technique could be more generally used to separate two sets of signals which have large difference in intensity. Also it provides some ideas to model other dynamical imaging methods.

A

Deutsche Zusammenfassung

Das wissenschaftliche Interesse an photoakustischer Tomographie (PAT) hat in den letzten Jahrzehnten stark zugenommen. Die Gründe dafür sind vielfältig, unter anderem liegt dies an der hohen Auflösung, dem starken Kontrast, sowie der guten Genauigkeit der Methode. Dennoch vernachlässigen die meisten aktuellen Artikel einen wichtigen Aspekt, die Dämpfung. Da das meiste Gewebe viskoelastische Eigenschaften aufweist, würde sich die Energie während der Ausbreitung einer akustischen Welle verringern. Lässt man die Dämpfung dabei außer Acht, könnte dies die Qualität der finalen Rekonstruktion verschlechtern.

Dies ist eine kumulative Dissertation, bestehend aus drei Artikeln aus dem Bereich der medizinischen Bildverarbeitung.

Die ersten beiden Artikel beschäftigen sich mit PAT unter Berücksichtigung von akustischer Dämpfung. Unser erstes Ziel ist es ein dazugehöriges mathematisches Modell zu entwickeln. Bekannte Forschungsergebnisse diesbezüglich gibt es bisher kaum. Einige der fundamentalen Probleme, wie zum Beispiel die Frage danach wie sehr ein Problem schlecht gestellt ist und die Existenz einer expliziten Rekonstruktionsformel, verbleiben offen.

Im ersten Artikel wird zuerst ein Überblick über bekannte photoakustische Dämpfungsmodelle gegeben. Anschließend präsentieren wir ein allgemeines Modell unter Berücksichtigung der Dämpfung und zeigen Existenz und Eindeutigkeit der Lösung. Außerdem untersuchen wir das asymptotische Verhalten der Singulärwerte des direkten Problems und geben eine notwendige und hinreichende Bedingung für die endliche Ausbreitungsgeschwindigkeit einer akustischen Welle an.

Nach der Behandlung des direkten Problems beschäftigen wir uns im zweiten Artikel mit dem inversen Problem, das heißt, unser Ziel ist es die anfängliche Druckverteilung zu rekonstruieren. Es gibt einige bekannte Methoden zur Lösung dieses Problems, jedoch keine bekannte Rekonstruktionsformel. Wir stellen neue Rekonstruktionsformeln basierend auf der allgemeinen Rückprojektionsformel vor. Numerische Resultate zeigen vielversprechende Ergebnisse mit ähnlichem rechnerischen Aufwand wie Rückprojektionsformeln.

Im dritten Artikel entwickeln wir eine Methode zur Teilung des Signals in sub-zellulärer optischer Kohärenztomographie (OKT). Dies rührt daher, dass das Hintergrundsignal in OKT Bildern, verursacht durch Kollagen oder andere interzelluläre Teilstücke, so stark ist, dass wichtige Informationen im Inneren der Zelle verborgen bleiben. Unser Ziel ist es den Einfluss dieses Signals zu minimieren, um so die benötigten Informationen zu isolieren. Dazu untersuchen wir zunächst die Modellierung des Hintergrundsignals sowie die Zellaktivität und schlagen, unter Verwendung der Singulärwertzerlegung, eine effiziente Methode vor, um das Problem zu lösen.